A CELLULAR AND BEHAVIORAL ANALYSIS OF PREFRONTAL CORTICAL FUNCTION AND ITS MODULATION BY DOPAMINE

By

JEREMY KEITH SEAMANS

B.Sc., McGill University, 1991
M.A. University of British Columbia, 1993

A THESIS SUBMITTED IN PARTIAL FULFILLMENT
OF THE REQUIREMENTS FOR THE DEGREE OF

DOCTOR OF PHILOSOPHY

in

THE FACULTY OF GRADUATE STUDIES

(Department of Psychology; Biopsychology)

We accept this thesis as conforming
to the required standard

THE UNIVERSITY OF BRITISH COLUMBIA
JANUARY 1998

© Jeremy Keith Seamans, 1998

In presenting this thesis in partial fulfilment of the requirements for an advanced degree at the University of British Columbia, I agree that the Library shall make it freely available for reference and study. I further agree that permission for extensive copying of this thesis for scholarly purposes may be granted by the head of my department or by his or her representatives. It is understood that copying or publication of this thesis for financial gain shall not be allowed without my written permission.

Department of Psychology

The University of British Columbia
Vancouver, Canada

Date Jan 17 /98

DE-6 (2/88)

Abstract

The activity of neurons in the prefrontal cortex (PFC) may underlie working memory processes in the brain. Both the performance of working memory tasks and the activity of PFC neurons are modulated by dopamine. The goal of the present thesis was to gain insight into the neural basis of working memory by studying the PFC, and the DA system in the PFC, from both a behavioral and cellular perspective.

The functional contribution of the PFC to working memory processes in the rat was assessed in Chapter 2 of the present thesis using memory-based foraging tasks on an 8-arm radial maze. The results of these studies indicated that lidocaine-induced inactivations of the PFC selectively disrupted the ability to use mnemonic information to guide foraging, but not the ability to acquire or retain such information. The ability to use mnemonic information to guide foraging was also disrupted by microinjection of a D1 but not D2 receptor antagonist into the PFC.

Chapters 3-5 investigated how PFC neurons process synaptic inputs to their dendrites to produce spike output. The intrinsic membrane properties and synaptic responses at the soma and dendrites of deep layer PFC pyramidal neurons were recorded using sharp intracellular or whole-cell patch-clamp techniques in a brain-slice preparation. Different passive and active membrane properties of the soma and dendrites of PFC neurons were observed. The distal dendrites of PFC neurons responded most effectively to strong, highly coincident

synaptic inputs. Ca^{2+} currents near the soma both amplified the effects of these inputs and modulated the spike output pattern. Spike output at the soma was also controlled by the interplay of slowly-inactivating Na^{+} and K^{+} currents. Chapter 6 investigated the modulation of PFC neurons by DA. DA or a D1 but not D2 receptor agonist increased the evoked firing of PFC neurons via a D1-mediated modulation of slowly-inactivating Na^{+} and K^{+} currents. Concurrently, D1 receptor activation reduced burst firing in PFC neurons, due to a attenuation of Ca^{2+} currents. D1 receptor activation also increased both $GABA_A$ IPSPs and NMDA EPSPs.

The final chapter of this thesis integrated these data into a cellular model of PFC function and its modulation by DA. It is proposed that DA may tune PFC neurons such that they respond selectively to strong synchronized inputs from other cortical areas. In the presence of DA, working memory processes mediated by the PFC may be influenced selectively by stimuli of behavioral significance.

TABLE OF CONTENTS

LIST OF TABLES AND FIGURES

ACKNOWLEDGMENTS

First, I would like to thank God.

I would like to acknowledge all those involved in reviewing and critiquing this thesis, including, Drs. Catherine Rankin, Dimitri Papageorgis, Peter Reiner, Robert Douglas and Lawrence Ward. I would also like to thank Dr. Ward for many long and interesting debates. I also thank Daniel Durstewitz for his many insightful and thoughtful comments.

This thesis was made possible by the combined efforts and support of many people. To begin I would like to that all those associated with the laboratories of Drs. Phillips and Yang. Most notably, Dr. Charles Blaha who has been so supportive on a variety levels, and has been a valued friend. The contribution of Dr. Natalia Gorelova to my development as a neurophysiologist is immeasurable. She has been a valued teacher and mentor.

I would also like to acknowledge the support of my friend and colleague, Stanley Floresco. Much of the behavioral work in this thesis was a direct result of the our many heated yet thoroughly enjoyable discussions. He has been a tremendous help to me both on a practical level and on as a friend.

I would also like to thank Drs. Anthony Phillips and Charles Yang, I could not have asked for better supervisors. They have exhibited extreme patience over the years, under sometimes very trying circumstances. I truly appreciate the countless hours Charles spent in the laboratory with me, providing both guidance and support. For the past six years, Tony has always been there for me and I have come to respect his opinions more than anyone else's. They have had a tremendous influence on my life, both as scientists and people, and they have my deepest respect.

Finally, I would like to thank the two most important women in my life, Krista and Betty Seamans. Betty, my mother, has been there since day one and has always believed in me. She has been a constant source of support and encouragement. If it weren't for her, there wouldn't be a thesis. Krista, my wife, has put up with a lot, given the long hours and tough times associated with research. She has been a constant source of stability.

Thank you Krista for your constant support, patience and love.

Dedication

This thesis is dedicated to the memory of my father, Dr. Keith Byron Seamans. He is responsible for my interest in pursuing the mysteries of the brain.

Chapter 1

General Introduction

"Thinking is done by the cells of the brain behind the forehead... if the forehead cells do not know how to think, the mind cannot make use of memories. We say that such a person is a fool."

Overton, 1897.

The capacity to use mnemonic information to plan and organize forthcoming action is a key cognitive ability necessary for the survival of a number of species. It is proposed that the ability to envision and manipulate scenarios internally was more fully developed in early humans relative to Neanderthals, and this ability was a determinate of the success of our ancestors (Diamond 1992). The prominent prefrontal cortex (PFC, see Table 1 for list of abbreviations) in modern humans is hypothesized to be responsible for our well developed ability to use internalized representations to flexibly and insightfully guide action (Stuss & Bensen 1986).

The ability to hold and manipulate information during the performance of a wide range of cognitive tasks has been defined as working memory (Baddeley & DeSalla 1996; Baddeley & Hitch 1974). Baddeley (1986) proposed the term working memory to replace the concept of passive short-term memory and to emphasize the on-line *manipulation* of information. According to Baddeley & Hitch (1974), working memory is composed of a central executive, which controls interconnected slave systems. One of these interconnected slave systems is a visuo-spatial sketch pad which holds visuo-spatial information temporarily. The

transient nature of information in the sketch pad separates working memory from other types of memory such as semantic or procedural memory which are long-lasting. Goldman-Rakic (1991; 1995) and Fuster (1971; 1991) have argued that the activity of PFC neurons underlies the ability to hold transiently information that will be used to guide action (see below). The active retention of information is also a unique attribute of working memory systems in the brain, as theories of the neural basis of long-term memory emphasize 'passive' storage, whereby information is stored as changes in synaptic weights (e.g. Barnes 1996).

The distinction between working memory and other forms of memory in the brain has been emphasized by a number of investigators. Goldman-Rakic (1996) has stated that although damage to the PFC does not impair knowledge about the world or long-term memory, it does impair the ability to use such knowledge to guide behavior. Likewise, Fuster (1993) has stated "frontal memory, above all, is memory for action". This type of memory for action embodies the concept of working memory as defined by Baddeley (1986) as it emphasizes the executive control of memory used to guide action.

The Contribution of the PFC to Working Memory, NOT Short-term Memory

In 1936, Jacobsen first demonstrated that lesions of the PFC of primates impair performance of the delayed-response working memory task and this finding has been replicated by numerous investigators (see Funahasi & Kubota 1995 for review). However, there has been considerable difficulty in understanding the nature of this deficit. Early theories suggested that the PFC

may be involved in short-term memory. Working memory and short-term memory have been related theoretically, therefore there has been a lasting tendency to view working memory processes mediated by the PFC simply as short-term memory processes. This is not correct as there is considerable evidence against the idea that the PFC simply subserves short-term memory.

First, there has never been a reported case of amnesia after selective PFC damage (Petrides 1996). Patients with PFC damage show no deficits on traditional short-term memory tasks of recognition or recall (Petrides 1989). Such patients have a normal digit span and are unimpaired in the memory component of intelligence tests (Hebb 1939; 1977; Stuss et al. 1982; Petrides 1989). In fact, some authors have reported a significant post-operative improvement of scores on the Weshler memory scale following bilateral excision of the PFC (Smith et al. 1977) most likely as a result of reduced anxiety about the test situation. Moreover, primates with PFC lesions perform normally on recognition memory tasks, delayed matching to sample tasks and delayed object alternation tasks (Bachevalier & Mishkin 1986; Passingham 1975; Petrides 1995).

Consistent with the role of the PFC in working memory, PFC lesions affect the *manipulation* of information in short-term memory. For instance, PFC patients are severely impaired on self-ordered pointing tasks, which require subjects to sort through a set of cards pointing at each stimulus only once, while monitoring or editing responses to avoid pointing to previously selected stimuli. Moreover, PFC lesions also impair the ability to use memory to plan events in everyday life or plan responses on laboratory tasks (Shallice 1982; Shallice & Burges 1989;

Robbins 1996). Robbins and colleges (Robbins, 1996; Owen et al. 1990; 1995) have shown that PFC patients are particularly impaired on a modified Tower of London task. This task requires subjects to plan the moves which are needed to stack discs on a ring in accordance with a 'goal' configuration set by the experimenter.

The distinction between the role of the PFC in *working*, as opposed to *short-term* memory is made especially clear when one examines the effects of PFC lesions on tasks requiring response flexibility. On such tasks PFC patients commit repeated errors that they are consciously aware of and that they can report, but cannot use to update behavior (Milner 1965; Konow & Pribram 1970). A classic example of this is observed in PFC patients with the Wisconsin Card Sorting task (Milner 1963). This task requires subjects to formulate a card sorting strategy based on feedback from an experimenter. PFC-damaged patients are able to deduce, remember and verbalize the correct sorting strategy to the experimenter, but are unable to alter their sorting strategy based on this knowledge. As a result they perseverate in their initial response strategy, unable to shift to a strategy they know to be correct. Primates with lesions of the PFC also perseverate on their initial response strategy during performance of the analogous "A-not-B" task (Diamond & Goldman-Rakic 1989). In the "A-not-B" task primates must learn that one of two spatially distinct wells initially contains food while the other does not. After training, the well containing food is switched. Normal animals quickly go to the newly baited food well, while lesioned animals continue to revisit a previously rewarded spatial location, indicating that they had

specific knowledge about the spatial location where food was presented previously, yet they could not use this knowledge to update their behavior. In contrast, primates with hippocampal damage perform randomly on this task, alternating their responses between correct and incorrect food wells (Diamond & Goldman-Rakic 1989). This indicates an anatomical dissociation between the short-term retention of spatial-reward contingencies and the ability to use this knowledge to guide behavior (working memory), with the former involving medial temporal lobe regions and the latter involving the PFC. PFC lesions produce a deficit on delayed tasks because animals or humans are unable to use mnemonic information to guide action.

According to Petrides (1994, 1995, 1996) the PFC may act alone or in concert with other brain regions to guide working memory under different conditions. He has suggested that ventrolateral regions of the PFC are involved in the active organization of behavior based on the retrieval of information from posterior association corticies while dorsolateral regions are involved in holding information for monitoring and manipulation in accordance with willed actions. Based on this hypothesis, information may be retained within the PFC or in other brain regions but the critical function of the dorsolateral PFC relates to the ability to manipulate and use information to guide thought or action, i.e. working memory. I argue that a complete understanding of working memory will require a detailed understanding of the PFC at a basic level. Therefore the next section reviews the basic anatomy and physiology of the PFC.

Functional Anatomy of the PFC

Brodmann initially defined the PFC as the region rostral to motor and premotor areas which possessed a granular layer IV. More recently, the PFC has been defined as the prominent cortical projection area of the medial dorsal (MD) nucleus of the thalamus (Rose & Woolsey 1948; Uylings & van Eden 1990; Nauta 1961; Groenewegen et al. 1990). The MD projects to the dosrolateral, ventrolateral and ventromedial PFC and the medial and lateral PFC (Uylings & van Eden 1990) (Fig 1-1A).

In the rat the medial PFC is divided into several subregions, with the most dorsal region being the anterior cingulate, the middle region being the prelimbic (PL) and the most ventral region, the infralimbic cortex (Fig 1-1A). According to Uylings and Van Eden (1990) the PL region of the rat is equivalent to area 32 (Broadmann), or ventral medial PFC in the primate cortex. The rat lacks the anatomical equivalent of the dorsolateral PFC (area 46) in the primate. However, the PFC is thought to have evolved from both an archicortical and paleocortical moiety (Pandya & Yeterian 1990). From the archicortical moiety arose proisocortical areas 24 (anterior cingulate), 25 (infralimbic) and 32 (prelimbic) which gave rise to dorsomedial and dorsolateral PFC regions in the primate (Panya & Yeterian 1990). Thus the PL, may be viewed as a primitive version of the dorsolateral region of the primate PFC, that is also anatomically related to the primate ventral medial PFC (Kolb 1984). Unless stated otherwise, the primate or

Figure 1-1: Location and relative size of a layer V PFC neuron. **A)** Brain slices were taken from the PFC at the location illustrated by the parallel lines. **B)** Coronal slice at the point illustrated in A. Layer V neurons were recorded from the prelimbic (PL) region of the PFC that is flanked dorsally by the anterior cingulate (AC) region, ventrally by the infralimbic (IL) region, and laterally by the corpus callosum (CC). Images taken from the computer atlas of Paxinos & Watson (1997). **C)** Layer V PFC neuron (left) relative to a layer V somatosensory cortex neuron (right). The image of the somatosensory cortex neuron was taken from Cauller & Connors (1992).

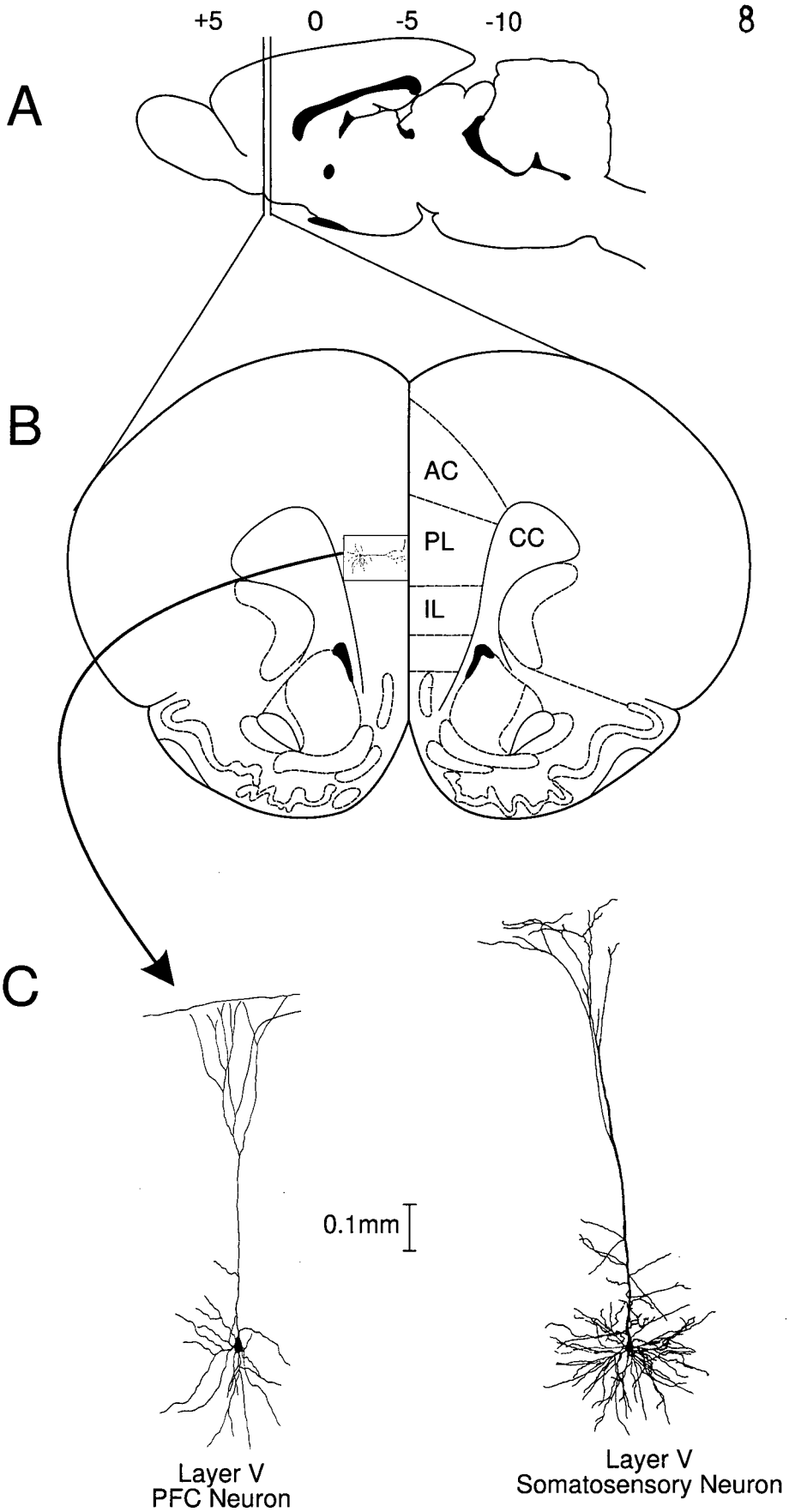
+5
0
-5
-10
A
B
AC
PL
CC
IL
C
0.1mm
Layer V
PFC Neuron
Layer V
Somatosensory Neuron

human dorsolateral PFC and the rat medial PFC will henceforth be referred to simply as the PFC.

The subiculum and overlying temporal corticies send projections to both the rat and primate PFC (Jay & Whitter 1989; Uylings & van Eden 1990; Conde et al. 1990). Likewise, the parietal cortex in the primate and the somatosensory cortex in the rat also project to the PFC (Goldman-Rakic 1988; Mitchell & Cauller 1997; Conde et al. 1990). Moreover, the PFC of both species also projects to the striatum (Sesack et al. 1989; Uylings & van Eden 1990; Groenewegen et al. 1990). The PFC is therefore situated to receive inputs from regions involved in the encoding and storage of spatial and object-related information (i.e. parietal and temporal corticies), while projecting to regions involved in response initiation (i.e. basal ganglia). Such an anatomical profile is required for a structure involved in using internal representations to guide action (i.e. working memory).

Cellular Analyses of Working Memory

The delayed response task has been used extensively to investigate the cellular bases of working memory processes (see Goldman-Rakic 1987, 1990, 1995 for review). In the original delayed response task monkeys observed an experimenter bait one of two covered food wells. An opaque screen was then lowered to block the monkey's view of the covered food wells. After a delay, the screen was raised and the monkey must chose the previously baited well to obtain the reward. More recently an oculomotor delayed response task has been used to asses working memory. In this task a monkey is placed in front of a video

screen and must initially fixate on a center dot of light. During the *cue* phase a light is flashed in one of 8 spatial locations on the screen which are equidistant from the center fixation light. The fixation and cue light are then extinguished for a few seconds in the *delay* period. During the *response* phase which follows the delay, the monkey is required to perform a saccade to the spatial location on the screen where the light was flashed. Since the cue light was extinguished the saccade must be directed based on mnemonic information. In rats a similar task was used in the two published studies analyzing unit activity in the medial PFC during delayed responding (Bateuv et al. 1990; Orlov et al. 1988). In these tasks a light was flashed above a food well to the right or left of the rat. After a delay of 5sec, the rat was allowed to visit the previously lighted food well. Bateuv et al. (1990) and Orlov et al. (1988) found that approximately 54% of PFC neurons responded preferentially during the delay while the firing of 85% was correlated with the response.

The contribution of neurons in the primate PFC to working memory processes have been studied much more extensively. Neurons in the primate PFC increase in activity during the cue, delay and response phases of the original (Fuster 1973) and oculomotor delayed response task (Funahashi et al. 1989). Most attention has been paid to the delay-active neurons in the PFC. The activity of these neurons may underlie the ability to retain information transiently (Goldman-Rakic 1989;1995). There are a number of findings which suggest that the activity of these neurons represents an active neural trace of previously encountered external stimuli. First, delay-period activity is not observed on 'mock'

trials, when the monkey does not observe a food well being baited (Fuster 1984; 1991), Second, delay-active neurons have 'memory fields' in that individual neurons fire during the delay period of the task, only if a cue was presented previously in a specific spatial location (Funahashi et al. 1989; Goldman-Rakic 1990). Third, if the activity of these neurons decreases throughout the delay, the animal is highly likely to make an error (Niki & Watanabe 1976; Funahashi & Kubota 1994; Funahashi et al. 1989). Fourth, these neurons show sustained firing during the delay even if the animal is required to make a response in the opposite location from the initial cue, indicating that the activity is related to the memory of the previously presented stimuli and not the mechanics of the response itself (Funahashi et al. 1993). Finally, activity during the delay increases or decreases uniformly as the delay interval increases or decreases (Kojima & Goldman 1982).

Delay-active neurons are also found in other areas of the brain such as the parietal, inferotemporal cortex and hippocampus (Fuster 1990; Koch & Fuster 1989; Watanabe & Niki 1985), suggesting that copies of recently-presented task-relevant stimuli are distributed. This may explain why PFC lesions alone do not impair short-term memory. However these brain areas interact during the performance of delayed tasks since PFC cooling disrupts delay-period activity in the inferotemporal cortex (Fuster et al. 1985) while cooling of the parietal cortex or inferotemporal cortex disrupt task related activity in PFC neurons (Fuster et al. 1985; Quintana et al. 1989).

Miller & Desimone (1994) and Miller et al. (1996) have pointed out key differences between activity in PFC and inferotemporal or parietal neurons. According to these authors, the activity of PFC neurons is less stimulus dependent but exhibits greater 'match-non-match' effects on delayed matching and nonmatching to sample tasks. This suggests that PFC neurons are more involved in the manipulation of information in memory. In addition, only PFC neurons exhibit progressives increases in activity during the delay period. The progressive increase in activity of PFC neurons during the delay has been termed "climbing activity" and is related to the probability of a correct forthcoming response (Quintana & Fuster 1992). The climbing activity in the PFC may be related to the prospective memory of the upcoming response (Quintana & Fuster 1992). Response-correlated activity in PFC neurons is also observed on simple non-delayed tasks without a memory component, such as Go/No Go tasks (Watanabe 1986a,b). Furthermore, on more complex conditional tasks, the activity of motor-set units can precede that of delay-active neurons in well trained animals. In such tasks the color of a cue light instructs experienced monkeys where to direct their response following a delay. The activity of motor set neurons often begins to increase as soon as the light cue is presented, presumably because information about the direction of a forthcoming response is given completely by the color of the cue light (Fuster 1991). Thus, on both working memory tasks and conditional memory tasks the discharge of the motor-set units in the PFC may predict the direction of the impending motor response. Fuster (1989; 1991; 1995) has proposed that mnemonic information encoded by delay-

active cells may be communicated to response-active PFC neurons to ensure a forthcoming response is directed to the correct location.

Deep Layer PFC Neurons and Working Memory

Delay and response-active pyramidal neurons are often in very close proximity to each other in the cortex (Fuster et al. 1982). Typically these neurons are found in deep layers III or V-VI of the PFC (Sakai & Hamada 1981; Suzuki & Azuma 1977; Fuster 1973). Layer III-V neurons have a number of characteristics that may make them well suited for PFC-dependent working memory processes.

Layer III-V PFC neurons have a long ascending apical dendrite which spans from the cell body in layer III-V to the pial surface in layer I. As noted above, the inferotemporal cortex, parietal cortex and possibly hippocampus affect task-related activity in PFC neurons. Inputs from the parietal/somatosensory cortex synapse in superficial layers I-II, while hippocampal afferents synapse in layers II-V (Mitchell & Cauller 1997; Goldman-Rakic 1988; Conde et al. 1991). Deep layer PFC neurons are therefore situated to receive sensory information about the task at hand.

Layer III-V neurons possess horizontally projecting axons which connect nearby neurons (Kritzer & Goldman-Rakic 1995). Dual cell recordings from deep layer cortical neurons have indicated that excitatory inputs from a few connected pyramidal neurons may be sufficient to depolarize the post synaptic neuron to spike threshold (Thomson & Deuchars 1997; Markram 1997; Markram et al. 1997). The activity of nearby PFC neurons synchronizes within a fraction of a

second during the delay period of a delayed response task (Vaadia et al. 1995). Connected PFC neurons may form functional cell-assemblies which mutually excite each to maintain firing throughout the delay period, in order to maintain an active trace of recently acquired information (Goldman-Rakic 1995a,b; 1996)

In general, deep layer neurons in the cortex are the projection neurons and send axons out of the cortical region. With regards to the PFC, deep layer neurons project to regions involved in response initiation such as the striatum (Sesack et al. 1989; Gorelova & Yang 1996). It has been hypothesized that plans generated in the PFC may be translated into action via interactions with the striatum (Robbins 1991; Mogenson et al. 1993). Collectively these properties make deep layer PFC neurons well suited to receive sensory information, maintain an active representation of this information through recurrently active cell assemblies, and use this information to generate a response via the striatum.

In addition to the striatum, delay-active neurons are functionally connected to neurons in the parietal cortex and inferotemporal cortex (Goldman-Rakic 1988; Fuster et al. 1985; Quintana et al. 1989; Goldman-Rakic & Chaffe et al. 1994). It has been hypothesized that afferents from the PFC tune the delay-activity in the inferotemporal cortex such that the activity of inferotemporal neurons is more tightly tuned to stimuli of behavioral significance (Miller et al. 1996). Indeed the PFC may play a particularly important role in signaling behavioral significance.

Cellular Working Memory and Behavioral Significance.

Considerable evidence suggests that task-related activity of PFC neurons is associated with the behavioral significance of the stimuli. Although PFC

neurons respond to visual cues not associated with reward, such activity is significantly enhanced if stimuli are of particular behavioral significance (Bruce 1988). In contrast, cells in other cortical association areas typically code only for specific stimuli, regardless of their significance (Miller et al. 1996). PFC neurons may respond similarly to different stimuli with the same behavioral significance while responding differently to identical stimuli of varying behavioral significance (Watanabe 1981;1986; 1990; 1996).

In non-delayed tasks, some PFC neurons respond simply to the presentation of a primary reward, and this activity is abolished if the rewarding value of the stimuli is decreased by adding quinine to the food (Inoue et al. 1985). Likewise, on delayed response tasks, the delay-period activity of PFC neurons is dependent strongly on the nature of the reward, as cues associated with palatable reward produce significantly greater activity in delay-active PFC neurons (Watanabe 1996). Moreover, activity of delay-active neurons was more vigorous if food itself served as a cue relative to a stimulus previously paired with food. Furthermore, Yajeya et al (1988) showed that PFC neurons fired more vigorously to stimuli predictive of reward relative to equivalent stimuli which were irrelevant to the monkey.

Watanabe (1990) investigated the effect of associative significance on PFC unit activity using a novel associative learning task which varied the significance of stimuli, while keeping the mnemonic and response demands constant. On such tasks the animal must release a lever to begin a trial, however, reward is delivered only on trials where a discriminative cue had been

presented several seconds earlier. As in the delayed response task, subsets of PFC units were active during the cue, delay and response phases of the task. However, a majority of these task-related neurons showed increased activity only on trials where the discriminative cue was presented, regardless of its physical attributes. Collectively, these data indicate that that the rewarding value of stimuli and expectancy of reward is coded by PFC neurons during performance of working memory tasks.

Role of Dopamine in Determining Behavioral Significance

Reward related information in the brain may be coded specifically by the activity of midbrain dopamine neurons (Shultz 1992; Shultz et al. 1997). Accumulating evidence indicates that dopamine neurons in the ventral tegmental area (VTA) respond selectively to stimuli of behavioral significance. DA neurons respond in short phasic bursts to appetitive or novel stimuli (Romo & Shultz 1990). However, the response of DA neurons to the same stimuli changes as the salience of the stimulus changes. For example, novel stimuli which evoke a vigorous response initially do not activate DA neurons when the animal is familiar with the stimuli. DA neurons also change their response to stimuli paired with reward (Romo & Schultz 1990; Ljungberg et al. 1992). Initially DA neurons respond immediately after the receipt of reward. With repeated pairings of the conditioned stimulus (CS) and the primary reward (unconditioned stimulus, US) , the phasic activation of DA neurons neurons shifts from the time of delivery of reward to the time of CS onset. Following this shift, DA neurons no longer

respond to the primary reward. The shift in the activity of DA neurons is related to the shift in the monkeys' appetitive behavioral reaction from the US to the CS (Schultz et al. 1997). DA neurons therefore code for both the *a priori* and learned significance of stimuli.

Although the activity of both DA neurons and PFC neurons is related to the significance of stimuli, there are notable differences in their activation characteristics. First, DA neurons in the VTA tend to respond homogeneously to a given stimulus (Shultz 1991). In contrast, the activity of PFC neurons exhibits considerable heterogeneity as the response of individual neurons varies depending on the attributes of the object, its location and when it is presented in time. Second, the response of DA neurons to the same stimulus can be very different depending on its significance in a given context. The response of PFC neurons is less dependent on the ascribed significance of the stimulus. The significance only serves to modify the responses of PFC neurons to other task-related variables. Given these properties, DA neurons appear to code specifically for the behavioral significance of a stimulus, while the activity of PFC neurons is only modified by behavioral significance. Schultz (1991) has postulated that behavioral significance of a stimulus may be signaled to the PFC via the release of DA from the terminals of VTA neurons. He suggested that DA released in the PFC may focus the activity of PFC neurons such that this activity is restricted to the processing of the most prominent or behaviorally significant inputs.

Anatomy of DA Innervation of the PFC

Anatomical data are consistent with the proposed DA dependent modulation of PFC activity. In the primate, DA neurons in the VTA send axons to the PFC which terminate on the dendrites of deep layer pyramidal neurons (Smiley & Goldman-Rakic 1993; Goldman-Rakic et al. 1989). In the rat, there is a sparse band of DA inputs to layers II-III of the anterior cingulate region (Berger et al. 1991). Layers II-II is where inputs from the hippocampus, parahippocampal/ entorhinal and parietal/somatosensory corticies converge (Conde et al. 1995; van Eden et al. 1992; Goldman-Rakic 1988). However, layer V of the PL is the region of greatest overlap between hippocampal and DA afferents (Carr & Sesack 1996; van Eden et al. 1987; Jay & Witter 1991; Descarries et al. 1987). While hippocampal and DA terminals do not converge onto a common post-synaptic target, these terminals are often found in apposition to one another on layer V PFC neurons (Carr & Sesack 1996). In addition, on the dendrites of PFC neurons, DA terminals converge with axon collaterals from neighboring neurons. Given this anatomical arrangement it is likely that DA could modulate hippocampal afferents, or local connections within the PFC (see below).

D1 and D2 receptors are found on both pyramidal and non-pyramidal neurons in the PFC (Vincent et al. 1996). However the PFC contains a greater number of D1 receptors relative to D2 (Gasper et al., 1995; Farde et al., 1987). D1 receptors are located primarily on the dendritic spines and shafts of pyramidal neurons in the PFC (Bergson et al. 1995). D1 receptors are also found on the dendrites and axon terminals of parvalbumin-containing fast spiking neurons in

the PFC (Muly et al. 1997). DA may therefore exert both direct and indirect effects on the excitability of PFC neurons via the D1 receptor. D1 receptor activation could therefore influence the activity of PFC neurons related to working memory.

DA Modulation of Working Memory Processes Mediated by the PFC

Dopamine (DA) strongly modulates both working memory performance and the activity of task-dependent neuronal activity within the PFC. 6-OHDA lesions or microinjection of DA D1 receptor antagonist into the PFC disrupts performance on delayed-response tasks (Sawaguchi et al. 1990b; 1994; Brozoski et al. 1979). Paradoxically, pharmacologically-induced high rates of DA turnover in the PFC also produce deficits in delayed-tasks (Murphy et al. 1996). Similarily, iontophoresis of either DA *or* a D1 antagonist at low ejection currents enhance delay period activity, relative to 'background' activity, on a delayed response task (Williams et al. 1995; Sawaguchi 1987; Sawaguchi & Matsumura 1985; Sawaguchi et al. 1986; 1990). Thus the action of DA in the PFC is highly complex and both increases and decreases in DA activity can enhance or attenuate performance on working memory tasks and task-related neural activity. The neuronal mechanisms underlying the complex actions of DA in the PFC are presently unknown.

Another puzzling aspect of the DA dependent modulation of delayed responding is that DA neurons in the VTA do not show sustained activity throughout the delay period of a delayed response task (Shultz & Romo 1990;

Ljungberg et al 1991). In order to reconcile these data it has been argued that during delayed responding, DA release may be modulated at the terminal level in the PFC (Shultz 1990). Alternatively, DA released at the outset of the task may modulate the activity of PFC neurons for prolonged periods via second messenger signaling pathways coupled to the D1 receptor. However, since the activity of DA cell bodies in the VTA may not be relevant to performance of working memory tasks, it raises the possibility that the modulation of PFC activity by DA could be assessed adequately in a brain slice preparation in which VTA axons have been severed.

Action of DA on PFC Neurons

The actions of DA on pyramidal cells in the PFC have been studied predominately using extracellular recording techniques on anaesthetized rats *in vivo*. Most studies have shown that DA exerts an inhibitory effect on pyramidal cell excitability (Pirot et al. 1992; Mantz et al. 1982; Sesack & Bunney 1989; Ferron et al. 1984; Godbout et al. 1991; Bunney & Aghajanian 1976; Mora et al. 1976). However, in a critical experiment, Pirot et al. (1992) showed that this inhibitory effect was abolished if the $GABA_A$ antagonist bicuculline was iontophoresed prior to DA suggesting that the inhibitory action of DA was an indirect effect on GABAergic interneurons. This finding is consistent with that of Penit-Soria et al. (1987) who reported that DA substantially increased spontaneous IPSPs in PFC pyramidal neurons. Thus DA may suppress the activity of PFC pyramidal neurons via interneurons.

In contrast, DA appears to enhance the effects of excitatory stimuli directly onto PFC pyramidal neurons. DA has been shown to enhance the excitatory responses of PFC neurons to subthreshold doses of NMDA or acetylcholine (Cépeda et al., 1992; Yang and Mogenson,1990). Likewise, although VTA stimulation reduced the activity of PFC neurons evoked by hippocampal stimulation (Jay et al. 1995), iontophoresis of DA had the opposite effect, enhancing the activity PFC neurons evoked by hippocampal stimulation and long-term potentiation in the hippocampal PFC pathway (Jay et al. 1996). The reasons for these differences are not presently clear.

When viewed collectively, the studies to date indicate that DA has multiple, often contradictory effects on the activity of PFC pyramidal neurons. There is no internally consistent theory that explains these data, due in part to a lack of knowledge regarding the specific cellular actions on PFC neurons.

Cortical Pyramidal Neurons

It should be clear from the preceding paragraphs that an understanding of deep layer PFC neurons and their modulation by DA is central to our understanding of working memory processes mediated by the PFC. The physiological properties of PFC pyramidal neurons are not known since they have not been studied systematically. Furthermore, until recently, most studies have investigated the properties of cortical neurons via recordings from the soma. Classically, *in vitro* somatic recording studies of layer V pyramidal neurons have focused on neurons from the somatosensory cortex, beginning with the

seminal paper of Connors et al. (1982). For comparison, the morphology of a typical layer V PFC and somatosensory cortex pyramidal neuron are shown in Fig 1-1B. As shown in Fig 1-1B, deep layer cortical neurons possess a long ascending apical dendrite that spans all cortical layers. Although PFC neurons are smaller that somatosensory neurons there is still a considerable distance from the soma to the distal branches of the apical tuft. As a result, somatic recordings may be unable to probe dendritic function adequately (Spruston et al. 1993; 1994). The behavior of the dendritic region of cortical pyramidal neurons has been examined only recently via whole-cell patch-clamp recordings from the dendrites of somatosensory neurons (Kim & Connors 1993; Stuart & Sakmann 1994). The present thesis will examine the properties of deep layer PFC neurons from the soma and apical dendrites.

Theorists have speculated that the dendrites of pyramidal neurons may process synaptic signals in a computationally rich manner (see Mel 1994 for review). On one hand, the passive cable properties of pyramidal neurons may act as low pass filters to reduce EPSPs en route to the soma. EPSPs may be further reduced by dendritic outward K^+ currents (Hoffman et al. 1997). On the other hand, recent Na^+ and Ca^{2+}-imaging data and single channel analyses have revealed that the apical dendrites of hippocampal and somatosensory cortical pyramidal neurons are endowed with a variety of voltage-gated inward currents (Yuste et al. 1994; Jaffe et al. 1992; Magee & Johnston 1995a,b). It is widely believed that these currents aid in signal transduction from the distal apical dendrites to the soma by acting as voltage or current amplifiers (Bernander et al.

1994; Rhodes 1997; Johnston et al. 1996). The functional interactions of these inward and outward currents to signal integration in cortical neurons is still poorly understood. Moreover, the properties of the dendrites of PFC neurons have never been studied, even though the dendrites are where inputs from other cortical regions, neighboring neurons and DA axons converge. Thus an understanding of the physiological properties of the soma and dendrites of PFC neurons is central to a complete understanding of the function of the PFC.

Overview and Objectives

The PFC is involved in working memory processes that appear to be mediated by the activity of subgroups of deep layer neurons. DA modulates working memory processes in the PFC and the activity of deep layer PFC neurons. The exact contribution of DA to working memory processes mediated by the PFC is not entirely clear although it may be related to behavioral significance. There is also a considerable lack of knowledge regarding the physiological properties of deep layer PFC neurons in general and how these neurons respond to DA. Therefore, the objectives of the present thesis are as follows:

1. To determine the specific role of the PFC in working memory processes. To this end, behavioral procedures were developed to separate short-term memory processes from working memory processes. As noted above, the use of traditional delayed response tasks with a few second delay period, has resulted in confusion regarding the role of the PFC in short-term memory versus working

memory. In the behavioral experiments of the present thesis a long delay-response task was used in combination with transient inactivations of the PFC by lidocaine. On this task with a 30 min. delay, the PFC could be inactivated prior to the acquisition, during the retention or prior to the use of trial-unique information. This approach could therefore be used to segregate aspects of working memory which would not be possible using traditional delayed response tasks, and thereby determine whether the PFC was involved specifically in the acquisition, retention or retrieval/use of recently acquired information. Based on the arguments presented above, it is hypothesized that the PFC may have a selective role in the retrieval/use of mnemonic information rather than its acquisition or long-term storage.

2. To determine the functional role of DA to working memory processes mediated by the PFC as assessed by the long delay, delayed response task. It is hypothesized that D1 but not D2 receptor blockade will selectively disrupt the use of mnemonic information to direct prospective responding towards behaviorally relevant locations in the environment.

3. To determine the physiological properties of deep layer PFC neurons. To obtain sufficient insight into how these neurons translate synaptic inputs into spike train output it is important to explore the passive and active membrane properties of PFC neurons at the soma and the apical dendrites. It is also necessary to examine the responses of PFC neurons to synaptic inputs to the apical dendrites. It is expected that the soma and apical dendrites posses very

different electrophysiological properties that will provide important insights into how PFC neurons process synaptic signals to different regions of the neuron.

4. To determine how the physiological properties of PFC neurons are modulated by DA. DA terminals are located predominately in the deep layers of the rat PFC (see above), therefore the main focus will be on how DA modulates ionic currents located near the soma, and on how DA modulates synaptic inputs *enroute* to the soma. It is hoped that the present experiments will provide a mechanistic explanation of the important yet confusing effects of DA on delay and response-related activity of PFC neurons on working memory tasks.

The experimental data in this thesis will be presented in the following five chapters. Each chapter will have a short introduction, which will provide the rationale for each experiment. In each chapter there will also be a discussion section which deals with specific aspects of the data presented in each chapter. The final General Discussion will not deal with specific aspects of the data but will attempt to integrate findings from each Chapter into a global picture of PFC function and its modulation by DA.

TABLE 1: List of Abbreviations

AC	Anterior Cingulate
AHP	After Hyperpolarization
DA	Dopamine
DAP	Depolarizing Afterpolarization
FS	Fast Spiking
I_A	Transient A-type K^+ current
IB	Intrinsic Bursting
I_D	Slowly-Inactivating K^+ current
I_h	Hyperpolaration-activated mixed cationic current
IL	Infralimbic
I_{NAP}	Persistent or Slowly-Inactivating Na^+ current
LS	Low threshold Spiking
LT	Late Spiking
LTS	Low Threshold Ca^{2+} Spike
mPFC	Medial Prefrontal Cortex
PFC	Prefrontal Cortex
PL	Prelimbic
RF	Random Foraging
R_{in}	Input Resistance
R_m	Membrane Resistance
ROB	Rythmic Oscillatory Bursting
RS	Regular Spiking
SWSh	Spatial Win Shift
V_m	Membrane Voltage
vSub	Ventral Subiculum
VTA	Ventral Tegmental Area

Chapter 2:

The Role of the PFC in Working Memory : Modulation by DA

Introduction

Chapter 2 will be divided into two sections. Section 1 will examine behavioral functions mediated by the rat medial prefrontal cortex while section 2 will examine how these functions are affected by local manipulation of dopamine activity.

Working memory, as defined by Baddeley involves the temporary storage and retrieval of information from short-term memory buffers, via the attention function of a central executive system (Baddeley, 1986). According to this view, information retained for a short period of time is used by the central executive to guide behavior. There is abundant evidence for a role of the PFC in working memory (see General Introduction) whereby mnemonic information is used to guide behavior. Aside from the well known delay-period active 'memory' neurons in the PFC (Goldman-Rakic 1995a,b), other PFC neurons are relatively inactive at the start of the delay period but increase in activation as the delay progresses, until a correct response is initiated. Fuster (1991,1995) has termed these latter neurons 'anticipatory' units and suggests that these neurons are involved in generating a prospective memory for the upcoming response. According to Fuster it is the interaction between the short-term memory and preparatory motor set functions of the PFC that allows primates to respond to information from different sources that is related in context but separated temporally.

There is evidence that the human PFC may subserve a similar function as patients with PFC lesions cannot use past responses to order ongoing behavior (Milner & Petrides, 1984). In the rat, lesions of the PFC cause deficits in various radial arm maze tasks used to evaluate memory for the temporal ordering of a series of spatial events (Kesner & Holbrook, 1987) and the ability to make assessments of recency (Kesner, 1989).

A complimentary role for the PFC emphasizes flexibility in the use of recently acquired information. Performance on delayed alternation (van Haaren et al. 1988; Wikmark et al. 1973), delayed non-matching to position (Rogers et al. 1992), delayed non-matching to sample, reversal learning (Doar et al. 1987; Wolf et al. 1987) and go/no go alternation (Sakuria & Sugimoto, 1985) tasks are disrupted by PFC lesions in rats. Likewise, humans with PFC damage are impaired on the Wisconsin Card Sort task (Milner, 1963) and are slow to shift their sorting strategy on the basis of newly acquired information. Furthermore, primates with PFC lesions show the "A-B error pattern" on the A not B task, and continue to respond to a previously rewarded spatial location despite receiving information that the location of reward has changed (Diamond & Goldman-Rakic, 1989). These learning tasks all require the integration of information from specific stimuli with the demands of the task at hand. As such, the deficits are consistent with Shallice's (1982) observation that "non routine" tasks, which require constant monitoring of new information in order to plan appropriate responses, are particularly susceptible to prefrontal damage.

A clear segregation of the role of the PFC in the short-term retention of information versus flexible use of mnemonic information has not been demonstrated. The delayed response tasks have proven useful in elucidating a role for the PFC in the short-term active retention of information, however, because such tasks utilize a very brief delay interval (i.e. <6s) it is difficult to separate mnemonic processes from processes involved in response organization and generation. For instance is activity of PFC neurons throughout the delay interval completely linked to retention of information, or does this activity represent processes underlying the ability to use this information to guide a response? During the delay period, delay active neurons show discrete changes in their activity level which has been hypothesized to represent changes in underlying mental processes (Vaadia et al. 1996).

The present study sought to determine the role of the PFC using previously acquired information to guide responding as separate from the short-term retention of this information. To this end two variants of Olton's (Olton & Papas, 1979) radial arm maze tasks were employed. The first has been termed the delayed spatial win-shift task (Packard et al., 1989; Packard et al. 1990) or simply the delayed task. This task consists of a training phase and a test phase, separated by a delay. On the training phase, the rat is required to locate food on 4 of 8 arms of a spatially-cued radial arm maze while the remaining 4 arms are blocked. Following a 30min delay, during the test phase, all arms are unblocked and the rat must approach the 4 previously baited arms while avoiding the 4 arms which contained food during the training phase. The second task is identical

to the test phase of the delayed task, but omits the preceding training phase. In this single phase task, the rat is required to obtain food from 4 randomly chosen arms while avoiding arms which it has already visited. To examine the contribution of the rat medial PFC to the acquisition and retention versus retrieval and use of information, reversible lidocaine-induced inactivations of the main subdivision of the rat medial PFC, the prelimbic region (PL) will be delivered prior to the training phase or test phase of the delayed task or prior to the non-delayed task (see Fig 2-1).

The relatively short-lived anesthetic action of lidocaine (~15min) microinjections immediately prior to the training phase of the delayed task will inactivate the PL for the entire training phase and part of the delay period. If the PL is involved solely in the acquisition or retention of information then deficits on test phase performance would be expected following inactivations of the PL prior to the training phase. In contrast, if the PL is involved in the ability to use previously acquired information to guide a response, deficits on test phase performance would be expected following inactivations of the PL prior to the test phase of the delayed task. Inactivations of the PL prior to the non-delayed responding task serve as a useful control for possible effects of PL lesions on motivational or motoric processes and spatial navigation or response flexibility.

A The Delayed Radial Maze Task

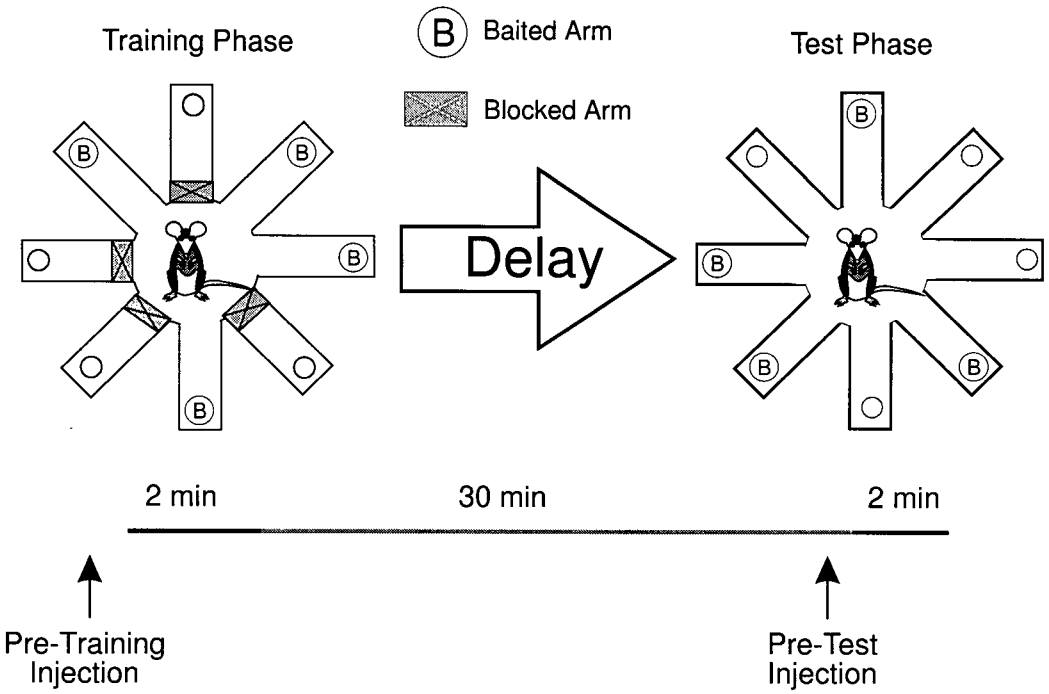

B The Non-Delayed Task

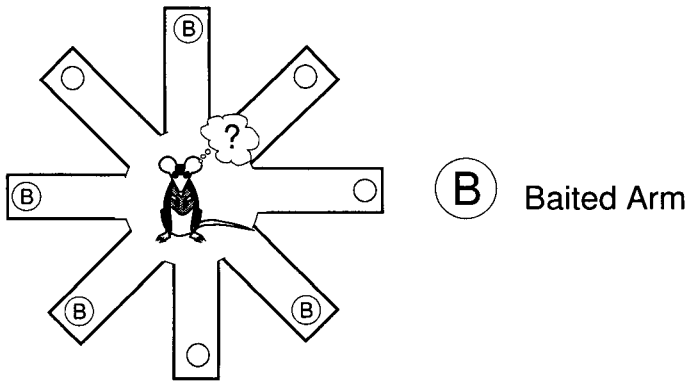

Figure 2-1: Schematic representation of the radial-arm maze tasks used in Section 1. A) The delayed task consisted of a training and test phase separated by a 30 min delay. In the training phase 4 of 8 randomly chosen arms were open and baited. After the delay, the previously blocked arms were baited. Intracerebral injections were delivered prior to the training phase or prior to the test phase. B) The non-delayed task was identical to the test phase of the delayed task except there was no prior training phase. 4 of 8 arms were chosen randomly each day and baited. In the absence of a prior training phase, information was not available regarding the expected location of food on the maze. Intracerebral injections were delivered prior to placing the rats on the maze.

METHODS

1. Subjects

The subjects were male Long Evans rats weighing between 300-450 g prior to surgery. All rats were given free access to water and were maintained at 85% of their free-feeding weight by providing 25-30 g of Purina lab chow pellets once daily. Rats were tested 5 to 7 days a week.

2. Surgery

Rats were anesthetized with 100 mg/kg of ketamine hydrochloride and 7 mg/kg xylazine. Twenty three gauge stainless-steel guide cannulae were implanted into the brain regions using standard stereotaxic techniques. The stereotaxic coordinates (flat skull) were derived from Paxinos and Watson (1986). Cannulae were implanted bilaterally into prelimbic (PL) region of the medial PFC (AP = +2.6 mm, ML =± 0.7 mm from bregma, and DV = -3.0 mm from dura) alone, or in combination with bilateral cannulae implanted into the ventral subicullum region of the hippocampus (AP = -6.0 mm from bregma, ML = +/- 5.5 mm from midline, and DV = -5.3 +/- 0.3 mm from dura). This region of the hippocampus was chosen because it sends dense projections to the PL region of the PFC in the rat (Jay et al. 1991; Condé et al. 1995). Thirty gauge obdurators flush with the end of the guide cannulae remained in place until the injections were made. Each rat was given at least 7 days to recover from surgery prior to testing.

3. Micro-infusion Procedure

On injection days, the obdurators were removed and 30 gauge stainless-steel injection cannulae were inserted 0.8 mm beyond the tip of the guide cannulae. In Experiment 1, lidocaine (20 μg in 0.5 μl of saline, Astra Pharmaceuticals and Research Biochemicals Inc.) was delivered bilaterally into the PL. In Experiment 2, the D1 antagonist SCH-23390 (0.05, 0.5, 5 μg in 0.5μl dissolved in physiological saline), the D2 antagonist Sulpiride (0.05, 0.5, 5 μg in 0.5μl dissolved with a drop of NaOH in phosphate buffered saline) (Research Biochemicals Inc.) or vehicle injections were delivered into the PL at a rate of 0.5 μl /1.2 min by a microsyringe pump (Sage Instruments Model 341). In Experiment 3, SCH-23390 or vehicle injections were made unilaterally into the PFC, while lidocaine (20 μg in 0.5 μl of saline) was delivered to the contralateral ventral subiculum. Injection cannulae were left in place for an additional 1 min following each injection to allow for diffusion. All SCH-23390, Sulipiride and corresponding vehicle injections were made 15-20 min. prior to testing to ensure an optimal blockade of DA receptors (Sawaguchi & Goldman-Rakic 1994). Lidocaine and corresponding vehicle injections were made 3min. prior to testing. Efforts were made to keep those conducting behavioral testing blind to the experimental condition.

4. Apparatus

An eight-arm radial maze was used for all experiments. The maze had an octagonal center platform 40 cm in diameter connected to eight, equally spaced arms, each measuring 50 cm x 9 cm, with a cylindrical food cup at the end. Removable pieces of white opaque plastic (9 cm x 13 cm) were used to block the arms of the maze. The maze was elevated 40 cm from the floor and was surrounded by numerous extra maze cues (i.e., cupboards, posters, doors, the experimenter etc.), in a room 4 m x 5 m x 3 m, which was illuminated with overhead fluorescent lights (100 W).

5. Foraging Tasks

The two foraging tasks used in the present study were the delayed spatial win-shift (SWSh) and the non-delayed random foraging (RF) tasks.

The delayed SWSh task. This task was adapted from Packard et al., (1990) and has been described in detail elsewhere (Seamans and Phillips, 1994; Seamans et al., 1995). On the first two days of testing, rats were habituated to the maze environment. Subsequent training trials were given once daily. These trials consisted of a training phase and a test phase, separated by a delay. Prior to the training phase, a set of four arms was chosen randomly and blocked. Food pellets (Bioserv™, Frenchtown, NJ) were placed in the food cups of the four remaining open arms. During the training phase, each rat was given 5 min to retrieve the pellets from the four open arms, and then was returned to its home

cage for the delay period (see below). During the test phase of each daily trial, all arms were open, but only the arms that were previously blocked contained food. Rats were allowed a maximum of 5 min to retrieve the four pellets during the test phase.

The initial delay between training and test phases was 5 min. After achieving criterion performance in which all four pellets were retrieved in five or fewer choices during the test phase for two consecutive days, the delay was increased to 30 min. The first intracranial injections were administered after attaining two consecutive days of criterion performance at a 30 min delay. Following the first injection day, animals were again retrained to a criterion performance. The following day, a second intracranial injection was administered. This procedure was repeated until an animal had received all the designated sequence of injections, according to the protocols described below (see Design and Procedure).

On injection days the number and order of arm entries were recorded. An arm entry was recorded when a rat moved down the entire length of an arm and reached the food cup at the end of the arm. Errors were scored as entries into non-baited arms, and further broken down into two error subtypes. An *across-phase* error was defined as any initial entry to an arm that had been entered previously during the training phase. A *within-phase* error was any re-entry into an arm that had been entered earlier during the test phase. The latencies to reach the food cup of the first arm visited and to complete the phase were also recorded.

The non-delayed RF task. This task has also been described elsewhere (Seamans and Phillips, 1994; Seamans et al., 1995). Habituation to the maze during the first two days of training was identical to the delayed SWSh procedure described above. On subsequent daily trials animals were required to forage for pellets placed at random in the food cups of 4 of the 8 arms. A novel set of arms was baited each day. Animals were trained to a criterion of no more than one re-entry error per daily trial for four consecutive days. The day after criterion performance was achieved, the first intracranial injections were administered. Following the first injection day, animals were retrained to criterion for two consecutive days. As with the delayed SWSh task, this procedure was repeated until each animal had received all the designated injections.

Errors were scored as re-entries into arms entered previously within a trial. These errors were broken down further into re-entries into baited arms (arms that had been baited at the start of the trial) and re-entries to non-baited arms (arms that were not baited prior to the start of the trial). The number of re-entries errors made on each of the injection days were recorded and used for data analysis. As with the delayed SWSh paradigm, the latencies to reach the first food cup (either baited or non-baited) after being placed on the maze and the time required to retrieve all four pellets were also recorded.

6. Experimental Design and Procedures

Experiment 1: Bilateral Injections of Lidocaine into the PL: Three separate groups of rats were used in Experiment 1. Groups 1 and 2 were trained on the delayed

SWSh task. The day after criterion performance was attained at a 30 min delay, the first injection of lidocaine or saline was made prior to the Training phase (Group 1) or Test phase (Group 2). Following the first injection, rats were subsequently retrained until they could retrieve 4 pellets in 5 or fewer choices for 2 consecutive days at a 30 min delay. On the following day, rats received the second counterbalanced injection of lidocaine or saline prior to the Training phase (Group 1) or Test phase (Group 2). Rats in Group 3 were trained on the RF task. The day after criterion performance was achieved on this task , the first injection of either lidocaine or saline was delivered into the PL. Following the first injection, animals were again trained to criterion for two consecutive days. The following day, a second injection of lidocaine or saline was delivered to the PL prior to the daily trial in a counterbalanced order.

Experiment 2: Bilateral SCH-23390 or Sulpiride Injections into the PL. A within-subjects design was used for all four conditions of Experiment 2. Four groups of rats with bilateral cannulae implanted into the PL were trained on either the delayed SWSh task or the RF task. Rats in group 1 received bilateral infusions of either SCH-23390 or vehicle into the PL in a counterbalanced order prior to the test phase of the delayed SWSh task. Rats in group 2 received bilateral infusions of either Sulpiride or vehicle into the PL in a counterbalanced order prior to the test phase of the delayed SWSh task. Rats in group 3 received bilateral infusions of either SCH-23390 or vehicle into the PL in a counterbalanced order prior to a daily trial of the non-delayed RF task. Rats in group 4 received bilateral infusions of either Sulpiride or vehicle into the PL in a counterbalanced order prior to a

daily trial of the non-delayed RF task. After the first infusion each subsequent infusion was administered when the rats re-attained criterion performance for two consecutive days. The order of injections was counterbalanced between rats using a quasi-Latin square design.

Experiment 3: Lidocaine Inactivation of the vSub in combination with SCH-23390 injections into the contralateral PL. Experiment 2 utilized a modified version of the transient disconnection procedure. A within-subjects design was used for this experiment. Well-trained rats received a total of four injections, prior to the test phase of the delayed SWSh task. The following combinations of asymmetrical bilateral inactivations were employed: 1) a unilateral inactivation of the vSub in combination with a contralateral injection of SCH-23390 (0.5 μg in 0.5 μl of saline) into the PL; 2) a unilateral inactivation of the vSub in combination with a vehicle injection into the contralateral PL; 3) a unilateral injection of SCH-23390 (0.5 μg in 0.5 μl of saline) into the PL and a vehicle injection into the contralateral vSub; 4) unilateral injection of vehicle into the vSub and contralateral PL. The order of injections was counterbalanced between animals using a quasi-Latin square design. The counterbalancing ensured that a given sequence of injections was not repeated. The hemisphere (left or right) used for the first injection was also counterbalanced, and was alternated for subsequent injections. The injection procedure was repeated until the animal had received all four microinjections.

7. Histology

Upon completion of behavioral testing, the rats were sacrificed in a carbon dioxide chamber. Brains were removed and fixed in a 10% formalin solution. The brains were frozen and sliced in 50 μm sections prior to being mounted and stained with Cresyl Violet. Placements were verified with reference to the neuroanatomical findings of Jay and Witter (1991), Condé et al., (1995), and Paxinos and Watson (1986).

8. Data analysis

The number and type of errors made on the day prior to the first injection sequence and for all injection days for each experiment were analyzed using separate two-way, between/within, mixed design analyses of variance (ANOVA) with the Injection order as a between-subjects factor, and Treatment-day as a within-subjects factor. Main effects of treatment were further analyzed using Tukey's *post hoc* tests for repeated measures. Whenever a significant main effect of treatment was observed, one planned comparison was made, analyzing the number of each type of error made on drug injection days that differed significantly from control injections.

The latency data to reach the first food cup, and the average time per subsequent choice on injection days were analyzed with a one-way repeated measures ANOVA. The average time per subsequent choice was calculated using the formula:

[(Time to complete trial - Time to initiate trial) ÷ Number of choices for trial].

Whenever a significant main effect of treatment was observed in Experiment 2, three, one-way ANOVAs were conducted, assessing the number of errors made on injection days, with the side of the injection as a between-subjects factor. This analysis was conducted to rule out the possibility that unilateral inactivations in one hemisphere would lead to a greater increase in errors than inactivations of the other hemisphere.

Results: Section I

Delayed Task, Pre-Training Injection

The effects of bilateral lidocaine injections delivered prior to the Training or Test phase of the delayed radial arm maze task were examined. There was large variabilities, and no significant differences in the latencies to reach the first food cup during the Training phase, following pre-Training injections of lidocaine ($\bar{x}$=69.4s) versus saline ($\bar{x}$=96.7s) into the PL. Nor was there a significant difference in the average time to make each subsequent arm choice following either treatment (lidocaine $\bar{x}$=34.6s, saline $\bar{x}$=34s). There were no significant effects of the injection order on performance during the Training phase or Test phase of the delayed task. Furthermore, no significant differences in performance following pre-Training lidocaine injections were observed during the Training phase, or Test phase, as compared to the day prior to the first injection or the day of the pre-Training saline injection. The mean number of errors made

during the Test phase by rats on days prior to the first injection, and on saline and lidocaine test days are presented in Fig. 2-2 A.

Delayed Task, Pre-Test Injection

In a separate group of rats, injections of lidocaine into the PL, prior to the Test phase also did not produce a significant change in the latency to reach the food cup of the first arm visited (saline $\bar{x}$=102.3s, lidocaine $\bar{x}$=115.3s) or in the average time to make subsequent arm choices (saline $\bar{x}$=32.4s, lidocaine $\bar{x}$=31.2s). However, rats made significantly more errors on the day of the pre-Test lidocaine injections than on the day of the pre-Test saline injections ($F(1,6)=15.42$, $p<0.001$). Subsequent analysis of the type of errors made following lidocaine injections revealed an equal number of *across-phase* and *within-phase* errors. No significant differences of injection order were found nor was there a significant Order X Treatment interaction effect. Finally the number of errors made by rats on the days prior to the first injections and on the day of the saline injections did not differ significantly. The mean number and types of errors made by rats on days prior to the first injection, and on the days of the saline and lidocaine injections are presented in Fig. 1-1B.

Non-delayed Task

The effects of bilateral injections of lidocaine into the PL were also examined on the non-delayed radial arm maze task in a separate group of rats. A two-way repeated measures ANOVA revealed no significant differences in the latency to reach the first food cup (lidocaine $\bar{x}$=112.3s, saline $\bar{x}$=72.7s) or to

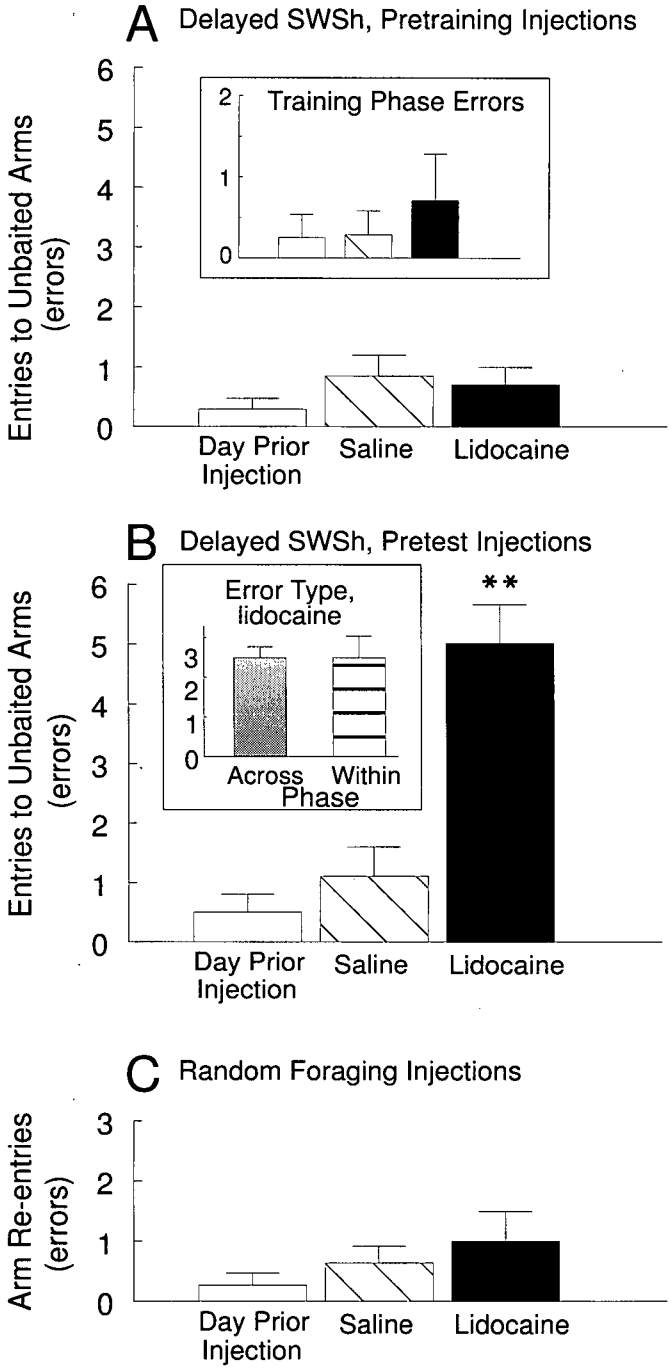

Figure 2-2: The effects of bilateral lidocaine-induced inactivation of the PL on performance of the delayed and non-delayed tasks. In A-C, the number of errors (mean ± SEM) are presented for the day before the first injection (open bar), after bilateral infusions of saline into the PL (hatched bar), and after bilateral infusions of lidocaine into the PL (black bar). A) Bilateral lidocaine-induced inactivation of the PL prior to the training phase did not affect training phase performance (inset) or subsequent test phase performance at a time when the anesthetic effects of lidocaine had dissipated. B) Bilateral lidocaine-induced inactivation of the PL prior to the test phase significantly disrupted test phase performance (** $p<0.01$ versus all other treatment conditions). Inset shows the number of across phase (gray bar) and within-phase (horizontal-stripped bar) errors made by rats following the lidocaine injections. C) Bilateral lidocaine-induced inactivation of the PL prior to the non-delayed task had no effect on task performance.

make subsequent arm choices following lidocaine ($\bar{x}$=22.8s) as compared to saline ($\bar{x}$=35.8s) injections. The error data were analyzed using a two-way repeated-measures ANOVA and there were no significant differences in the total errors committed on lidocaine test days as compared to saline test days. There was no significant effect of injection order or Order X Treatment interaction. The mean numbers of errors made on saline and lidocaine test days are presented in Fig.2-2C.

Histology

The placements for all rats receiving bilateral infusions of lidocaine into the PL prior to the Test phase of the delayed task are illustrated in Fig. 2-5. Filled circles represent the locations of the cannulae tips and shading represents the region in which incidental necrosis was observed as a consequence of intracerebral injection of the vehicle. Shading does not represent the extent of the functional spread of lidocaine. This was not measured directly in the present study. There are different estimates of the functional spread of lidocaine within the brain which appear to depend on the rate of infusion. Using an infusion rate of 1µl/min, Welsh and Harvey (1991) estimate that the functional spread is 1.4 mm in the cerebellum from the site of infusion. The functional spread of lidocaine in the oculomotor nucleus was estimated to be 0.5 mm with an infusion rate of 4µl/15min (Albert & Madryga 1980). Based on these considerations, an infusion rate of 1µl/2min utilized in the present study, could be expected to produce a

functional spread of approximately 1±0.5mm. This means that the PL was anesthetized selectively by the lidocaine injections while the adjacent anterior cingulate subregion was spared. Furthermore, anterior cingulate inactivations have functionally different effects on delayed and non-delayed foraging behavior, relative to PL inactivations (Seamans et al. 1995), and unilateral PL inactivations do not disrupt performance of the delayed task (Floresco et al. 1997). Given the proximity of the PL and AC and hemispheres of the PL, it suggests that the functional spread of lidocaine is indeed 1mm or less.

Discussion of Section 1

The Results of Section 1 demonstrate that transient inactivations of the PL prior to the test phase but not prior to the training phase of a delayed foraging task, disrupt test phase performance. Similar inactivations of the PL had no effect on performance of the non-delayed task. These results suggest that in the context of delayed foraging, the PL has a selective role in the use of previously acquired information.

There are many previous reports that lesions of the mPFC, including the PL, produce selective impairments on delayed tasks (Bubser & Schmidt, 1990; Brito & Brito, 1990; Dunnett, 1990). However, because these were permanent lesions, the precise role of the mPFC in the encoding, storage or retrieval of information cannot be specified from these studies. Moreover, on oculomotor delayed response tasks in primates, the delay period is so brief, it is not possible

to dissociate the roles of the PFC in the acquisition, retention or retrieval of recently acquired information.

The results of Part 1 demonstrate that rats with transient PL lesions are impaired on the delayed task but not the single phase non-delayed task. The fact that lidocaine injections in the PL prior to training phase of the delayed task did not affect test phase performance argues against a role for this region in the acquisition or storage of trial-unique information. Given that pre-test lesions of the PL significantly disrupted Test phase performance, it may be assumed that activity in the PL is involved in the retrieval or utilization of information retained during a delay.

The pattern of errors displayed by the rats on the radial arm maze after PL lesions is essentially random, as predicted by the failure of a processing mechanism for a prospective pattern of motor responses. The specificity of this deficit is underscored by the fact that PL lesions in the rat failed to disrupt behavior on the RF task which does not require prospective planning, when animals were trained exclusively on this task. Thus the rat PL, like the primate dorsolateral PFC, plays an important role in the utilization of mnemonic information related to planning (Petrides 1994).

Although spatial information must play a critical role in predicting the probable location of food in the test phase of the delayed SWSh task, such information need not be retained within the PL throughout the 30 min delay. The temporal lobe is one candidate for the storage of spatial memory, from where it may be accessed by processing mechanisms within the PL responsible for

planning a prospective sequence of motor responses (Petrides 1994; 1995). Indeed, Floresco et al (1997) have shown recently that unilateral lidocaine injections into the PL with contralateral injections into the ventral hippocampus prior to the test phase of the delayed task, transiently disconnect these two brain regions and selectively disrupt test phase performance. Similar transient disconnections had no effect on performance of the non-delayed task. Thus, on the delayed foraging task information is transferred from the hippocampus to the PL at the time a series of responses are to be organized and initiated.

Electrophysiological data from neurons in the PFC of monkeys during delayed responding indicate that the memory functions of the PFC must be coordinated with computation of plans for subsequent motor responses (Fuster, 1993; Goldman-Rakic, 1992). In his description of a delay task, Fuster (1995) states that it involves complex behavior requiring both retrospective and prospective activity. Two categories of memory, the procedural memory of the rules of the task and the trial-specific memories of the cue, must be coordinated with the prospective memory of the motor response. When monkeys with lesions of the PFC are tested at longer delays (>20s), they fail to retain the perceptual memory of the cue and it also fails to evoke the prospective memory of the motor response. The delayed SWSh task used here with rats differs greatly from the delayed response tasks used with monkeys in both the duration of the delay period (30 min vs. seconds). Collectively, these data suggest that at short delays information stored transiently and used by PFC neurons to guide forthcoming responses. In contrast, at longer delays information is not stored within the PFC,

but rather is likely stored in temporal lobe regions and transferred to the PFC at a time when responses are to be organized and initiated. Thus one consistent function of the PFC across species and tasks is the ability to use mnemonic information to guide behavior.

Section 2: DA Modulation of PFC Function

Introduction

The integrity of the active short-term memory trace within the PFC appears to be regulated by the activity of a dopamine (DA) system, as destruction of DA terminals in the PFC disrupts performance on delayed-response or delayed-alternation tasks (Bubser & Schmidt., 1990; Brozoski et al., 1979). The administration of high doses of DA antagonists into the PFC also impairs performance on delayed-response tasks and decreases delay-period activity of PFC neurons (Sawaguchi and Goldman-Rakic, 1994; Williams et al., 1995; Sawaguchi et al., 1990b).

In addition to active retention of information over very short delays, the PFC in collaboration with a variety cortical and subcortical regions, may control more complex cognitive processes, also linked to working memory (Baddeley, 1986; Baddeley and Della Sala 1996) such as the ability to use mnemonic information to guide behavioral responses (see Part 1; and Shallice, 1982; Shallice and Burgess, 1996). The results of Part 1 demonstrated an essential role for the rat PL in foraging when previously acquired spatial information is

used to guide responding after a 30min delay, but not in foraging based solely on mnemonic information about previous arm choices within a single trial.

Several features of the delayed foraging procedure are consistent with the engagement of a working memory process. First, the rat acquires trial-unique spatial information in the training phase that may be stored in a 'spatial memory buffer'. During the test phase, this information will be retrieved from the spatial memory buffer and integrated into a prospective search strategy enabling the rat to retrieve four food pellets efficiently from eight possible locations on the maze. Transient disconnections of the PL and ventral hippocampus prior to the test phase of the delayed task but not prior to the non-delayed task disrupted foraging (Floresco et al. 1997). Thus, the spatial memory buffer may be located in the temporal lobe, while the integration of spatial information into a prospective search strategy is performed by the PFC (Floresco et al. 1997). At present it is unknown whether such cognitive processes related to working memory are modulated by DA in the PFC.

The present research examined the effects of D1 and D2 receptor blockade in the PFC on delayed and non-delayed radial arm-maze foraging (Seamans and Phillips, 1994, Seamans et al.,1995). The present study also investigated whether endogenous DA activity within the PFC specifically modulated hippocampal afferents during the performance of the delayed task. To this end, a modified version of the transient disconnection procedure was employed. In the standard transient disconnection procedure (Floresco et al., 1997) unilateral lidocaine injections were delivered to the origin of the

hippocampal-PFC pathway in the vSub and the termination of this pathway in the contralateral PL (Jay and Witter, 1991; Condé et al., 1995). This procedure caused a selective disruption of delayed SWSh performance, whereas unilateral injections into either site had no effect on working memory (Floresco et al. 1997). The logic underlying the use of this disconnection procedure to identify components of a functional neural circuit is based on the assumption that information is transferred serially from one structure to an efferent region, on both sides of the brain in parallel. Furthermore, the design assumes that dysfunction will result from blockade of neural activity at the origin of a pathway in one hemisphere (i.e. hippocampus) and the termination of the efferent pathway in the contralateral hemisphere (i.e. PFC). In the present study, an injection of the D1 antagonist SCH-23390 was substituted for the non-specific lidocaine injection into the PL. A critical role for D1 receptors in the PFC would be revealed if working memory was disrupted selectively by the combination of the D1 antagonist in the PL and lidocaine in the vSub.

Results: Section II

The Effects of Bilateral injections of SCH-23390 or Sulpiride into the PL

Delayed Task: SCH-23390: Prior to the test phase of the delayed task, seven rats received bilateral counterbalanced infusions into the PL of vehicle and three doses of SCH-23390 (0.05, 0.5, or 5 μg in 0.5 μl of vehicle) on separate days. Analyses of the number of errors made on vehicle and all drug injection days revealed a significant main effect of Treatment ($F(3,18)= 4.96$, $p<0.05$)(Fig. 2-

3A). Tukey's *post hoc* analysis for repeated measures showed that rats made significantly more errors following injections of 0.5 μg and 5.0 μg of SCH-23390 relative to vehicle and 0.05μg SCH-23390 treatments ($p<0.05$). Subsequent planned comparisons on the type of errors made on SCH-23390 injection days revealed that following injections of either 0.5 μg or 5.0μg of SCH-23390 into the PL, an equal number of across- and within phase errors were made (all F's < 2.0, n.s.). There were no significant effects of Injection Order, or Treatment X Order interactions (all F's < 1.8, n.s.).

Sulpiride: Prior to the test phase of the delayed task, seven rats received bilateral counterbalanced infusions of either vehicle or three doses of Sulpiride (0.05, 0.5, or 5 μg in 0.5 μl of vehicle) into the PL on separate days. Analyses of the number of errors made on vehicle and all drug injection days revealed no significant main effect of Treatment ($F(3,18)= 1.62$, n.s) (Fig. 2-3B). There were also no significant effects of Injection Order, or Treatment X Order interactions (all F's < 1.8, n.s.).

Non-delayed RF Task: SCH-23390: Prior to a daily trial of the non-delayed task, seven rats received counterbalanced bilateral infusions of either vehicle or SCH-23390 (0.05, 0.5, or 5 μg in 0.5 μl of vehicle) into the PL on separate days. Analysis of these data revealed no significant main effect of Treatment ($F(3,18)$ = 2,27, n.s.) (Fig 2-4A). There also were no significant effects of Order of injection or Order x Treatment interactions (all F's < 2.3, n.s.).

Sulpiride: Prior to a daily trial of the non-delayed task, seven rats received bilateral counterbalanced infusions of either vehicle or Sulpiride (0.05, 0.5, or 5

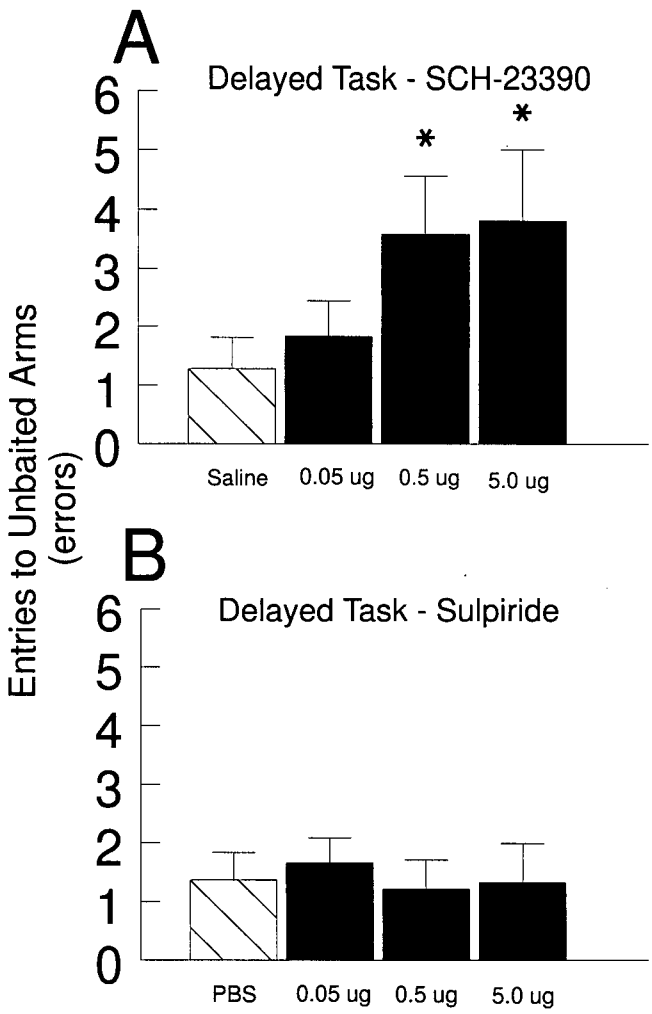

Figure 2-3: The effects of bilateral injections of D1 or D2 receptor antagonists into the PL of rats well trained on the delayed task. **A)** Number of errors (mean ± SEM) made during the test phase by rats receiving saline (hatched bar), 0.05μg, 0.5 μg, and 5 μg SCH-23390 (black bars) into the PL. **B)** Number of errors (mean ± SEM) made during the test phase by rats receiving PBS (phosphate buffered saline) (hatched bar), 0.05μg, 0.5 μg, and 5 μg Sulpiride (black bars) into the PL. * $p<0.05$ relative to saline injections.

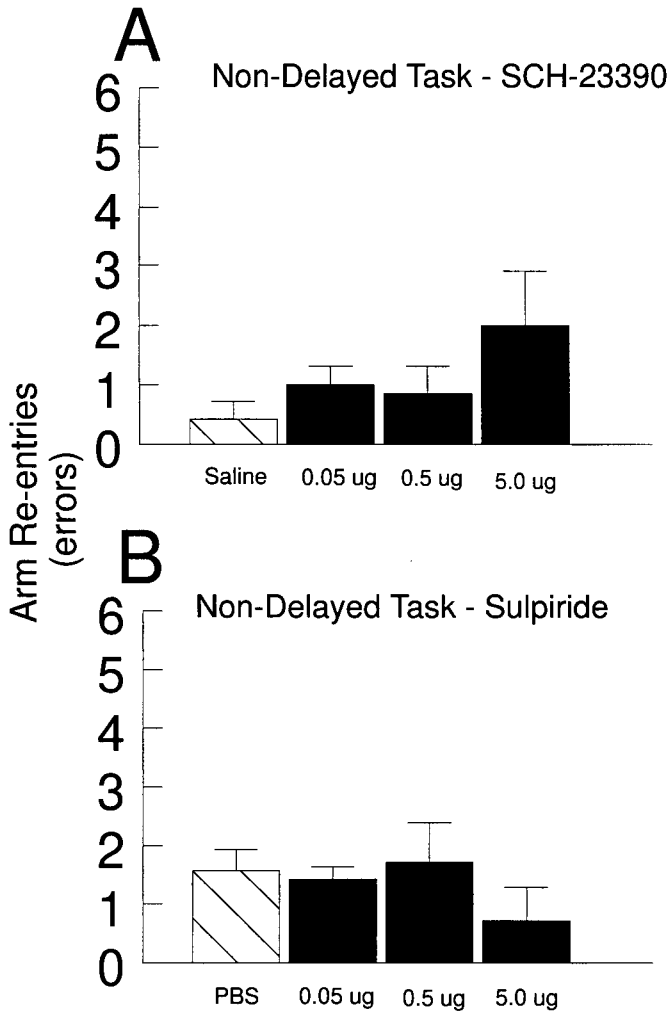

Figure 2-4: The effects of bilateral injections of D1 or D2 receptor antagonists into the PL of rats well trained on the non-delayed task. **A)** Number of errors (mean ± SEM) made during the non-delayed task by rats receiving saline (hatched bar), 0.05μg, 0.5 μg, and 5 μg SCH-23390 (black bars) into the PL. **B)** Number of errors (mean ± SEM) made during the non-delayed task by rats receiving PBS (phosphate buffered saline) (hatched bar), 0.05μg, 0.5 μg, and 5 μg Sulpiride (black bars) into the PL.

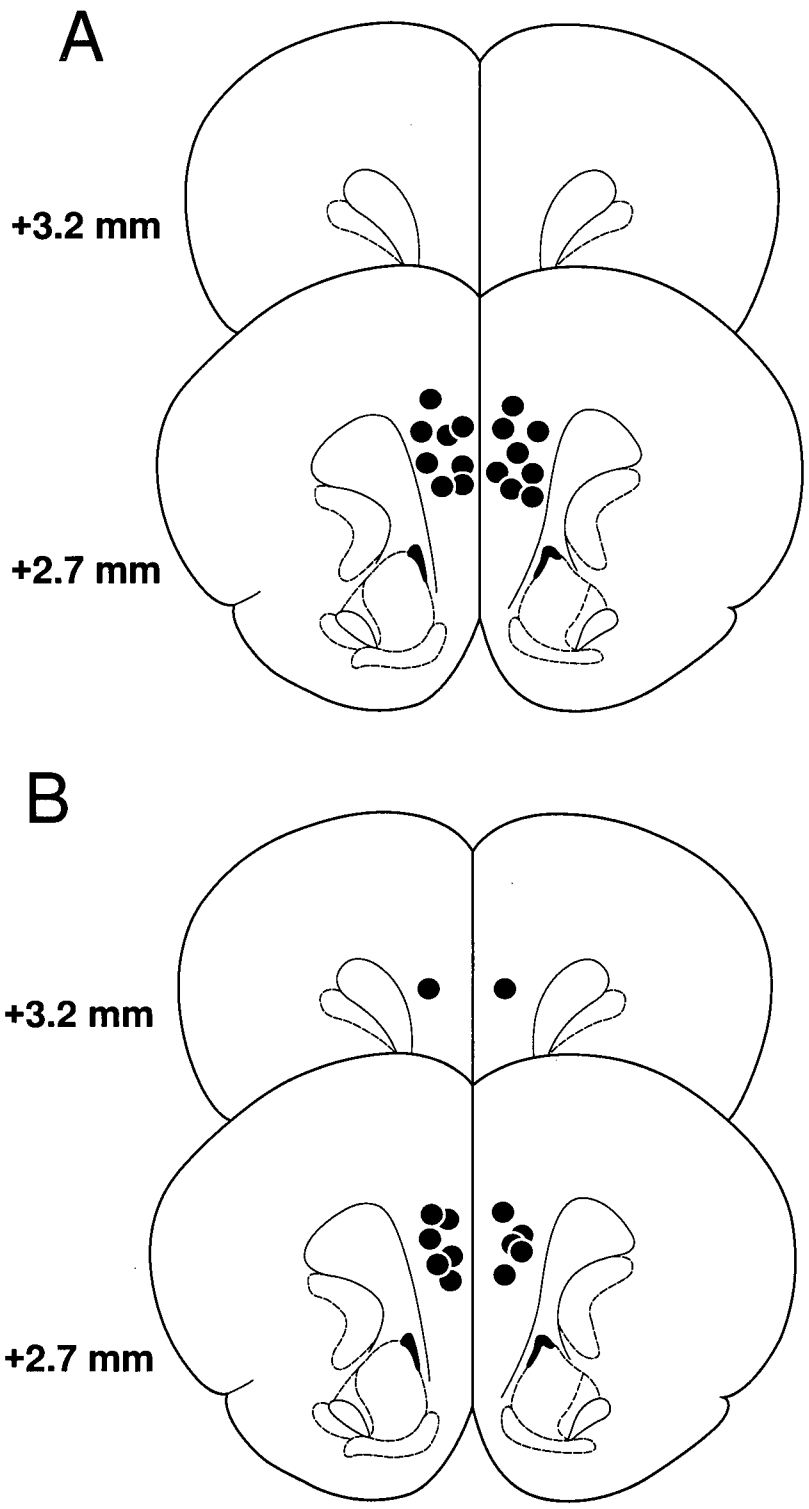

Figure 2-5: Schematic representation of injection sites. **A)** Dots represent the location of cannulae tips for all rats receiving bilateral injections of lidocaine and saline into the PL prior to the test phase of the delayed task. **B)** The location of cannulae tips for all rats receiving bilateral injections of SCH-23390 and saline into the PL prior to the test phase of the delayed task. Numbers to the left indicate the distance of the coronal section from bregma.

μg in 0.5 μl of vehicle) into the PL on separate days. Analysis of these data revealed no significant main effect of Treatment ($F(3,18) = 0.56$, n.s) (Fig 2-4B). There were also no significant effects of Order of injection or Order x Treatment interactions (all F's < 0.7, n.s.).

Histology

The location of the cannulae tips for all animals receiving bilateral SCH-23390 injections into the PL prior to the delayed task are shown in Fig. 2-5B. Placements were similar for the other groups. Data from animals whose placements were not located in the PL region of the PFC were not included in the data analysis.

Unilateral injection of SCH-23390 into the PL combined with inactivation of the contralateral vSub on the Delayed Task.

A group of 7 rats with two sets of bilateral cannulae implanted into the PL and the vSub received the injection protocol described above, prior to the test phase of the delayed task, on four occasions. Statistical analyses revealed a highly significant main effect of Treatment ($F(3,18) = 9.720$, $p<0.001$)(Fig 2-6A). Tukey's *post hoc* analysis for repeated measures revealed that rats made significantly more errors when unilateral infusions of SCH-23390 into the PL were paired with contralateral infusions of lidocaine into the vSub ($p<0.001$). There were no other significant differences in the number of errors made on any of the other injection days. Subsequent planned comparisons on the type of errors

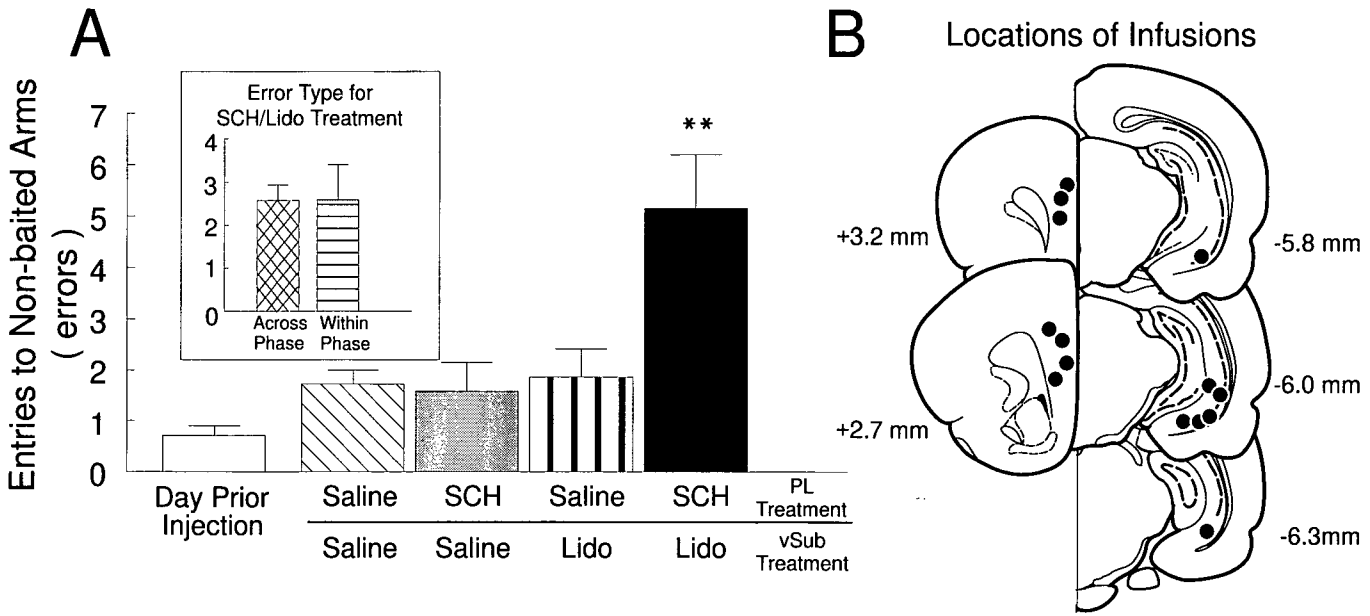

Figure 2-6:The effects of unilateral inactivation of the vSub in combination with unilateral injections of SCH-23390 into the PL of the contralateral hemisphere. A) Number of errors (mean ± SEM) made during the delayed task by rats on the day before the first injection (open bar), after unilateral infusions of saline into both the PL and vSub (hatched bar), unilateral infusions of SCH-23390 (SCH, 0.5 μg) into the PL and contralateral infusions of saline into the vSub (gray bar), unilateral infusions of saline into the PL and contralateral infusions of Lidocaine into the vSub (stripped bar) and unilateral injections of SCH (0.5 μg) into the PL and contralateral injections of Lidocaine into the vSub (black bar). ** $p<0.01$ versus all other treatment conditions. Inset shows the number of across phase (cross-hatched bar) and within-phase (horizontal-stripped bar) errors made by rats following the SCH/Lidocaine injection condition. B) Schematic representation of the SCH-23390 injection sites into the PL and lidocaine injection sites into the vSub for rats in the SCH/lidocaine condition. Black dots represent the location of cannula tips.

made following unilateral PL infusion of SCH-23390 and contralateral vSub inactivations showed that rats made an identical number of across- and within-phase errors ($F(1,6) = 0.0$, n.s) (Fig. 2-6A, inset). Furthermore, there were no significant effects of Injection Order, Error type, or any significant interactions (all F's <1.4, n.s.). Collectively these results showed that D1 receptors selectively modulate hippocampal afferents to the PL during the performance of a long-delay SWSh task.

A separate series of tests revealed no evidence of hemispheric biases on the number of errors made following unilateral vSub inactivations or unilateral SCH-23390 injections into the PL (all F's <0.7, n.s.). However, rats which received unilateral inactivations of the right vSub made significantly more errors than those rats which received left vSub inactivations ($F(1,5) = 7.10$, $p<0.05$). This effect was not observed previously following identical unilateral vSub lidocaine injections (Floresco et al., 1997). Given the large number of comparisons made in the present study, this increase in errors following right unilateral vSub inactivations is likely to be a spurious finding. Moreover, the total number of errors made by rats following unilateral vSub inactivations, combined for both hemispheres, did not differ significantly from other control treatments.

Histology

The location of the cannulae tips are represented in Fig. 2-6C. Bilateral placements in the vSub were similar to those observed by Floresco et al. (1997). Similarly, bilateral placements in the PL were within the same region of the PFC as those observed in Fig 2-5.

Analysis of Response Latencies

The latency data for Part 2 are presented in Table 2. The latency data for each experimental condition were analyzed separately. These analyses revealed that none of the bilateral drug injections significantly affected the latency to initiate the trial or the average time per subsequent choice (all F's <1.5, n.s.). SCH-23390 PFC microinjections paired with vehicle injections into the vSub significantly reduced initiation times ($p<0.05$). Since neither bilateral SCH-23390 injections or unilateral vSub vehicle injections did not affect response latencies in the other conditions, this result may not be a real effect.

Table 2: Response latencies for Section 2 of Chapter 2.

Biltaeral Injections

Delayed SWSh	**SCH-23390**	**saline**	**0.05 µg**	**0.5 µg**	**5.0 µg**
	Initiate	31.6 (3.2)	29.7 (13.1)	42.1 (10.0)	25.6 (5.1)
	Average time per choice	28.1 (2.6)	21.8 (2.8)	18.9 (2.4)	20.0 (2.3)
	sulpiride	**saline**	**0.05 µg**	**0.5 µg**	**5.0 µg**
	Initiate	18.3 (2.0)	10.2 (2.7)	8.7 (4.0)	16.8 (5.2)
	Average time per choice	20.1 (2.3)	17.8 (1.9)	11.8 (1.1)	11.8 (2.9)
Non-delayed RF	**SCH-23390**	**saline**	**0.05 µg**	**0.5 µg**	**5.0 µg**
	Initiate	23.8 (4.8)	25.5 (8.0)	20.6 (4.8)	23.3 (4.6)
	Average time per choice	19.4 (3.8)	24.1 (7.2)	19.1 (3.5)	24.3 (4.8)
	sulpiride	**saline**	**0.05 µg**	**0.5 µg**	**5.0 µg**
	Initiate	16.3 (8.0)	22.1 (8.1)	21.4 (3.0)	26.0 (10.1)
	Average time per choice	13.1 (2.1)	29.1 (10.9)	17.9 (1.3)	37.9 (18.1)

Asymetric Injections

	saline(PL) & saline (vSub)	**saline (PL) & Lido (vSub)**	**SCH (PL) & saline (vSub)**	**SCH (PL) & Lido (vSub)**
Initiate	43.2 (8.4)	46.4 (18.7)	26.8 (8.8)*	65.0 (16.2)

Discussion of Section 2

The present results demonstrate that D1, but not D2, receptors in the PL modulate delayed responding on a delayed foraging task. These data are consistent with those of Bubser and Schmidt (1990) who showed that 6-OHDA lesions of the rat PL selectively impaired delayed, but not spontaneous alternation on a T-maze. Furthermore, D1 receptor blockade in the PFC of primates or rats produces deficits on delayed-response tasks but typically not those without a delay component (Sawaguchi and Goldman-Rakic, 1994; Sawaguchi et al., 1990b; Williams & Goldman-Rakic, 1995; Broersen et al. 1995b). Abnormally high levels of DA activity in the PFC also disrupts delayed responding in rats as shown by impaired performance of delayed alternation on a T-maze, after pharmacologically-induced high rates of DA turnover in the PFC, or administration of high doses of D1 agonists into the PFC (Arnsten 1997; Murphy et al. 1996a,b; Zhart et al. 1996). These data indicate that maintenance of D1 activity in the PFC within an optimal range is essential for working memory.

Although D2 receptor blockade in the PFC has been reported to affect certain memory tasks in rats (Bushnell and Levin, 1983), most studies do not find an effect of D2 antagonists on delayed responding (Sawaguchi and Goldman-Rakic, 1994; Sawaguchi et al., 1990b; Broersen et al., 1995b). These behavioral findings are consistent with receptor localization studies showing that; 1) the rat PFC, in common with the primate PFC, contains a greater number of D1 receptors relative to D2, and 2) D1 receptors have a higher affinity for DA in the micromolar range (Gasper et al., 1995; Farde et al., 1987; Seeman, 1987).

Moreover, D1 receptors modulate pyramidal cell function in the PFC, whereas the role of D2 receptors is less clear (Yang and Seamans, 1996). D2 receptors may modulate pyramidal cell function indirectly via GABAergic interneurons (Rétaux et al., 1991). Thus D1 receptors appear to be more important than D2 receptors in cognitive and physiological functions of the PFC. However, it has been suggested that D2 receptor modulation of cognitive function may play a more predominate role in older animals (Arnsten et al., 1995).

The deficit observed here following microinjections of a D1 antagonist into the PL was specific to performance of the delayed task, as similar injections had no effect on foraging during the non-delayed single trial procedure, even though such non-delayed tasks required the short-term retention and use of trial unique information. It has been postulated that imposing a delay in a radial arm maze task, bias rats to forage prospectively while non-delayed tasks bias rats to forage retrospectively (see Part 1 and Cook et al., 1985; Floresco et al., 1997). Thus, spatially-mediated foraging based on a series of planned responses, or prospective memory appears to be critically dependent on D1 receptor activity in the PFC.

Foraging based on a planned series of responses also depends on interactions between the hippocampus and PFC (Floresco et al., 1997). The results of Part 2 demonstrated that D1 receptor blockade in the PL coupled with inactivation of the vSub in the contralateral hemisphere disrupted performance on the delayed foraging task. In this context it is important to emphasize that unilateral injection of SCH-23390 in the PL in combination with vehicle injections

into the vSub had no effect on memory for the location of food. In previous "disconnection" studies asymmetrical injections of lidocaine into both the PL and vSub were used to demonstrate a critical role for a hippocampal - PFC circuit in the working memory function that enabled rats to anticipate the location of food in complex environment (Floresco et al., 1997). The fact that blockade of D1 receptors in the PL in one hemisphere disrupted delayed foraging when combined with a reversible lesion of the contralateral vSub, is consistent with an important gating function for D1 receptors during the transmission of information in a hippocampal-PFC circuit. On the basis of these data, it may be inferred that D1 receptors modulate *specifically* hippocampal inputs to the PFC during the test phase of the delayed task at which time spatial information acquired 30 min. previously must be accessed and incorporated into a prospective plan for the efficient discovery of food in a complex environment.

The present data compliment and extend previous reports that application of a D_1 antagonist into the PFC in primates disrupts the active retention of information during a brief delay (<6s) oculomotor delayed response task (Williams & Goldman-Rakic 1995). Taken together these studies indicate that PFC neurons and modulation of neuronal activity by D1 receptors in the PFC, appear to play an important role in at least two different aspects of working memory: a) the ability to hold information in an active state for a short time, and b) the recall of information from a spatial memory buffer via a hippocampal-PFC circuit, and possibly the integration of spatial memory into a prospective response strategy.

The pattern of errors committed by rats receiving injections of the D1 antagonist into the PFC provide important insights into the possible mechanisms of action of DA in the PFC. In the present study, rats receiving injections of a D1 antagonist responded randomly on the delayed task as they made an equal number of across and within phase errors. Yet on the non-delayed tasks, similar injections did not increase within-phase errors despite the fact that the non-delayed task assesses specifically the propensity to commit such errors.

The D1 antagonist-mediated disruption of the delayed task could not be interpreted as a short-term memory deficit, as such a deficit would be expressed in a greater number of across relative to within-phase errors. Moreover, it was not a spatial deficit or a problem in response initiation as no deficits were observed on the spatially-mediated non-delayed task. Rather the present data indicate that D1 receptor blockade disrupts selectively the ability to use previously acquired information to organize efficient foraging behavior.

Following D1 receptor blockade, foraging was not directed by mnemonic, task-related information, but rather was completely unorganized. A qualitatively different impairment has been observed following local microinjections of D1 agonists into the PFC. Recently, Zhart et al. (1997) have shown that such injections also impair delayed responding by rats on a T-maze. But rather than causing random modes of responding, the errors were perseverative, as rats tended to revisit the previously rewarded spatial location. It therefore appears that too much or too little D1 receptor stimulation in the PFC can disrupt working memory, but in different ways. Insufficient D1 receptor stimulation in the PL

results in random responding that is not guided by task relevant stimuli, while excessive D1 receptor stimulation causes responding to be directed only to previously significant stimuli in the environment.

In order to attain a more complete understanding of working memory processes mediated by the PFC and modulation by D1 receptors, Chapters 3-6 will examine the electrophysiological properties of PFC neurons and how these properties are modulated by DA.

Chapter 3:

Electrophysiological and Morphological Characteristics of Principal Pyramidal PFC Neurons : Somatic Recordings

Introduction

The PFC is involved in both the short-term retention of information and the use of mnemonic information to guide behavior (see Chapters 1 & 2). Evidence for a role of the PFC in the short-term retention of information has come from extracellular single unit recordings from the PFC of primates performing oculomotor delayed response tasks. Many neurons exhibit sustained firing throughout the delay period of the task and there are a number of findings which suggest that the activity of these neurons represents an active neural trace of previously encountered external stimuli (see General Introduction). Other PFC neurons show a gradual increase in activity throughout the delay period, prior to a response (Quintana & Fuster 1992; Funahashi et al. 1989). These neurons have been termed 'anticipatory' or 'response related' neurons (Quintana & Fuster 1992; Fuster 1995). It is hypothesized that the coordinated activity of delay and anticipatory/ response-related neurons in the PFC underlie the ability to use previously acquired information to guide a response (Fuster 1995; Goldman-Rakic 1995a,b).

Many of the delay and response period -active neurons have a soma which resides in deeper layers of the cortex (Sakai & Hamada 1989; Fuster 1985). Neurons whose soma is located in layer V of the cortex have long ascending apical dendrites which is a key receptive zone for synaptic inputs from

other cortical areas (Peters 1987; Cauller & Conners 1992; 1994; Goldman-Rakic 1988) and the delay-period activity of layer V PFC neurons is dependent on inputs from other cortical regions, such as the parietal or inferotemporal cortex (Wilson et al. 1993; Fuster et al. 1985; Quintana et al. 1989). Moreover layer V PFC neurons project out of the PFC to regions involved in response generation, such as the striatum (Sesack et al. 1989; Gorelova & Yang 1996). Deep layer PFC neurons are positioned to process sensory information about the external world, actively retain this information via sustained firing throughout a delay, and use this information to subsequently guide a response.

If we are to obtain a more complete understanding of working memory processes mediated by the PFC it is necessary to understand at a basic level, how deep layer PFC neurons integrate synaptic signals. Chapter 2 will examine the intrinsic membrane properties of layer V PFC in a brain slice preparation as a first step in determining how such neurons may processes inputs and generate spike output.

METHODS

The methods for all electrophysiological experiments included in the present thesis (Chapters 3-6) are described below.

1. Brain Slice Preparation

Young adult male Sprague-Dawley rats (80-100 g, University of British Columbia colony) were used in this study. Following decapitation, the brain was rapidly dissected and immersed for 1 minute in cold (4 °C) oxygenated (with 95%

O_2 + 5%CO_2) artificial cerebrospinal fluid (ACSF) (in mM): NaCl (126), KCl (3), $NaHCO_3$ (26), $MgCl_2$ (1.3), $CaCl_2$ (2.3), glucose (10). The lateral halves of the brain were removed from each hemisphere. A coronal cut was made just caudal to the optic chiasma, isolating the forebrain.

Each tissue block was glued onto the cutting stage of a vibratome (Vibraslice) by cyanoacrylic-based glue and anchored by a block of agar (4% in saline). 450 μm thick oblique slices that retained the PFC and the NAc were cut from each hemisphere using the vibotome. The slices were incubated in oxygenated ACSF for 1 hour at room temperature before electrophysiological recordings commenced.

2. Recordings

In the recording chamber (Medical System Corps. U.S.A.), the slice was held by a nylon net and perfused by gravity-fed ACSF (maintained at 34°C) at a rate of 3-4 ml per min. Standard sharp electrode intracellular recordings of layer V-VI PFC neurons were made in current-clamp mode while whole-cell patch-clamp recordings were made in current-clamp or voltage-clamp mode. Sharp electrode intracellular recordings were made using thick-walled borosilicate micropipettes (1.2 mm O.D., 0.6 mm I.D. Sutter Instruments Inc.) which were prepared on a horizontal micropipette puller (Flaming-Brown P-87). Sharp microelectrodes were filled with 1.5% biocytin (Sigma) in 3M potassium acetate or 3M cesium acetate. For recordings of synaptic responses sharp micropipettes were filled with 3M potassium acetate alone or 2M potassium acetate, 1M cesium acetate and 80-100mM QX-314. It should be noted that, in addition to blocking

Na^+ channels, QX-314 also reduces pertussis-toxin-sensitive G-protien coupled K^+ currents, such as those linked to $GABA_B$ receptors (Aghajanian & Wang 1986) as well as an inwardly-rectifying hyperpolarizing-activated curent (Perkins & Wong 1995).

The electrodes had a final resistance between 90 -130 MΩ. Patch pipettes (1.5mm O.D., 1.1mm I.D.) were filled with (in mM): K-gluconate (130), KCl (10), ethylene glycol-bis(β-aminoethyl ether)- N,N,N',N'-tetraacetic acid (EGTA) (1), $MgCl_2$ (2), NaATP (2), N-2-hydroxyethylpiperazine-N'-2-ethanesulfonic acid (HEPES) (10) and 0.3% biocytin and had a resistance between 8-12 MΩ for dendritic recordings and <5 MΩ for somatic recordings. In some experiments QX-314 (1mM) and/or CsCl (10mM) was also added to the internal patch solution. Seal resistance before break-in was >2GΩ, and after break-in, access resistance was routinely 60-90 MΩ for dendritic recordings and <20 MΩ for somatic recordings

Microelectrodes were connected to the headstage of an Axoclamp-2B amplifier (Axon Instruments) with Ag/AgCl wire. Changes in junctional potential at the indifferent electrode were minimized by connecting the Ag-AgCl reference electrode to an agar-bridge (a block of 4% agar in saline at the end of a glass pipette that is filled with 3M KCl solution). Bridge balance was continuously monitored on the oscilloscope (Tetronix D13) in order to subtract the voltage drop across the electrode resistance. Capacitance transients were also optimally compensated. Voltage-clamp recordings were obtained using the Axoclamp-2B in continuous single-electrode voltage-clamp (SEVC) mode. Series resistance

was 80% compensated and the gain was increased up to 25mA/mV. Data were filtered at 10 kHz. The recorded signals were amplified in current-clamp bridge-mode or SEVC mode were digitized by a Digidata 2000 A/D board (Axon Instruments), and sampled on-line using a PC based computer. The captured data were analyzed off-line using pClamp software (Version 5.5 and 6.10, Axon Instruments).

The resting membrane potential was estimated by taking the difference between the V_m reading when the electrode was inside the cell (with no DC current injected) and the V_m reading when the electrode was outside the cell at the end of the recording period. Neuronal input resistance (R_{IN}) was determined by dividing the difference in membrane voltage in response to a hyperpolarizing current pulse which caused a voltage deflection ≈ 10mV by the amount of current injected. The membrane time constant (τ) was fitted from the onset of the response to a hyperpolarizing pulse to the beginning of the steady state condition. Although some cells showed clear indications of more than one fast equalizing time constant, only the final single slow time constant fitting is reported in this study. For group data, all values presented correspond to the mean and standard error of the mean.

3. Drug Applications

All drugs were bath-applied by gravity. Complete exchange of the bathing solution took ≈2 mins. 4-aminopyridine (4-AP, 2mM), tetraethylammonium hydrochloride (TEA, 20mM), tetrodotoxin (TTX, 0.5-1mM) were obtained from

Research Biochemical Inc. or Sigma (U.S.A.). In order to isolate Na^+ currents, Ca^{2+} currents were blocked by Cd^{2+} or Co^{2+}($NaHCO_3$ was replaced with Tris (base) and the pH of the solution was adjusted to 7.4 after oxygenation in order to prevent divalent cation precipitation), and K^+ currents were blocked by $[Cs^+]_i$, TEA and/or 4-AP. In order to isolate K+ currents, TTX and Co^{2+} or Cd^{2+} was applied to block Na^+ and Ca^{2+} currents respectively. In experiments in which Ca^{2+} spikes were evoked by intracellular current pulses TTX in combination with $[Cs^+]_i$ TEA and/or 4-AP were applied to block Na^+ and K^+ channels respectively. In other experiments $NiCl_2$ (100uM) was bath-applied to block low threshold Ca^{2+} currents.

4. Biocytin Staining

To trace the entire soma-dendritic profile of recorded PFC neurons, biocytin was injected iontophoretically during intracellular recordings either continuously, or by means of anodal current pulses (200ms, 100 to 300 pA, 1 Hz), for at least 20 mins. After the recording sessions, brain slices were fixed in 4% paraformaldehyde in 0.1M phosphate buffer (pH 7.4) for 1 hr at room temperature. Slices were then transferred to 0.05M Tris buffer containing 1 % Triton X-100 and stored at 4°C for 48 hrs. After this period, the endogenous hydrogen peroxidase activity was then neutralized with 30% hydrogen peroxide in methanol (1:60 dilution) for 30 mins. Following washing with Tris-Triton, the tissue was incubated with a streptavadin-horseradish peroxidase complex (1:200 dilution) containing 3% fish gelatin (Sigma) in Tris-Triton for 2 hrs at room temperature. After washing with Tris-buffer, the tissue was incubated with

diaminobenzidine (1 mg) and hydrogen peroxide for 5 mins. Finally, the reaction was stopped by washing in 0.1 M phosphate buffered saline. After dehydration of the slices through a series of alcohol, the tissue was cleared in methylsalicylate and the entire 400-450 μm slice was mounted for examination using light microscopy. Camera lucida drawings and photographs of the entire stained neurons were made. The exact locations of these neurons were verified with reference to identical sections counter-stained with cresyl violet.

Dendritic tuft recordings were made by patch pipettes in layers I-II, and biocytin passively diffused throughout the neuron during the course of the experiments. At the end of each experiment brain slices were fixed and stained for biocytin (Yang et al. 1996a). Dimethylsulphoxide was used as the mounting medium for cover-slipping. When viewed under a microscope, the soma of stained neurons were located in layers III-VI, and the corresponding recording was in the apical tuft. In some cells the recording site could be observed clearly on the stained dendrite as a small notch.

5. Synaptic Stimulation

For synaptic stimulation experiments a concentric bipolar stimulating electrode (SNE-100, David Kopf Co.) was placed in layers I-II or V-VI. Electrical stimulation (0.2ms, 50-500 μA) was delivered at low frequencies (≤ 0.1 Hz) and consisted of monophasic square pulses delivered via an optically isolated stimulation unit (ISO-FLEX, A.M.P.I., Israel). Stimulation frequencies were programmed by a Master-8 pulse generator (A.M.P.I., Israel).

In some experiments, in order to isolate layer I-II inputs, a vertical cut from the corpus callosum to layer II was made using a 30.5 g syringe needle mounted on a micromanipulator. The stimulation electrode was then placed at least 0.3mm to one side of the cut (Cauller & Connors 1994). In other experiments 300mM L-glutamic acid monosodium salt (Sigma Chemicals) plus Fast Green (Sigma Chemicals) was applied to layers I-II via a glass pipette (tip diameter 1-2mM) using a Picospritzer II (General Valve Corp., NJ) pressure ejection device (using 10-500ms pressure pulses, 20-50psi) and diffusion was monitored visually under a microscope.

An NMDA-mediated EPSP was isolated by bath application of DNQX (10μM) and bicuculline (0.5-10μM). An AMPA / kinate-mediated EPSP was isolated by bath application of APV (50μM) and bicuculline. $GABA_A$ IPSPs were isolated by co-application of APV and DNQX. In most experiments $GABA_B$ responses were blocked by QX-314 in the micropipette (Nathan et al. 1990). All glutamatergic and GABAergic antagonists were obtained from Precision Biochemicals Inc. (Vancouver, Canada).

6. Focal Drug Applications

To determine the site of electrogenesis of Ca^{2+} mediated potentials, $CdCl_2$ (2-50mM in puff pipette) plus Fast Green was pressure ejected focally (using 100-500ms pressure pulses, 20-50 psi) to the apical dendritic stem at the region between the dorsal borders of layer III and V (100 - 200μm from the soma), the border between layers II-III (300-400μm from the soma) or to layers I-II (>500μm from the soma, <200μm from pia) via a glass pipette (tip diameter 1-2μM) using a

Picospritzer II pressure ejection device (General Valve Corp., New Jersey). To minimize spreading small diameter pipettes were used and the speed of perfusion was increased to 5 ml / min. Diffusion was monitored visually through a microscope.

Results

Stable intracellular or patch-clamp recordings were obtained from the soma or dendrites of >300 neurons whose soma was located in layers V-VI of the prelimbic and dorsal infralimbic regions of the PFC for all electrophysiological experiments in this thesis. Only PFC neurons with action potentials which overshot 0 mV were included in the data analysis.

Four distinct groups of pyramidal neurons in layers V-VI of the PFC were classified based on their evoked firing pattern at the soma in response to intracellular depolarizing pulses and morphological profiles. We have classified them as *regular spiking (RS)*, *intrinsic bursting (IB)*, *repetitive oscillatory bursting (ROB)*, and *intermediate (IM)* cells (Yang et al. 1996). The majority of deep layer PFC neurons were of the *IB* type, and the remainder of the thesis will deal mainly with these neurons.

IB (also called phasic-tonic firing in other studies e.g., van Brederode and Snyder, 1992) made up 63% of all deep layer PFC neurons recorded. Nine *IB* layer V-VI PFC neurons were stained with biocytin. All were pyramidal cells with a thick ascending apical dendritic trunk which bifurcated into arborized branches terminating in layer I-II (Fig. 3-1A). Proximal dendrites also arose from the deep

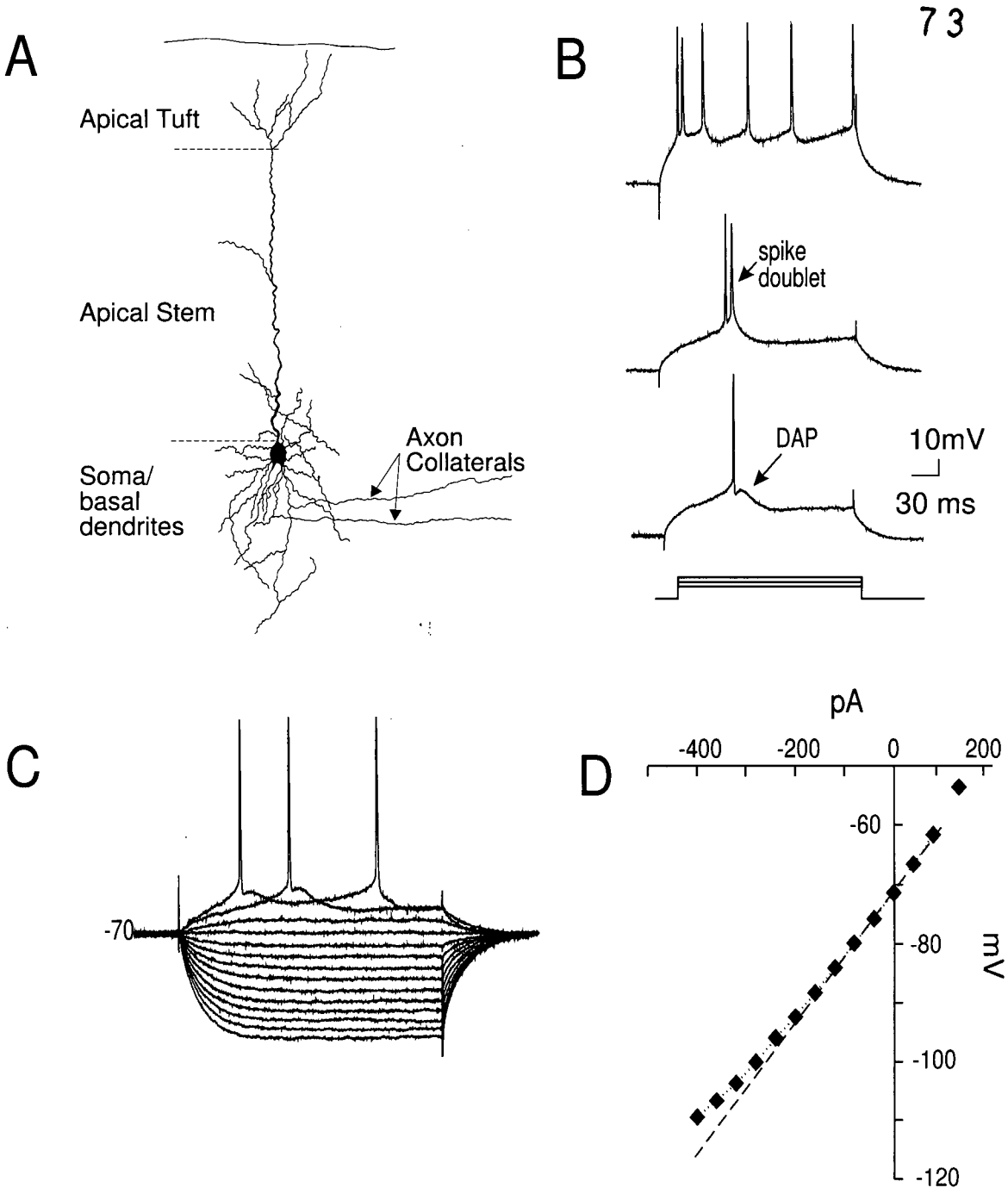

Figure 3-1: Morphological and electrophysiological properties of *IB* PFC neurons recorded from the soma. **A)** Camera Lucida drawing of an *IB* neuron that was stained with biocytin-streptavidin-DAB. **B)** Responses at the soma of an *IB* neuron to progressively increasing depolarizing current steps from rest. DAP denotes the presence of a depolarizing after potential. **C)** Voltage deflections to injection of a series of hyperpolarizing and depolarizing current steps (200ms, 40pA per step) to the soma. **D)** Voltage-current plots and slope resistance for an *IB* cell recorded at the soma.

layer somatic region and bifurcated profusely. Dendritic spines were prominent in both the apical dendrites and in the basal proximal dendrites. The projection of the axon could be traced to the white matter in most stained neurons. Collateral axons arose from the main branch and projected perpendicularly and horizontally within layers V-VI.

IB neurons had a mean resting V_m of -72 ± 1.2 mV. The voltage-current plot of this type of PFC cell was linear in the membrane voltage between -60 to -95 mV, yielding a mean slope resistance of 109 ± 8 MΩ. The mean membrane time constant (τ) of the *IB* PFC neurons was 17.9 ± 0.9 ms and the mean firing threshold was -51.8 ±1 mV as assessed using intracellular recordings (the R_{IN} and τ were considerably larger using patch-clamp recordings, as reported in Chapter 4).

When activated from rest by an intracellular current pulse, *IB* cells showed a distinctive depolarizing afterpotential (DAP) which followed immediately after each incompletely repolarized action potential (Fig. 3-1B). Injection of a fixed amplitude depolarizing pulse evoked a doublet of fast spikes rising over a depolarizing envelope. After the initial spike-doublet, *IB* neurons fired single spikes with progressive spike frequency adaptation (Fig. 3-1B).

Intrinsic Membrane Oscillations

IB neurons exhibited two types of membrane oscillations. One type showed narrow frequency band subthreshold oscillations (*type 1*, 18 out of 60, 30%, Fig 3-2A). Spike clusters sometimes occurred between periods of

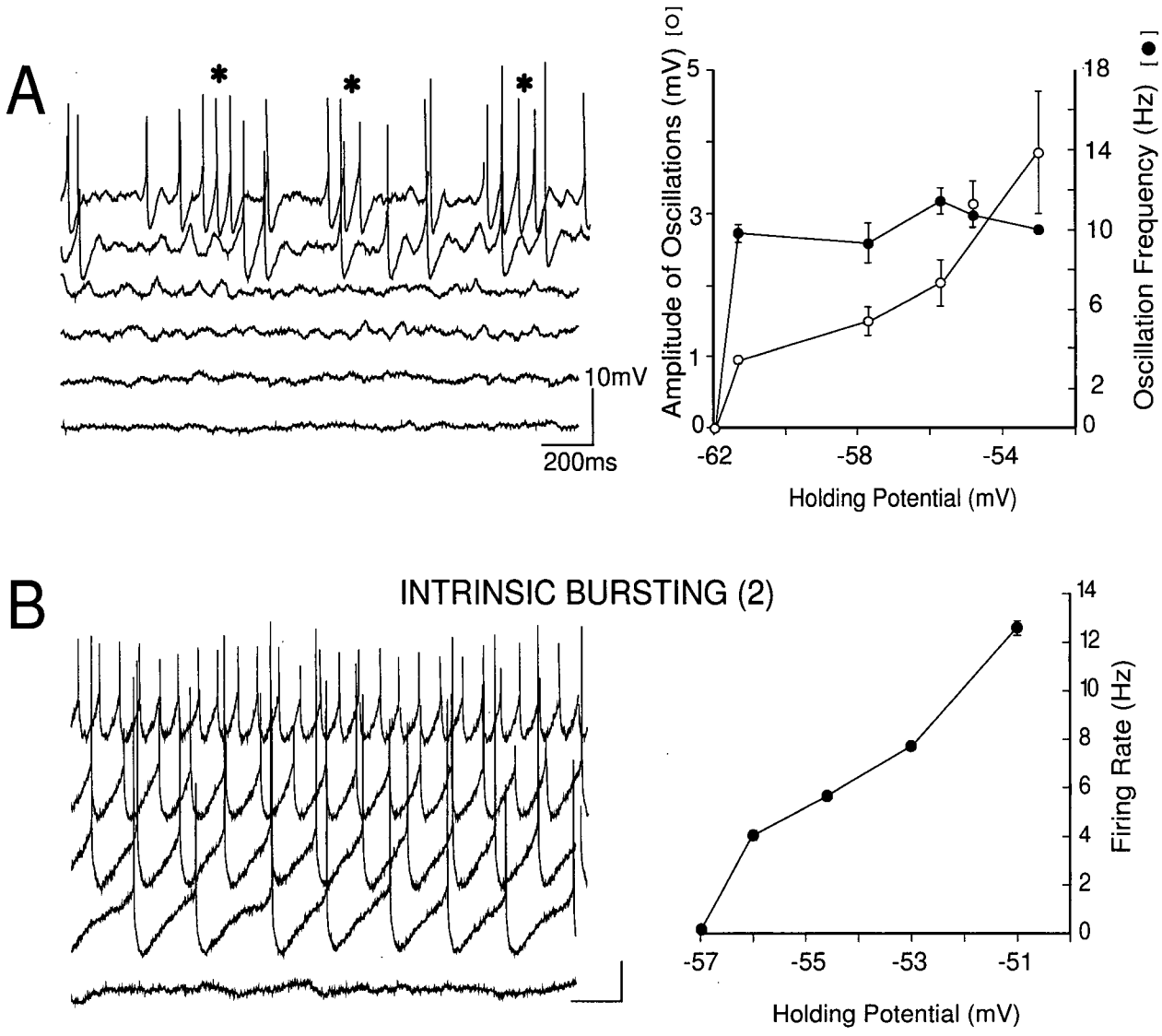

Figure 3-2: Voltage dependent subthreshold membrane oscillations and rhythmic pacemaker-like firing in *IB* PFC neurons. **A)** (LEFT) A third of all *IB* PFC neurons (type-1) recorded at the soma exhibited subthreshold membrane oscillations. When spikes were present they occurred in clusters (*). (Right): The oscillatory frequencies (filled circles) were restricted within a narrow bandwidth of 8-12 Hz perhaps due to strong outward rectification. However, the amplitude of the oscillations (open circles) progressively increased with membrane depolarization. **B)** In contrast, the majority (two thirds) of all *IB* PFC neurons (type-2) fired in a rhythmic pacemaker-like mode with membrane depolarization.

membrane oscillations in these cells (Fig. 3-2A, filled asterisks). The narrow frequency subthreshold oscillations were limited by the voltage-dependent activation of a delayed outward rectifying conductance which also prevented sustained membrane depolarization.

In a second subtype of *IB* neurons (*type 2*, 42 out of 60, 70 %, Fig 3-2B), spike firing was superimposed on the oscillating waves of the membrane potential. In contrast to type-1 *IB* neurons, oscillations in type-2 *IB* neurons were unaffected by membrane outward rectification. As a result, there was a linear increase in firing frequency with membrane depolarization, leading to a broad frequency pacemaker-like firing.

The persistent Na^+ current (I_{NAP}) has been shown to mediate subthreshold membrane oscillations in pyramidal neurons (Alonso & Llinas 1992; Stuart & Sakmann 1995; Stafstrom et al. 1982; 1985). In PFC neurons, the narrow-frequency membrane oscillations were blocked by bath application of TTX (1μM, n=8) or intracellular injection of the lidocaine derivative Na^+ channel blocker QX-314(n=5)(not shown), indicating that they were Na^+ mediated.

Na^+ Potentials

A time-dependent slow membrane inward rectification was observed in most *IB* PFC neurons in the voltage range more positive than -70 mV. This inward rectification resulted in an upward bend in the depolarized range of the V-I plot (Fig. 3-3A). The inward rectification was blocked by bath-application of TTX (1μM) or intracellular injection of QX-314, suggesting that it was mediated by a TTX-sensitive Na^+ current (Fig. 3-3A, n= 9 / 9 cells). This TTX- and QX-314-

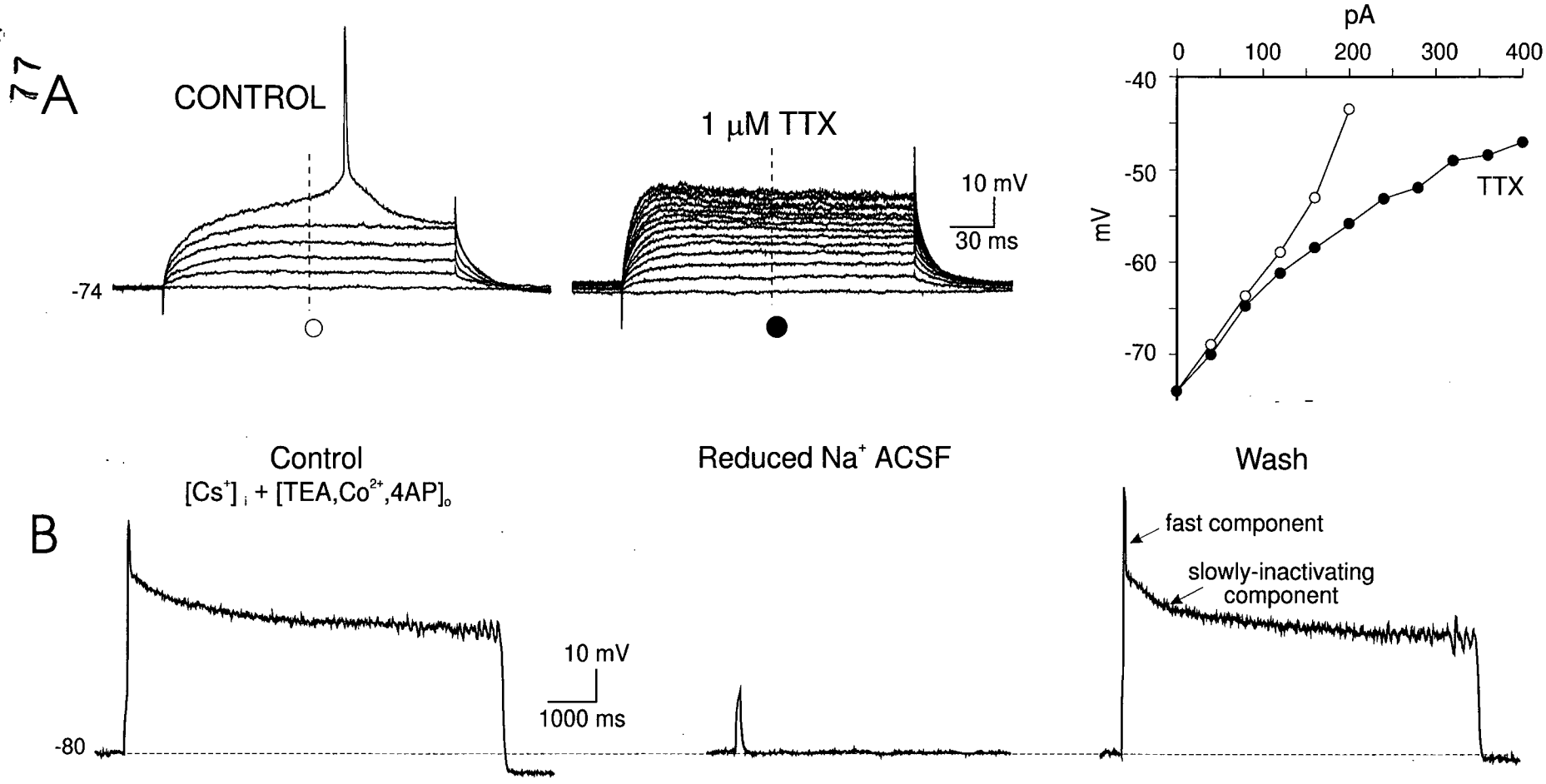

Figure 3-3: Voltage-dependent inward rectification in the depolarized voltage range at the soma of an *IB* PFC neuron. **A)** (Left) The underlying current that mediates the inward rectification in the depolarized range was sensitive to TTX (1 μM). The V-I plot in TTX (filled circles) was linearized relative to the control (open circles). **B)** Following blockade of K^+ and Ca^{2+} currents by $(Cs)_i$, TEA, 4-AP and Co^{2+}, a small depolarizing current step evoked a large plateau potential composed of a fast and slow component. Reduction of Na^+ in the ACSF prevented activation of the plateau.

sensitive inward membrane rectification has been observed previously in other cortical neurons and is the result of I_{NAP} (Connors et al. 1982; Stafstrom et al. 1985; Alzheimer et al. 1993). In current-clamp mode this persistent Na^+-mediated current was observed as a long-lasting plateau potential as shown in Fig 3-3B. Reduction of $[Na^+]_O$ to half (63mM) markedly reduced the amplitude and duration of the plateau, confirming that it was Na^+ mediated (Fig 3-3B, n=3).

Ca^{2+} Potentials

In PFC neurons as with other types of central neurons (Franz et al., 1986; Llinas, 1986), low threshold Ca^{2+} spikes (LTS) were often triggered following the offset of a hyperpolarizing current pulse. The LTS was observed most consistently in *IB* and *ROB* PFC neurons. The generation of the LTS depended on multiple factors. At membrane potentials more positive than -55mV, low threshold Ca^{2+} currents are inactivated (Tsien et al. 1988). Hyperpolarizing the membrane from -55mV to potentials more negative than -70 mV for 100-500 ms is necessary to achieve a voltage- and time-dependent removal of inactivation of the low threshold Ca^{2+} conductance (Fig.3-4A). The LTS also shows a time-dependent increase in amplitude which is observed most clearly when Na^+ and inwardly rectifying K^+ conductances are blocked by TTX (1μM) and CsCl (2.5 mM), respectively (Fig. 3-4A). Consistent with a previous study performed in frontal cortical neurons (Ye and Akaike, 1993), the LTS is blocked by 100-400μM Ni^{2+} (Fig 3-4A).

Figure 3-4: Characteristics of low threshold Ca^{2+} spikes (LTS) and currents in PFC neurons. **A)** (Left) In TTX and $(Cs)_o$, a LTS was evoked at the rebound of a hyperpolarizing current step. This LTS was blocked by bath application of 200μM Ni^{2+}. (Right) A graph showing the time-dependent activation of the LTS, with progressive increases in LTS amplitude as the duration of the hyperpolarizing pulses were prolonged. Open circles = TTX (0.5 μM), Filled squares = TTX + Cs^+ (2 mM), Filled triangles = TTX + Cs^+ Ni^{2+} (200μM). **B)** Voltage-clamp analysis of the low threshold Ca^{2+} current in PFC neurons. (Left) In the presence of internal QX-314 and Cs, voltage steps from -105mV to -65 / -50mV evoked a transient inward current that was blocked by 200μM Ni^{2+}. (Right) A graph showing the voltage dependent activation of the low threshold current in the control (open circles), and in Ni^{2+} (open squares). The filled circles are the control minus the Ni^{2+} response and illustrates the total current that is blocked by Ni^{2+} .

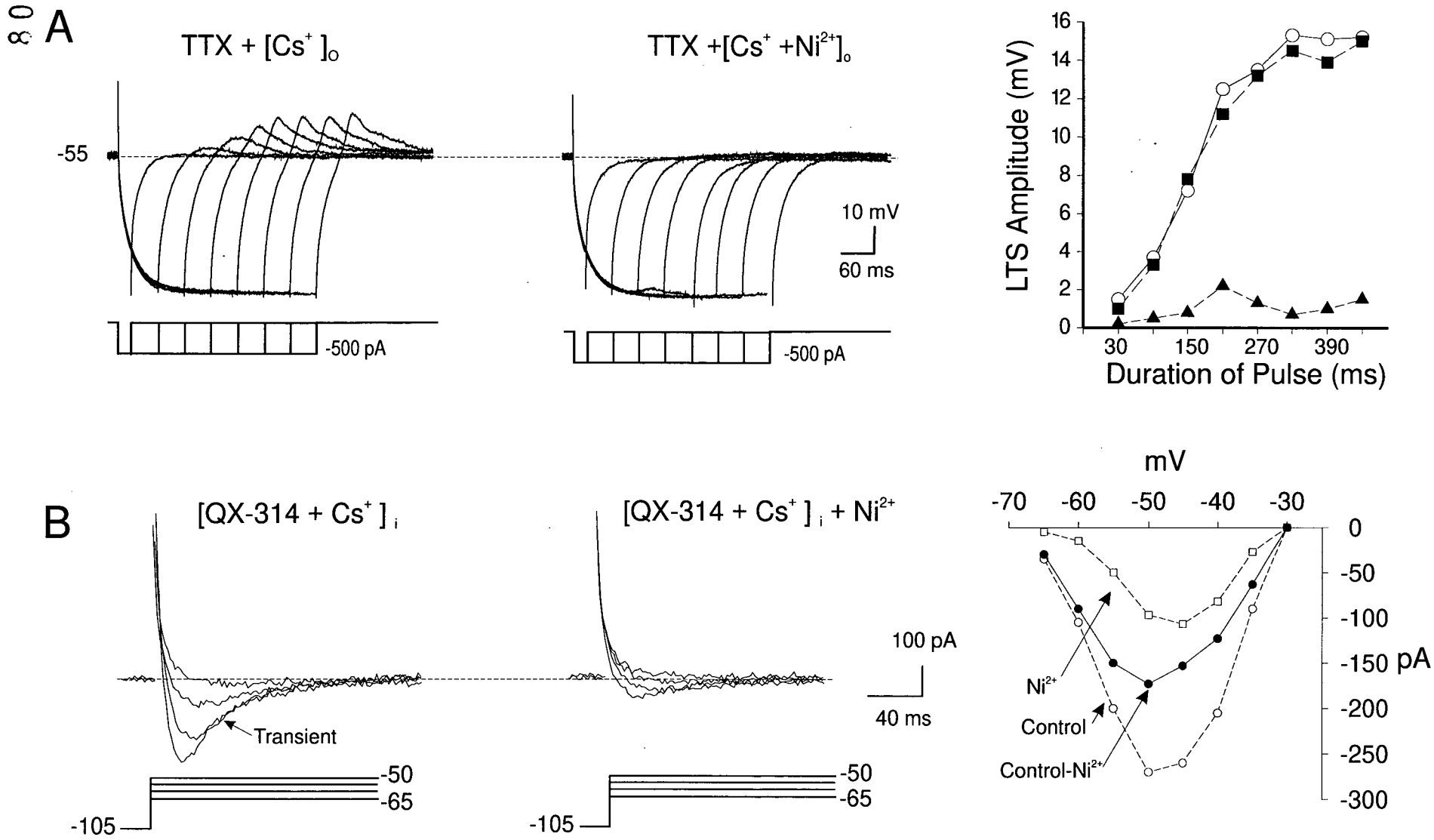
A
TTX + [Cs+]o
TTX +[Cs+ +Ni2+]o
-55
10 mV
60 ms
-500 pA
-500 pA
LTS Amplitude (mV)
16
14
12
10
8
6
4
2
0
30
150
270
390
Duration of Pulse (ms)
B
[QX-314 + Cs+] i
[QX-314 + Cs+] i + Ni2+
Transient
100 pA
40 ms
-50
-65
-105
-50
-65
-105
mV
-70
-60
-50
-40
-30
0
-50
-100
-150 pA
-200
-250
-300
Ni2+
Control
Control-Ni2+

In 2 PFC neurons studied under voltage-clamp, a Ni^{2+}-sensitive low threshold Ca^{2+} current was evoked by delivering a series of voltage steps from a holding potential of -105mV (Fig 3-4B). The low threshold current increased in size with larger depolarizing steps. Thus in PFC neurons there is a time and voltage-activated low threshold Ca^{2+} current activated in the subthreshold voltage range.

In PFC neurons, other Ca^{2+} currents were also activated in the subthreshold voltage range. A 'hump' potential was evoked by intracellular current pulses prior to action potential initiation (Fig 3-5A). Although slightly reduced, this 'hump' potential was still present following blockade of Na^+ currents by QX-314 or TTX (n>100).

Following blockade of Na^+ channels and/or K^+ channels (by QX-314 and $(Cs)_i$), the 'hump' potential was observed prior to the initiation of a high threshold Ca^{2+} spike (Fig 3-5B). Although the 'hump' potential was activated in the subthreshold voltage range, Ca^{2+} spikes were evoked only following blockade of Na^+ channels and at membrane potentials above action potential threshold. In some neurons (~ 30%) the 'hump' potential was not prominent until $(Cs^+)_i$ or 4-AP was present to block K^+ currents (Fig. 3-5C). In all cells tested, the 'hump' potential was greatly reduced or blocked by 200μM Cd^{2+} (n=9/9, Fig 3-5C), indicating that it was mediated by a Ca^{2+} current.

Ca^{2+} channels are distributed throughout the soma and dendrites of pyramidal neurons (Westenbroek et al. 1992). In order to determine the site where the 'hump' potential was initiated, Cd^{2+} was applied focally via a pressure-

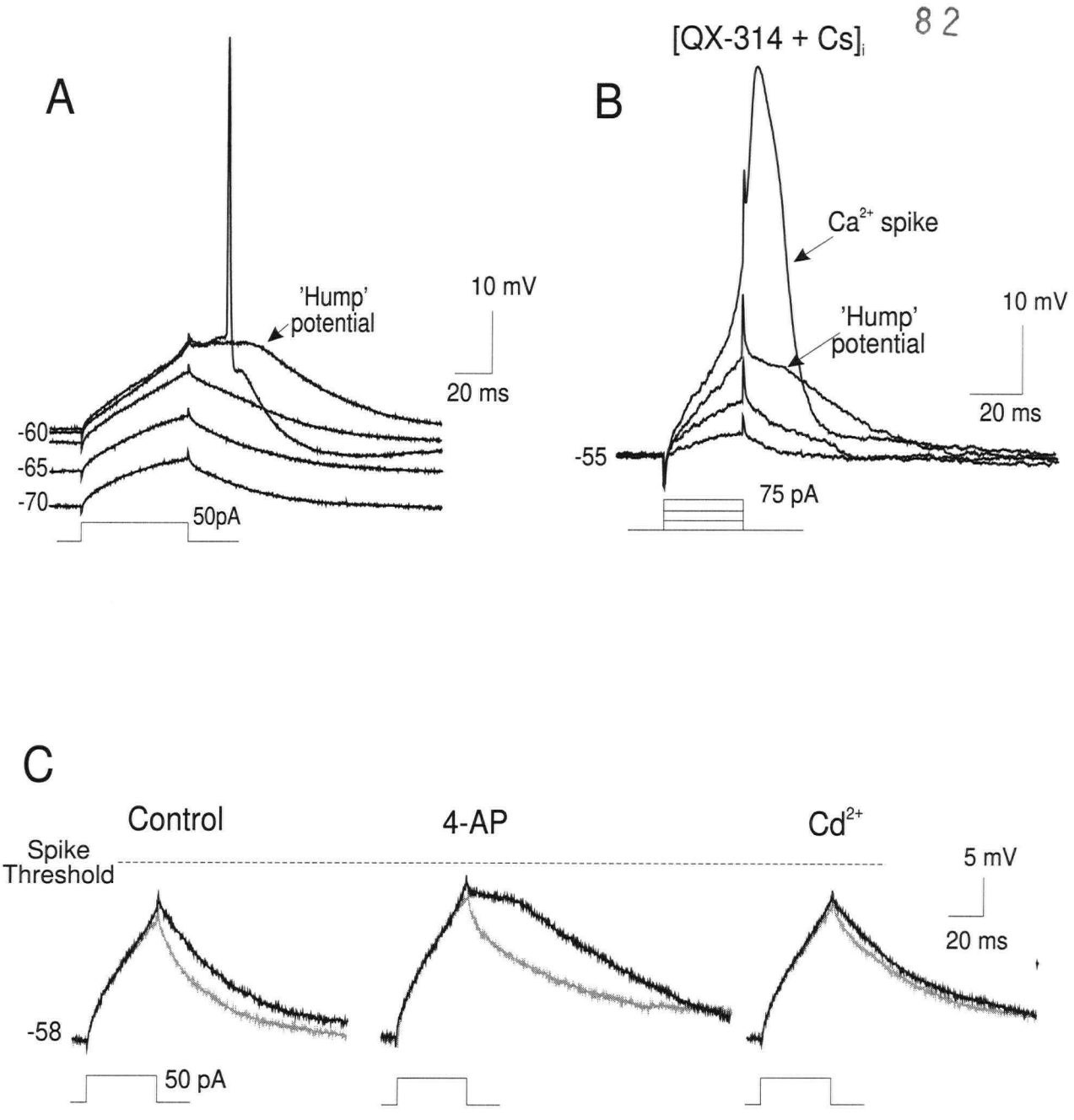

Figure 3-5: The subthreshold 'hump' potential. **A)** A short depolarizing current step often triggered a large 'hump' potential prior to an action potential during progressive membrane depolarization. **B)** The 'hump' potential was reduced in amplitude but still present in internal QX-314 and Cs^+. Larger current pulses triggered a Ca^{2+} spike under these conditions. **C)** In the subthreshold voltage range, the 'hump' potential was evoked by a depolarizing current pulse more readily in the presence of 4-AP (2mM), and was eliminated completely by Cd^{2+} (200μM).

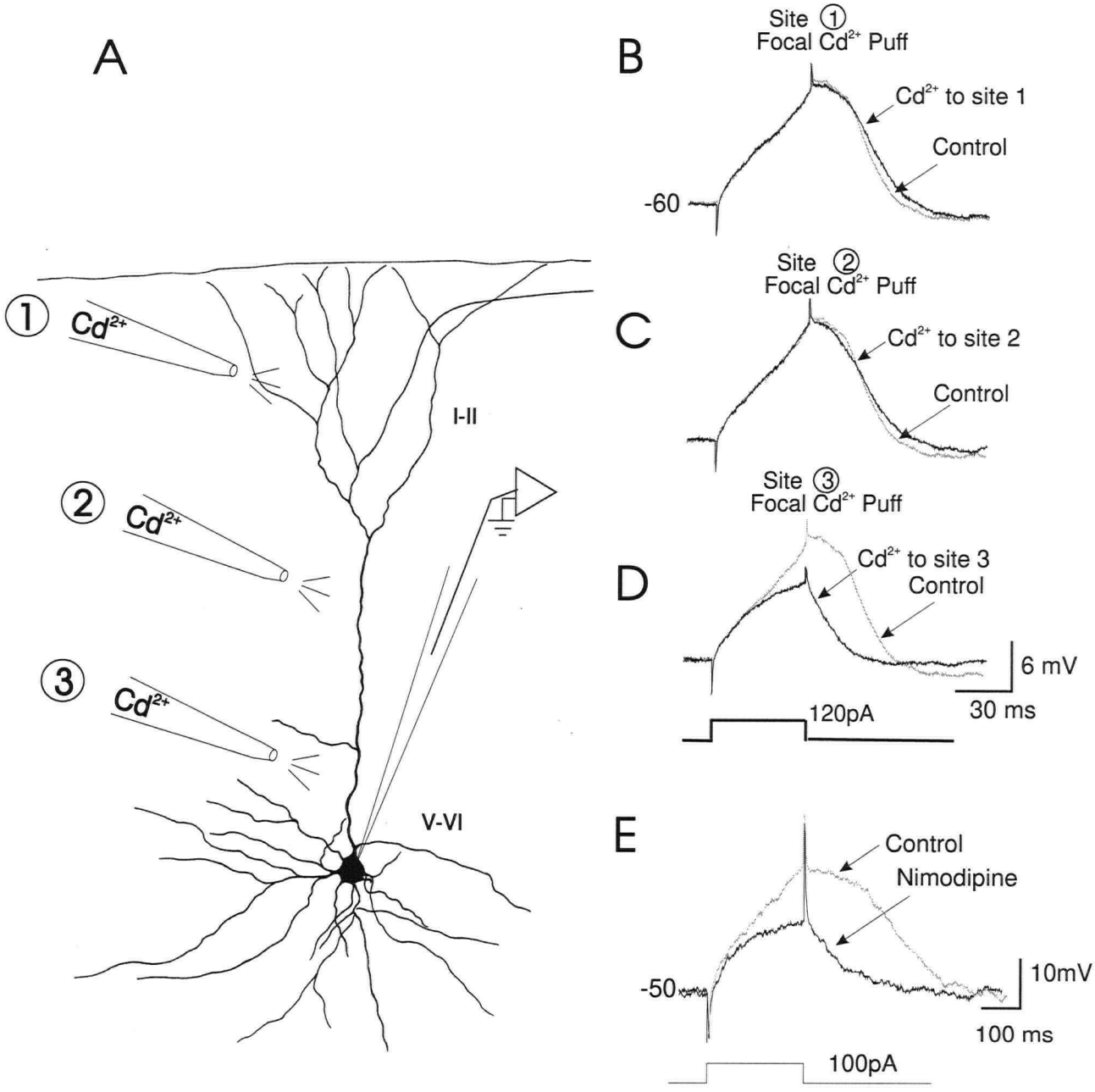

Figure 3-6: Sites of electrogenesis of the 'hump' potential. **A)** Camera Lucida tracing of a typical layer V PFC neuron and three sites where Cd^{2+} was applied focally: The apical tuft (site 1), the distal apical dendritic stem (site 2) and the proximal apical dendritic stem (site 3) during somatic recordings with pipettes filled with QX-314 and Cs^{+}. The 'hump' potential was evoked by an intrasomatic depolarizing current pulse (50ms, 120pA). **B)** Focal Cd^{2+} application to the apical tuft (site 1) or **C)** distal apical dendritic stem (site 2) had no effect on the 'hump' potential recorded from the soma. **D)** The 'hump' potential was blocked by focal Cd^{2+} application to the proximal apical dendritic stem (site 3). **E)** Bath application of the L-type Ca^{2+} channel blocker, Nimodipine (10μM) also greatly reduced the 'hump' potential.

ejection pipette to block Ca^{2+} channels in specific regions of the neuron prior to evoking the 'hump' potential via an intracellular current pulse (Fig 3-6A). Cd^{2+} was applied focally by pressure ejection to the apical dendritic tuft (>500μM from the soma, <100μM from pia, site 1 Fig. 3-6B), the distal dendritic stem (300-500μM from soma site 2, Fig. 3-6C), or the proximal dendritic stem/soma (100-300μM from soma, site 3, Fig. 3-6D). The 'hump' potential was blocked specifically by Cd^{2+} application to site 3, the apical dendritic stem/soma (Fig 3-6D). Cd^{2+} application to the same site also reduced Ca^{2+} spikes, as shown previously by Yuste et al. (1994) (not shown, n=4). Given that L-type Ca^{2+} channels are clustered specifically at the soma and the base of the apical dendrite of pyramidal neurons (Westenbroek et al. 1990; Magee & Johnston 1995b), and L-type Ca^{2+} channels mediated Ca^{2+} influx in the subthreshold voltage range (Avery & Johnston 1996; Kavalali & Plummer 1996; Hernandez-Lopez et al. 1997), the effects of L-type Ca^{2+} channel antagonists on the 'hump' potential were examined. Bath application of the L-type Ca^{2+} channel antagonists nimodipine or nifedipine, greatly reduced the 'hump' potential in cells recorded with QX-314 and Cs^{+} containing electrodes (Fig 3-6E, n=4/4). Thus L-type Ca^{2+} channels proximal to the soma were important for initiating the 'hump' potential.

Ca^{2+} currents also contribute to the firing pattern of PFC neurons in the *suprathreshold* voltage range where they played an important role in burst generation, as in other cortical neurons (Friedman & Gutnick 1989; Connors et al. 1982). As shown in Fig 3-7, bursts typically rode atop a DAP in *IB* and *ROB* PFC neurons. Removal of extracellular Ca^{2+} (plus an addition of 10 mM Mg^{2+})

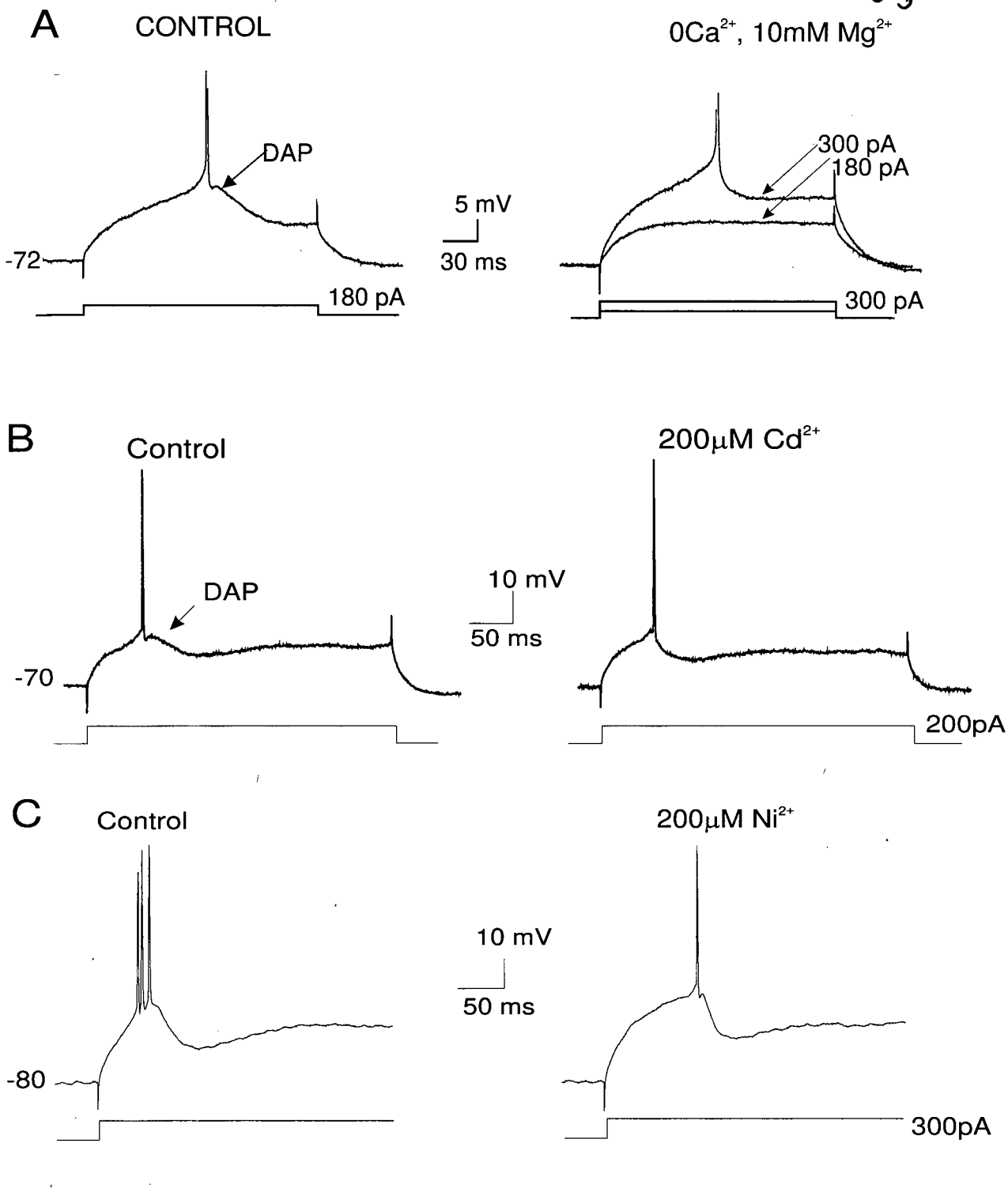

Figure 3-7: Contribution of Ca^{2+} currents to DAP generation at the soma. **A)** Reduction of $(Ca^{2+})_o$ and elevation of $(Mg^{2+})_o$ eliminated the DAP in PFC neurons. Larger current pulses were required to evoke spikes in reduced Ca^{2+} media. **B)** Bath application of the high threshold Ca^{2+} channel blocker, Cd^{2+} also reduced the DAP. **C)** Bath application of the low threshold Ca^{2+} channel blocker, Ni^{2+} reduced the DAP and bursting evoked by depolarizing current pulses from negative holding potentials.

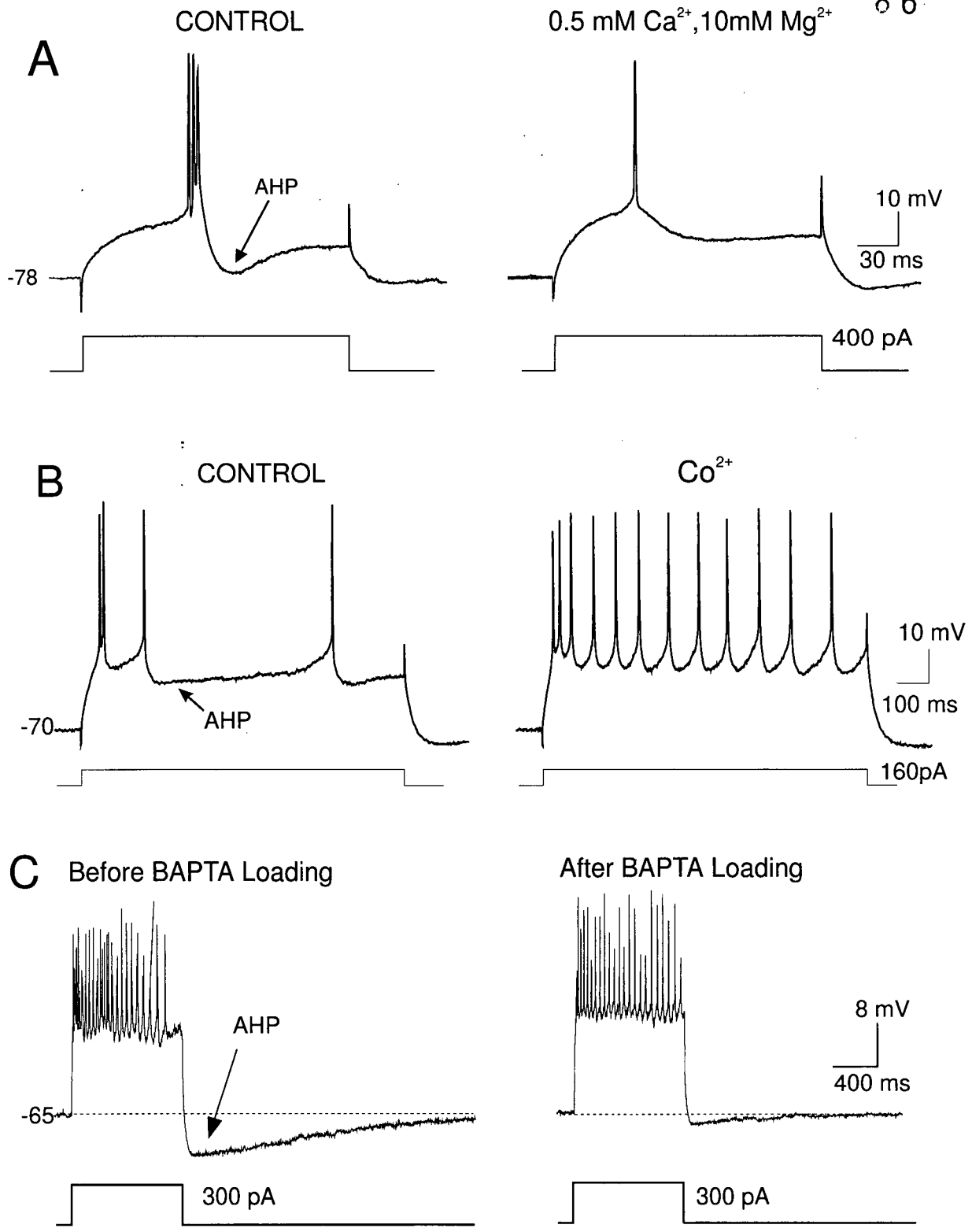

Figure 3-8: Contribution of Ca^{2+} currents to AHP generation. **A)** Reduction of $(Ca^{2+})_o$ and elevation of $(Mg^{2+})_o$ eliminated the slow AHP in bursting PFC neurons. **B)** Bath application of the high threshold Ca^{2+} channel blocker, Co^{2+} also reduced the slow AHP allowing more spikes to be triggered by the same depolarizing current pulse. **C)** Chelation of $(Ca^{2+})_i$ by BAPTA reduced the post-burst AHP evoked by large depolarizing current pulses.

blocked the post-spike DAP (Fig. 3-7A). The DAP was dependent on high threshold Ca^{2+} currents as it was greatly reduced by bath application of 200μM Cd^{2+} (Fig 3-7B). If the V_m was held more negative than -60mV, the DAP was also reduced by the low threshold Ca^{2+} channel blocker Ni^{2+} (200μM, Fig. 3-7C, n=3). Thus both low and high-threshold Ca^{2+} currents contributed to the DAP underlying bursts in PFC neurons.

K^+ currents: AHP

Ca^{2+} channels in PFC neurons also contributed to the generation of after hyperpolarizations (AHPs). In *IB* and *ROB* cells, the bursting complex and the accompanied post-burst AHP was eliminated by; 1) lowering $[Ca^{2+}]_O$ (0.5mM) and elevating $[Mg^{2+}]_O$ (10mM) (Fig 3-8A, n=3), 2) bath application of the Ca^{2+} channel blockers Cd^{2+} or Co^{2+} (Fig. 3-8B, n=5) or, 3) diffusion of the internal Ca^{2+} chelator BAPTA (Fig. 3-8C, n=5). Following blockade of the AHP by Co^{2+} or Cd^{2+}, the firing pattern of *IB* and *ROB* cells was changed from bursts with interspersed AHPs to more or less repetitive spike output (Fig 3-8B). Thus Ca^{2+} currents modulate the AHP in PFC neurons and indirectly regulate the spike output pattern.

K^+ Currents: I_D

The effects of strong membrane depolarizations in PFC neurons were counteracted by K^+ currents. Following Na^+ channel blockade by TTX or QX-314 a clear membrane outward rectification was revealed. In *IB* and *RS* cells the membrane response following an incremental series of long (1-3 sec.) sustained

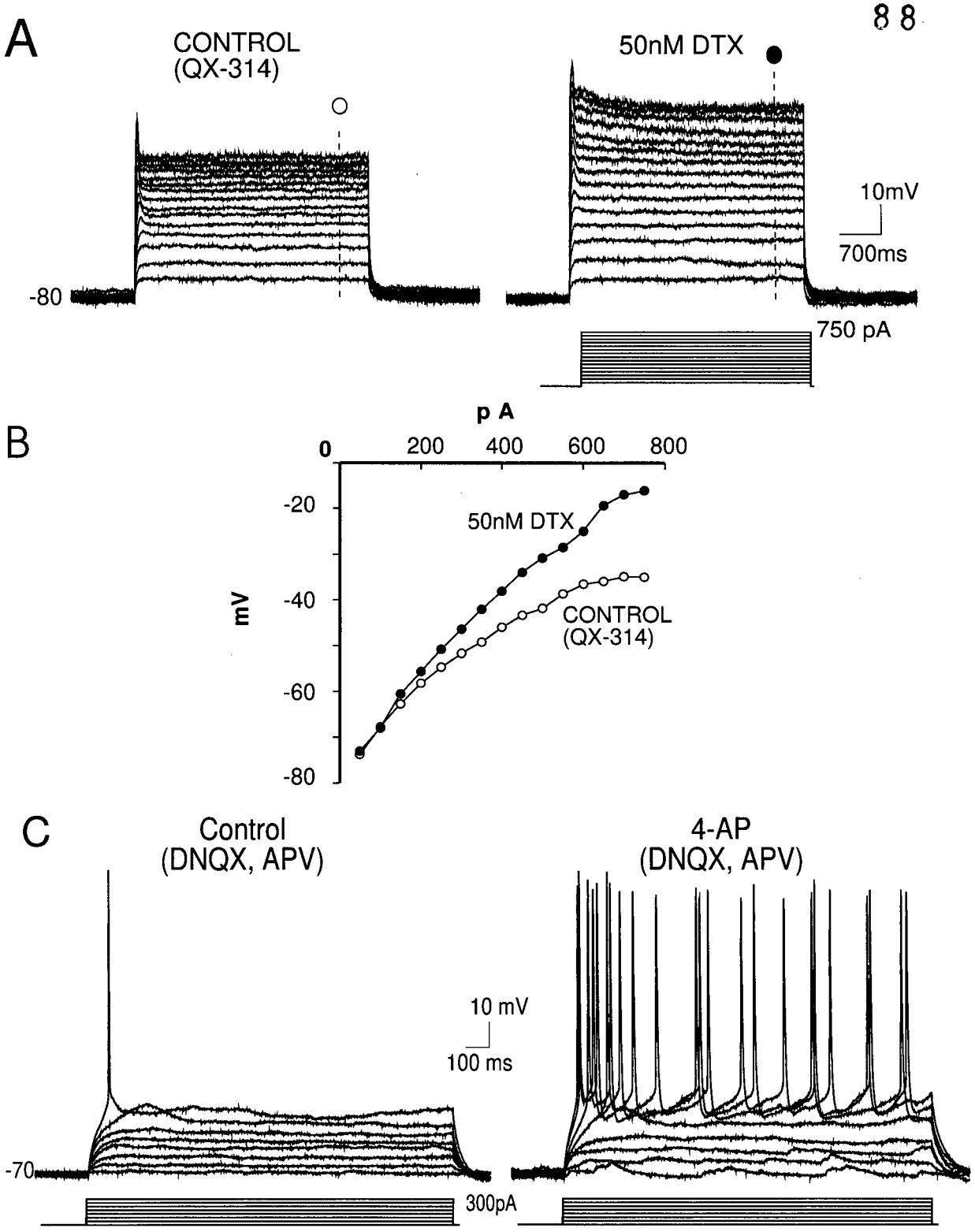

Figure 3-9: Outward rectification in the depolarized voltage range. **A)** In the presence of QX-314 pronounced membrane outward rectification was evoked by depolarizing current pulses and blocked by dendrotoxin (DTX, 50nM). **B)** Application of DTX linearized the V-I plot. **C)** In the presence of DNQX (10μM) and APV (50μM), to block synaptic transmission, bath application of 4-AP (2mM) greatly increased spike firing, probably due to blockade of I_D.

depolarizing pulses revealed a delayed membrane outward rectification which tended to bring the V_m towards rest (Fig. 3-9A). This outward rectification counteracted depolarizions due to injections of positive current. Hence, the steady-state V-I plot showed a typical downward bend as illustrated in Fig. 3-9B. The outward rectification was blocked by Dendrotoxin (50nM, n=4), 4-AP (2 mM, n=7) , or $(Cs^+)_i$ (n=10) causing an increase in the slope of the voltage-current plot (Fig 3-9A,B). Since the outward rectification was blocked by 4-AP and dendrotoxin it was likely mediated by I_D. However, there are many subtypes of slowly-inactivating K+ currents (Foehring & Surmeier 1991), and in the absence of voltage-clamp data, it is presently unclear as to which subtypes contribute to the outward rectifiction observed in the present voltage traces. At membrane potentials more negative than -45mV, I_D activates quickly but is slow to inactivate (Storm, 1993; Hammond & Crepel 1992) and therefore counteracts the effects of prolonged membrane depolarization and repetitive spiking. As shown in Fig 3-9C, blockade of I_D by 4-AP evokes repetitive and continuous firing in PFC neurons (see also Hammond & Crepel 1992).

Mixed K+/Na+ current: I_h

In the hyperpolarized voltage range, a transient "sag" potential was observed from the soma of < 10% PFC cells, all but one was of the *ROB* type. In the hyperpolarized voltage range this "sag" tended to push the membrane potential back towards resting values (Fig 3-10). This "sag" potential was likely mediated by the mixed cationic conductance I_h, and was absent 10min after bath

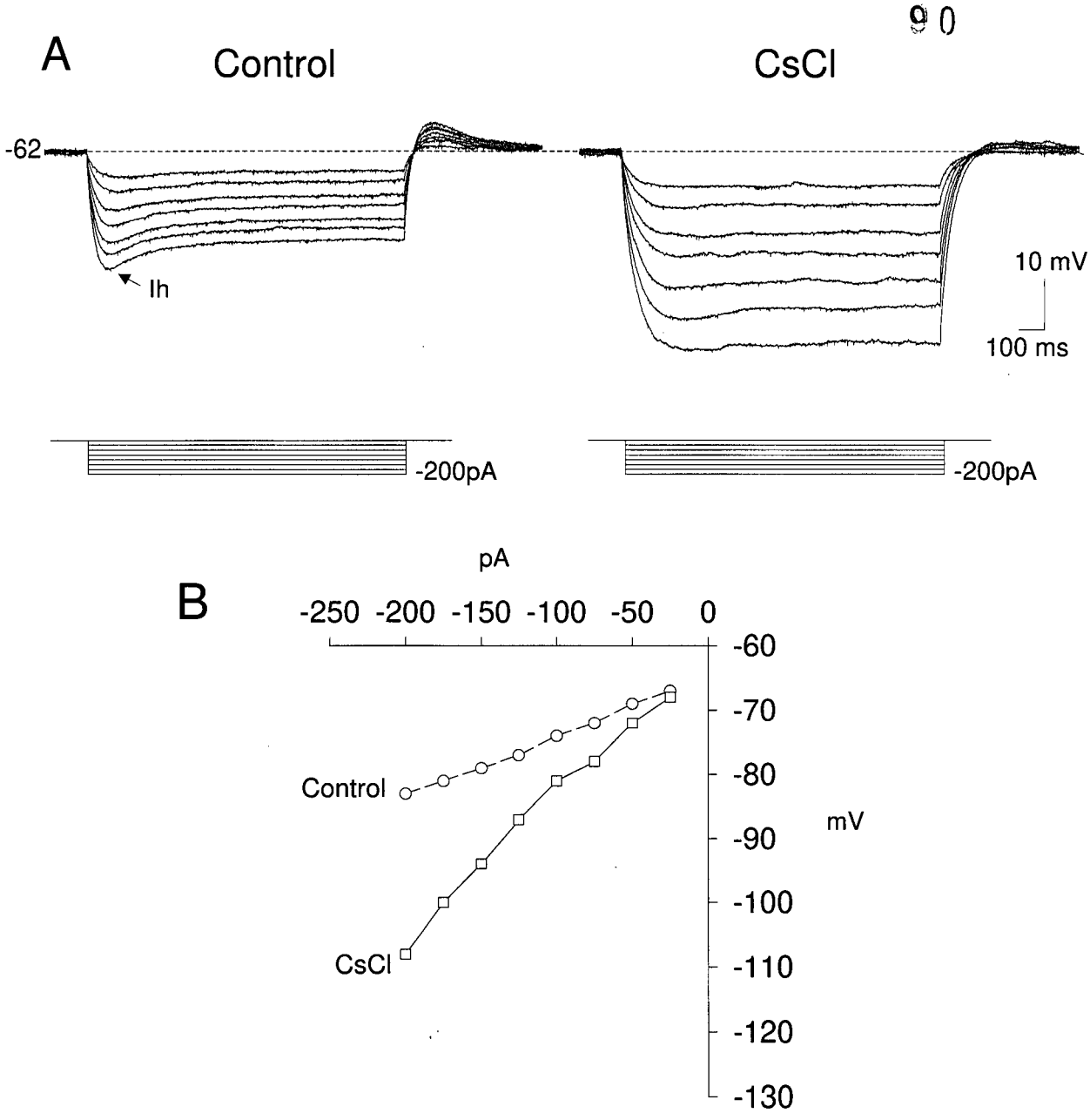

Figure 3-10: Anomalous rectification in the hyperpolarized voltage range. **A)** In a small minority of PFC neurons recorded from the soma, hyperpolarizing current pulses evoked a 'sag' potential characteristic of the mixed hyperpolarizing-activated mixed cationic current, I_h. Blockade of the I_h-like 'sag' by CsCl increased the passive R_{in} and τ. **B)** V-I plot showing that blockade of the 'sag' by CsCl removed inward rectification in the hyperpolarized voltage range and increased the slope resistance.

application of CsCl (2mM) in an *IB* neuron (Fig 3-10A) (Spain et al. 1987; 1991). Blockade of I_h had two important effects on PFC neurons: 1) The input resistance (Fig 3-10B) and membrane time constant were increased. 2) The depolarization following the offset of the hyperpolarizing pulse was correspondingly reduced. This indicates that I_h in these neurons speeds the passive membrane response and may enhance the effects of depolarizing inputs arriving after membrane hyperpolarization.

Discussion

Intrinsic bursting (*IB*) PFC neurons were the most frequently encountered cell type in layers V-VI. *IB* cells fired an initial spike doublet, followed by single spikes with post-spike DAPs. These neurons had a single thick main ascending apical dendrite. Bursting cells with thick ascending apical dendrites have also been found in the deep layers of rat somatosensory and visual cortices (Chagnac-Amitai et al., 1990; Mason and Larkman 1990). *IB* had basal dendriteswhich were confined within layer V-VI. Thus, this type of neuron may only be influenced by inputs to deep layer V-VI, from adjacent PFC neurons or from regions such as the thalamus.

Firing Threshold

The firing threshold of PFC neurons was determined by the interaction of at least three cationic conductances. First, up to 30 mV from resting, a TTX-sensitive, slowly inactivating Na^+ current (I_{NAP}), was clearly activated in *RS* and *IB* cells. This current was also responsible for the inward rectification of these

cells in the subthreshold voltages and had a functional role in setting the firing threshold for regenerative fast repetitive spike firing (Schwindt, 1992).

Second, the depolarizing action of this current was counteracted by a 4-AP sensitive, outwardly rectifying K^+ current. This K^+ current was inactive above -50mV and required prior hyperpolarization to remove the inactivation fully (Hammond & Crepel 1992). While this current was activated in 100-200ms, it took many seconds to inactivate (Storm 1988; Hammond & Crepel 1992). This voltage-dependent ionic current resembles the slowly inactivating outward K^+ current, I_D or I_{Ks} (Foehring and Surmeier 1993; Schwindt et al., 1989; Storm, 1988; Hammond and Crepel, 1992). As I_D functionally prevented excessive and sustained membrane depolarization, it effectively delayed spike firing. Because both the Na^+ and K^+ currents were slow to inactivate, they may be involved in regulating the neurons general membrane excitability over long time courses.

The third current involved in regulating membrane excitability in the subthreshold voltage range is the transient low threshold Ca^{2+} current that mediates the low threshold spike (LTS) present in *IB* and *ROB* cells. Although an LTS can be evoked from resting potential ($\approx$ -75 mV), it is more pronounced following prior membrane hyperpolarization. The slowly inactivating Na^+ currents may provide steady-state inward rectification, the magnitude of which can be transiently enhanced by the rapidly inactivating LTS (Sutor and Zieglgänsberger, 1987). Thus, the transient LTS contributes to subthreshold membrane excitability, especially when the neuron received prior membrane hyperpolarization (see below).

Subthreshold Membrane Voltage Oscillations

All 4 PFC cell types showed subthreshold membrane voltage oscillations in response to a sustained membrane depolarization. All *RS* and a third of the *IB* neurons (*type 1*) oscillated in a narrow frequency range (5-12 Hz). Oscillations in this frequency range have been reported previously in the PFC, cingulate, association and entorhinal cortices (Alonso and Llinas, 1989; Alonso and Klink, 1993; Llinas et al., 1991; Steriade et al., 1993). These oscillations were abolished by bath-application of TTX or intracellular injection of QX314, suggesting that they were mediated by an intrinsic Na^+ current, most likely the same slowly inactivating Na^+ current that underlies the subthreshold inward rectification discussed above (Alonso and Klink, 1993; Alonso and Llinas, 1989; Klink and Alonso, 1993; Stafstrom et al.,1982;1985; Taylor, 1993). Computer simulations suggest that the range of these oscillations may be determined by the action of I_D (Wang 1993). In addition, depolarizing and hyperpolarizing synaptic inputs may provide an extrinsic regulation of membrane oscillations in vivo when the entire cortical network is intact (Cowan and Wilson, 1994; Steriade et al., 1993).

Neuronal membrane oscillations may functionally synchronize the activity of a given network of neurons, thus ensuring that neuronal groups that resonate at the same frequency will fire in synchrony. A common mode of oscillation shared by cortical neurons from adjacent columns (often connected by horizontally projecting pyramidal neurons) could constitute a synchronizing

mechanism from which the activity patterns of multiple inputs are co-ordinated (Alonso and Klink, 1993; Singer, 1993; Lampl and Yarom, 1993). In the PFC, membrane oscillations transferred through the tangentially projecting axons of *IB* and *ROB* neurons may synchronize firing at sites both proximal and distal to the site of generation.

Low Threshold and High Threshold Ca^{2+} Conductances

Prominent high and low voltage activated Ca^{2+} currents govern the bursting behavior of the *IB* and *ROB* PFC neurons. As activation of the LTS requires removal of inactivation by voltage excursions from about -55 to > -70 to -100 mV for at least 50-100 ms, the LTS may be triggered physiologically as a rebound response to a powerful long duration IPSP mediated by $GABA_B$ receptors (Connors et al., 1988). Once activated, the LTS generates a depolarizing envelope which serves to trigger 1-5 fast spikes. The occurrence of this event is dependent on factors such as the length of time which the membrane potential has been hyperpolarized and the time since the last LTS was triggered (Jahnsen and Llinas, 1984; McCormick and Feeser, 1990).

In the subthreshold range a 'hump' potential was also activated. The 'hump' potential was present in TTX or QX-314 but was blocked by the non-selective Ca^{2+} antagonist Cd^{2+} (Seamans et al. 1997). The effects of focal puff application of Cd^{2+} suggested that the 'hump' potential was generated in the proximal apical dendrite. Immunocytohistochemical data which shows a clustering of L-type Ca^{2+} channels along the proximal apical dendrite and soma

of pyramidal neurons (Westenbroek et al. 1990; 1992). Accordingly, the 'hump' potential was blocked or greatly reduced by L-type Ca^{2+} channel antagonists but not the T-type Ca^{2+} channel blocker, Ni^{2+}. Collectively these data suggest that the 'hump' potential was generated by L-type Ca^{2+} channels located proximal to the soma of PFC neurons.

It is believed that L-type Ca^{2+} channels are 'high voltage-activated'. However, based on whole-cell voltage clamp data from cortical neurons (Brown et al. 1993) there may some channel activation in the subthreshold voltage, depending of course, on the threshold of action potential initiation. Given the high density of these channels in regions proximal to the soma, and their large single channel conductance (Tsien et al. 1988), even a little channel activity could produce a significant whole-cell current. Recently using physiological channel densities and kinetic properties of L-type channels derived from previous voltage-clamp studies (Magee & Johnston 1995a,b; Brown et al. 1993) we have shown in a computer model of a PFC neuron, that a hump potential mediated by L-type Ca^{2+} currents is evoked in the subthreshold voltage range (Durstewitz & Seamans 1997). However, there is accumulating evidence for an L-type Ca2+ channel that is active at or near rest, thereby providing significant Ca^{2+} influx in the subthreshold voltage range (Avery & Johnston 1996; Kavalali & Plummer 1996; Hernandez-Lopez et al. 1997; Magee et al. 1995). Moreover, neurotransmitters, such as noreadrenaline are know to shift the activation of L-type Ca^{2+} channels by about 10mV in the hyperpolarized direction, thereby raising the possiblity that, in vivo the subthreshold contribution of L-type Ca^{2+}

channels may be even greater. Thus the traditional classification of L-type channels as "high voltage-activated" may need revision.

Using the present techniques it was not possible to determine whether L-type channels in the soma or proximal apical dendrite made the greatest contribution to the 'hump' potential. However the proximal location of the 'hump' potential may help to amplify distal EPSPs near the soma, as suggested for subthreshold Ca^{2+} potentials in anterior cingulate neurons (Higashi et al. 1991). The contribution of the 'hump' potential to amplification of distal EPSP will be examined in Chapter 5.

A similar Ca^{2+} mediated 'hump' potential has been observed in rat subiculum neurons (Taube et al. 1991) and cat layer V sensorimotor neurons (Stafstrom et al. 1985). However, Stafstrom et al. (1985) argued against a significant Ca^{2+} current in the subthreshold range of sensorimotor neurons, but rather emphasized the importance of I_{NAP} in this voltage range. In contrast, in neurons from the anterior cingulate region of the PFC which is just dorsal to the prelimbic region, subthreshold inward rectification was mediated by both a TTX-sensitive Na^+ current and a Co^{2+} sensitive Ca^{2+} current (Tanaka et al. 1991). Thus in neurons from the PFC there is both Na^+ and Ca^{2+}-mediated inward rectification in the subthreshold voltage range.

In the suprathreshold voltage range, short current pulses triggered large amplitude and long duration Ca^{2+}-mediated high threshold spike following blockade of the Na^+ and K^+ channels by TTX and TEA, respectively. Unique to the *IB* and *ROB* neurons was their ability to elicit regenerative Ca^{2+} spikes once a

single Ca^{2+} spike was triggered (Amitai et al., 1993). Voltage-dependent activation of the dendritic Ca^{2+} spike by incoming synaptic signals, or by back-propagated action potentials from the soma may, in turn, amplify the dendritic synaptic signals (Bernander et al., 1994; Magee and Johnston, 1995; Mel, 1994; Miller et al., 1985; Shepherd et al., 1985). In addition, local Ca^{2+} spike-mediated dendritic depolarizations may briefly relieve the voltage-dependent Mg^{2+} block of the NMDA receptor channel complex, resulting in changes in synaptic efficacy (Hirsch and Crepel, 1990; Sah and Nicoll, 1991). Perhaps most importantly, Ca^{2+} spikes may provide the depolarization and Ca^{2+} entry required to support burst firing in pyramidal neurons (see below).

Burst Generation: The DAP and AHP

IB, *ROB* and *IM* cells all possessed a post-spike DAP. In *IB* cells, the post-spike DAP triggers a second spike resulting in a spike doublet. In *ROB* neurons, a bursting complex was derived from the DAP that followed a single action potential. The DAP is critical for burst generation but mechanisms responsible for this DAP are somewhat controversial. There are at least three hypotheses relating to the origins of the DAP in central neurons.

One hypothesis is that they arise passively due to discharge of capacitive current from the axon or dendrite into the soma following the initial axon potential (Spritzer 1984; Jiang & North 1991).The geometry of bursting and non-bursting cortical neurons is consistent with this hypothesis, since IB cells have a larger apical dendrite which emerges gradually from the soma, while RS cells have an

abruptly emerging apical dendrite (Chagnac-Amitia et al. 1990) with presumably less charge capacity than the thick proximal dendrite of *IB* and *ROB* cells.

The second hypothesis about DAP generation is that it is the result of I_{NAP} (Konnerth et al. 1986; Franceschetti et al. 1995; Guatteo et al. 1996). Low concentrations of TTX which do not affect spike amplitude, reduce the DAP in cortical neurons. This finding is in direct contrast to reports showing that DAP or bursting is reduced or abolished by Ca^{2+} channel blockade in trigeminal motoneurons (Kobayashi et al. 1997), pancreatic β cells (Rosario et al. 1993), hippocampal CA1 and CA3 cells (Shindou et al. 1994; Hablitz & Johnston 1981; Wong & Stewart 1992) and cortical neurons (Friedman & Gutnick 1989; Connors et al. 1982; Tanaka et al. 1991). Likewise, in the present study, removal of extracellular Ca^{2+} or blockade of high or low threshold Ca^{2+} channels greatly reduced DAPs in PFC neurons (Fig 3-7). One resolution of these data with those of Franceschetti et al. (1995) and Guatteo et al. (1996) is that TTX application, while not affecting somatic spike amplitude, may have seriously compromised the back propagation of Na^{+} spikes into the dendrites, thereby decreasing activation of dendritic Ca^{2+} currents. Indeed spike propagation in the dendrites is much less reliable than spike propagation along the axon (P. Mackenzie personal communication). While additional experiments are needed to resolve these issues conclusively, it appears that in most cases Ca^{2+} currents are at least partially responsible for DAP generation and burst discharges in pyramidal neurons.

RS neurons were the only cells which did not posses DAPs. In contrast, these cells exhibited a prominent post-spike AHP which was most likely mediated by a Ca^{2+}- activated K^+ current (Schwindt et al., 1988; 1992). These post-spike AHPs largely determined the degree of spike frequency adaptation during repetitive firing. In *ROB* neurons, a post-burst AHP followed each burst. Both burst firing and post-burst AHPs were dependent on extracellular Ca^{2+} entry since they were abolished in Ca^{2+}-free media. Together, these data suggest a critical role for entry of extracellular Ca^{2+} in triggering bursts and activation of Ca^{2+} dependent K^+ currents that underlie post-burst AHPs as well as the DAP (Schwindt et al., 1988).

Anomalous Rectification in the Hyperpolarized Voltage Range.

Both *IB* and *ROB* neurons show hyperpolarization-activated inward rectification. A weak, time-dependent, cesium-sensitive inward rectification was associated with *IB* neurons recorded with intracellular sharp electrodes. A prominent transient "sag" mediated by an external cesium-sensitive hyperpolarization-activated time-dependent inward rectification was present in ~ 1% of *IB* cells recorded by patch-clamp electrodes and in all *ROB* neurons in the PFC. This transient "sag" is likely to be mediated by voltage- and time-dependent hyperpolarization-activated mixed cationic current, I_h.

This current slowly repolarizes the neuron following prolonged hyperpolarization, e.g., by a $GABA_B$ receptor-mediated IPSP or a post burst AHP (McCormick and Pape, 1990; Kamondi and Reiner; 1991; Schwindt, et al., 1988). The end of the repolarization by I_h may also trigger a rebound LTS-

mediated spike burst. In this manner, the interaction of I_h and the LTS may underlie the unique bursting behavior of *ROB* neurons in the PFC (McCormick and Pape, 1990; Foehring & Waters, 1991).

I_h also served to alter the passive membrane properties of *IB* and *ROB* cells. I_h is open at rest in the dendrites of pyramidal neurons, and speeds repolarization of local EPSPs (Spruston & Stuart 1996). Application of external Cs^+ blocked I_h and greatly enhanced the cell's R_{IN} and τ. Since the voltage change of a membrane is determined by the product of the current flowing across it and the membrane resistance, a decrease in R_{IN} will reduce the amplitude of an EPSP. Since the passive repolarization of a membrane is determined by the membrane τ, a reduction in τ will speed the rate of repolarization. Thus I_h may normally reduce the amplitude and duration of synaptic inputs to PFC neurons, by altering the neurons passive membrane properties. Smaller, faster PSPs may allow the neuron to faithfully respond to fast input patterns while avoiding summation of PSPs.

Functional Considerations.

Much of what we understand about the intrinsic membrane properties of neocortical neurons has been used to explain changes in membrane excitability that ultimately lead to the regulation of firing activity (Schwindt, 1992). The various instrinsic membrane properties described in this Chapter may influence neuronal excitability in the mammalian PFC. For example, computer modeling studies indicate that the ability of PFC neurons to sustain repetitive firing throughout a delay period may depend upon the complex interplay of the slowly

inactivating Na^+ and K^+ currents which regulate firing threshold, and the Ca^{2+}-activated K^+ currents which regulate inter-spike intervals. The membrane oscillations exhibited by layer V-VI PFC neurons may synchronize the output of large groups of PFC neurons, thus allowing a coherent signal to be transmitted to subcortical areas such as the nucleus accumbens for response initiation. Finally, the I_{NAP} and high and low threshold Ca^{2+} currents observed in PFC neurons may amplify synaptic signals as in other types of pyramidal neurons (Gillesen & Alzheimer 1996; Schwindt & Crill 1995; Stuart & Sakmann 1995; Markram & Sakmann 1994). These currents may therefore influence the processing of inputs from regions such as the posterior parietal cortex or thalamus. This may be of particular importance given that the PFC interacts reciprocally with these areas during the performance of a delayed response task (Goldman-Rakic, 1995a; 1995b; Goldman-Rakic & Chaffe 1994; Quintana et al. 1989).

Chapter 4:

Electrophysiological Properties of PFC Neurons: Dendritic Recordings.

Introduction

The preceding chapter examined the intrinsic membrane properties and morphology of layer V-VI PFC neurons recorded from the soma. Stained neurons possessed a long ascending apical dendrite which bifurcated into the fine branches of the apical tuft (see Fig 1-1B and 3-1A). The apical tuft, located in layers I-II is a major receptive zone for synaptic inputs (Peters 1987). Layer II of the PFC receives inputs from a variety of cortical regions including the parietal/somatosensory cortex and temporal/perirhinal cortex and hippocampus (Conde et al. 1995; Goldman-Rakic 1988; Hirose et al. 1992; Mitchell & Cauller 1997; van Eden et al. 1992). These inputs are important for PFC-dependent working-memory processes since inputs from the parietal and temporal cortex influence unit activity in the PFC and performance of delayed response tasks (Fuster et al. 1985; Quintana et al. 1989; Wilson et al. 1993) and blockade of hippocampal-PFC interactions impaired delayed responding in the rat (Floresco et al. 1997).

The apical dendrite of layer V PFC neurons extends a considerable distance (500-700μm) from the soma (Fig 1-1). A number of intervening factors influence the transference of signals from the apical dendrite to soma. For instance, EPSPs arriving in the apical tuft are strongly filtered by the dendrite's

passive cable properties before reaching the soma (e.g. see Cauller & Connors 1992; Johnston et al., 1996; Mel 1994; Spruston et al. 1994; Yuste et al., 1996), while strong K^+ currents limit depolarization of the distal dendrites of pyramidal neurons (Hoffman et al. 1997; Durstewitz & Seamans, 1997). It is also thought that Na^+ (Schwindt & Crill 1995) and Ca^{2+} (Bernander et al., 1994; Mel, 1994; Shepherd et al., 1985) currents located along the apical dendrite amplify distal EPSPs. Although Ca^{2+} and Na^+ imaging studies have shown that significant influx of these ions into the dendrites of pyramidal neurons occurs following synaptic stimulation or back-propagating action potentials (Jaffe et al. 1992; Johnston et al. 1996; Müller & Connor, 1992; Miyakawa et al. 1992; Rehger & Tank 1992; Schiller et al. 1995; Svoboda et al. 1997; Yuste et al. 1994) the relative contribution of Na^+ and Ca^{2+}-dependent potentials to the electrical properties of pyramidal neurons are unclear. Moreover, recordings have never been made from the dendrites of PFC neurons. For these reasons it is difficult to determine how layer V neurons process synaptic inputs to their dendrites based solely on recordings from the soma. The goal of the present Chapter was to investigate the intrinsic membrane properties of the apical dendrites of layer V PFC neurons in order to gain insights into how these neurons process and integrate synaptic signals from other cortical regions.

Results

Whole-cell patch-clamp recordings were made from the apical dendritic tuft (n=15) or apical stem (n=10) of layer V PFC neurons. Two additional apical

tuft recordings were made from neurons whose soma was located in layer III. All recordings were made using the 'blind' approach except 3 from the apical stem which were performed under visual control with the aid of differential interference contrast optics enhanced with infrared video microscopy. All but 4 neurons were stained for biocytin and the recording site was often observed as a small notch along the dendrite. Dendritic recordings made from the apical tuft were analyzed separately from recordings made from the apical stem. Since simultaneous recordings from the soma and dendrite were not performed, it was not possible to accurately determine the somatic cell type from which the dendritic recordings were made. However, based on the morphological features of the biocytin-stained neurons, most were of the *IB* type.

Passive Membrane Responses

The membrane response of the apical tuft, apical stem and soma as assessed by patch-clamp techniques are presented in Table 3.

Table 3: Regional Membrane Properties of PFC Neurons

Site	N	Resting V_m (mV)	R_{IN} (MΩ)	τ (ms)	Strong I_h	Threshold AP (mV)	sEPSP Ampl. (mV)	sEPSP τ (ms)
Apical Tuft	18	-58 ± 1.7 -71 to -48	158 ± 22 60 to 350	10 ± 1.8 2.2 to 22	42%	-14±2.7 -37 to -1	2.6 ±0.3 0.9 to4.5	14.5 ± 2 5.1 to 28
Apical Stem	10	-57 ± 1.3 -64 to -53	162 ± 19 100 to 274	18 ± 1.8 8.5 to 25	40%	-33±2.5 44 to 22	2.4 ±0.3 1.3 to 3.9	22 ± 3.5 10.7 to 38
Soma	13	-66 ± 1.7 -75 to -63	163 ± 17 65 to 268	32.6 ± 3 16.4 to 55	0.7%	-44 ±0.7 -49 to -41	4.1 ±0.5 2.3 to 6	69 ± 7.3 24 to 99

In each box, values on top are Means ± S.E.M., while values on bottom are the absolute ranges.

The apical tuft dendrites had a mean resting V_m of -58.6 ± 2.7mV and a mean R_{IN} of 158 ± 21.9MΩ (range: 60 MΩ to 350 MΩ). The time course of the membrane voltage response to a hyperpolarizing current pulse could be fitted by one or two exponentials with the longest τ of 10 ± 1.8ms, but varied considerably from cell to cell with a range between 2.3 - 22 ms (Fig 4-1B). Spontaneous EPSPs (average amplitude: 2.6 ± 0.28mV) recorded from the apical tuft repolarized with a τ of 14.5 ± 2.18 ms (Fig 4-1B).

The apical dendritic stem had a mean resting potential of -57.2 ± 1.3mV. The mean R_{IN} recorded from the apical stem was 162.2 ± 19.7 MΩ (range: 100 MΩ to 274 MΩ). In the apical stem, the time course of the membrane voltage response to a hyperpolarizing current pulse could be fitted by one exponential with mean time constant of 17.8 ± 1.8 ms (range: 8.5 to 25ms)(Fig 4-1B). Spontaneous EPSPs (average amplitude: 2.4 ± 0.26mV) recorded from the apical stem repolarized with a τ of 22.5 ± 3.5 ms.

For comparison, τ of the membrane response to a hyperpolarizing current pulse recorded from the soma of *IB* cells using whole-cell patch-clamp techniques was 39.9 ± 2.9 ms (Fig 4-1B, n=7), while spontaneous EPSPs recorded at the soma repolarized with a τ of 69.9 ± 7.3 ms. This τ was considerably longer than that reported for *IB* cells in Chapter 3. This is because the intracellular electrodes used in Chapter 3 produce a current shunt, reducing the membrane resistance and allowing charge to leak into the extracellular

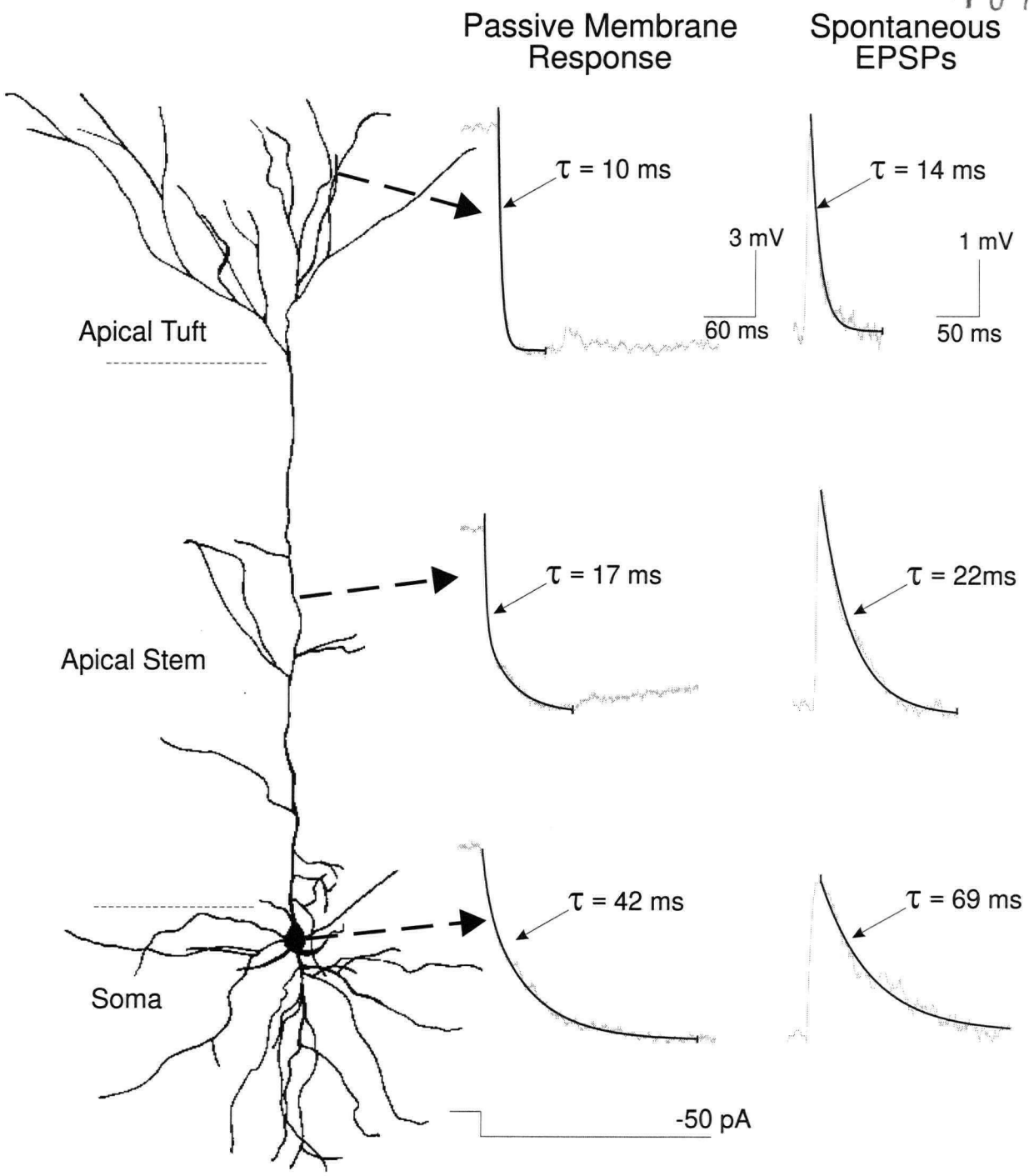

Figure 4-1: Regional differences in passive membrane properties of *IB* PFC neurons. **A)** Camera Lucida tracing of a layer V PFC neuron with the apical tuft, apical stem and soma demarcated. Responses in B were obtained from 3 different PFC neurons. **B)** The passive membrane response to a -50pA pulse (left column) and spontaneous EPSPs (right column) recorded from the apical tuft (top), apical stem (middle) or soma (bottom). Mean values for τ are presented next to each representative trace.

space. Since $\tau = R_{esistance} \times C_{apacitance}$ such a shunt speeds the rate at which the membrane charges. The giga-ohm seal formed by patch-clamp pipette on the membrane reduces the shunt considerably (Spruston et al. 1993).

Mixed Na+/K+ current: I_h

In response to a hyperpolarizing current step, the membrane potentials recorded from the apical tuft and stem were strongly influenced the time-dependent mixed cationic current, I_h. Unlike the majority of somatic recordings, hyperpolarizing current pulses evoked the typical "sag" potential in many apical dendritic stem recording (Fig 4-2A). This 'sag' was blocked by bath application of CsCl, and following blockade, the R_{IN} and τ increased by 47.3 ± 7.5% and 138.5 ± 32% respectively (Fig 4-2A, n=4).

In the apical tuft there was considerable heterogeneity in I_h, as it was very prominent in some recordings (strong I_h dendrites) and weak in others (weak I_h dendrites) (Fig 4-2B). In 3 apical tuft dendrites the "sag" was considerably larger than that observed during any somatic or apical dendritic stem recording. These 3 apical tuft dendrites possessed the shortest τ (4.1 ± 1ms) and the smallest R_{IN} (65 ± 4 MΩ). The "sag" potential recorded in the apical tuft was blocked by either $[Cs^+]_i$ or $[Cs^+]_o$ (Fig 4-2C). By blocking I_h both the R_{IN} and τ were increased in the apical tuft by 47 ± 14% and 53 ± 26% respectively (n=3). Adding CsCl to weak I_h dendrites increased the R_{IN} and τ such that strong I_h dendrites had membrane properties similar to weak I_h dendrites (Fig 4-2B,C). Thus I_h strongly influenced the membrane properties of the apical tuft of PFC neurons.

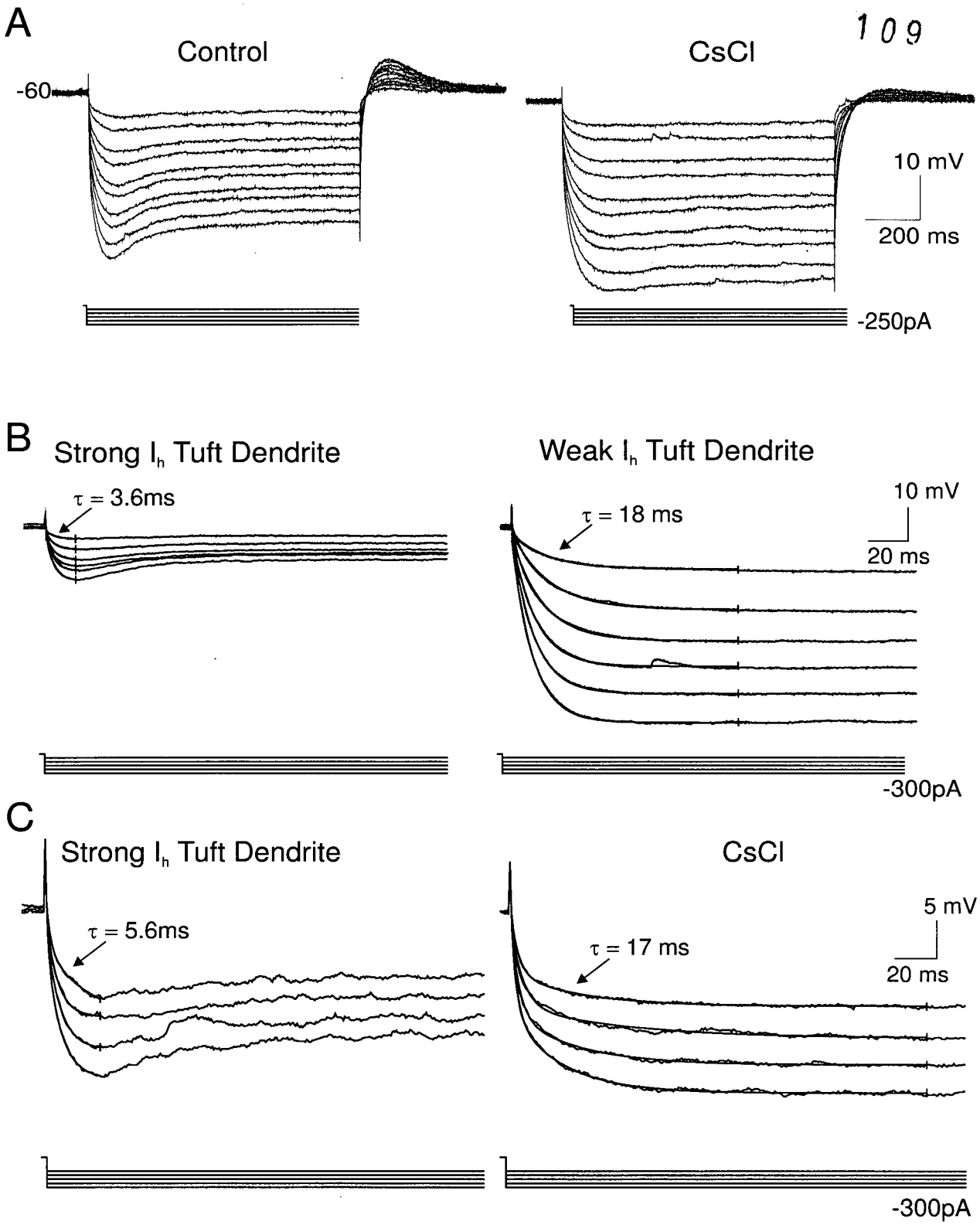

Figure 4-2: Effect of I_h in the apical dendrites on passive membrane properties. **A)** In the apical stem a 'sag' potential was evoked by hyperpolarizing current pulses. The sag was blocked by CsCl, resulting in an increase in R_{in} and τ. **B)** The apical tuft dendrites possessed either a strong (left) or weak I_h (right), which influenced τ. **C)** Blockade of I_h by internal CsCl in a strong I_h dendrite caused the passive membrane τ to increase from 5.6ms to 17ms.

Na^+ Currents and Spikes

The response of the apical dendritic tuft to depolarizing current pulses was very linear in the subthreshold voltage range(Fig 4-3A). In the apical tuft, the V-I plot was unaffected by bath application of TTX or by intracellular blockade of Na^+ channels by QX-314 (Fig 4-3A, n= 4 total). Likewise the response of the apical stem (>200μm from soma) to depolarizing current pulses was also linear in the subthreshold voltage range, and TTX had no effect on the V-I plot (Fig 4-3B, n=6) in the apical stem. Thus, unlike the soma (see Fig 3-3) there was no evidence of a persistent Na^+ current in the apical dendrites of layer V PFC neurons. Also unlike somatic recordings (see Figs 3-3, 3-9) , outward rectification was not observed following blockade of Na^+ channels.

Spikes were observed in 14/16 apical tuft dendrites tested at a mean threshold of -14.8 ± 2.7 mV. In most cases, a spike doublet was initiated, while repetitive firing after the initial doublet was observed in only 2 apical tuft dendrites (Fig. 4-4B).

Spikes were observed in all 9 apical stem dendrites at a mean threshold of -33.5 ± 2.5 mV. However, the spike threshold appeared to vary with distance from the soma (Fig 4-4C,D; Kim & Connors 1993). For distal apical stem recordings (>200 from soma to the main bifurcation) the mean spike threshold was -29.1 ± 3.4 mV (Fig 4-4C, n=4). Very proximal to the soma (20-200μm) the mean spike threshold was -40.3 ± 1.9 mV (Fig 4-4D, n=4). In one dendrite recorded from the apical stem, very close to the soma, spikes sometimes appeared spontaneously at ~ -55mV (Fig.

Figure 4-3: Lack of subthreshold inward rectification in the apical dendrites of PFC neurons. **A)** The response of an apical tuft dendrite to depolarizing current pulses under control conditions (left) and in TTX (middle). (Right) The V-I plot at the points marked in the traces, open circles=control, filled circles=TTX. **B)** The response of a distal apical stem dendrite (~ 350μm from soma) to depolarizing current pulses under control conditions (left) and in TTX (middle). The V-I plot (right) is constructed from the points marked in the traces. Open circles=control, filled circles=TTX.

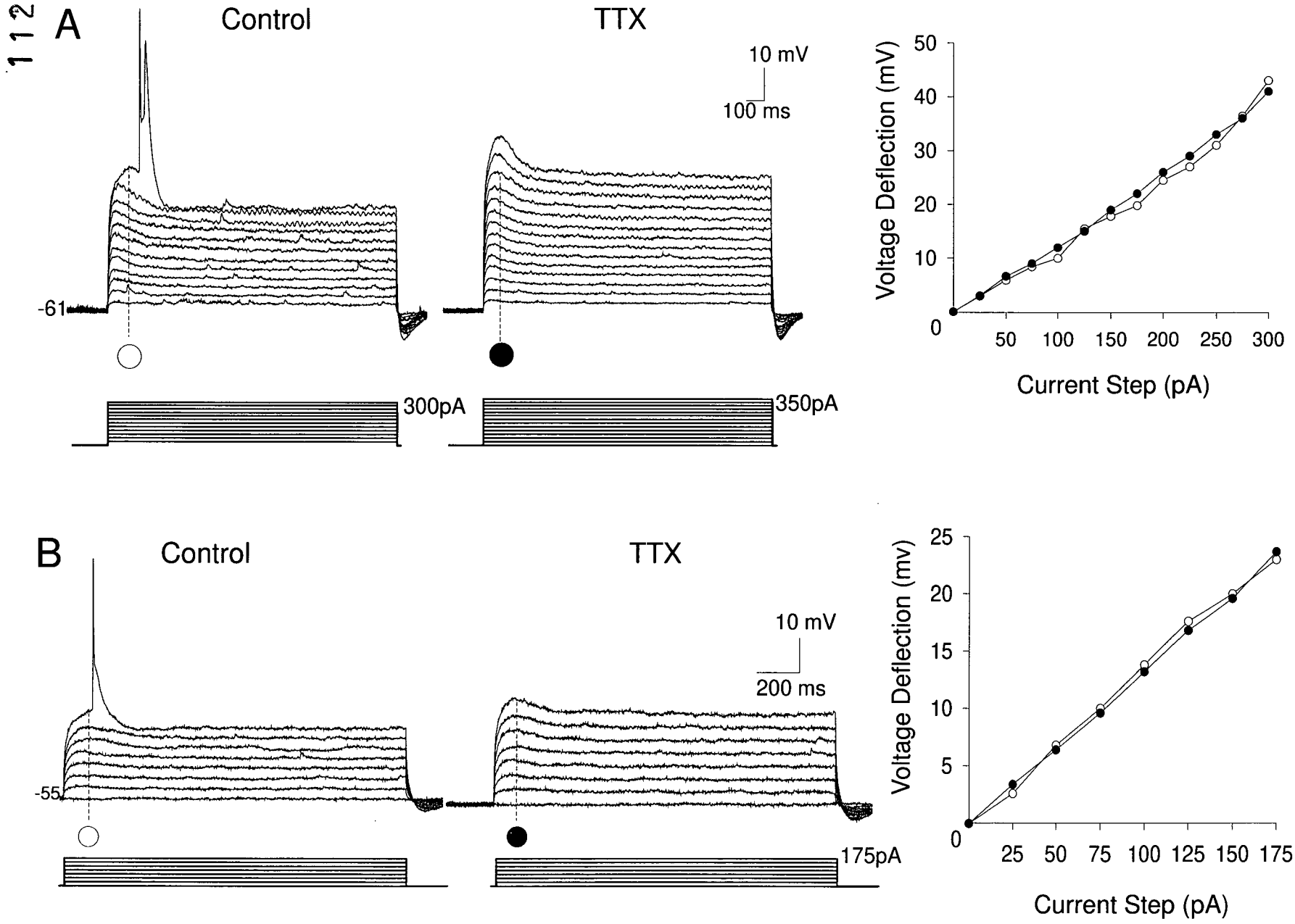
A
Control
TTX
10 mV
100 ms
-61
300pA
350pA
Voltage Deflection (mV)
Current Step (pA)
B
Control
TTX
10 mV
200 ms
-55
175pA
Voltage Deflection (mv)
Current Step (pA)

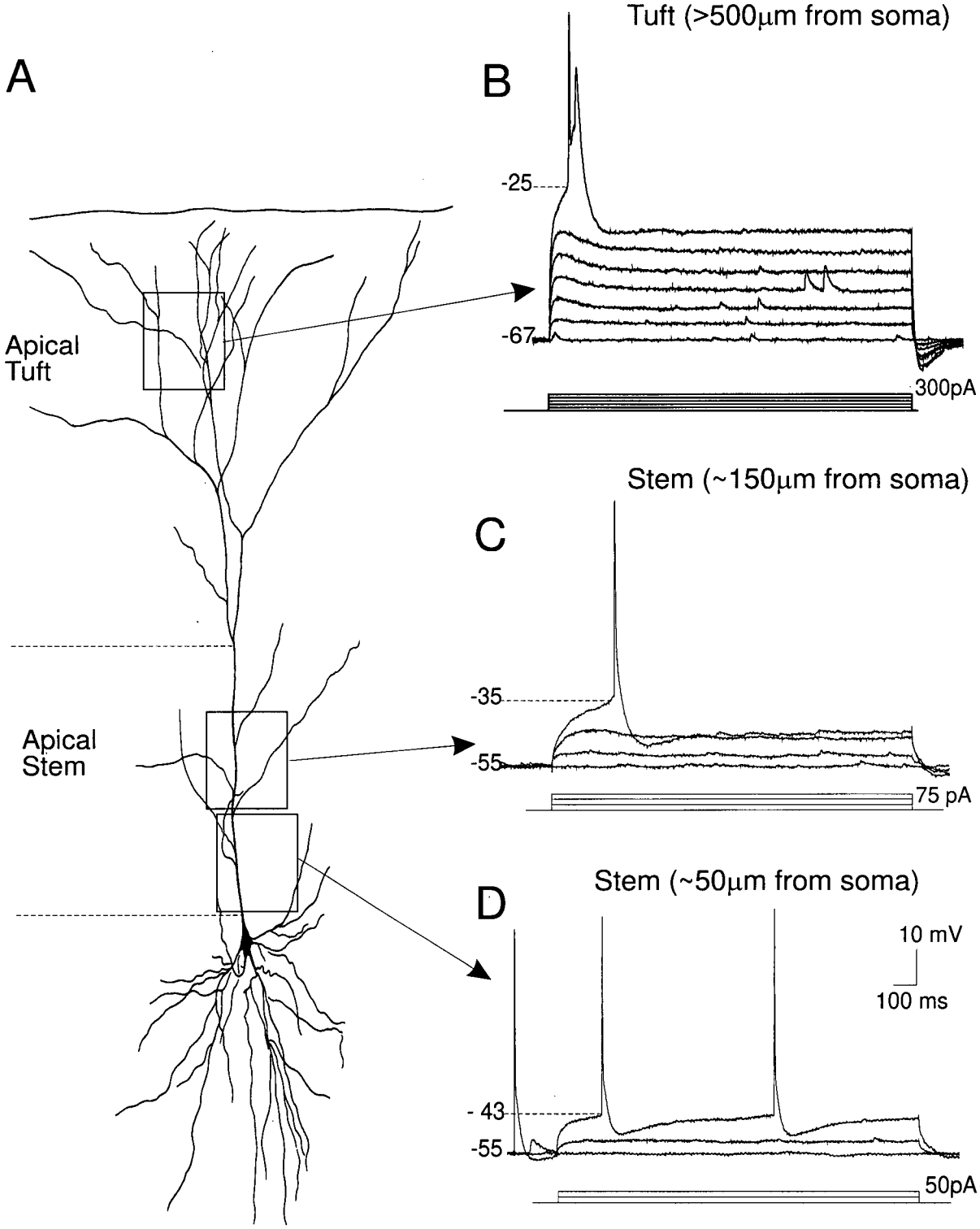

Figure 4-4: Spike threshold increased with distance from the soma. **A)** A camera lucida tracing of a layer V PFC neuron with the approximate recording sites demarcated. Responses in B-D were obtained from 3 different PFC neurons. **B)** Depolarizing current pulses into the apical tuft evoked a single spike doublet at a threshold of -25mV. **C)** In the apical stem ~150μm from the soma, depolarizing current pulses evoked spikes at a threshold of -35mV. **D)** In the apical stem <50μm from the soma, depolarizing current pulses evoked repetitive spikes at a threshold of -43mV, although spontaneous spikes could be observed at more hyperpolarized potentials.

4-4D). In contrast to the apical tuft, it was common for more than one spike to be triggered at threshold during recordings from the apical stem (Fig. 4-4D).

K^+ currents: I_D

At the soma, both the initiation of the 'hump' potential and repetitive firing were suppressed by the 4-AP, dendrotoxin, and $(Cs^+)_i$-sensitive I_D-like current, as shown in Fig 3-9. During recordings from the apical stem, bath application of 4-AP augmented the 'hump' potential (Fig 4-5A). Initiation of the 'hump' potential allowed a previously subthreshold current pulse to evoke an action potential recorded along the proximal apical stem (Fig. 4-5A). Larger current pulses, which triggered only 1-2 spikes, evoked repetitive firing following bath application of 4-AP (Fig. 4-5B, n=4). This indicated that a 4-AP-sensitive current inhibited repetitive spikes from invading the apical stem.

Current pulses which were unable to evoke spikes in the apical tuft produced repetitive firing following blockade of K^+ currents by $(Cs^+)_i$ or 4-AP (n=4, Fig. 4-6). As shown in Fig 4-6A1, bath application of 4-AP caused spikes to be evoked at various thresholds by current pulses which evoked no spikes under control conditions. In the presence of 4-AP an apparently spontaneous spike doublet was observed when the steady-state V_m was maintained at -55mV (Fig 4-6A2). Smaller amplitude events (>15mV) were also observed in the presence of 4-AP (Fig 4-6A2). $(Cs)_i$ produced similar effects in another apical tuft dendrite shown in Fig 4-6B. These findings suggest that excitability within the apical tuft is

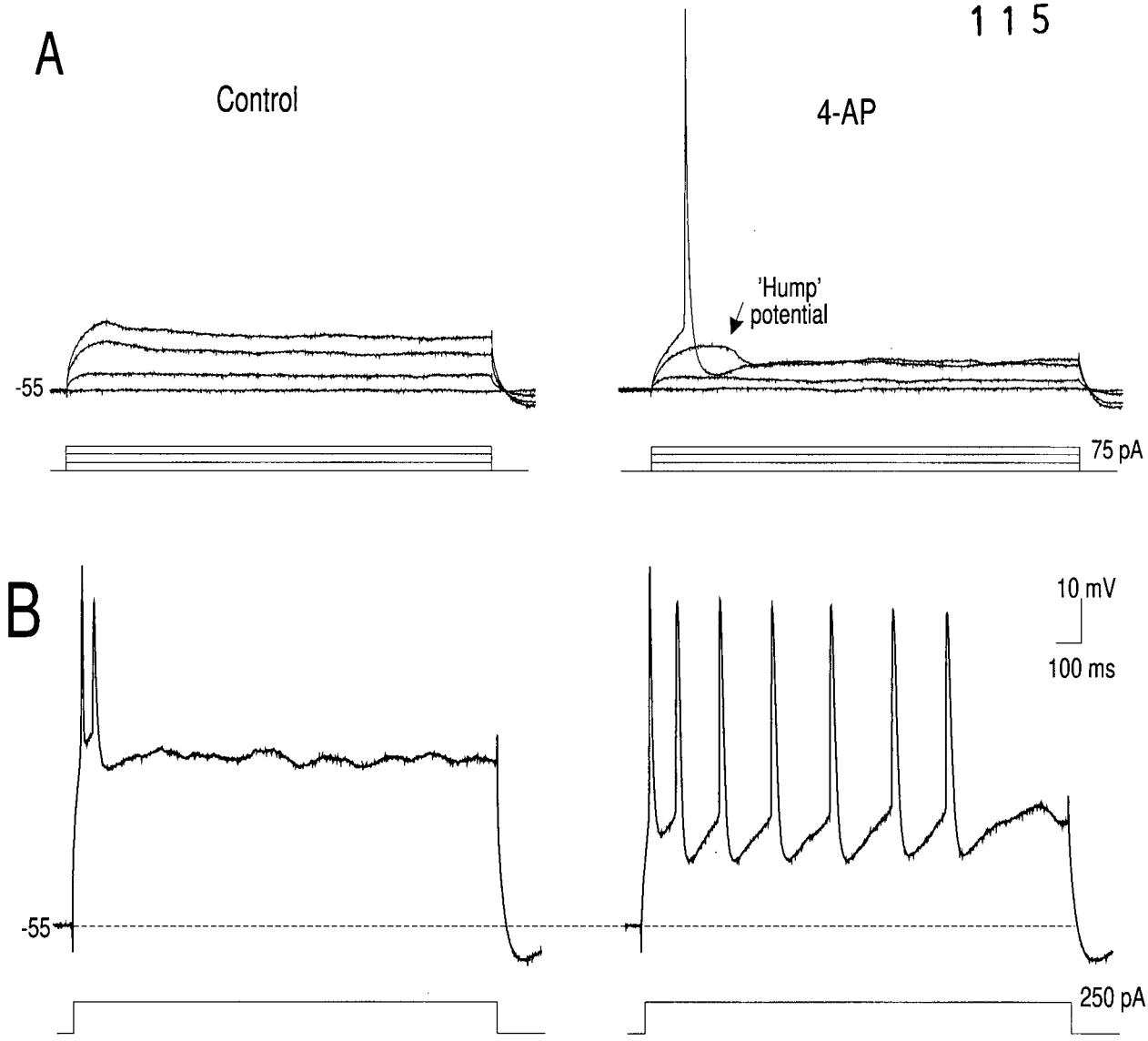

Figure 4-5: K+ current modulation of spiking in the apical stem. **A)** (Left) Current pulses which were subthreshold for action potential generation in the apical stem (recording ~100μm from soma) triggered the 'hump' potential and action potentials in the presence of 4-AP (right). **B)** Larger depolarizing current steps which evoked a single spike doublet (left) evoked repetitive firing in 4-AP (right).

Figure 4-6: K^+ modulation of excitability of the apical tuft. **A1)** (Left) In the apical tuft from a layer III neuron, spikes were not evoked by depolarizing current pulses under control conditions. (Right) In the presence of 4-AP, spikes appeared at various thresholds evoked by the same depolarizing current pulses. **A2)** Two main types of responses were triggered in 4-AP, large amplitude spike doublets (left) and lower amplitude, long duration events of unknown origin (right). **B)** A different apical tuft dendrite recorded from a layer V neuron using a CsCl-filled patch-pipette. Spikes were not evoked by depolarizing current pulses at break-in (left) , but were evoked by the same current pulses 13min later when CsCl had diffused into the cell and blocked K^+ currents.

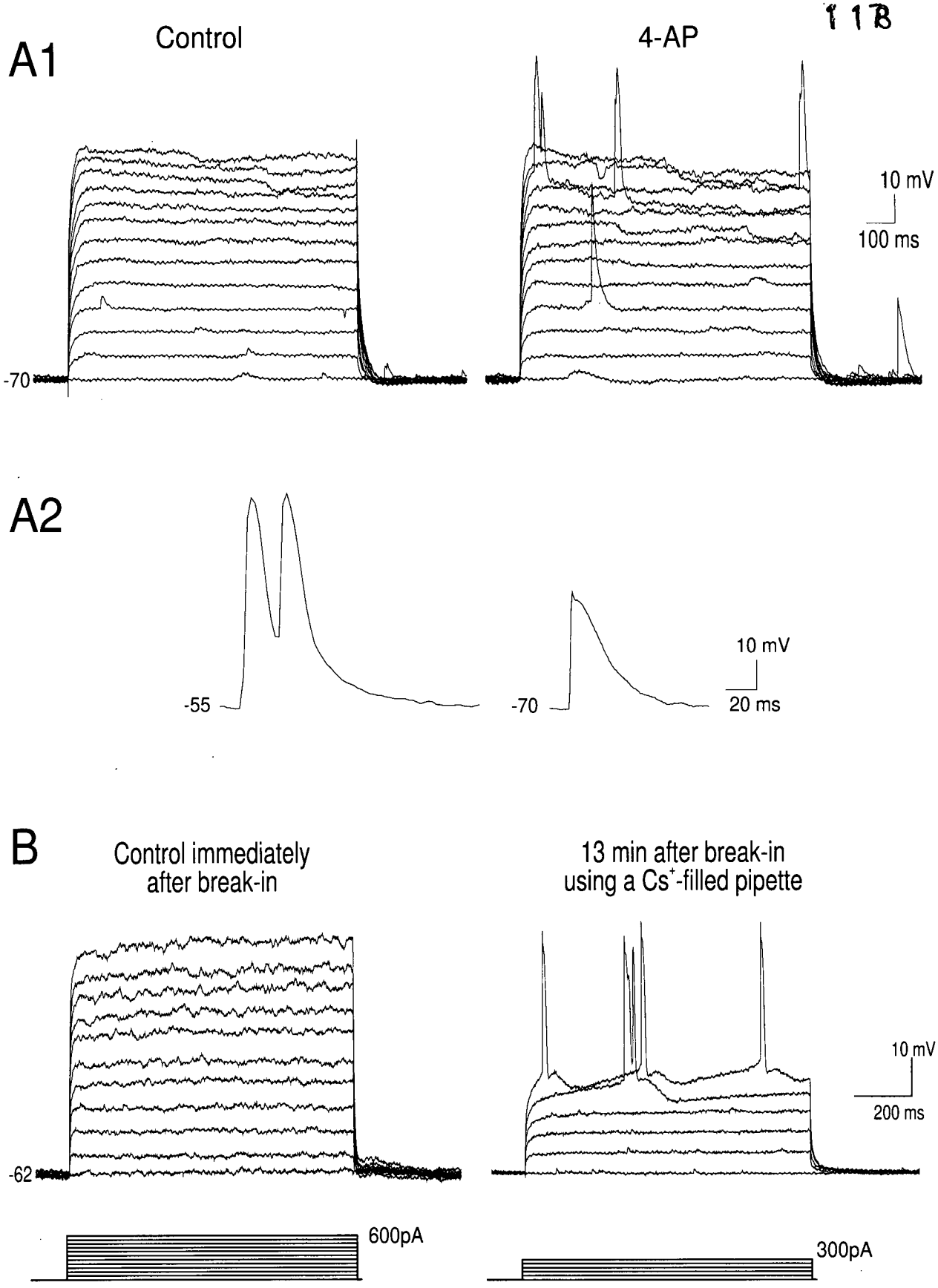
A1
Control
4-AP
10 mV
100 ms
-70
A2
-55
-70
10 mV
20 ms
B
Control immediately
after break-in
13 min after break-in
using a Cs+-filled pipette
10 mV
200 ms
-62
600pA
300pA

controlled by strong 4-AP and $(Cs)_i$-sensitive K^+ currents which curtail local spike initiation and EPSP amplitude.

4-AP and $(Cs)_i$ -are effective in blocking both I_D and the transient K^+ current I_A (Hammond & Crepel 1992; Andreasen & Hablitz 1992; Schwindt et al. 1989). At the soma of cortical neurons and in the dendrites of hippocampal neurons I_A inactivates in ~6ms (Hoffman et al. 1997; Schwindt et al. 1989), while I_D requires several hundreds of milliseconds to inactivate (Hammond & Crepel 1992; Storm 1988). Since repetitive spikes were recorded in the apical stem well after 6 ms from the onset of the depolarizing current pulse, it indicates that the effect of 4-AP illustrated in Fig. 4-6 may have primarily been the result of a blockade of I_D. As noted in the preceeding chapter, it is presently unclear as to which subtype(s) of slowly-inacting K^+ currents are expressed in PFC neurons. However, activation of any slowly-inactiving K^+ current will supress repetitive spiking both at the soma and back into the dendrites, whereas a transient K^+ current may have the opposite effect in that only the first spike would be affected.

Ca^{2+} potentials

In the proximal apical stem (<200μm from soma), a 'hump' potential was evoked prior to a Na^+ spike in 67% of the dendrites (Fig 4-7A). Following blockade of Na^+ channels, the 'hump' potential was evoked at a mean threshold of -35 ± 5 mV and Ca^{2+} spikes at a mean threshold of -26.5 ± 6 mV (n=3).

The amplitude of the 'hump' potential in the proximal stem in TTX alone or in combination with 4-AP was reduced by 63 ± 10.5% by bath application of the

L-type Ca^{2+} channel antagonist Nimodipine (10μM) (n=3, Fig. 4-7B). Although Ca^{2+} spikes were still evoked in Nimodipine, their amplitude was reduced by 56.3 ± 12.7% (n=3). Thus L-type Ca^{2+} channels in the proximal apical stem contributed to sub- and suprathreshold Ca^{2+} electrogenesis, however other subtypes of high voltage-activated channels may also be involved.

In contrast to the proximal apical dendrite, Ca^{2+} electrogenesis within the distal apical stem or apical tuft was rare. Under control conditions neither a 'hump' potential or Ca^{2+} spike was observed in the distal apical stem (>250μm from soma) prior to a Na^{+} spike. Following blockade of Na^{+} channels, a 'hump' potential was evoked in the distal apical stem at a mean threshold of -19 ± 7mV and Ca^{2+} spikes at a mean threshold of + 12.9 ± 3 mV (n=3, not shown).

During 7/10 apical tuft recordings all spike components were removed when QX-314-filled pipettes were used (n=7), or TTX (n=3) was bath applied. No Ca^{2+}-mediated 'hump' potential or Ca^{2+} spikes were evoked by intradendritic current injection these dendrites (Fig 4-8A). In the remaining 3 tuft dendrites only a broad, low amplitude 'hump'/spike could be evoked at a mean threshold of +10 ± 5.8mV (Fig 4-8B). This spike was blocked by bath application of 200μM Cd^{2+} (Fig. 4-8B), indicating that it was Ca^{2+} mediated. Thus spikes recorded within the apical tuft appeared to be initiated by a Na^{+} current and Ca^{2+} channels contributed little to local electrogenesis of Ca^{2+} potentials.

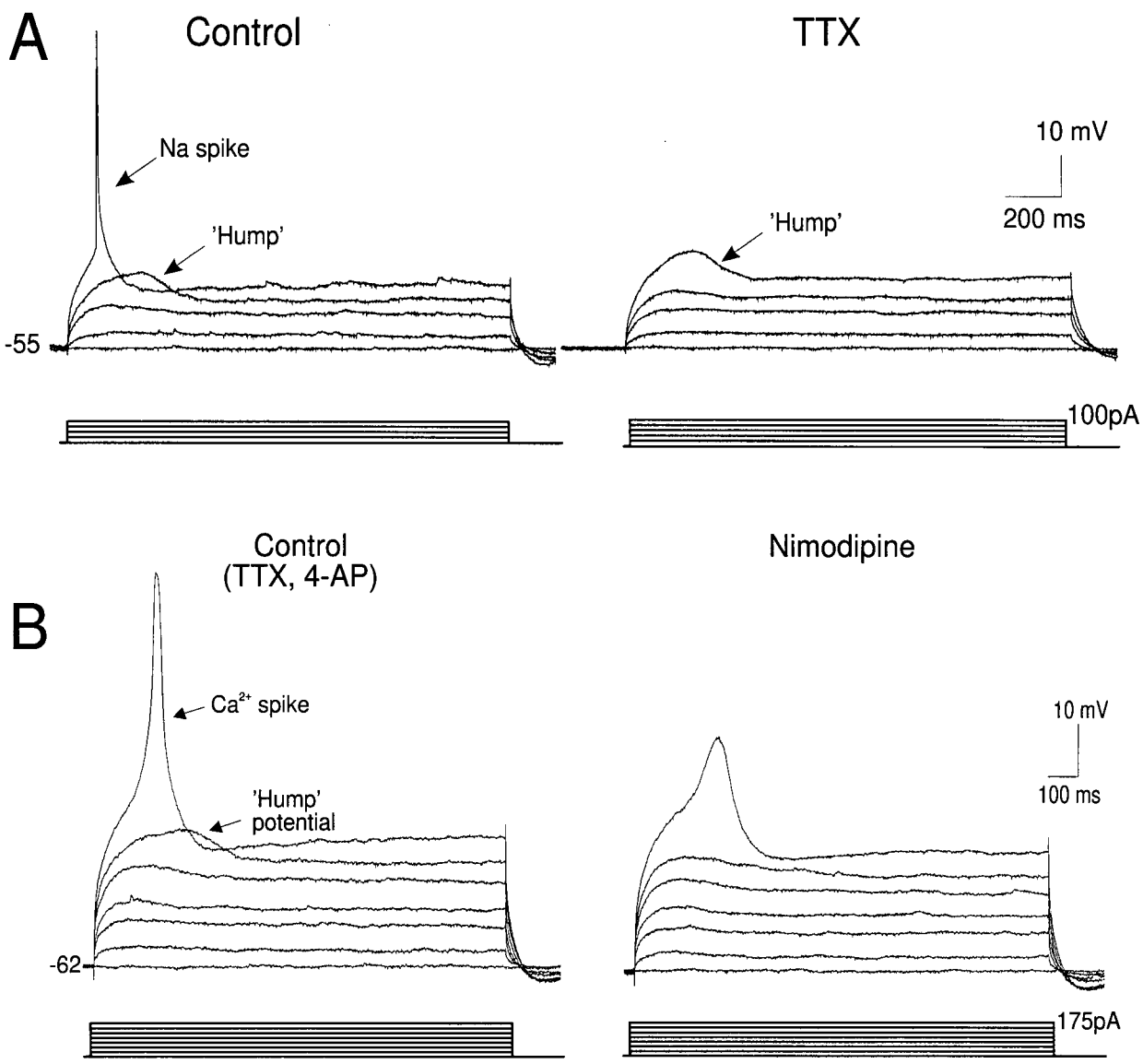

Figure 4-7: Ca^{2+} electrogenesis in the apical stem. **A)** A recording from the proximal apical stem (~150μm from soma) in which a 'hump' potential was evoked prior to a Na^{+} spike by intradendritic depolarizing current pulses (left). Application of TTX blocked the Na^{+} spike but not the 'hump' potential (right). **B)** In a different apical dendrite (recorded ~200-250μm from the soma), a 'hump' potential and Ca^{2+} spike were evoked in TTX and 4-AP (left). Bath application of the L-type Ca^{2+} channel blocker, nimodipine (10μM) reduced the size of the 'hump' potential and Ca^{2+} spike (right).

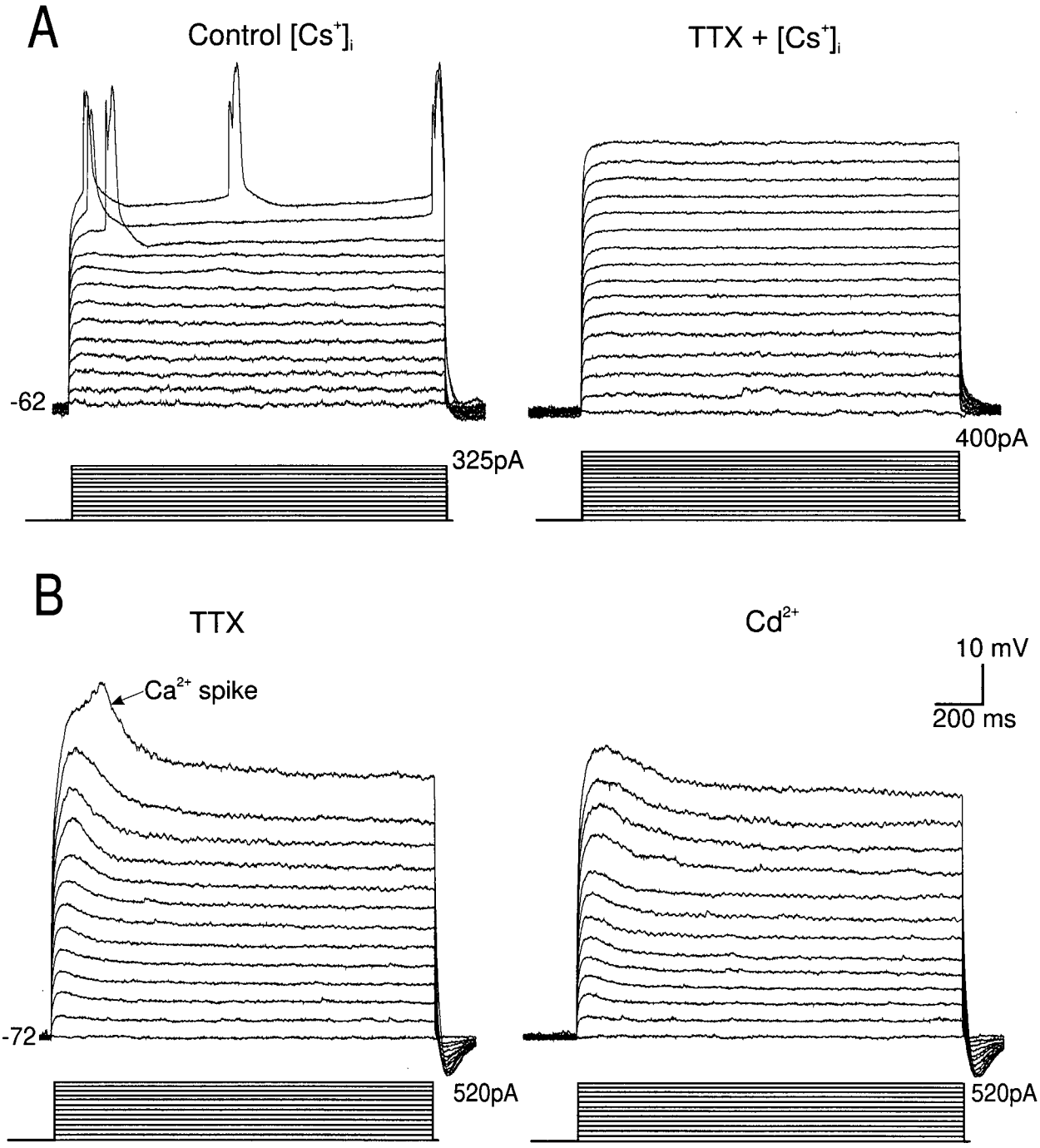

Figure 4-8: Electrophysiological responses of apical tuft dendrites following blockade of Na^+ and Ca^{2+} channels. **A)** In a dendrite recorded using a Cs^+-filled electrode, spikes evoked by injecting depolarizing intradendritic current pulses (left) were blocked by bath application of TTX (right). **B)** In a different tuft dendrite it was possible to evoke Ca^{2+} 'spikes' by injecting large depolarizing intradendritic current pulses in TTX (left). Ca^{2+} spikes were blocked by bath application of Cd^{2+} (200μM) (right).

Discussion

The results of Chapter 4 show that the apical dendritic stem and apical tuft exhibit clearly different electrophysiological properties from the soma of deep layer PFC neurons. Most notably, the τ is shorter in the apical tuft, and the spike initiation threshold is higher with the apical tuft. Moreover, the apical stem but not the apical tuft appears to be a critical initiation zone for Ca^{2+} electrogenesis. Both dendritic regions posses the mixed cationic conductance, I_h, and the excitability of both regions is controlled by a 4-AP-sensitive K^+ current.

The membrane properties of the apical stem and tuft are clearly different from those of the soma, when studied using whole-cell patch-clamp techniques. Although recordings were not made from the basal dendrites, it is expected that they would posses even faster time constants than the apical tuft because they are attached to the large current sink at the soma (Softkey 1994). Conversely, the current injected into the soma will also spread into the basal dendrites, speeding the measured τ. The differences in somatic and dendritic time constants are in accordance with those predicted by theoretical modeling techniques (Koch et al. 1996). Most notably, the τ is much shorter in the apical dendrites. There are several possible reasons for these differences in τ. The first is that the membrane capacity of the fine apical dendrites is considerably smaller than that of the large soma. Although the thickness of the somatic and dendritic membranes are not known, it can be assumed that the specific membrane

capacitance is equal. However, current injected into the dendrites equalizes (Rall 1964; Koch 1996) such that current at the source in the dendrites spreads out spatially and charges nearby dendrites, branch points and the soma.

A second reason for the shorter τ is that the apparent R_{IN} is nearly equivalent in the dendrites and the soma (since $\tau = R_{esistance} \times C_{apacitance}$). This finding implies nonuniform membrane resistance (R_m) of the soma and dendrites because membrane resistance is related to membrane area, and the somatic area is considerably larger than dendritic area at the site of current injection. If the R_{IN} is equivalent for the soma and dendrites as suggested by the present experiments, then $R_{membrane}$ of the soma should be larger than that of the dendrites (since $R_{IN} \propto R_{membrane}$ / area). The smaller dendritic R_{IN} appears to be attributable to a stronger I_h in the dendrites relative to the soma. As noted in Chapter 3, I_h was very rare at the soma, and was usually only present in *ROB* cells, whereas many dendrites possessed I_h. The presence of I_h and the reduction in R_{IN} and τ in the apical tuft may have important implications for single neuron computation in the PFC (see General Discussion).

Spike Initiation in PFC neurons

The present data indicate that Na^+ spikes can be recorded in the apical tuft of PFC neurons. However it is not clear whether such spikes are initiated at the soma or locally within the tuft. The site of spike initiation is determined by source versus load considerations whereby the source refers to the density and activation properties of Na^+ channels while the load is determined by the

diameter, length and axial resistance of a given neuronal segment (Mainen et al. 1995).

Imaging and single channel records indicate that the axon, soma and apical dendritic stem contain a relatively uniform density of Na^+ channels (Colbert & Johnston 1996; Jaffe et al. 1992; Heugenard et al. 1989; Stuart & Sakmann 1994), suggesting that the source does not vary from axon to the main bifurcation of the apical dendrite. While the density of Na^+ channels in the apical tuft is not known, large and fast rising action potentials were recorded in the apical tuft in the present experiments, indicating that Na^+ channels are present locally. However, these channels have very different activation and inactivation kinetics from somatic Na^+ channels as depolarization to -15mV was required to evoke a spike in the apical tuft. Similar depolarizations of the soma would inactivate the fast Na^+ channels nearly completely (Alzheimer et al. 1993) and prevent action potential initiation. Moreover, there is no evidence of persistent Na^+ channels in the apical dendrites as the V-I plot was linear up to spike threshold. Thus the apical tuft of PFC neurons appears to have fast and not persistent Na^+ channel gating, but the activation and inactivation kinetics of fast gating is shifted in the depolarized direction.

The persistent Na^+ current in the axon and soma helps to overcome the considerable load of the soma and basal dendrites (Mainen et al. 1995; Colbert & Johnston 1996). If the soma charged passively, a considerable amount of Na^+ channel inactivation would occur before spike threshold is reached, given the long τ of the soma. The persistent Na^+ current is activated prior to the fast Na^+

current and helps to charge the soma. In contrast, the load of the axon is very small and thus it can depolarize to spike threshold before significant Na^+ channel inactivation occurs. The load of the tuft is also small, and the activation and inactivation kinetics of Na^+ channels appear to be shifted in the depolarized direction such that significant depolarization appears to occur without significant channel inactivation. Furthermore, the electrotonic distance from the tuft to the axon, provides electrical isolation of the tuft from the strong spike generating mechanisms in the axon. Computer simulations of realistic PFC neurons indicate that as the electrotonic distance between tuft and soma increases, spike initiation in the tuft is more likely (D. Durstewitz personal communication). These factors make local spike initiation within the apical tuft possible, in spite of the evidence against spike initiation in the apical stem (Stuart & Sakmann 1994). Indeed, recent dual cell recordings from the tuft and soma of somatosensory neurons indicate that current pulses into the tuft evoke action potentials in the tuft prior to the soma (Zhu & Sakmann 1997). Local spike initiation in the apical tuft has important implications for single neuron computation in the PFC (see General Discussion).

Ca^{2+} Spike Electrogenesis

In contrast to the clear evidence for Na^+ mediated events in the apical tuft, Ca^{2+} electrogenesis was extremely rare. In most neurons it was difficult to generate a Ca^{2+} potential in the absence of Na^+ currents. This was in marked

contrast to the soma and proximal apical stem where Ca^{2+} spikes were evoked readily. Unlike Na^{+} spikes, Ca^{2+} spikes do not propagate effectively from the site of initiation (Rhodes 1997; Schwindt & Crill 1997). Thus even if conditions were unfavorable for local spike initiation, Na^{+} but not Ca^{2+} spikes could back propagate from more proximal regions of the neuron. Therefore, unlike Na+ spikes, it is clear that Ca^{2+} spikes were not evoked in the apical tuft.

In contrast to the apical tuft, both sub- and suprathreshold Ca^{2+} electrogenesis was observed in the apical stem. In the proximal apical dendritic stem, synaptic activation of Ca^{2+} channels might overcome certain problems associated with effective synaptic signal processing in layer V-VI pyramidal neurons. The axial resistance of the main apical dendritic stem strongly limits the axial current that enters the soma (Bernander et al. 1994). In contrast, there is little loss of synaptic current to membrane capacitance along the dendrite because the apical dendritic stem is very thin. However, a considerable portion of synaptic current is lost at the soma due to charging the large somatic membrane (Rall & Rinzell 1973). Hence, synaptic activation of voltage-gated Ca^{2+} channels in the proximal apical dendritic stem would dramatically enhance the synaptic current prior to entering the signal-attenuating capacitive sink at the soma. In this way Ca^{2+} channels located in the proximal apical dendritic stem may serve as effective current amplifiers for distally generated EPSCs. If Ca^{2+} channels proximal to the soma were to make a contribution to voltage amplification of distal EPSPs, they would have to be activated prior to an axosomatic action potential. At the soma (see Chapter 3) and apical stem, the 'hump' potential was

observed prior to action potential initiation. Thus, Ca^{2+} channels proximal to the soma may act as voltage amplifiers of synaptic signals. Chapters 5 examines the properties of synaptic inputs to PFC neurons and their amplification by proximal Ca^{2+} channels.

Chapter 5:

Synaptic Responses and Synaptic Amplification in Layer V-VI PFC Neurons

Introduction

Much of our understanding of the role of the PFC in working memory processes has come from single unit recordings of behaving primates. While this single unit activity is very good predictor of the future performance of the animal on the task (Niki & Watanabe 1976; Funahashi et al. 1989), it is clear that a single PFC neuron does not control behavior. Rather, it has been proposed that individual PFC neurons receive task-relevant information from other brain regions, retain this activity by recurrent activity and use this information to guide behavior via efferents to motor output regions (Goldman-Rakic 1988; 1995; Robbins 1991; Seamans et al. 1995; Mogenson & Yang 1990; Fuster 1985; Quintana et al. 1989).

Synaptic contacts from such as the somatosensory/parietal cortex, entorhinal/temporal cortex and hippocampus terminate both in the superficial layers I-II and deep layers V-VI of the PFC (Mitchell & Cauller 1997; Conde et al. 1991). Information relayed from these areas may then be coded and stored within the PFC by re-entrant loops of interconnected neurons (Hebb 1968; Abeles 1982; Vaadia et al. 1995). Recent evidence indicates that within the PFC, activity of many individual cells quickly become synchronized during the performance of a delayed response task in the primate (Vaadia et al. 1995). It is

proposed that neighboring neurons co-activate each other when the common synaptic drive is increased (Vaadia et al. 1995). Layer V PFC neurons posses long axons with collaterals which connect neighboring neurons (Fig 3-1A; Kritzer & Goldman-Rakic 1993). In the neocortex, strong functional contacts are made onto the basal and apical oblique dendrites of neighboring neurons in layer V which are capable or generating EPSPs or action potentials in the adjoined cell (Markram et al. 1997; Thomson & Deuchars 1997).

Excitation among connected cells is balanced by GABA mediated inhibition, as interneurons synapsing on the soma can suppress repetitive firing in pyramidal neurons while interneurons synapsing on the dendrite can inhibit Ca^{2+} spikes and shunt distally generated EPSPs primarily via the $GABA_A$ receptor (Miles et al. 1996; Thomson et al. 1996; Thomson & Deuchars 1997). In the cortex, GABA-mediated inhibition is present in the deep layers V-VI but is particularly dense in the superficifical layers I-II where the apical tufts of layer V neurons are located (Kanter et al. 1996; van Brederode & Spain 1995).

GABA inputs may limit the effectiveness of inputs to the distal tuft from reaching the soma. Although these inputs are of potential importance, their effectiveness is further reduced by the dendrite's passive cable properties (Cauller & Connors 1992) and strong K^+ currents in the dendrites (Figs 4-5, 4-6; Hoffman et al. 1997). One solution to overcome such problems has been to suggest that voltage-gated ionic conductances in the dendrites of pyramidal neurons boost the effects of local synaptic inputs by acting either as voltage or current amplifiers (Bernander et al. 1994; Shepherd et al. 1985; Spencer &

Kandel 1961, Yuste et al. 1994). Slowly inactivating Na^+ currents have been shown to enhance distal EPSPs and currents evoked by iontophoresis of glutamate onto the apical dendrites of layer V-VI cells (Schwindt & Crill 1995; Stuart & Sakmann 1995). In addition, both low and high threshold Ca^{2+} currents have been recorded in the dendrites of pyramidal neurons and might also serve to amplify synaptic signals (Fig 4-4, 4-7; Amitai et al. 1993; Deisz et al. 1991; Kim & Connors 1993; Magee & Johnston 1995a,b; Magee et al. 1995; Markram & Sakmann 1994).

Evidence from immunocytochemical and electrophysiological studies indicate that while Ca^{2+} channels are located throughout the dendrites of pyramidal neurons, there is a clustering of large conductance (L-type) high threshold Ca^{2+} channels at the base of the major dendrites (Magee & Johnston 1995b; Westenbroek et al. 1990). As shown in Chapters 3,4 these channels likely are responsible for the generation of the 'hump' potential in the subthreshold voltage range. Furthermore, the results presented in Chapter 4 suggested that Ca^{2+} electrogenesis occurs primarily in the proximal apical stem and not the apical tuft of layer V PFC neurons. Collectively, these data suggest that high voltage-activated Ca^{2+} channels proximal to the soma, but not within the apical tuft of PFC neurons amplify distal EPSPs. If so, these channels play an important role in ensuring distal synaptic inputs, from other cortical regions, effectively influence the output of PFC neurons.

The present Chapter will test the hypothesis that proximal Ca^{2+} potentials amplify distal EPSPs by using a combination of bath and focal puff application of

Ca^{2+} channel blockers and direct patch-clamp recordings from different regions of PFC neurons. However, prior to investigating this hypothesis I will examine the basic synaptic responses recorded from the soma and dendrites of PFC neurons to stimulation of the superficial and deep layers.

Results

Synaptic Responses at the Soma

Synaptic responses were evoked by a stimulating electrode in layers I-II or V-VI during somatic or apical dendritic tuft recordings. In order to study synaptic responses more clearly, neurons were recorded using QX-314-filled electrodes to block Na^+ spikes. Synaptic stimulation of layers I-II or V-VI evoked a mixed PSP under control conditions (Fig. 5-1).

There was tremendous variability from cell to cell with the responses of individual cells being dominated by either an EPSP or an IPSP at various membrane potentials. In cells in which the synaptic response was dominated by an EPSP rather than an IPSP, application of a low dose (0.5μM) of the $GABA_A$ antagonist, bicuculline enhanced the response amplitude. Even in cells where the evoked IPSP was less prominent (Fig 5-2A) addition of 0.5μM bicuculline also enhanced the response amplitude (Fig 5-2B,C). This suggested that an IPSP of variable strength was co-activated by stimulation of layers I-II or V-VI.

In the cortex, 0.5μM bicuculline blocks only 10-20% of $GABA_A$ receptor function (Chagnac-Amitai & Connors 1989). At higher doses of bicuculline (2-

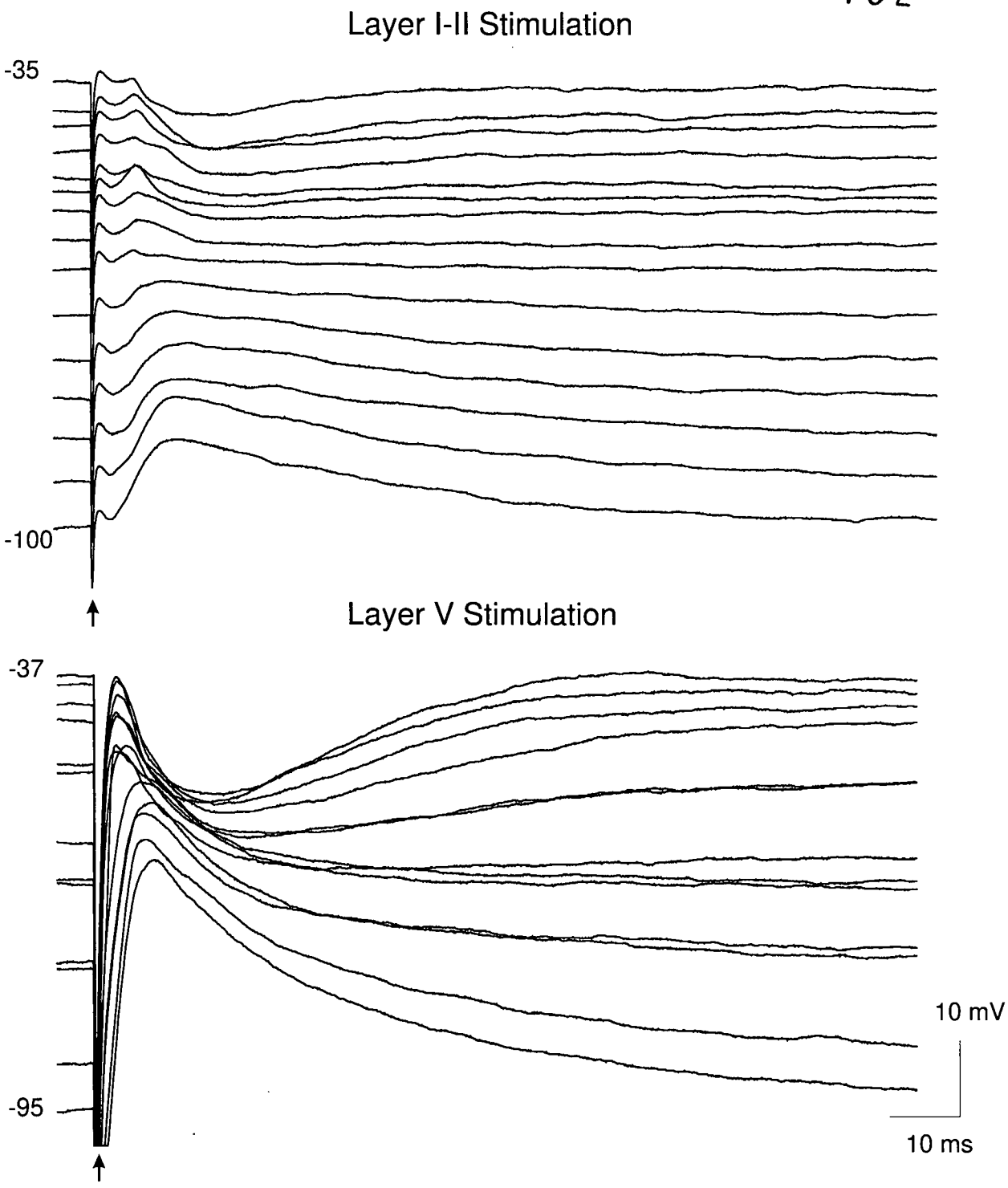

Figure 5-1: Basic synaptic responses of PFC neurons recorded at the soma. Synaptic responses evoked by layer I-II (top) or layer V-VI (bottom) stimulation consisted of multiple components, with a prominent IPSP at depolarized membrane potentials. This cell was recorded using an intracellular electrode containing QX-314 and 1M CsAc in 2M KAc.

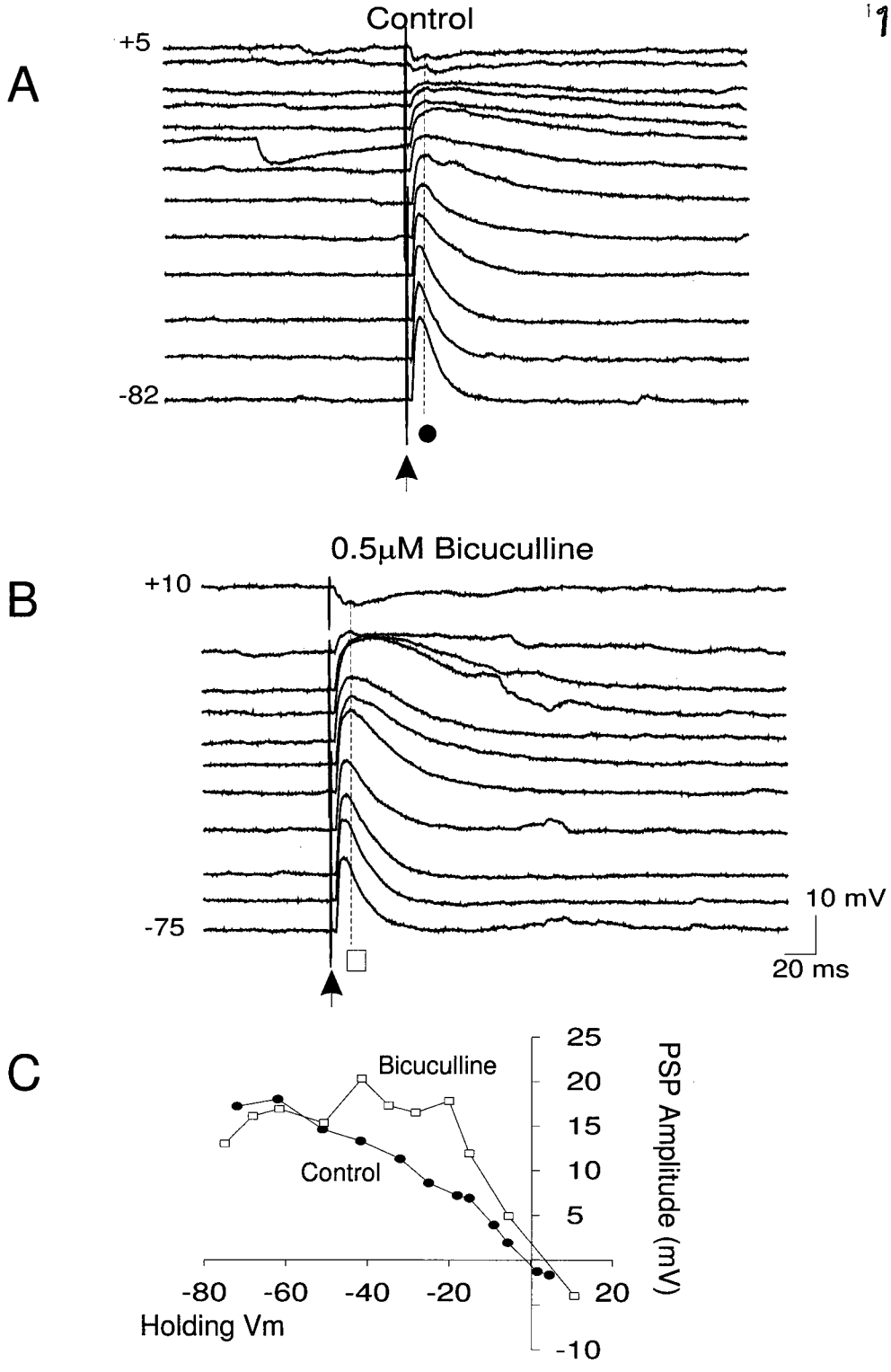

Figure 5-2: $GABA_A$ modulation of layer I-II IPSPs. **A)** A neuron which lacked a prominent IPSP following stimulation of layers I-II. **B)** In this neuron bath application of low doses of the $GABA_A$ receptor antagonist, bicuculline, increased PSP size. **C)** Plot of PSP amplitude at the points marked by the black circles and open squares in A and B, versus holding potential. Note the significant increase in PSP amplitude at depolarized holding potentials in the presence of this low dose of bicuculline. This cell was recorded using an intracellular electrode containing QX-314 and 1M CsAc in 2M KAc.

10μM), an epileptiform discharge was evoked by layer I-II or V-VI stimulation. This epileptiform discharge was likely a giant polysynaptic EPSP as suggested by Johnston & Brown (1981). The giant EPSP evoked in bicuculline was still present in APV (50μM) and consisted of a fast and slow component (Fig 5-3A-C). The first fast component reversed in polarity at ~ 0mV (not shown), while the second, slow component reversed in polarity at ~ -60mV (Fig 5-3, n=15). While it was probable that the first, fast component was a giant AMPA-mediated EPSP, the ionic basis for the second component is not known. It was not mediated by a voltage-gated current however because strong hyperpolarizing pulses (-3000 pA / 50ms) could not inactivate it (n=8, not shown).

In APV and higher concentrations of bicuculline (>2μM), the transition from a small EPSP to a giant EPSP occurred within a very narrow stimulation intensity range which was independent of the membrane potential (Fig. 5-3C). The all-or-none nature, and variable onset latency of the giant EPSP in APV and bicuculline, suggested that it was mediated by recurrent circuit activation whereby many neurons were activated synchronously *en masse* at a threshold stimulation intensity. As a result of these complications, it was not practical to work with isolated AMPA-mediated EPSPs in PFC slices.

In contrast, in the presence of DNQX and bicuculline the giant EPSP was not triggered but rather an isolated NMDA-mediated EPSP was evoked with a constant onset latency. If the stimulation intensity was increased or the V_m was depolarized, the NMDA EPSP increased in size and an overridding Na^+ spike or Ca^{2+} spike (in QX-314) was triggered (Fig. 5-3D). Ca^{2+} spikes may have been

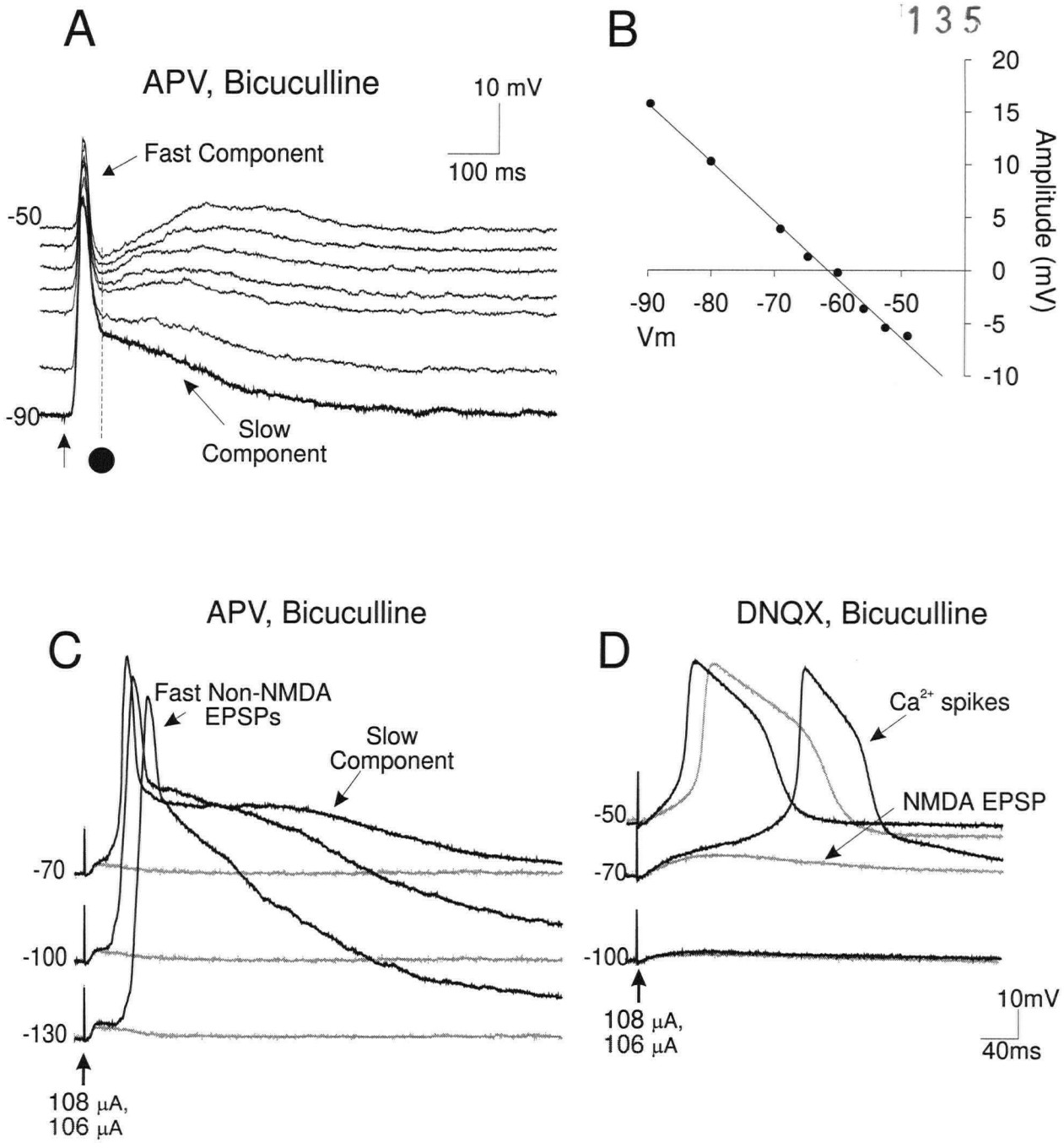

Figure 5-3: Isolated NMDA and non-NMDA synaptic responses. **A)** In the presence of APV (50μm) and bicuculline (5μM), a large response was evoked by layer I-II synaptic stimulation which consisted of a fast and slow component. **B)** Plot of the amplitude of the slow component at the point demarcated by the black circle in A, versus holding potential. The slow component reversed in polarity at V_m of -60mV. **C)** In a different cell, the large layer I-II evoked PSP in APV and bicuculline was triggered by the same stimulation intensity (108μA) at all holding potentials from -130mV to -70mV. **D)** In the same cell APV was washed out and DNQX (10μM) was added. The transition from a small NMDA EPSP to a Ca^{2+} spike occurred in a voltage-dependent manner when using 108μA stimulation. Cells in A and C,D were recorded using intracellular electrodes containing QX-314 and 1M CsAc.

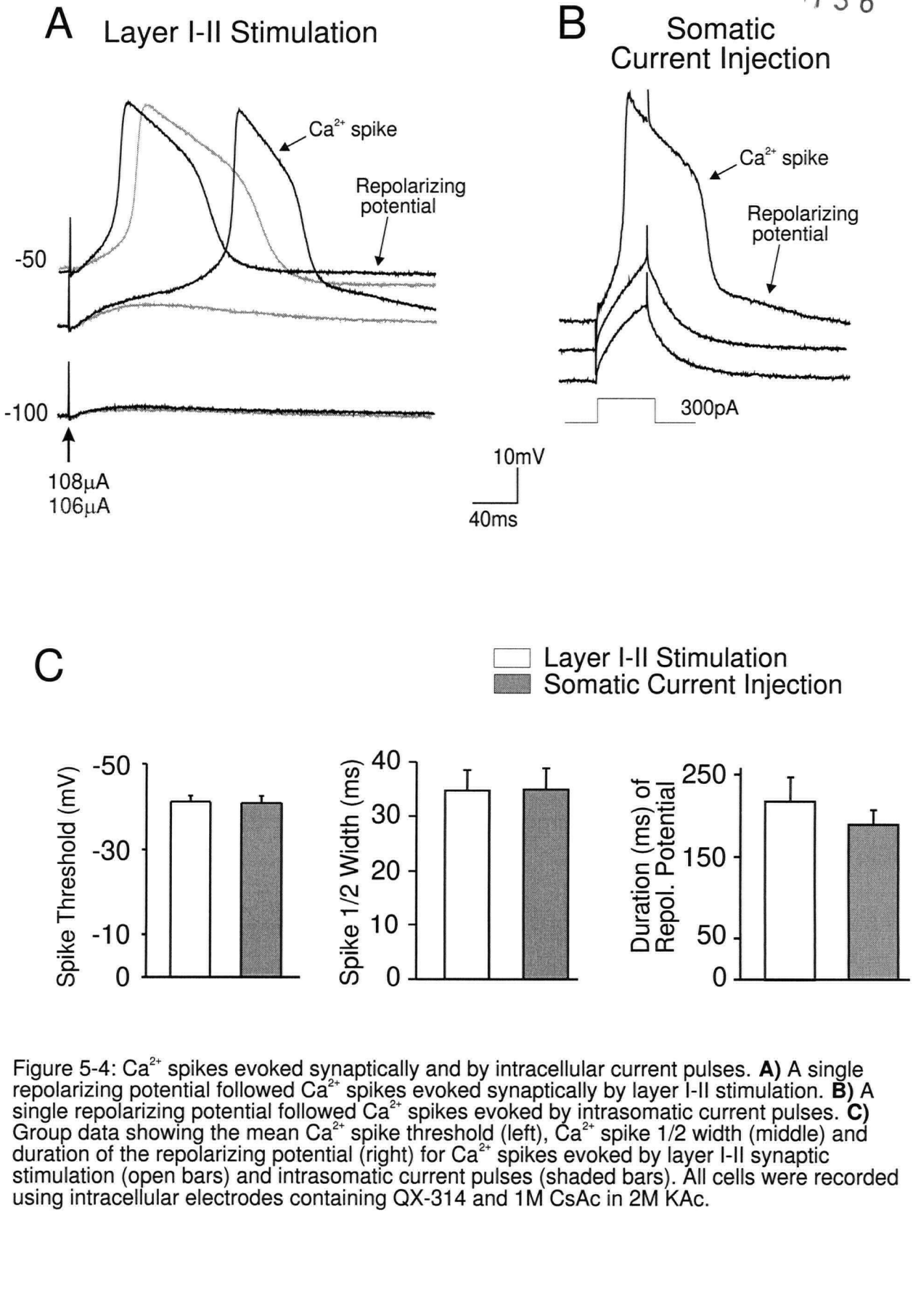

Figure 5-4: Ca^{2+} spikes evoked synaptically and by intracellular current pulses. **A)** A single repolarizing potential followed Ca^{2+} spikes evoked synaptically by layer I-II stimulation. **B)** A single repolarizing potential followed Ca^{2+} spikes evoked by intrasomatic current pulses. **C)** Group data showing the mean Ca^{2+} spike threshold (left), Ca^{2+} spike 1/2 width (middle) and duration of the repolarizing potential (right) for Ca^{2+} spikes evoked by layer I-II synaptic stimulation (open bars) and intrasomatic current pulses (shaded bars). All cells were recorded using intracellular electrodes containing QX-314 and 1M CsAc in 2M KAc.

triggered in APV and bicuculline but were completely occluded by the giant EPSP described above.

The Ca^{2+} spike evoked synaptically in DNQX and bicuculline, was followed by a single repolarizing potential (Fig 5-4A). A similar single repolarizing potential followed Ca^{2+} spikes evoked by intracellular current injection in a combination of TTX and TEA or QX-314 and $(Cs)_i$ (Fig 5-4B). Ca^{2+} spikes evoked synaptically by the NMDA EPSP had similar thresholds and durations to Ca^{2+} spikes evoked by intracellular current injection in QX-314 and $(Cs)_i$ (n=15, Fig. 5-4C). This suggested that distally-generated NMDA EPSPs and intrasomatic current pulses activated a similar population of Ca^{2+} channels. Therefore, co-application of DNQX and bicuculline allowed a stable monosynatic EPSP to be evoked, which was capable of activating voltage-gated currents in PFC neurons without generating an epileptiform discharge.

Synaptic Responses in the Apical Tuft

The apical tuft is a main input zone for synaptic afferents to layer V cortical neurons (Peters 1987; Cauller & Connors 1992) but given its electrotonic distance from the soma, it is difficult to determine the properties of local synaptic integration within the apical tuft from somatic recordings. The same patch-clamp techniques that allowed stable recordings from the apical tuft of layer V PFC neurons in Chapter 4, were used to examine directly the responses of cortical neurons at this important input zone.

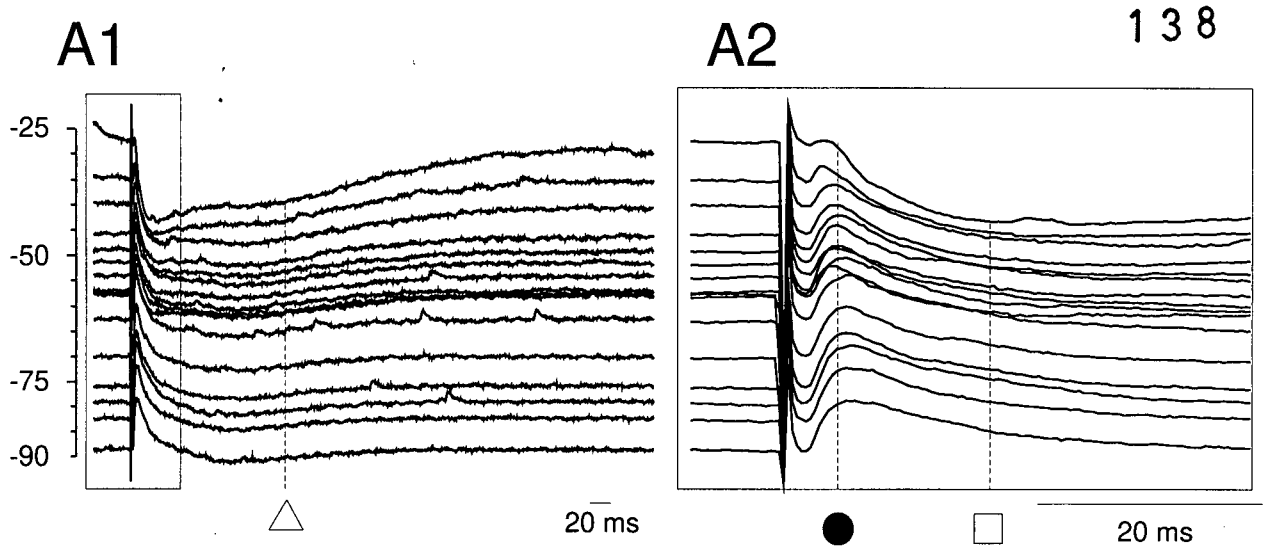

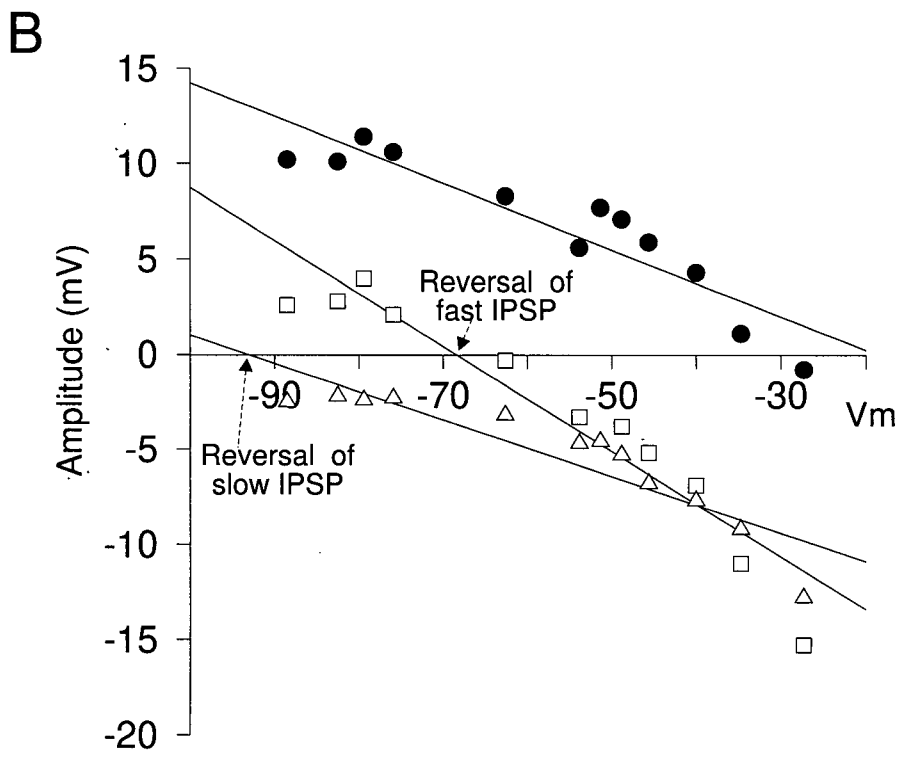

Figure 5-5: Basic synaptic responses of the apical tuft. **A1)** Layer I-II synaptic stimulation evoked PSPs in the apical tuft which consisted of both an EPSP and a fast and slow IPSP that varied in size with the membrane holding potential. **A2)** Responses in the box shown in A1 on an expanded time scale. **B)** Plot of the membrane potential versus response amplitudes at the points demarcated by the open triangle in A1 (slow IPSP) and the filled circle (EPSP) and open square (fast IPSP) in A2. Note that the response demarcated by the open triangle in A1 (slow IPSP) reversed at ~ -92mV, while the response demarcated by the open square in A2 (fast IPSP) reversed at ~ -67mV. The EPSP demarcated by the filled circle in A2 was truncated by the fast IPSP, and reversed at ~ -20mV.

In most apical tuft dendrites, stimulation of layers I-II evoked a mixed PSP. This PSP consisted of multiple components which could separated based on their reversal potentials (Fig 5-5A1). The early component consisted of an EPSP which was truncated by an IPSP at depolarized membrane potentials. As a result the reversal of the EPSP occurred at approximately -20mV (Fig 5-5B). The early IPSP reversed at -67mV (Fig 5-5A1,B) and the late IPSP at -93mV (Fig 5-5A2, B). This is consistent with the reversal potentials for $GABA_A$ and $GABA_B$ receptor respectively.

In some cases an EPSP could be evoked in the absence of a clear IPSP. in the absence of QX-314 in the recording pipette, increasing stimulation intensity evoked fast, presumably Na^+-mediated spikes (mean 1/2 width = 5.3 ± 0.6ms) in 40% of these apical tuft dendrites (Fig. 5-6A). In 2 out of 16 dendrites, synaptic stimulation of layers I-II evoked an initial fast spike which was followed by an additional long duration 'spike' (mean 1/2 width = 50.5 ± 17.8 ms)(Fig 5-6B). In one of these two tuft dendrites, recorded close (~50μM) to the main bifurcation, long duration regenerative spikes were evoked (not shown) and appeared similar to putative dendritic Ca^{2+} spikes reported previously (Amitai et al. 1993). In the other tuft dendrite, synaptically activated mixed spikes were present immediately after break-in using a QX-314 electrode (Fig. 5-6B). However, spikes disappeared later during the recording session when QX-314 produced a sufficient block of Na^+ channels (Fig. 5-6B). Thus in 2 apical tuft dendrites Ca^{2+} spikes may have been triggered by QX-314-sensitive Na^+ spikes.

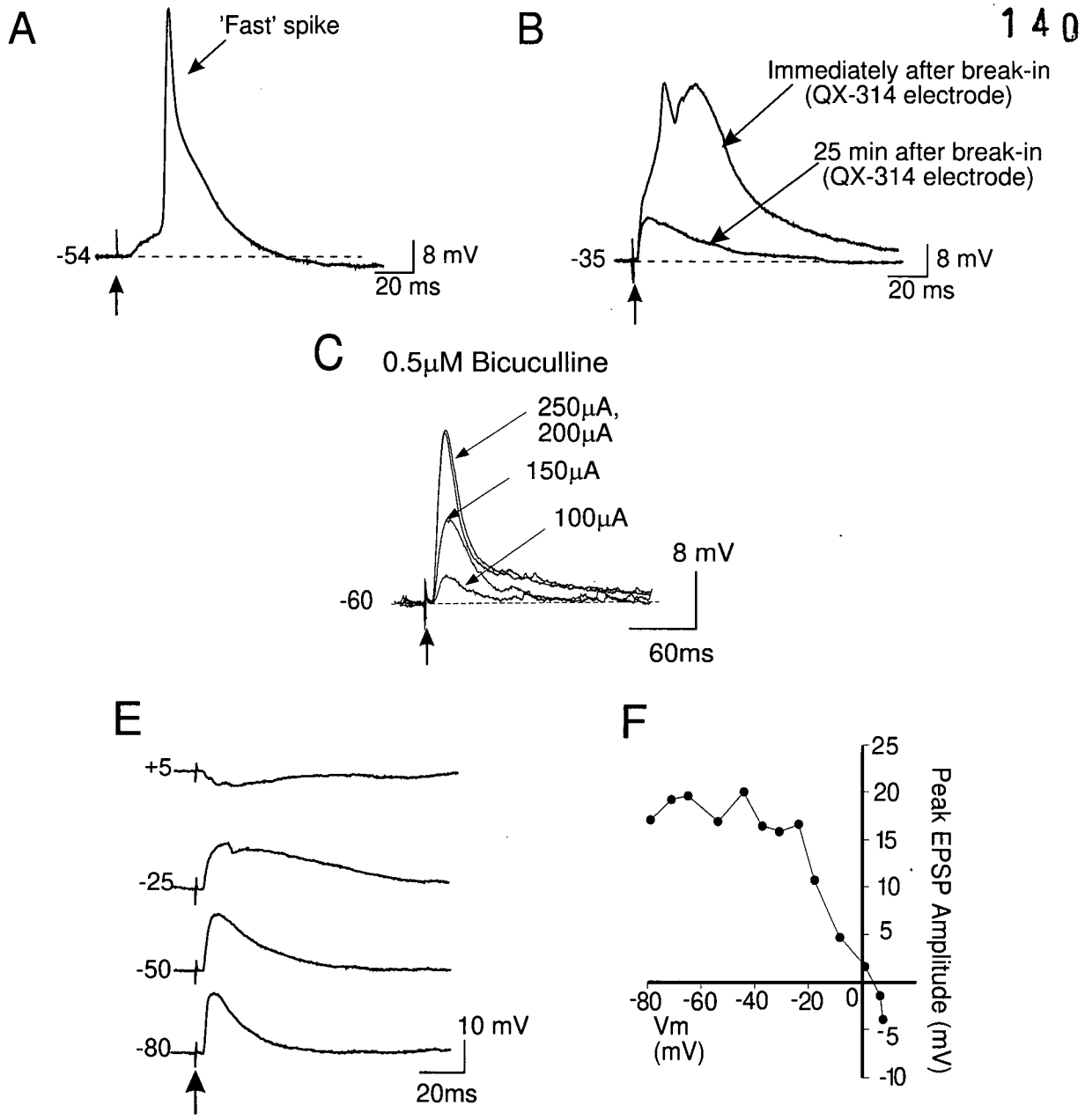

Figure 5-6: Synaptic responses of apical tuft dendrites following blockade of Na^+ channels and $GABA_A$ receptors. **A)** Synaptic stimulation of layers I-II often evoked an EPSP with an overriding fast spike. **B)** A dendrite recorded using a QX-314 filled electrode, fast and slow spikes were evoked by synaptic stimulation of layers I-II immediately after break-in of the dendritic patch. These spikes disappeared during the recording period as QX-314 blocked Na^+ channels, leaving an EPSP. **C)** After QX-314 sufficiently blocked Na^+ channels, synaptic stimulation of layers I-II evoked a subthreshold EPSP in low concentrations of bicuclline (0.5μM) which increased in amplitude uniformly with increases in stimulation intensity. No Ca^{2+} spikes were evoked synaptically. **D)** (Left) In a different dendrite recorded in the presence of 0.5μM bicuculline, EPSPs decreased in amplitude as the dendritic membrane was current-clamped from -80mV, and reversed at ~ +5mV. Note that EPSP duration was enhanced with membrane depolarization from -80mV to -25mV due to activation of NMDA receptors. (Right) A graph showing the changes in the amplitude of the layer I-II EPSP with changes in dendritic membrane voltage.

In the presence of QX-314 (>25 min after break in) it was not possible to evoke spikes synaptically within the tuft by non-isolated glutamatergic EPSPs (in 0.5μM bicuculline, n = 7, Fig. 5-6C,D) even with strong synaptic stimulation or membrane depolarization. As shown in Fig 4-5C,D no 'hump' potential or Ca^{2+} spikes were evoked under these conditions. Thus in the apical tuft of PFC neurons, only Na^{+} and not Ca^{2+} mediated potentials could be evoked synaptically. Like somatic recordings, increasing the concentration of bicuculline to >2μM evoked a giant EPSP recorded with in the apical tuft (n=5, Fig 5-7). The transition from a small EPSP to a giant EPSP recorded in the apical tuft occurred within a very narrow stimulation intensity range. In fact, both small or giant variable onset EPSPs were often evoked using the same stimulation intensity (Fig. 5-7A). Note in Fig 5-7A that even very large stimulation intensities (400 μA) were insufficient to evoke a giant EPSPs in the absence of bicuculline.

Similar to giant EPSPs recorded from the soma, giant EPSPs recorded from the apical tuft were still present in APV but were slightly reduced in duration (n=3, Fig 5-7B). Following washout of APV, co-application of DNQX with bicuculline eliminated the giant EPSP and a stable monosynatic EPSP was evoked (Fig 5-7B,C).

In contrast to somatic recordings, Ca^{2+} mediated potentials were not triggered by NMDA EPSPs within the apical tuft even when using very strong stimulation intensities (400μA) or during membrane depolarization to beyond 0mV (Fig 5-7C). The amplitude of NMDA EPSPs recorded from the apical tufts was influenced by dendritic membrane voltage and reversed in polarity at 0mV

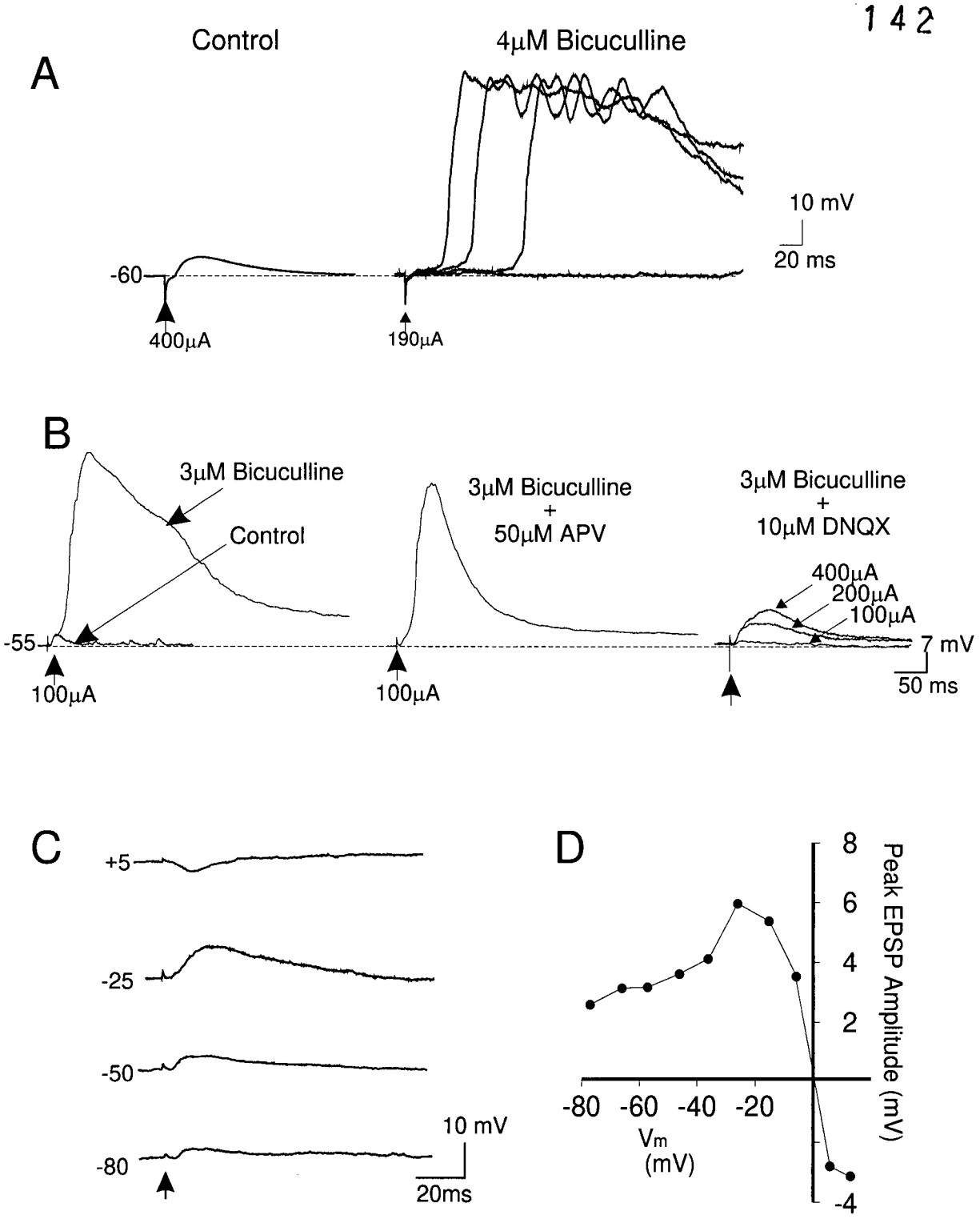

Figure 5-7: $GABA_A$-mediated inhibition of the apical tuft. **A)** In an apical tuft dendrite, synaptic stimulation of layers I-II evoked a small EPSP (left). Application of 4μM bicuculline evoked either a small EPSP or a gaint EPSP at variable onset latencies using the same low current intensity (190μA). **B)** In a different tuft dendrite, application of 3μM bicuculline transformed a tiny EPSP into a giant EPSP (left). Co-application of APV (50μM) reduced the duration of the giant EPSP (middle). Washout of APV and addition of DNQX (10μM) greatly reduced the EPSP. A stable NMDA-mediated EPSP could be evoked if the stimulation current intensity was increased. **C)** Voltage-depedence and reversal of the NMDA EPSP with membrane depolariation. **D)** Plot of the responses illustrated in C showing the typical voltage profile of an NMDA-mediated response. All recordings were performed using QX-314-filled patch-pipettes.

(Fig 5-7D). This finding indicated that: 1) The NMDA-mediated response had properties consistent with NMDA responses recorded from the soma (Hestrin et al. 1990; Nowak et al. 1984) and main stem of the apical dendrite (Spruston et al. 1995). 2) The high access resistance (60-80 MΩ) of the dendritic patch-pipette did not seriously alter the recorded membrane voltage.

Amplification of EPSPs by Proximal Voltage-Gated Ca^{2+} Channels.

To test the hypothesis that Ca^{2+} channels proximal to the soma amplified distal EPSPs, the Ca^{2+} channel blocker Cd^{2+} was applied focally to different regions of the neuron prior to synaptic stimulation of the apical tuft. Because Cd^{2+} blocks transmitter release pre-synaptically, it could block diffuse polysynaptic collateral inputs which contribute to the response evoked by layer I synaptic stimulation (Cauller & Connors 1994). It was therefore essential to ensure that polysynaptic collateral inputs did not contribute to the synaptic response.

Preliminary experiments revealed that in bicuculline alone, focal application of DNQX (100μM) but not APV (500μM) to the apical dendrite reduced the synaptic response evoked by layer I-II stimulation (n=3, not shown). Furthermore, as shown in Fig. 5.3, monosynaptic layer I-II EPSPs rather than giant polysynaptic EPSPs were evoked in the presence of bicuculline and DNQX. Thus polysynaptic collateral inputs were activated by layer I-II inputs and were mediated primarily by AMPA receptors.

In order to eliminate these polysynaptic collateral inputs, a vertical cut was made in the brain slices from layers VI-II and the stimulation electrode was

placed >0.3mm on the far side of the cut from the recording electrode to isolate layer I-II inputs (Cauller & Connors 1994). In addition, DNQX and bicuculline were co-applied during the course of all experiments, unless otherwise stated. Finally, in some experiments APV was applied focally to the region where Cd^{2+} had been applied to ensure blockade of collateral inputs were not the cause of any Cd^{2+}-mediated response attenuations.

Cd^{2+} (2-50mM in puff pipette) was pressure ejected focally to the apical dendritic stem or apical dendritic tuft. (Fig. 5-8). Layer I-II NMDA EPSPs which evoked action potentials (suprathreshold responses) were reduced significantly by Cd^{2+} application to the proximal apical dendrite and soma (n=8 / 9, Fig 5-8A). Following Cd^{2+} application, action potentials were not triggered synaptically unless the V_m was depolarized by at least 2-4mV more positive than the control V_m. In contrast, focal Cd^{2+} application to the proximal apical dendrite had no effect on subthreshold NMDA EPSPs evoked >5mV more negative than the threshold for triggering action potentials (Fig 5-8A). Thus, Cd^{2+} application to the apical dendritic stem reduced the suprathreshold synaptic responses evoked by synaptic stimulation of layers I-II.

In order to test whether Cd^{2+}-sensitive Ca^{2+} channels in the distal apical tuft also contributed to the suprathreshold response recorded at the soma, responses were evoked non-synaptically by focal glutamate application to the apical tuft (>500μm from soma). The glutamate-evoked suprathreshold response recorded from the soma was unaffected by focal Cd^{2+} application to the apical tuft (>500μm from the soma) just below the site of glutamate application (n = 5 /

Figure 5-8: Cd^{2+} sensitive currents proximal to the soma of layer V PFC neurons enhance responses evoked by stimulation of layers I-II. **A)** (From Left to Right) Schematic diagram of a layer V PFC neuron and the location of synaptic stimulation and Cd^{2+} (5mM in puff pipette) and APV (250μM in puff pipette) pressure ejection pipettes. Synaptic stimulation of layers I-II (in the presence of bath applied DNQX ,10μM and Bicuculline, 4 μM) evoked either a large subthreshold NMDA EPSP or a suprathreshold response at a V_m of -56mV. Note the 'hump'-like potential during the late portion of the subthreshold EPSP. At a V_m of -76mV a smaller subthreshold NMDA EPSP was evoked. Cd^{2+} application to the proximal apical dendritic stem region (100-200μm from the soma) reduced the large subthreshold EPSP and abolished synaptically evoked action potentials, while having no effect on the EPSP evoked at -76mV. Following partial recovery from the effects of Cd^{2+} application, focal application of APV to the same site had no effect on the evoked response. **B)** (From left to right) Schematic diagram of a layer V PFC neuron and the location of the glutamate and Cd^{2+} pressure ejection pipettes . Focal pressure ejection of glutamate to the apical tuft evoked a suprathreshold response recorded at the soma. Cd^{2+} application just below the glutamate pipette in the apical tuft did not block the gluatamate evoked response.

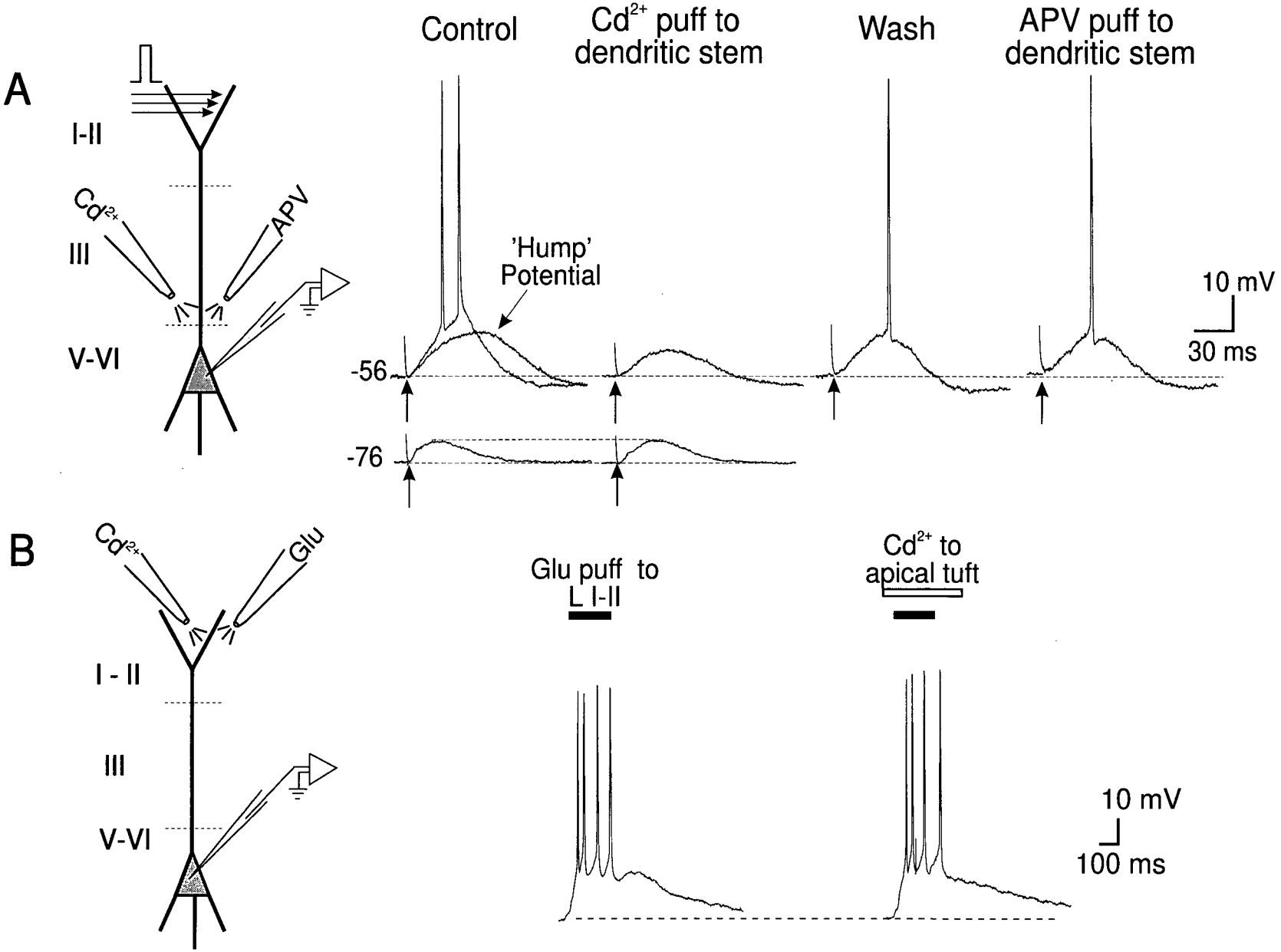
A
I-II
III
V-VI
Cd2+
APV
Control
Cd2+ puff to dendritic stem
Wash
APV puff to dendritic stem
'Hump' Potential
-56
-76
10 mV
30 ms
B
Cd2+
Glu
I - II
III
V-VI
Glu puff to L I-II
Cd2+ to apical tuft
10 mV
100 ms

5, Fig 5-8B). In contrast, Cd^{2+} application to the proximal apical dendrite (100-200μm from soma, n=8/8, not shown) reduced the glutamate-evoked response, however, using this preparation it was not possible to rule out that glutamate-activated collateral inputs were also blocked by Cd^{2+}. Collectively the results illustrated in Fig. 5-8 suggested that dendritic voltage-gated Ca^{2+} channels proximal to the soma and not within apical tuft functionally amplified distally evoked suprathreshold synaptic responses.

Properties of the Synaptically-Evoked 'Hump' Potential

As shown in Fig 5-9A, when the steady-state V_m was depolarized from rest, the late component of the synaptic response showed an abrupt increase in amplitude, just prior to the initiation of an action potential, corresponding to the generation of the 'hump' potential. The 'hump' potential was initiated in this manner during recordings from the soma (Fig 5-9A) or apical stem (Fig 5-9C). The increase in EPSP amplitude by the hump is illustrated graphically in Fig 5-9B for the soma and Fig 5-9D for the apical stem.

Following blockade of Na^+ channels by QX-314 the 'hump' potential recorded from the soma was evoked in a voltage-dependent manner by an isolated NMDA EPSP (Fig 5-10A, n=50). This indicated that the generation of the 'hump' potential was independent of Na^+ channels. In 5 additional cells in which a small EPSP could be evoked in APV and bicuculline without triggering a giant EPSP, epileptiform discharge (see above), the 'hump' potential was also generated in a voltage-dependent manner by the isolated AMPA-mediated EPSP

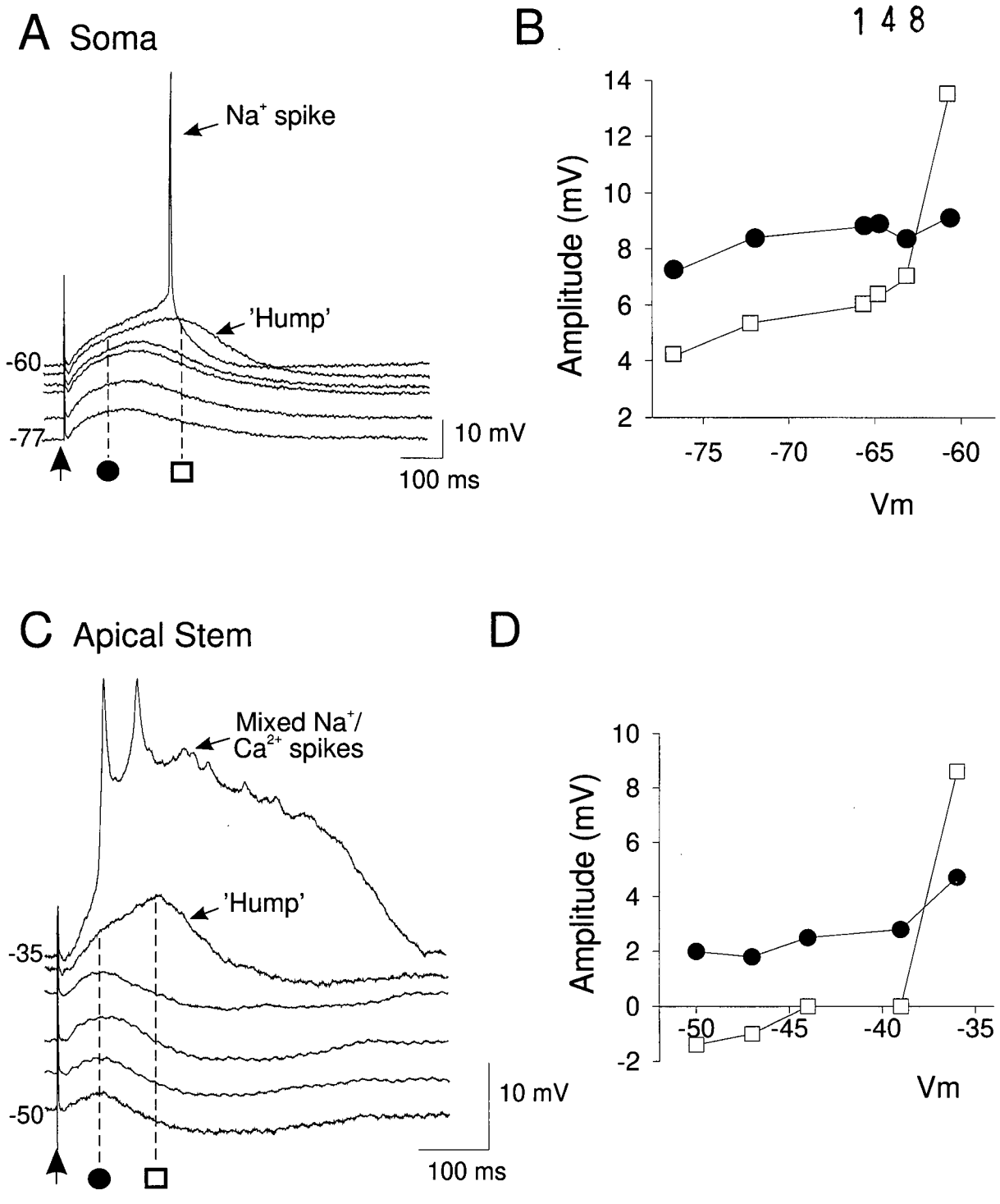

Figure 5-9: The synaptically-activated 'hump' potential recorded at the soma and apical stem. **A)** Layer I-II synaptic stimulation evoked a 'hump' potential prior to an action potential during progressive membrane depolarization of the soma. **B)** Plot of the holding potential versus response amplitude at the points demarcated by the black circle and open square in A. **C)** Layer I-II synaptic stimulation evoked a 'hump' potential prior to an action potential during progressive membrane depolarization of the apical stem. **D)** Plot of the holding potential versus response amplitude at the points demarcated by the black circle and open square in C. Responses in A and C were recorded in the presence of bicuculline (4μM) and DNQX (10μM).

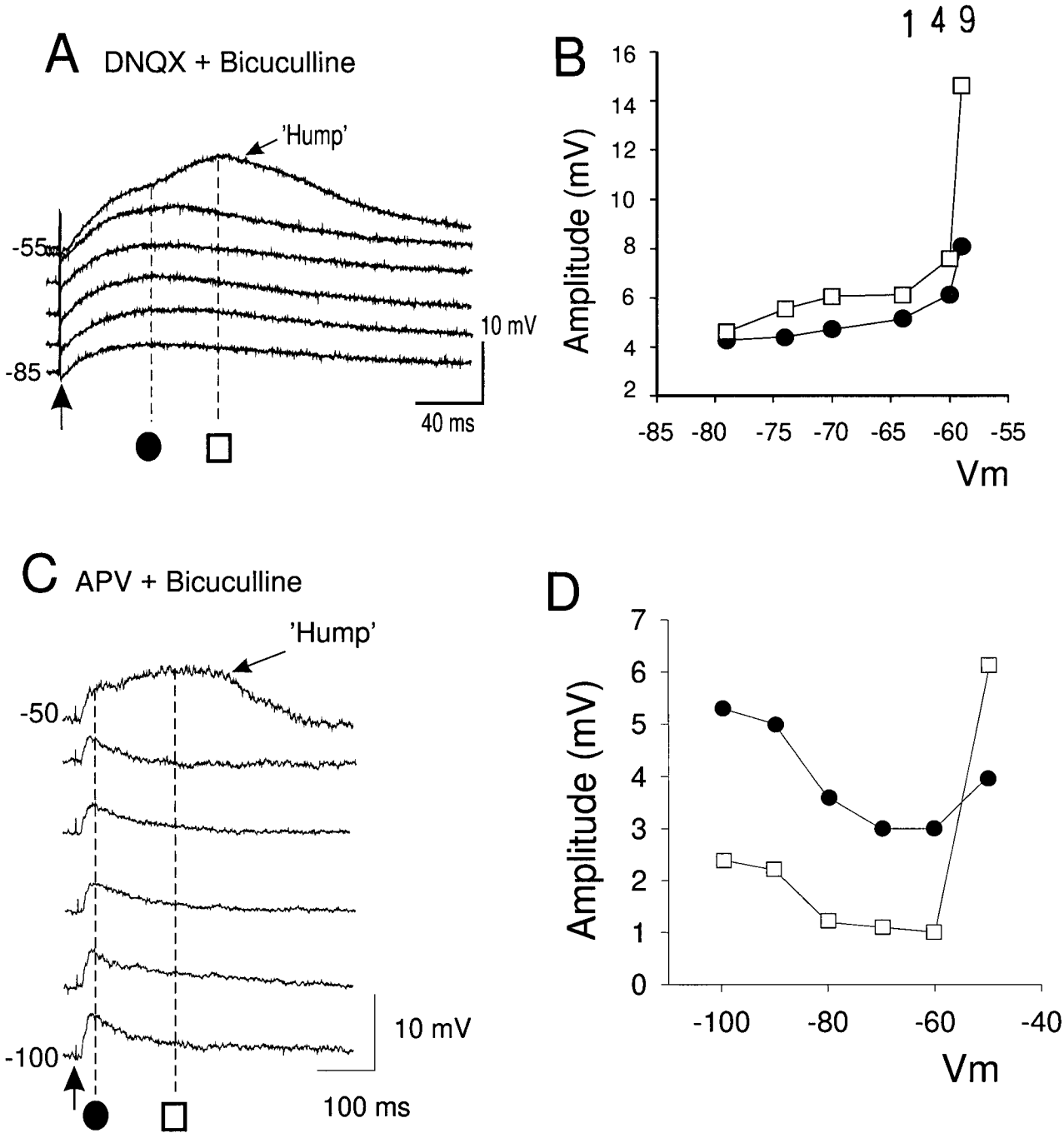

Figure 5-10: The synaptically-activated 'hump' potential evoked by NMDA and non-NMDA EPSPs. **A)** During a somatic recording in the presence of DNQX (10μM) and bicuculline (4μM), synaptic stimulation of layers I-II evoked a 'hump' potential at depolarized membrane potentials. **B)** Plot of the holding potential versus response amplitude at the points demarcated by the black circle and open square in A. **C)** During a somatic recording in the presence of APV (50μM) and bicuculline (4μM), synaptic stimulation of layers I-II also evoked a 'hump' potential at depolarized membrane potentials. **D)** Plot of the holding potential versus response amplitude at the points demarcated by the black circle and open square in C. Responses in A and C were recorded using an intracellular electrode containing QX-314, 1M CsAc and 2M KAc.

(Fig 5-10C). The 'hump' potential significantly enhanced the amplitude of the NMDA-mediated EPSP (Fig 5-10B) and the AMPA-mediated EPSP (Fig 5-10D).

To ensure that the 'hump' potential evoked synaptically was the same as that evoked by intracellular current pulses as described in Chapter 3, a number of additional experiments were performed. Results presented in Chapter 3 suggested that the 'hump' potential was generated by voltage-gated high threshold Ca^{2+} currents located proximal to the soma. If this were the case then it should be possible to evoke the 'hump' under current clamp conditions but not under voltage-clamp when the V_m was held below the activation threshold for the 'hump' potential. As shown in Fig 5-11A, in current clamp mode, the 'hump' potential was evoked synaptically in a voltage-dependent manner, e.g. at -50 to -55mV. However, in the same neuron, when the soma was voltage-clamped just below the activation threshold for the 'hump' potential only an EPSC was evoked synaptically (Fig 5-11A). This ruled out the possibility that a late polysynaptic input contributed to the 'hump' potential and indicated that the 'hump' was indeed mediated by a voltage-gated current.

As a result of the considerable space-clamp limitations associated with voltage-clamping large pyramidal neurons (Spruston et al. 1993), the data shown in Fig 5-11A also suggested that the 'hump' potential was generated electrotonically close to the soma in a region adequately voltage-clamped by the somatic electrode. In accordance with this hypothesis, the 'hump' potential was repolarized by a fast hyperpolarizing (-1 to -3nA / 10-20ms) somatic current pulse (Fig 5-11B, n = 5 / 5). Such fast intrasomatic hyperpolarizing pulses do not

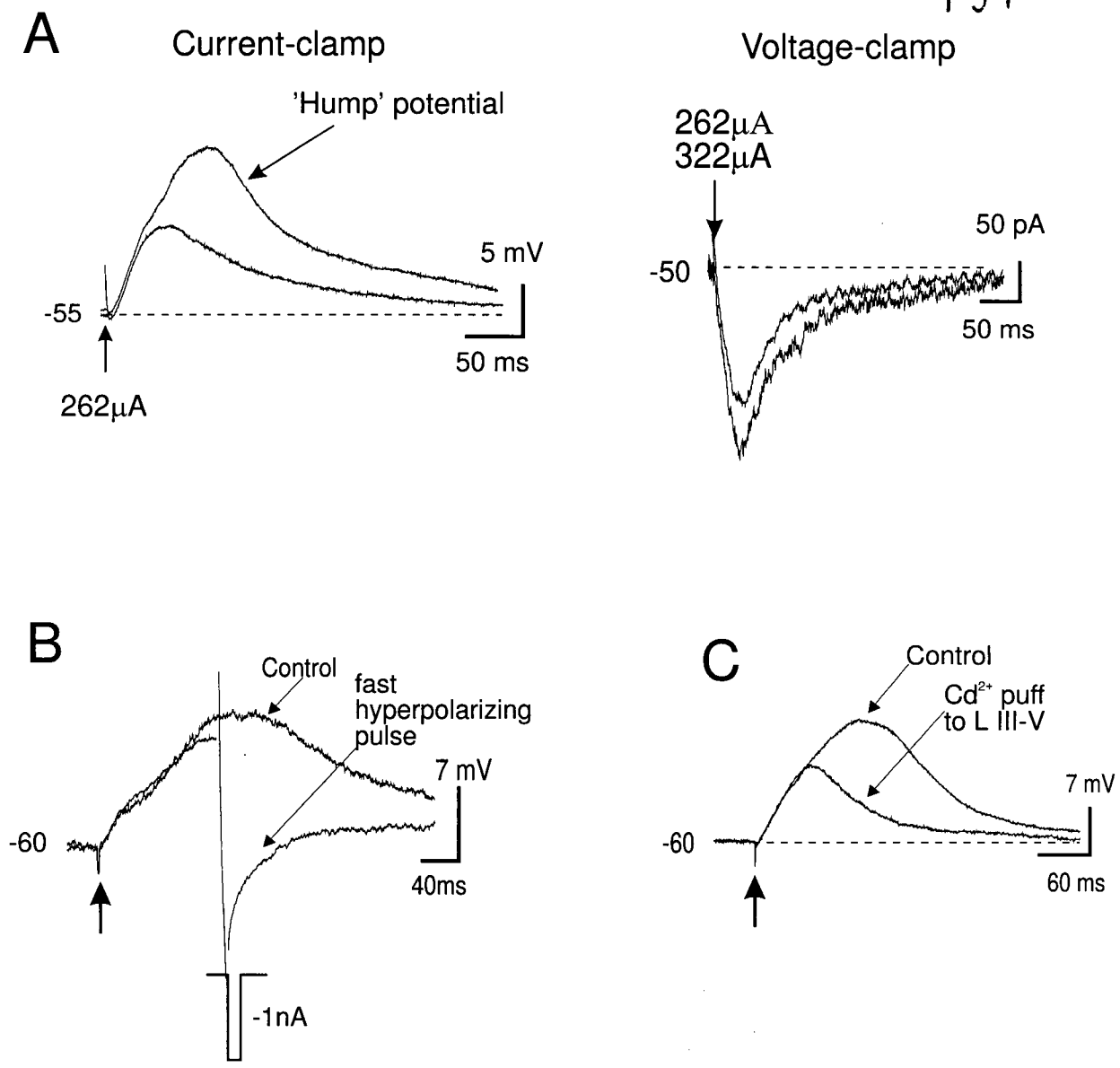

Figure 5-11: Properties of the synaptically-evoked 'hump' potential. **A)** The 'hump' potential was evoked synaptically in a voltage-dependent manner in current clamp mode (left). In the same neuron, the 'hump' potential was absent in voltage-clamp mode even when the stimulation intensity was increased from 262μA to 322μA (right), indicating that it was mediated by a voltage-gated current. **B)** The synaptically evoked 'hump' potential was repolarized by a fast hyperpolarizing somatic current pulse (-1000pA/10ms). **C)** The synaptically evoked 'hump' potential was blocked by focal Cd^{2+} puff to the proximal apical dendritic stem (100-200μm from soma). Responses in A-C were recorded using an electrodes containing QX-314 and CsAc.

propagate far from the soma because they are strongly filtered by the passive cable properties of the dendrites (i.e. estimated to be ~50% attenuation at 333μM from the soma) (Jack et al. 1975; Johnston & Brown, 1983; Spruston et al. 1993 & 1994; Spruston & Stuart 1996; Reuvini et al. 1993). Thus the 'hump' potential was generated by a voltage-activated current located electrotonically close to the soma.

As shown in Chapter 3 (Fig 3-6) the 'hump' potential evoked by intrasomatic current pulses was blocked by focal Cd^{2+} application to the apical stem. The 'hump' potential evoked synaptically was also blocked by focal Cd^{2+} application to the proximal apical dendrite (Fig 5-11C, n = 11 / 12). Thus, like the 'hump' potential evoked by intrasomatic current pulses, the synaptically-activated 'hump' potential was generated by Ca^{2+} currents in the proximal apical dendrite / soma.

Given the relatively high concentrations of Cd^{2+} that were applied focally (2-50mM) it was not possible to achieve a selective block of high threshold Ca^{2+} channels and thus it was not clear whether high or low threshold Ca^{2+} channels contributed to the synaptically-activated 'hump' potential. However, the 'hump' potential was not generated by a low threshold Ca^{2+} current because: 1) it was evoked at membrane potentials near -50mV (Fig 5-12) where T-currents are inactivated (Tsien et al. 1988), and 2) it was not blocked by Ni^{2+} (100μM) (n = 4 / 4,Fig. 5-12A).

In contrast, "high threshold" L-type Ca^{2+} channels made a significant contribution to the generation of the synaptically-evoked 'hump' potential.

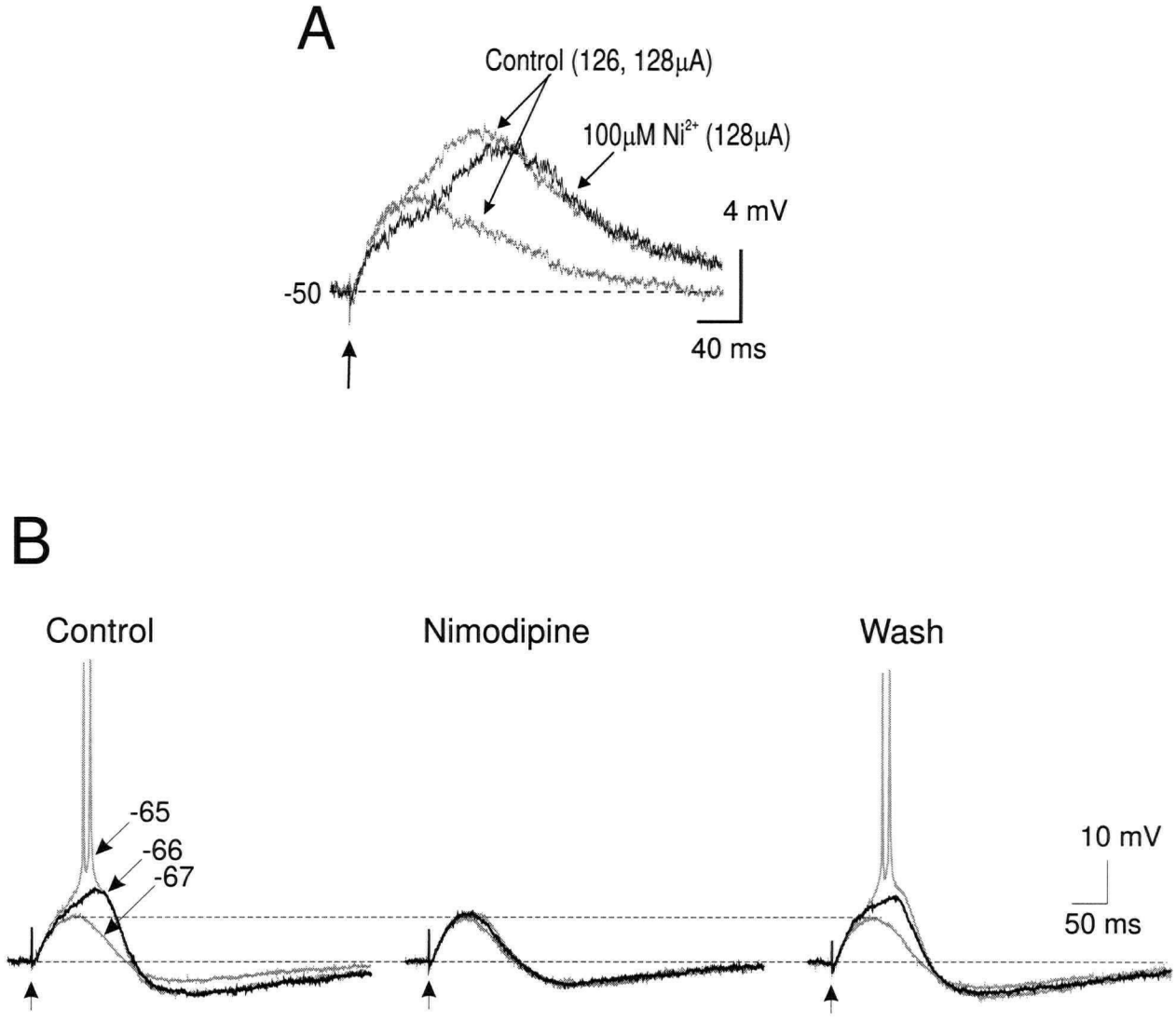

Figure 5-12: Ionic basis of the 'hump' potential. **A)** The 'hump' potential evoked by layer I-II synaptic stimulation was not mediated by a low threshold Ca^{2+} (T-type) current. The synaptically evoked 'hump' potential was evoked at a steady state V_m of -50mV and was not blocked by bath application of Ni^{2+} (100μM). **B)** An EPSP (gray trace), an EPSP plus 'hump' potential (black trace), and a suprathreshold response (gray trace with spikes) were evoked by layer I-II stimulation at somatic holding potentials of -67mV, -66mV and -65mV respectively (left). The 'hump' potential and suprathreshold response evoked by layer I-II synaptic stimulation were eliminated reversibly by bath application of the L-type Ca^{2+} channel blocker, nimodipine (10μM) (middle and right). Responses were recorded in DNQX and bicuculline.

Following blockade of L-type channels by nimodipine the amplitude of the synaptically-evoked 'hump' potential was reduced by 3.93 ± 0.54mV (Fig 5-12B, n=5). This meant that the neuron would have to be depolarized by nearly 4mV in order for the same EPSP to evoke spikes in the absence of L-type Ca^{2+} channels. Collectively, these data suggest that the 'hump' potential which amplified distal EPSPs was mediated primarily by L-type Ca^{2+} channels located close to the soma.

Discussion

The results of Chapter 5 revealed that synaptic responses of layer V PFC neurons are influenced strongly by GABA-mediated IPSPs. By blocking $GABA_A$ IPSPs, giant polysynaptic responses were recorded from the soma and apical tuft. These giant EPSPs were primarily AMPA mediated. Blockade of AMPA receptors by co-application of DNQX, resulted in a stable monosynaptic NMDA-mediated EPSP. This NMDA EPSP was able to evoke Ca^{2+} potentials during somatic recordings but not recordings from the apical tuft. A subthreshold Ca^{2+} potential was generated by L-type Ca^{2+} channels near the soma, which helped to boost distal EPSPs.

Synaptic stimulation of the deep or superficial layers of the cortex evoke both EPSPs and IPSPs of varying duration (Connors et al.1982; 1988). In the PFC as in other cortical areas, deep layer stimulation evoked an initial brief EPSP, followed by a fast and slow IPSP mediated by $GABA_A$ and $GABA_B$ receptors respectively (Connors et al. 1988). The fast $GABA_A$ response is Cl^--

mediated and reverses at approximately -70 while the slow $GABA_B$ response is K^+-mediated and reverses at approximately -90mV (present study, Connors et al. 1988; Kawaguchi 1993). The peak conductance of the fast IPSP is 10 fold larger than that of the slow IPSP in cortical neurons and is more effective at preventing spike firing in pyramidal neurons (Connors 1992; Connors et al. 1988; Deisz & Prince 1989; van Brederode & Spain 1995; Thomson & Deuchars 1997). Moreover, fast IPSPs appear to make a greater contribution to IPSPs generated in pyramidal neurons in the cortex (Thomson et al. 1993; Thomson & Deuchars 1997).

There is a high density of $GABA_A$ receptors in the superficial as compared to the deep layers (Jones 1993). Recordings from the soma of superficial or deep layer pyramidal cells in the cortex also suggest stronger GABA-mediated inhibition in superficial layers (van Brederode & Spain 1995; Silva et al. 1991). Furthermore, the fast IPSPs in dendritic but not somatic regions strongly modulates the NMDA response to burst-patterned stimulation (Kanter et al. 1996).

In the present Chapter, strong $GABA_A$ mediated IPSPs strongly limited the synaptic response recorded from the soma and apical tuft of PFC neurons to layer I-II stimulation. As in previous studies, following blockade of $GABA_A$-mediated IPSPs, a giant EPSP was recorded from the soma (Johnston & Brown 1981; Chagnac-Amitai & Connors 1989). The novel finding of the present experiments was strong excitatory drive to the apical tuft produces only small local EPSPs under normal conditions, and large EPSPs are only observed

following blockade of $GABA_A$ receptors. The excitatory synaptic drive to the apical tuft was clearly much greater in bicuculline since the doses of bicuculline used in the present experiments likely evoked synchronous activity across widespread regions of the cortex (Chagnac-Amitai & Connors 1989), and the giant EPSPs were clearly polysynaptic in origin given the large variability in onset latencies. However, it is evident that magnitude of the excitatory response onto the apical tuft is determined by $GABA_A$ IPSPs. Although K^+ currents exert a strong inhibitory effect on excitatory events within the apical tuft (see Chapter 4), in the absence of $GABA_A$-mediated inhibition, the apical tuft is nevertheless capable of generating massive EPSPs. Strong $GABA_A$-inhibition of the apical dendrites underlies penicillin-induced epileptiform activity in the hippocampus (Wong et al. 1979) and could conceivably play a similar role in the PFC.

The giant EPSP recorded from the soma or apical tuft in bicuculline was mediated by non-NMDA receptors, and was abolished by bath application of DNQX. A similar non-NMDA mediated giant EPSP has been reported in piriform cortex neurons (Hoffman & Haberly 1989). In the presence of bicuculline and DNQX a monosynaptic (constant onset latency) NMDA EPSP was recorded at both sites following stimulation of layers I-II. There has been considerable controversy regarding the spatial locations of NMDA receptors that mediate distally generated EPSPs. While NMDA R1 subunit immunoreactivity is found in virtually all lamina of the cortex (and PFC), including the superficial layers (Bröckers et al. 1994; Huntley et al. 1994; Rudolf et al. 1996), the electrical response of deep layer cortical neurons to iontophoresis of NMDA has been

reported to decrease with distance from the soma (Currie et al. 1994; Dodt et al. 1995). During tuft recordings, the initial synaptic response to layer I-II stimulation was greatly reduced by DNQX, but an NMDA EPSP could be evoked if the stimulation intensity was increased. This is consistent with the notion that the peak synaptic current is largely dependent upon activation of dendritic non-NMDA receptors (Spruston et al. 1995). Furthermore, in the absence of non-NMDA receptors, synaptic inputs will produce less membrane depolarization and therefore less relief of the voltage-dependent Mg^{2+} block of NMDA receptors. Thus, while NMDA EPSPs could be recorded within the tuft following layer I-II stimulation, NMDA receptor activation is likely dependent upon AMPA receptor stimulation normally.

A key difference between somatic and dendritic recordings was the lack of synaptically-evoked Ca^{2+} potentials in the apical tuft. This finding supports the conclusion made in Chapter 4 that the apical tuft is relatively devoid of Ca^{2+} electrogenesis. Furthermore, since the properties of the Ca^{2+} spike evoked by the NMDA EPSP and intracellular current pulses were virtually identical, it suggests that the Ca^{2+} spikes were generated by the same Ca^{2+} channels under both conditions. Thus, current flowing from the soma to dendrite and dendrite to soma were equivalent with respect to Ca^{2+} electrogenesis, and Ca^{2+} potentials were generated close to the soma in both cases.

A number of general conclusions can be made about the synaptic responses of PFC neurons: 1) $GABA_A$ IPSPs strongly limit excitatory responses evoked by a stimulating electrode in layers I-II or V-VI. 2) Stimulation delivered

after blockade of GABA receptors evokes a massive polysynaptic, AMPA-mediated EPSP. The presence of this giant EPSP makes it impractical to work with isolated AMPA EPSPs in PFC slices. 3) Co-application of bicuculline and DNQX evokes a monosynaptic stable, NMDA EPSP that can trigger Ca^{2+} potentials. 4) Ca^{2+} potentials are not easily evoked synaptically within the apical tuft of layer V PFC neurons. 5) A Ca^{2+}-mediated 'hump' potential is evoked by synaptic stimulation of layers I-II and it serves to amplify distal EPSPs.

A number of experiments were performed which investigated the ionic basis of the 'hump' potential. The 'hump' potential which rode atop layer I-II non-isolated or isolated NMDA EPSPs was clearly different from a late polysynaptic NMDA-mediated EPSPs described previously (Sutor & Hablitz 1989) because: 1) The 'hump' potential was evoked abruptly during membrane depolarization, 2)The 'hump' potential was evoked in media containing APV and low $[Ca^{2+}]_o$, high $[Mg^{2+}]_o$ or high $[Ca^{2+}]_o$ which block NMDA receptors and polysynaptic EPSPs respectively (Berry & Pentreath 1976). 3) The 'hump' potential was repolarized by a fast hyperpolarizing pulse. 4) The 'hump' potential was evoked by intrasomatic current pulses. 5) A monosynaptic EPSC but no 'hump' current was evoked synaptically when the soma was voltage-clamped below the activation threshold of the 'hump' potential. The present results also suggested that the 'hump' potential was not mediated by a QX-314-sensitive slowly inactivating Na^+ current or a Ni^{2+}-sensitive low threshold Ca^{2+} current (see Figs 2, 3A). Rather, the 'hump' potential was mediated by a slowly activating Ca^{2+} current located along the proximal apical dendritic stem, quite similar to that

recorded intradendritically in hippocampal pyramidal and Purkinje neurons (Benardo et al. 1982; Llinas & Sugimori 1980; Masukawa & Prince 1984). However, while Cd^{2+} application specifically to the proximal apical dendrite blocked the 'hump' potential and Ca^{2+} spikes, the spread of Cd^{2+} could have also affected Ca^{2+} channels in the basal dendrites and soma which may also contribute to Ca^{2+} potential electrogenesis.

As shown in Fig 5-12, the 'hump' potential was reduced by the L-type Ca^{2+} channel antagonist nimodipine. Accordingly, L-type Ca^{2+} channels are clustered along the proximal apical dendrite (Magee & Johnston 1995a,b; Westenbroek et al., 1992) and mediate subthreshold membrane depolarization (see Fig 2-6; Avery & Johnston 1996; Hernández-López et al. 1997). Collectively these data suggest that the Cd^{2+}-sensitive amplification of distal EPSPs was mediated by L-type Ca^{2+} channels located in the proximal dendrites/soma.

As noted in Chapter 4, there is a functional advantage to having Ca^{2+} potentials evoked synaptically within apical dendritic stem but not the apical tuft of PFC neurons: Inputs to the apical tuft would be curtailed temporally due to the fast passive membrane properties and large intrinsically generated Ca^{2+} spikes would not be initiated which would produce prolonged membrane depolarization. As a result the apical tuft would only firing a spike if many inputs arrived within a short temporal window (~10ms). Ca^{2+} channels in the proximal dendrite, activated by distal EPSPs, may inject current into the soma to charge the soma and basal dendrites. In this way, like the persistent Na^{+} current, Ca^{2+} channels clustered in the proximal dendrites may serve to overcome somatic capacitance

and ensure that distal EPSPs can depolarize the soma and axon to spike threshold.

Chapter 6:

Action of DA on PFC Neurons

Introduction

The prefrontal cortex (PFC) receives all major ascending monoaminergic projections, however the mesocortical dopaminergic input from the ventral tegmental area (VTA) has received much attention due to its perceived involvement in cognitive and neuropsychiatric processes (Goldman-Rakic, 1992; Jaskiw and Weinberger, 1992). The mesocortical DA input is crucial for processes in working memory processes mediated by the PFC (Brozowski et al., 1979; Goldman-Rakic, 1992). For example, performance on delayed response tasks is disrupted by administration of D1, but not D2, antagonists into the PFC (Goldman-Rakic,1992; Sawaguchi and Goldman-Rakic, 1994; Seamans et al., 1995; Smiley et al., 1994), while microiontophoretic application of DA or a very low iontophoretic dose of D1 antagonists enhance the firing rate of PFC neurons during the delay period of such tasks (Sawaguchi, 1987; Sawaguchi et al., 1990a; Williams & Goldman-Rakic, 1995). Given that this delay-period activity is highly correlated with task performance, and is thought to be a neural representation of short-term memory (Goldman-Rakic 1995a,b), these data indicates that DA modulates mnemonic aspects of working memory processes within the PFC.

Administration of DA into the PFC of primates also modulates the activity of neurons that are correlated with the initiation of a correct response on a

delayed-response task (Sawaguchi, 1987; Sawaguchi et al., 1990a). In rats, microinjection of D1 but not D2 receptor antagonists into the medial PFC disrupted foraging on a radial arm maze based on information acquired 30 min. previously, while similar injections had no effect on memory-based foraging within a single trial. These data suggest that D1 receptors in the PFC also modulate other aspects of working memory, specifically the ability to use mnemonic information to guide forthcoming responses. Inputs from the temporal lobe/hippocampus or parietal lobe (Floresco et al. 1997; Fuster et al. 1985; Goldman-Rakic 1988; Quintana et al. 1989) may provide mnemonic information to PFC which is used to guide forthcoming responses. Evidence presented in Chapter 2 suggested that D1 receptors in the PFC modulated the flow of information from the hippocampus to the PFC at a time when previously acquired information was to be used to guide forthcoming foraging behavior. Thus D1 receptors in the PFC modulate two important aspects of working memory, namely; 1) the short-term active retention of information and 2) the ability use mnemonic information to guide action. The neural mechanisms through which D1 receptors modulates these aspects of working memory are not known.

As discussed in the General Introduction and in Chapter 3, layer V-VI PFC neurons of are particular relevance to working memory processes mediated by the PFC since they; 1) show sustained activity throughout the delay period of a delayed response task (Fuster 1973; Sakai & Hamada 1981), 2) project out of the PFC to regions involved in response initiation such as the striatum (Gorelova & Yang 1997; Sesack et al. 1989) and 3) receive inputs from the hippocampus

(Carr & Sesack 1996; Gigg et al. 1994) and possibly parietal and temporal corticies (Goldman-Rakic 1988) which are essential for the performance of delayed responding (Floresco et al. 1997; Fuster et al. 1985; Quintana et al. 1989). For these reasons it was of interest to determine how DA modulates the intrinsic membrane properties and synaptic responses of layer V-VI PFC neurons.

As described in Chapter 3, the firing threshold of layer V-VI PFC neurons is controlled by two opposing voltage-dependent currents: the slowly-inactivating Na^+ and K^+ current. DA modulates threshold events in striatal neurons and reduces slow-inactivating Na^+ and K^+ currents directly (Cépeda et al., 1994; Calabresi et al., 1987; Surmeier et al., 1992; Kitai & Surmeier 1993). The effects of DA on these two major ionic conductances were therefore examined in PFC neurons. In addition, DA, via the D1 receptor, also reduces N- and P-type Ca^{2+} currents in striatal neurons (Surmeier et al. 1995). In PFC neurons, high threshold Ca^{2+} channels and DA receptors are localized the same region of the neuron (i.e. the soma and proximal dendritic region) (Chapter 3; Hell et al., 1993; Hillman et al., 1991; Smiley and Goldman-Rakic, 1993; Usowicz et al., 1992; Westenbroek et al., 1992; Yuste et al., 1994). Given the important role that these Ca^{2+} potentials play in burst generation (Chapter 3) and shaping EPSPs (Chapter 5) in PFC neurons, the effect of D1 receptor stimulation on high threshold Ca^{2+} potentials was also examined. Finally, the effects of DA on both inhibitory and excitatory synaptic inputs to PFC neurons was investigated.

Results

Effects of DA agonists on the passive membrane properties of PFC neurons

The effects of bath-application of DA, D1 or D2 agonists were examined on the passive membrane properties of 19 electophysiologically characterized PFC neurons (2 *RS*, 2 *IM*, 1 *ROB* and 14 *IB* neurons). In order to examine the effects of DA directly on the passive membrane properties of single PFC neurons, APV and bicuculline were added to the perfusate to block excitatory inputs and GABA inputs which are activated by DA (Penit-Soria et al. 1987; Retaux et al. 1991). Under these conditions, DA (20-50μM) induced no change in the membrane potential in 3 neurons (not shown), a small depolarization (2-5 mV) in 9 neurons, a hyperpolarization (2-8 mV) in 3 neurons, and a biphasic response consisting of a depolarization followed by a hyperpolarization in an additional 3 neurons (Fig. 6-1). In general, the effects of DA were long-lasting although some reversible responses were observed (n=4). The DA response desensitized quickly as subsequent application of DA induced either a smaller change or no change in the membrane potential. The effects of DA on the passive membrane properties were too variable to allow any clear conclusions to be drawn.

Actions of Dopamine on the Active Membrane Properties of PFC Neurons

DA is known to modulate the excitability of striatal and pyramidal PFC neurons in the subthreshold voltage range (Calabresi et al., 1987; Cépeda et al.,

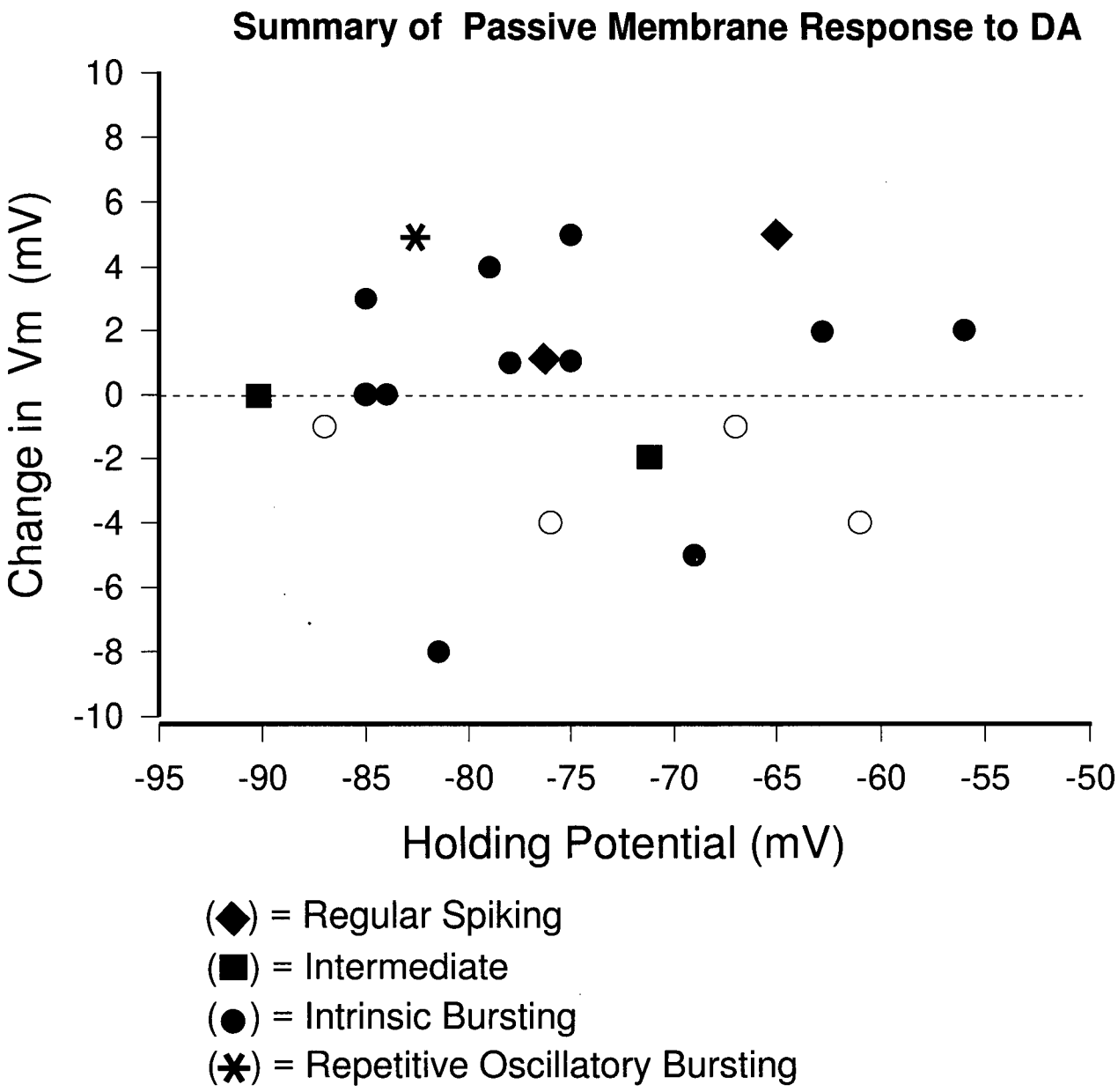

Figure 6-1: Graph summarizing the changes of the resting membrane potential following bath-application of DA on different cell types in the PFC. Open symbols represent responses to DA and filled symbols represent responses to DA in the presence of bicuculline (0.7 -10 μM) and APV (50 μM). Voltage responses above the dotted line indicate depolarization, and below, hyperpolarization.

1992; Penit-Soria et al., 1987), therefore the effects of DA, D1 or D2 agonists on subthreshold voltage responses of 30 PFC neurons were examined. No differences were observed between the 4 cell types with regard to their responses to DA, D1 or D2 agonists. Thus, data from all cell types were "pooled" (n = 12 for DA, n = 10 for SKF-38393, n = 8 for quinpirole). Bath-application of DA or the D1 agonist SKF-38393 reduced the overall first spike latency in 22 out of 23 neurons tested (DA: -39 ± 15% and SKF-38393: -38 ± 14%) (Fig. 6-2A). However, in one *RS* neuron, DA induced a marked increase in the 1st spike latency (159%). The first inter-spike interval (1st ISI) was also reduced by DA (-39 ± 13%) and SKF-38393 (-38 ± 5%). In the presence of the D1 agonist, spike frequency adaptation was greatly reduced and uniform interspike-intervals were observed.

The changes in input resistance induced by DA and SKF-38393 varied greatly with each individual neuron, but there was an overall small reduction in input resistance following DA (-17 ± 10%) application and a negligible change after SKF-38393 (-2 ± 4%). In marked contrast to the DA and D1 receptor-mediated responses, bath-application of the D2 receptor agonist quinpirole induced minimal changes in the first spike latency, first inter-spike interval and input resistance. Preliminary data from 1 apical dendritic tuft recording indicated that D1 receptor stimulation may also increase the number of spikes which invade the dendrites.

In response to a depolarizing input, D1 receptor stimulation not only produced more spikes and shorter first spike latencies, it also changed the firing

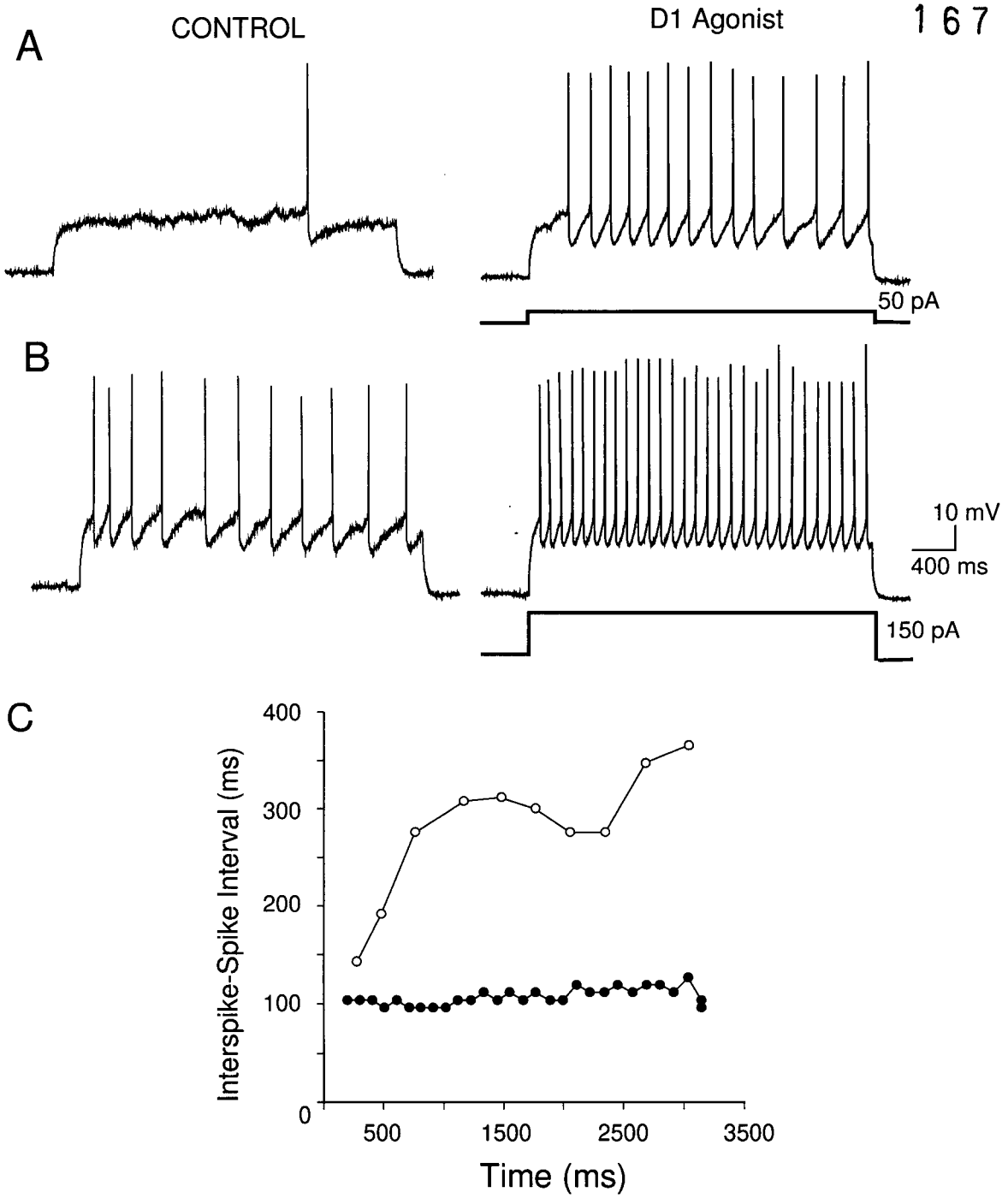

Figure 6-2: D1 receptor stimulation increased the response to an intracellular depolarizing pulse. **A)** (Left): A marked delay of first spike latency in response to a second long, 50 pA intracellular current pulse. (Right) Bath application of SKF38393 (20μM, for 25 secs) induced repetitive firing in response to the same 50pA intracellular current pulse. **B)** (Left) Increasing the intracellular current pulse to 150pA induced repetitive firing with variable inter-spike intervals and progressive spike frequency adaptation in the same *IB* neuron. (Right) Bath application of SKF38393 induced repetitive non-adapting firing in response to the same 150pA intracellular current pulse. **C)** A graph showing the inter-spike intervals of the control firing response (open circle) and the firing response following the application of SKF38393 (filled circles) during the 150pA intracellular current pulse injection. Note the very variable inter-spike intervals and the progressive spike frequency adaptation (e.g. the last inter-spike interval is much longer than the first inter-spike interval within the same spike train evoked, open circle). SKF38393 abolished the frequency adaptation, thus resulting in an overall uniform inter-spike intervals of approximately 100ms.

Figure 6-3: D1 receptor stimulation produced repetitive firng in bursting PFC neurons. **A)** (Left) In a *ROB* PFC neuron, depolarzing current pulses evoked a spike triplet with an AHP followed by a single spike and prominent DAP. (Right) The D1 receptor agonist, SKF-81297 (10μM) changed the initial triplet to a doublet, reduced the AHP and DAP following the second spike. An additional third spike was also evoked. **B)** In a different *ROB* neuron, two burst triplets separated by an AHP were evoked by depolarizing current pulses (Left). In the presence of the D1 receptor agonist SKF-38393, the initial triplet was still evoked but was followed by repetitive spiking (right). **C)** Histogram showing the mean percent change in AHP amplitude and duration and DAP amplitude due to D1 receptor stimulation. **D)** Illustration showing how the AHP and DAP were measured.

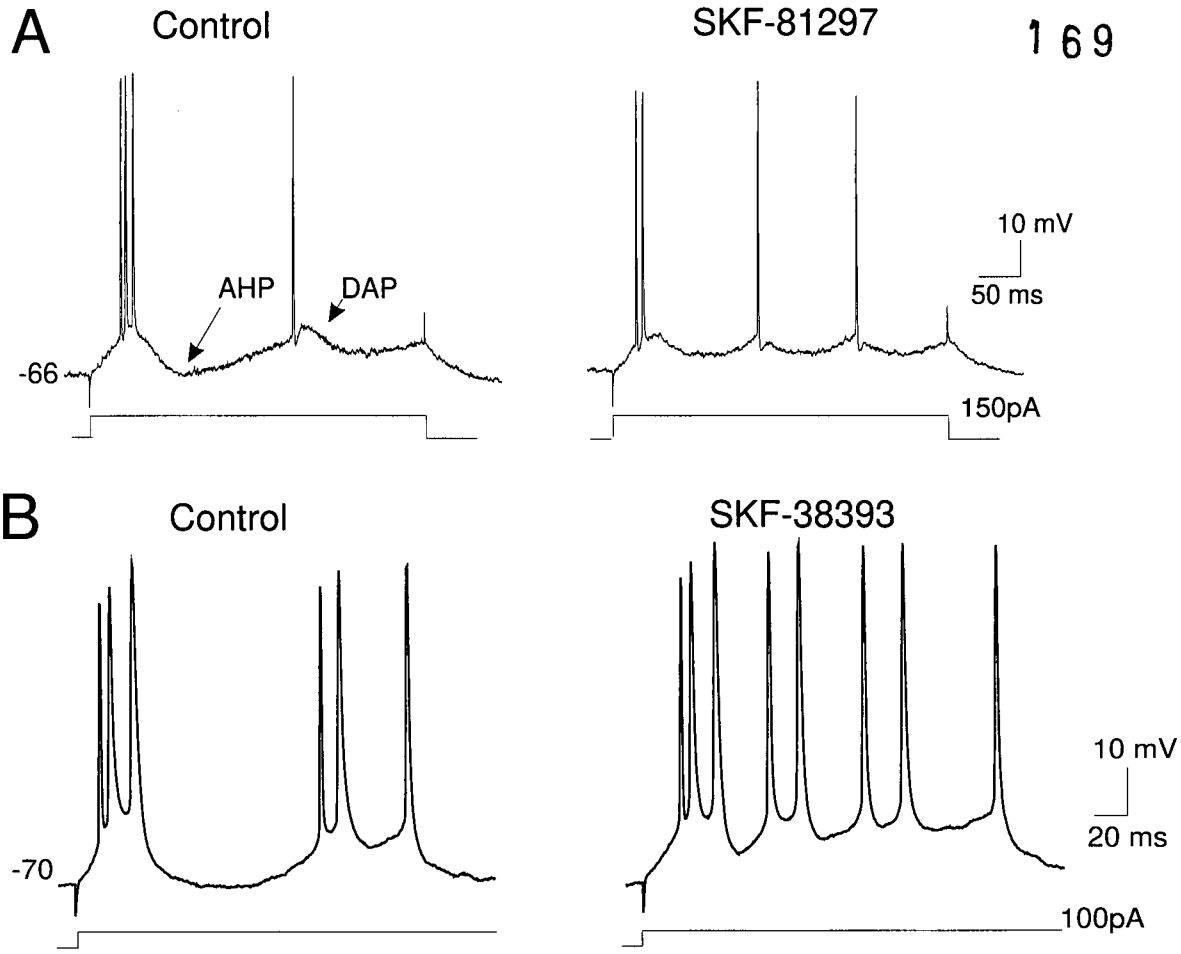
A
Control
SKF-81297
AHP
DAP
-66
10 mV
50 ms
150pA
B
Control
SKF-38393
-70
10 mV
20 ms
100pA

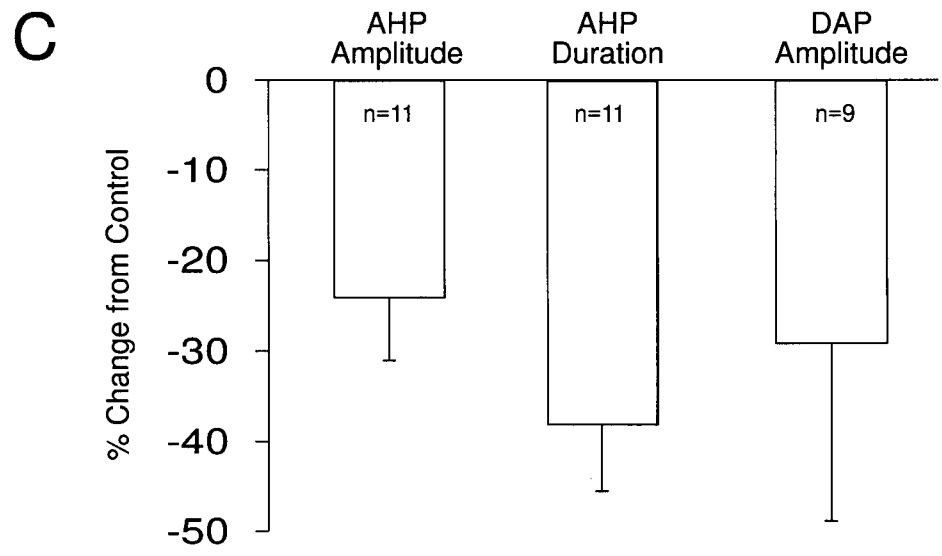
C
AHP Amplitude
AHP Duration
DAP Amplitude
n=11
n=11
n=9
% Change from Control
0
-10
-20
-30
-40
-50

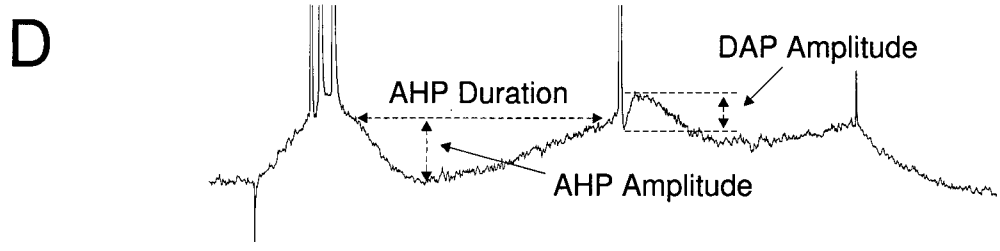
D
DAP Amplitude
AHP Duration
AHP Amplitude

pattern of burst-firing PFC neurons. As shown in Figs. 6-3A-C, bath application of the D1 agonists SKF-38393 or SKF-81297 reduced the DAP and AHP in burst-firing PFC neurons. In 11 *IB* and *ROB* neurons D1 receptor stimulation reduced AHP amplitude by 24 ± 6.9% and AHP duration by 38.1 ± 7.5% (Fig 6-3C). Likewise DAP amplitude was also reduced by 29.14 ± 19.7% in 9 neurons tested (Fig. 6-3C). As a result, in response to depolarizing current pulses, *IB* and *ROB* PFC neurons tended to fire more spikes in a repetitive pattern following D1 receptor stimulation (Fig.6-3A,B).

Actions Of D1 Receptor Agonists on the Slowly-Inactivating Na^+ and K+ Conductances

To determine how DA influences the excitability of PFC neurons, the effects of DA on two opposing currents which normally determine the firing threshold of PFC neurons were examined (see Chapter 3). The first was a TTX-sensitive slowly inactivating or persistent Na^+ current that is responsible for membrane inward rectification in the subthreshold voltage range (see Figs 2-4, 2-5; and Yang and Seamans, 1995; Stafstrom et al., 1985; Sutor and Zieglgansberger, 1987) and the second was a 4-AP-sensitive slowly inactivating K^+ current that is responsible for membrane outward rectification (see Fig 2-10 and Hammond and Crepel, 1992; Yang and Seamans, 1996). The slowly-inactivating Na^+ conductance was isolated by blocking Ca^{2+} channels with Co^{2+} or Cd^{2+} and blocking K^+ channels with a combination of $(Cs)_i$, TEA and 4-AP. The

Figure 6-4: D1 receptor stimulation increased the excitability of *IB* PFC neurons by directly interacting with a voltage-dependent slowly-inactivating Na^+ current: **A)** An isolated Na^+ plateau potential elicited by a depolarizing pulse (100ms, 100pA). Note the voltage-dependent changes in the duration of the Na^+ plateau. At -70mV, the same depolarizing pulse failed to elicit the Na^+ plateau potential. **B)** The D1 agonist SKF38393 (40 μM) markedly prolonged the duration, but not the amplitude, of the Na^+ plateau potential at all the holding potentials tested. Unlike in the control, the Na^+ plateau potential could be elicited at -70 mV in the presence of the D1 agonist (n=5). P1 and P2 indicate the early fast and the late slow components of the Na^+ plateau potential, respectively. **C)** Plot indicating the increase in the duration of the slow Na^+ plateau potential and the voltage shift in its activation following SKF38393 application (filled circles) when compared to the control (open circles). Mean data (± S.E.M.) dervied from 5 trials from the same neuron held at different voltages. **D & E)** Only small changes in the peak amplitude of the early fast (P1) and late slow (P2) components of the Na^+ plateau potential under the incluence of SKF39393 (filled circles) when compared to control (open circles).

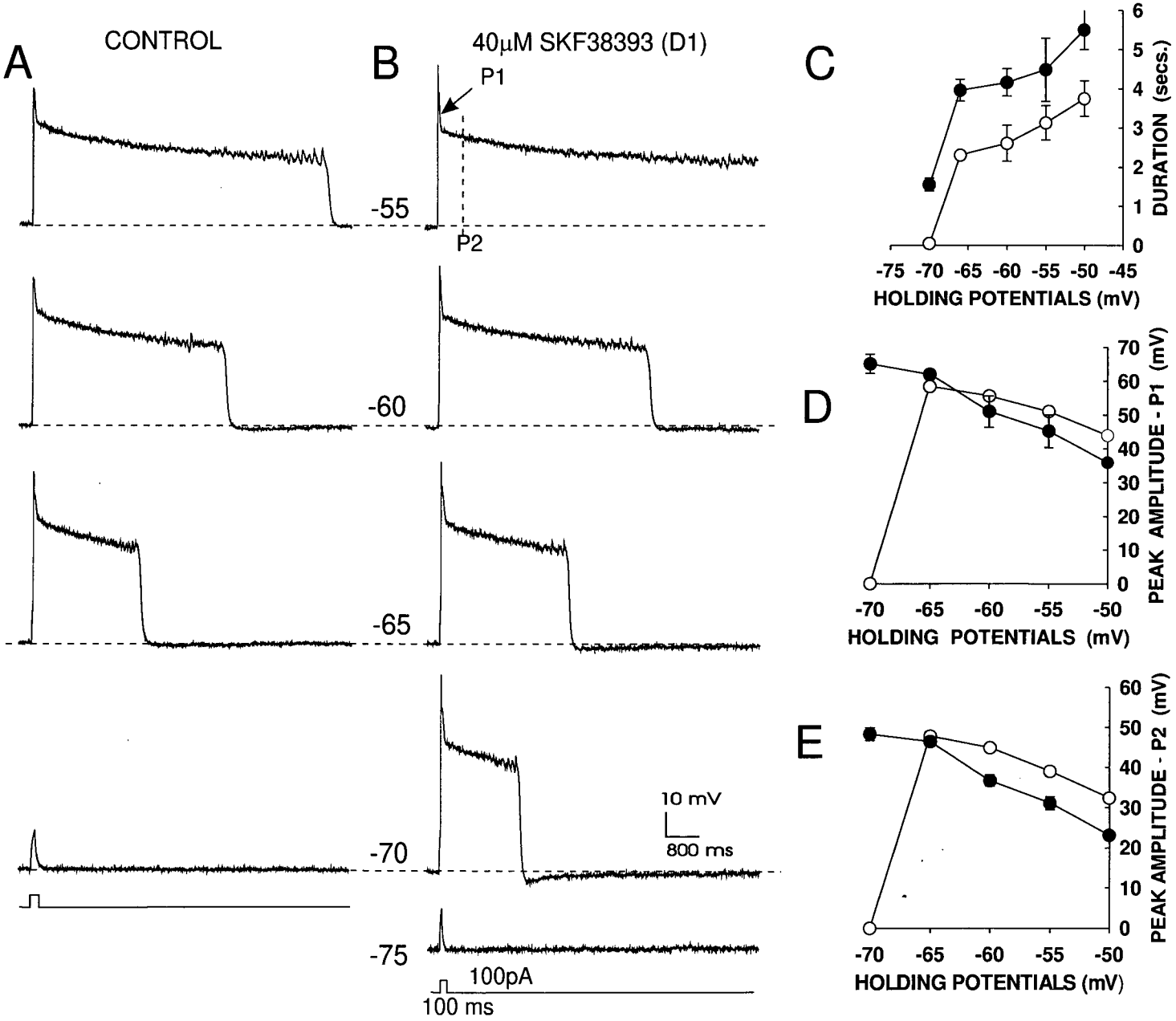
A
CONTROL
B
40μM SKF38393 (D1)
P1
P2
-55
-60
-65
-70
-75
10 mV
800 ms
100pA
100 ms
C
DURATION (secs.)
HOLDING POTENTIALS (mV)
D
PEAK AMPLITUDE - P1 (mV)
HOLDING POTENTIALS (mV)
E
PEAK AMPLITUDE - P2 (mV)
HOLDING POTENTIALS (mV)

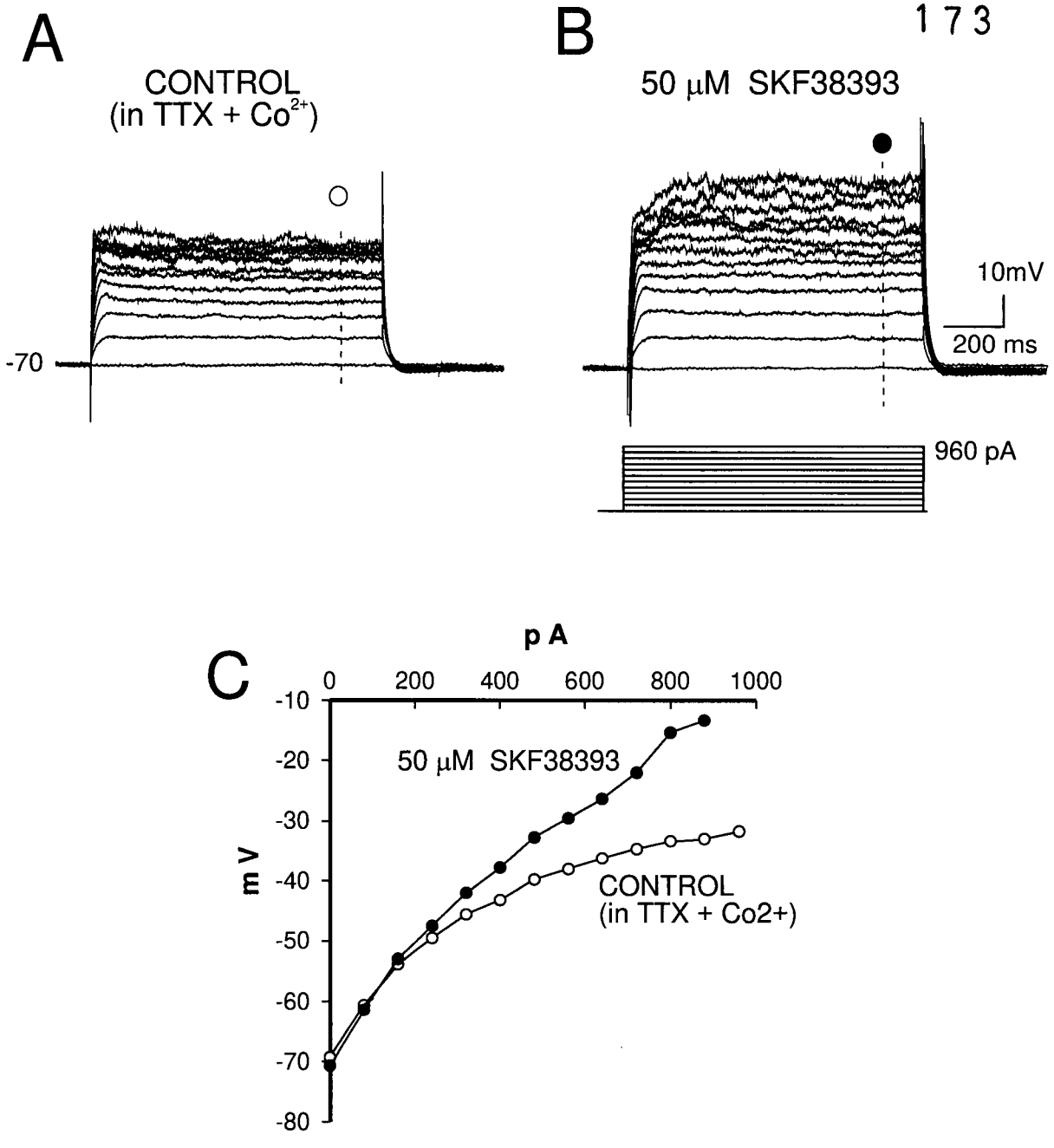

Figure 6-5: Reduction of a slowly inactivating outward rectifying current by a D1 agonist. **A)** Membrane voltage response in a PFC neuron following intracellular injection of a series of depolarizing pulses in the presence of TTX and Co^{2+} to block Na^{+} and Ca^{2+} currents. Note the slowly inactivating outward rectifying current which limits membrane depolarization beyond -50 mV. **B)** Bath-application of the D1 agonist 38393 (50μM) removed this outward rectification. **C)** Steady-state V-I plot showing the blockade of the outward rectifcation by SKF38393.

slowly-inactivating K^+ conductance was isolated by blocking Ca^{2+} channels with Co^{2+} or Cd^{2+} and Na^+ channels with TTX.

Bath application of SKF-38393 (10-50 μM) enhanced the duration of the slow Na^+-plateau potential mediated by I_{NAP} , and slightly reduced (≈10mV) its amplitude. SKF-38393 (40μM) also lowered the activation threshold of the plateau potential by 5mV (Fig.6-4, n=5). A lowering in the activation range of the persistent Na^+ current would allow spikes to occur at more hyperpolarized membrane potentials.

Bath-application of the D1 agonist SKF-38393 (40 μM), also removed the outward rectification and increased the slope of the V-I plot (Fig. 6-5A-C, n=5). This effect was similar to that observed following application of 4-AP or dendrotoxin (see Fig 2-10) and likely was due to a D1 mediated suppression of I_D. A reduction in outward rectification by I_D would allow greater membrane depolarization by I_{NAP} and thereby enhancing the probability of repetitive firing. Thus DA modulation of the slowly-inactivating Na^+ and K^+ currents lowers the firing threshold of PFC and produces more spikes at threshold.

Action of D1 receptor agonists on High Threshold Ca^{2+} Conductances

As shown in Chapter 3 (Fig 2-8, 2-9) , the burst firing in PFC neurons was regulated by high and low threshold Ca^{2+} currents. Specifically, bursts of spikes were triggered over the depolarizing envelope provided by the Ca^{2+}-dependent depolarizing after potential (DAP). Following the initial burst, a prolonged Ca^{2+}-dependent after hyperpolarization (AHP) occurred which prevented spike

Figure 6-6: DA D1 receptor stimulation suppressed Ca^{2+} spikes. **A)** (Left) Non-regenerative Ca^{2+} spikes were recorded using an intrasomatic, Cs^{+}-filled electrode in the presence of TTX and TEA in an *IB* PFC neuron. (Right) SKF-38393 attenuated the duration of the Ca^{2+} spikes. **B)** A histogram illustrating the mean (± S.E.M.) percentage changes in half-width of Ca^{2+} spikes following the bath application of the D1 agonist SKF-38393 (10-40 μM). **C)** In a *ROB* cell perfused with TTX and TEA, regenerative, voltage-dependent, Ca^{2+} spikes were elicited (left). SKF38393 markedly attenuated the Ca^{2+} spikes and completely suppressed regenerative firing (middle). Application of higher amplitude current pulses still triggered Ca^{2+} spikes but their amplitude and duration was markedly attenuated (right).

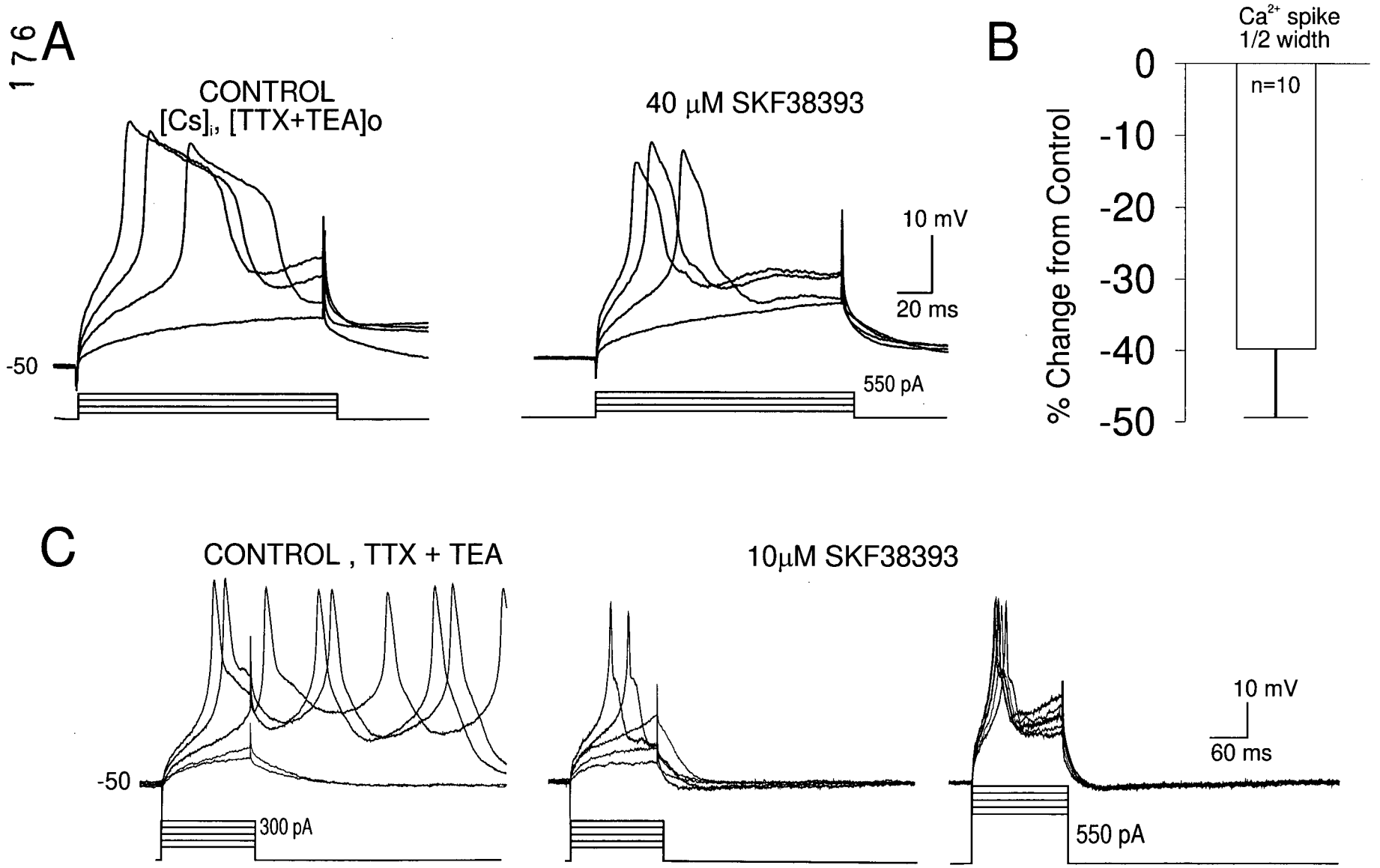
A
CONTROL
[Cs]i, [TTX+TEA]o
40 μM SKF38393
10 mV
20 ms
550 pA
-50
B
Ca2+ spike
1/2 width
n=10
% Change from Control
0
-10
-20
-30
-40
-50
C
CONTROL , TTX + TEA
10μM SKF38393
-50
300 pA
10 mV
60 ms
550 pA

initiation for 200-500ms. Given that D1 receptor stimulation reduced burst-firing in PFC neurons, it was of interest to determine how DA modulated the underlying Ca^{2+} potentials.

D1 receptor stimulation had clear effects on high threshold Ca^{2+} spikes in PFC neurons. DA reduced high threshold Ca^{2+} spikes evoked in the presence of TTX and $(Cs^{+})_i$/TEA (Fig 6-6A). During somatic recordings, bath application of the D1 agonist SKF-38393 reduced the half-width of Ca^{2+} spikes in 10 PFC cells tested (Fig. 6-6A,B). SKF-38393 also markedly suppressed the regenerative HTS in *ROB* cells (Fig 6-6C, n=3). As shown in Fig 6-6C, the D1-mediated suppression of Ca^{2+} spikes could be partially overcome by delivering larger depolarizing pulses. Thus D1 receptor stimulation may have interacted with the activation/inactivation properties of high threshold Ca^{2+} channels.

The inactivation of high threshold Ca^{2+} channels is voltage and Ca^{2+} dependent. The Ca^{2+} dependent inactivation is removed if Ba^{2+} is substituted for Ca^{2+} in the recording media (Hille 1984; Connors 1979). Following Ba^{2+} substitution a prolonged, non-inactivating Ba^{2+}-mediated plateau potential was evoked in the presence of TTX and TEA. The initiation of a Ba^{2+} -mediated plateau potential was reduced by SKF 38393 (Fig 6-7, n=3) indicating that the effects of D1 receptor stimulation were independent of the Ca^{2+}-mediated inactivation of high threshold Ca^{2+} channels. Instead D1 receptor stimulation likely altered the activation of Ca^{2+} currents in PFC neurons. However a detailed analysis of the effect of D1 agonists on Ca^{2+} currents under voltage-clamp is necessary to address this hypothesis directly.

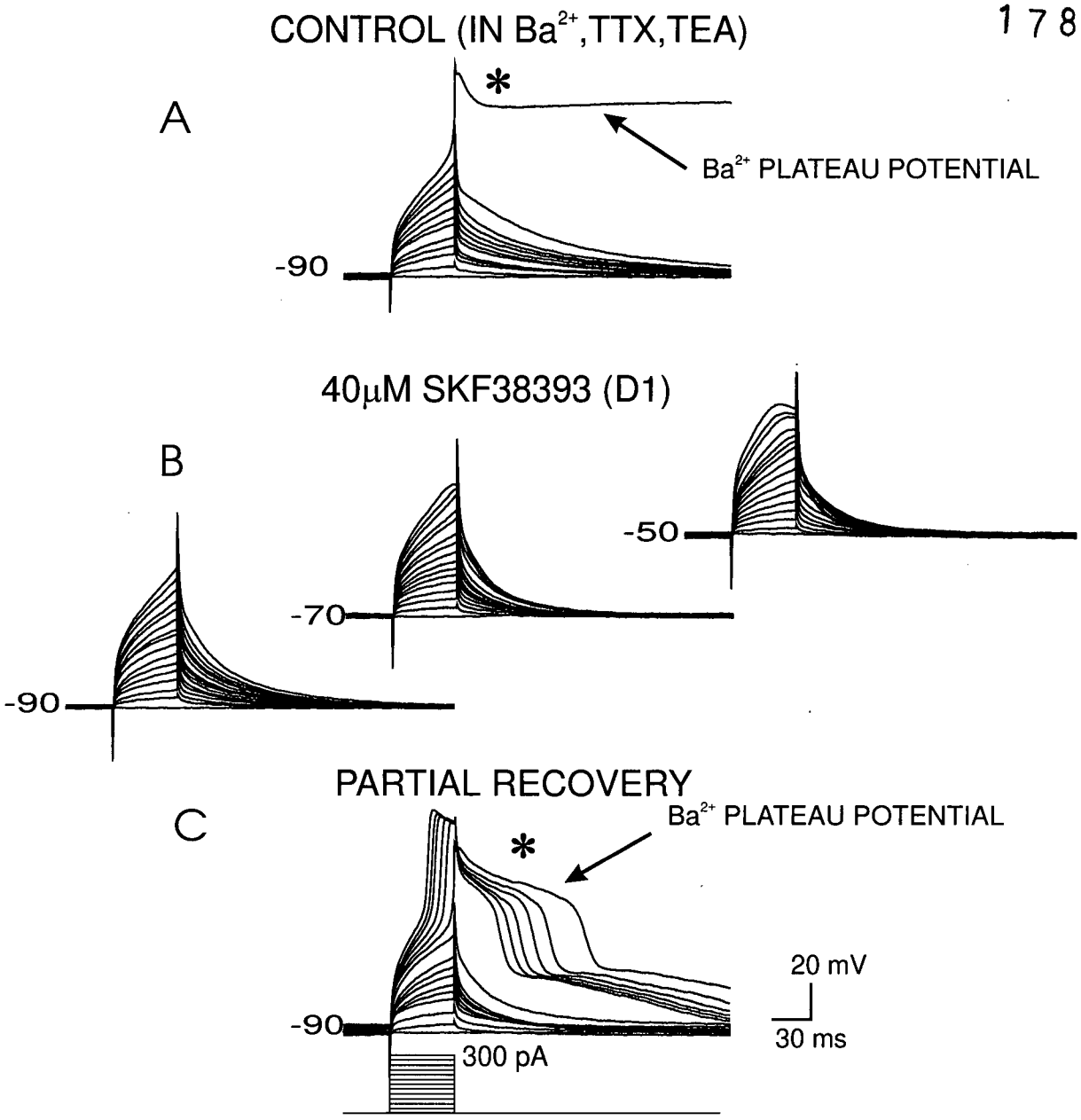

Figure 6-7: Direct D1 receptor suppression of Ca^{2+} spikes was not due to enhancements in the $(Ca^{2+})_i$-mediated inactivation of Ca^{2+} currents. **A)** When Ba^{2+} was used as the charge carrier for Ca^{2+} currents (in TEA and TTX) the $(Ca^{2+})_i$-mediated inactivation of Ca^{2+} currents was removed. Stepwise (20pA steps) increments in depolarizing current pulses eventually evoked an all-or-none, long lasting (100s), Ba^{2+} plateau potential (*). **B)** Following SKF-38393 application, similar current pulses delivered at various holding potentials no longer evoked the Ba^{2+} plateau potential. **C)** Partial recovery of the Ba^{2+} plateau potential (*) 14 mins after the application of SKF-38393.

Additional experiments were conducted to determine whether the suppression of the Ca^{2+} spikes by SKF-38393 was due to an action on L-type Ca^{2+} channels. This was not the case as a similar reduction in Ca^{2+} spike half-width (40 % reduction) following SKF-38393 administration was also observed in slices pre-treated with the L-type Ca^{2+} channel antagonist, nifedipine (n=5/5, not shown), suggesting that SKF-38393 acted primarily on P,N,Q,R-type high threshold Ca^{2+} channels.

Finally, the effects of D1 agonists on Ca^{2+} spikes evoked in the apical stem were also analyzed, with inconclusive results. D1 receptor stimulation had no observable effects on Ca^{2+} spikes in 4/5 dendrites tested, while in one dendrite, SKF-81297 reduced Ca^{2+} spike half width. The reason for the reduction in this one dendrite may have been that TTX and TEA were used, as in somatic recordings, rather than TTX and 4-AP as in the other 4 dendrites. In the presence of 4-AP Ca^{2+} spike repolarization was mediated primarily by the unblocked delayed rectifier. Following application of TEA the delayed rectifier was blocked and Ca^{2+} spikes repolarized as a result of Ca^{2+} channel inactivation (Reuvini et al. 1993). Given that D1 receptor stimulation decreased Ca^{2+} spike 1/2 width during somatic recordings, the effects may only be present when Ca^{2+} spikes repolarize on their own (in TTX and TEA). If confirmed in additional experiments, this observation may provide insights into the mechanisms of D1 mediated modulation of Ca^{2+} currents in PFC neurons.

The effect of D1 receptor stimulation was also examined on low threshold Ca^{2+} conductances. Since experiments were performed under current-clamp, it

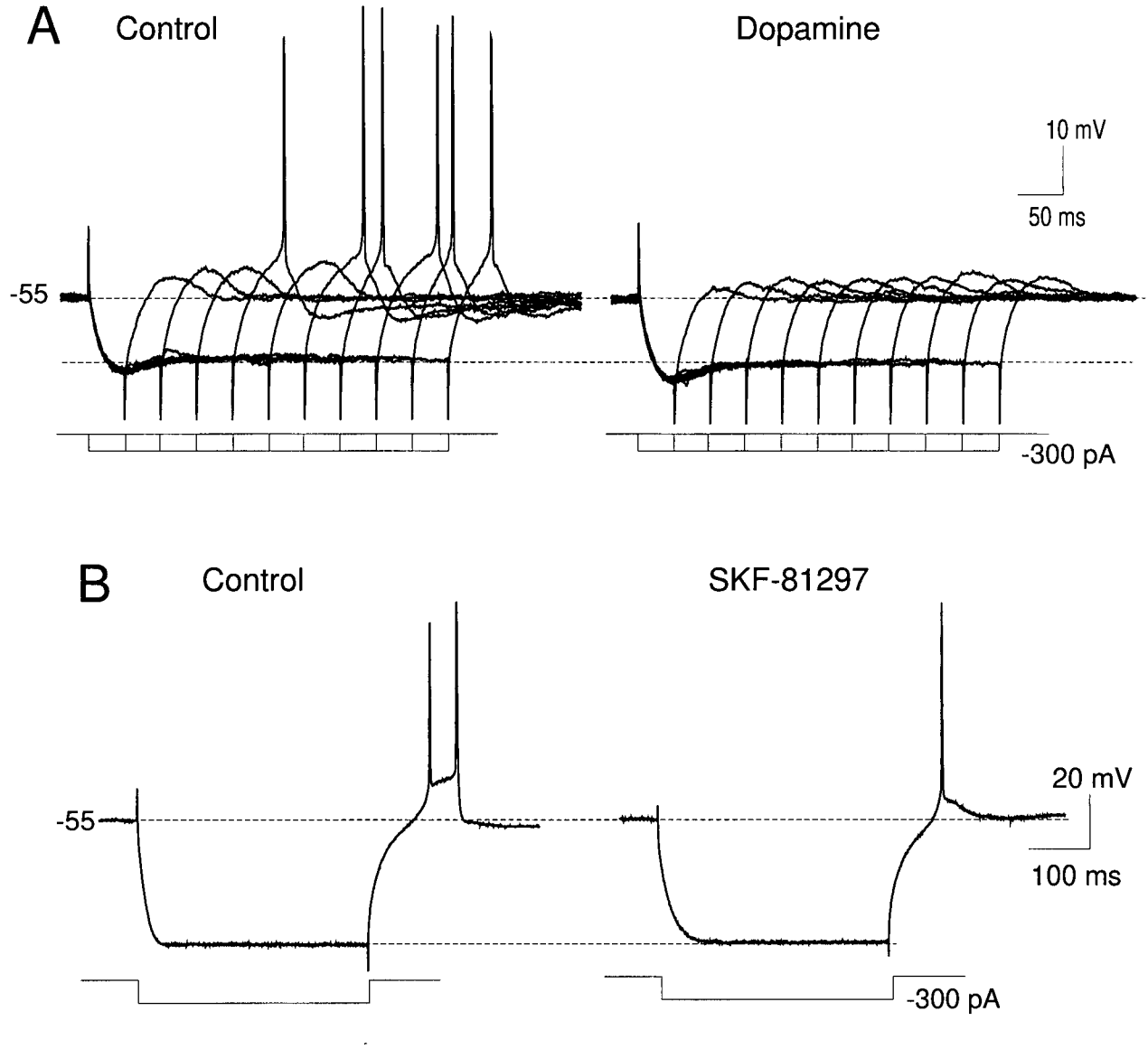

Figure 6-8: DA via the D1 receptor reduced low threshold Ca^{2+} spikes. **A)** Low threshold spikes (LTS) were evoked from the rebound of a hyperpolarizing current pulse, and often generated action potentials (left). Dopamine (20μM) decreased the LTS, such that spike threshold was not reached (right). **B)** In a *IB* PFC neuron, a spike doublet rode atop an LTS following a hyperpolarizing current step (left). In SKF-81297 (10μM) only a single spike was evoked at the offset of the hyperpolarizing current pulse.

was important to concurrently monitor changes in R_{IN}, since changes in V_m would influence the inactivation of low threshold Ca^{2+} channels. In 4 neurons in which no changes in R_{IN} were observed, bath application of SKF-38393 or SKF-81297 produced a -37.7 ± 9 % reduction in amplitude of low threshold Ca^{2+} spikes (LTS) (Fig 6-7A,B). Thus current-clamp data indicated that D1 receptor stimulation produced a moderate reduction in low threshold Ca^{2+} currents in PFC neurons. This conclusion is tentative and awaits confirmation based on voltage-clamp data. Thus the D1 mediated reduction in burst firing may have been due either to a reduction in high or low threshold Ca^{2+} currents.

Action of D1 receptor Agonists on Synaptically Evoked Responses

Non-Isolated PSPs

The effects of D1 receptor stimulation were examined on synaptic responses evoked by stimulation of layers I-II or V-VI. QX-314 was usually included in the recording pipette for these experiments to avoid possible confounding effects of D1 receptor stimulation on intrinsic Na^+ currents. QX-314 also produced a blockade of $GABA_B$ IPSPs (Nathan et al. 1990). All means reported below were recorded at the peak of the drug response.

D1 receptor stimulation produced a very small reduction in the amplitude of layer I-II and V-VI non-isolated PSPs (-4.5 ± 13% ,n=7 and -7.4 ± 15%, n=7 respectively) (not shown). Although the magnitude of the reductions were small this finding is consistent with that of Law-Tho et al. (1994) who showed that DA reduced non-isolated PSPs in PFC neurons. Because non-isolated PSPs are

made up of multiple synergistic and antagonist components (see Chapter 5), it was not possible to draw a conclusion regarding the exact action of DA on synaptic responses in the PFC.

Isolated NMDA EPSPs

The effect of D1 receptor stimulation on isolated NMDA EPSPs was examined. D1 receptor stimulation enhanced the layer I-II isolated NMDA EPSP (in DNQX and bicuculline, using a QX-314-filled electrode) by 25.6 ± 12.6% in 9/9 neurons tested (Fig 6-10 A-C). An enhancement in the NMDA EPSP was observed when the neuron was held at -66mV or more negative (Fig 6-9A). The reverse NMDA EPSP was also enhanced by SKF-38393 when the neuron was held more positive than 0mV (not shown, n=2). At such positive potentials voltage-gated currents could not affect EPSP amplitude, and D1 receptor stimulation modulated the NMDA EPSP directly.

However, if the membrane voltage was held within 10mV of firing threshold, a 'hump' potential was observed on top of the NMDA EPSP (Fig 6-9B1,B2). The enhancement of the synaptically-evoked 'hump' potential may have been caused by 1) the larger NMDA EPSPs in the presence of the D1 agonist, or 2) a direct effect on the 'hump' potential. Indeed in striatal neurons D1 receptor stimulation augments an identical 'hump' potential mediated by L-type Ca^{2+} channels (Hernandez-Lopez et al. 1997). Additional experiments were conducted to address these possibilities.

The effects of D1 receptor stimulation were examined on the 'hump' potential evoked from the soma (n=4) or proximal apical dendrite (n=4) by an

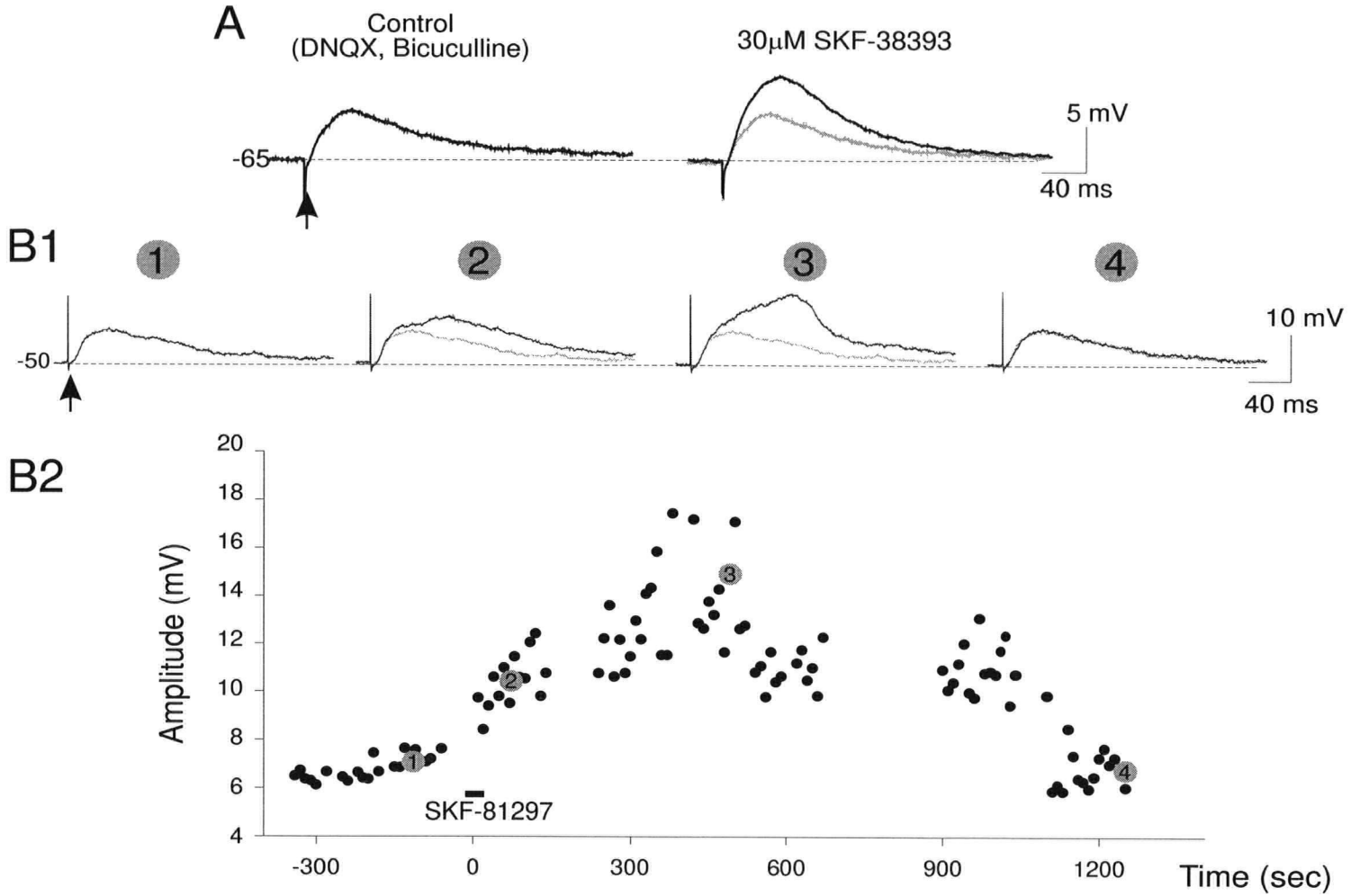

Figure 6-9: D1 receptor stimulation augmented layer I-II NMDA EPSPs. **A)** (Left) At a somatic V_m of -65 mV an isolated NMDA EPSP was evoked by layer I-II stimulation in the presence of DNQX (10μM) and Bicuculline (4μM). (Right) SKF-38393 (30μM) enhanced the amplitude of the NMDA EPSP. **B1)** (Trace 1) In a different neuron an isolated NMDA EPSP was evoked at a somatic V_m of -50mV. (Trace 2) Bath application of SKF-81297 (10μM, for 1min) enhanced the amplitude of the NMDA EPSP. (Trace 3) Eight minutes after SKF-81297 was applied the NMDA EPSP was large enough to trigger the voltage-gated 'hump' potential, which amplified the synaptic response further. (Trace 4) The augmentation of the synaptic response, recovered 20 minutes after SKF-81297 was applied. **B2)** Graph of the synaptic response amplitude before, during and after SKF-81297 application. The numbers in the grey circles show the times at which the traces shown in B1 were obtained. All responses were recorded using an intracellular electrode containing QX-314, 1M CsAc and 2M KAc.

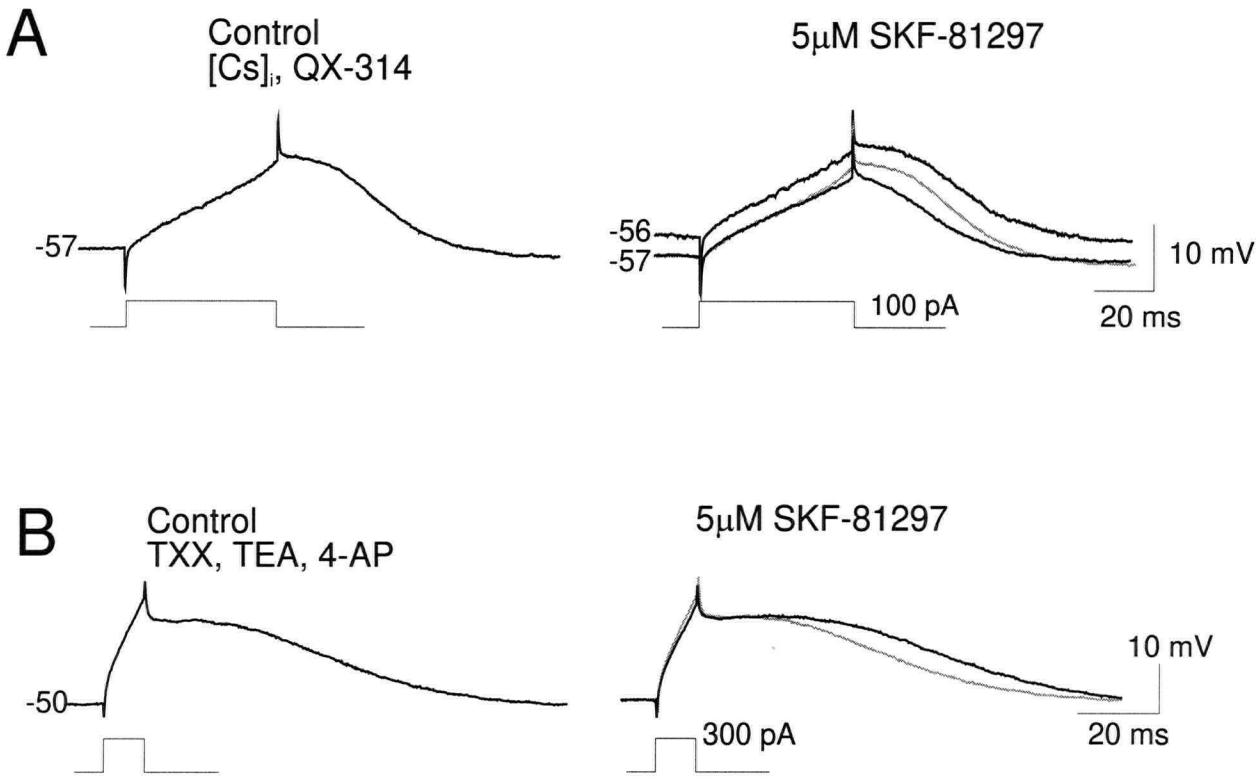

Figure 6-10: D1 receptor stimulation had inconsistent effects on the 'hump' potential evoked by current pulses. **A)** (Left) A 'hump' potential evoked by a current pulse during a recording from the soma using a pipette containing QX-314 and CsAc. (Right) The 'hump' potential evoked at a V_m of -57mV was reduced by SKF-81297 (5μM). However, a full blown 'hump' potential was evoked if the Vm was depolarized by 1mV to -56mV. **B)** (Left) A 'hump' potential evoked by a current pulse during a recording from the apical stem in the presence of TTX, TEA, and 4-AP. (Right) Bath application of SKF-81297 (5μM) had little effect on the 'hump' potential recorded from the apical stem.

intracellular current pulse in the presence of Na^+ and K^+ channel blockers, QX-314 and $[Cs]_i$ or TTX and 4-AP. Unfortunately the effects of D1 receptor stimulation on the 'hump' potential evoked by depolarizing current pulses was highly variable. The 'hump' potential was decreased in all somatic recordings. Fig 6-10A shows a recording from the soma of an *IB* cell in which an initial reduction in the size of the 'hump' potential was observed following administration of SKF-81297. In contrast, the hump potential was enhanced by D1 receptor stimulation in all 4 apical stem recordings. Fig 6-10B shows a cell recorded from the apical stem in which SKF-81297 produced an enhancement in the integrated area of the 'hump' potential. D1 receptor stimulation produced a 38.5 ± 16% in the amplitude of the 'hump' potential recorded from the apical stem (n=4/4). Overall, for all somatic and apical stem recordings, bath application of SKF-38393 or SKF-81297 produced a -3.7 ± 19% reduction in the amplitude of the 'hump' potential and a -13 ± 23 % reduction in the integrated area (n=8).

It is unclear as to why the 'hump' potential was increased during all stem recordings and decreased for all somatic recordings. Note however, if the V_m was depolarized by <1mV during somatic recordings, a 'hump' potential of equivalent size to that evoked in the control could be triggered following SKF-81297 administration (Fig 6-10A). Since the 'hump' potential was evoked in a relatively all-or-none manner (see Figs. 3-5, 5-9, 5-10), it is possible that the opposing effects of D1 receptor stimulation observed during somatic and dendritic recordings was due to inadequate voltage control. Additional experiments are required to determine the direct action of D1 receptor stimulation on the 'hump'

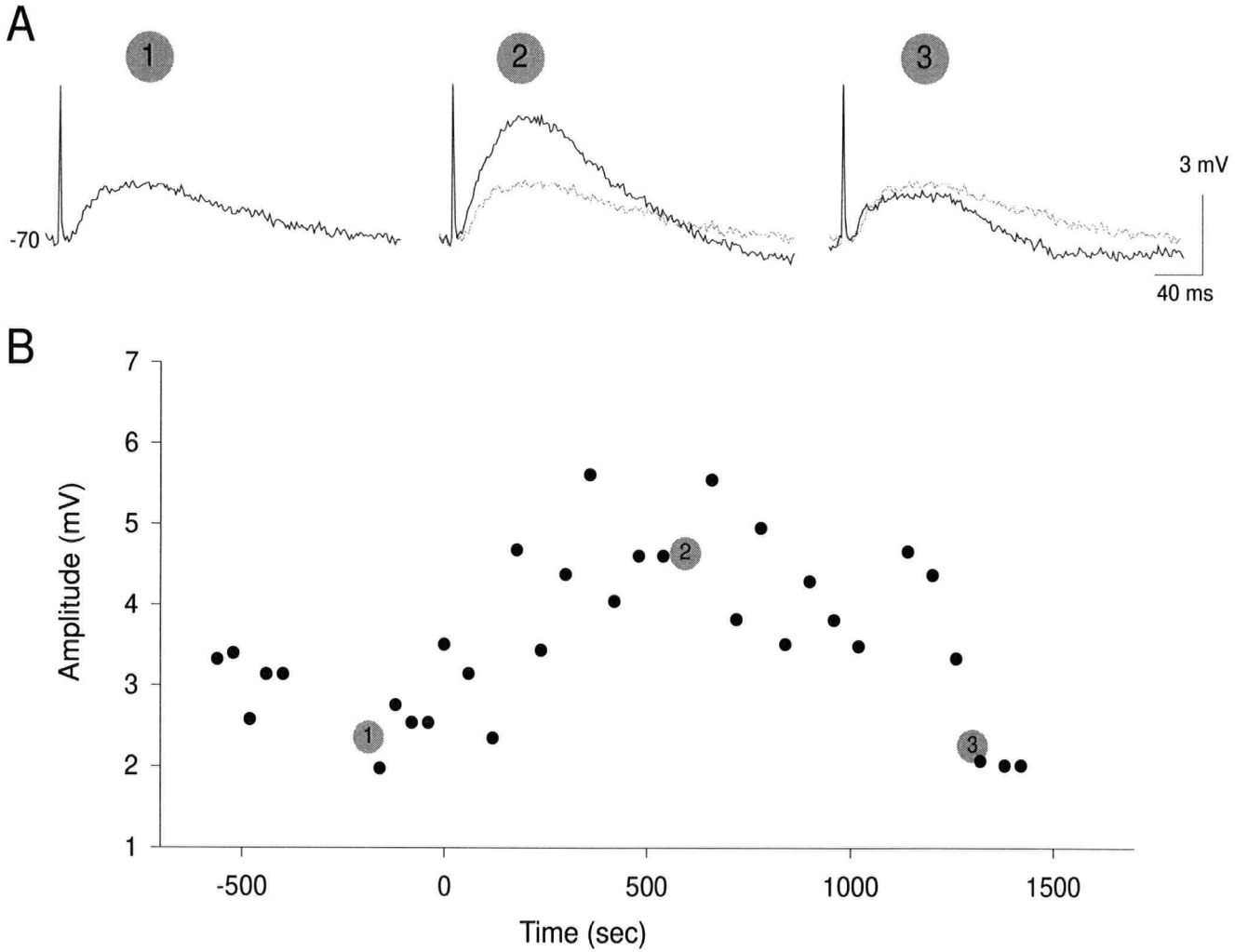

Figure 6-11: D1 receptor stimulation augmented layer V-VI NMDA EPSPs. **A)** (Trace 1) At a somatic V_m of -65 mV an isolated NMDA EPSP was evoked by layer V-VI stimulation in the presence of DNQX (10μM) and Bicuculline (4μM). (Trace 2) Bath application of SKF-81297 (10μM, for 1min) enhanced the amplitude of the NMDA EPSP. (Trace 3) The augmentation of the synaptic response, recovered 25 minutes after SKF-81297 was applied. **B)** Graph of the synaptic response amplitude before, during and after SKF-81297 application. The numbers in the grey circles show the times at which the traces shown in A were obtained. Responses were recorded using an intracellular electrode containing QX-314, 1M CsAc and 2M KAc.

potential. However, regardless of possible direct effects of D1 receptor stimulation on the Ca^{2+} potentials underlying the 'hump', D1 receptor stimulation enhanced layer I-II NMDA EPSP amplitude sufficiently to evoke the 'hump' potential synaptically as shown above.

Stimulation of D1 receptors also enhanced the amplitude of the layer V-VI NMDA EPSP (in DNQX and bicuculline) by 59 ± 17% in 5/8 neurons tested (Fig 6-11A,B). In 3/8 neurons tested, administration of a D1 agonist reduced the EPSP by -9 ± 3.5 %. For all 8 neurons, the overall effect of D1 receptor stimulation was a 30 ± 15.9% increase in EPSP amplitude. Thus although D1 receptor stimulation caused a small reduction in non-isolated PSPs in PFC neurons, it appeared to augment the NMDA EPSP.

$GABA_A$ IPSPs

Fast $GABA_A$ IPSPs were evoked by stimulating electrodes placed in layers I-II and V-VI in the presence of DNQX, APV while using QX-314 filled electrodes. Application of D1 agonists (SKF-38393 or SKF-81297) enhanced the amplitude of the layer I-II IPSP by 35.2 ± 17 %, (Fig 6-12, n=5) while administration of a D1 antagonist SCH-23390 reversibly reduced the layer I-II IPSP by -37 ± 11% (Fig 6-13 A,B, n=4). SCH-23390 also reduced the layer V-VI IPSP by -51 ± 9% (Fig 6-14A-B, n=6). D1 agonists increased layer V-VI IPSP amplitude by 27.7 ± 11.6% in 3 neurons (Fig 6-15). However, in an additional 2 neuron D1 agonists produced a -26 ± 1% reduction in IPSP amplitude (not shown). The reasons for

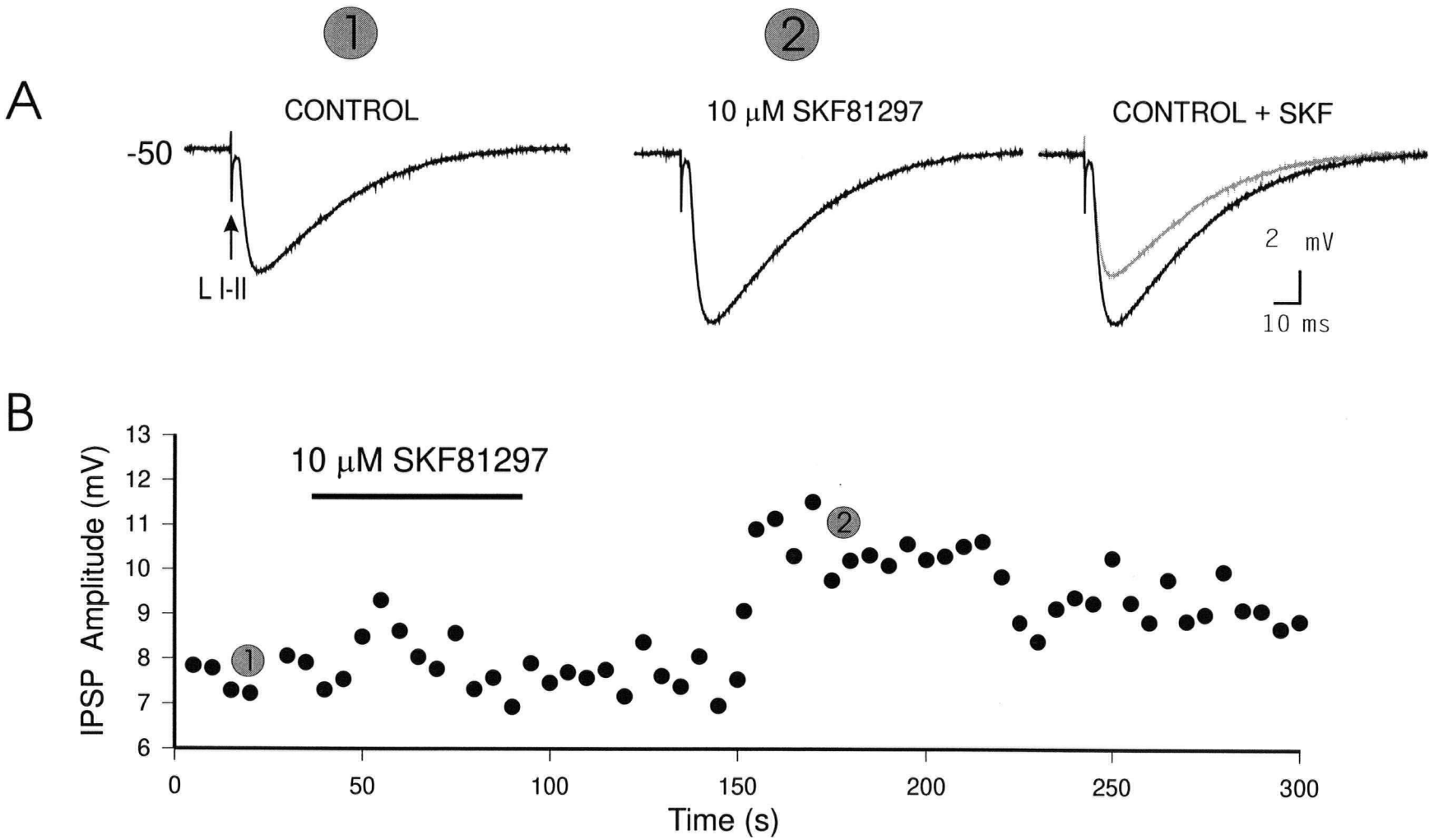

Figure 6-12: D1 receptor stimulation augmented layer I-II IPSPs. **A)** (Left) At a somatic V_m of -50 mV an isolated $GABA_A$ IPSP was evoked by layer I-II stimulation in the presence of DNQX (10μM) and APV (50μM). (Middle) Bath application of SKF-81297 (10μM, for 1min) enhanced the amplitude of the IPSP. (Right) The control and SKF-81297 response superimposed showing the magnitude of the ehnancement. **B)** Graph of the synaptic response amplitude before, during and after SKF-81297 application. The numbers in the grey circles show the times at which the traces shown in A were obtained. Responses were recorded using an intracellular electrode containing QX-314, 1M CsAc and 2M KAc.

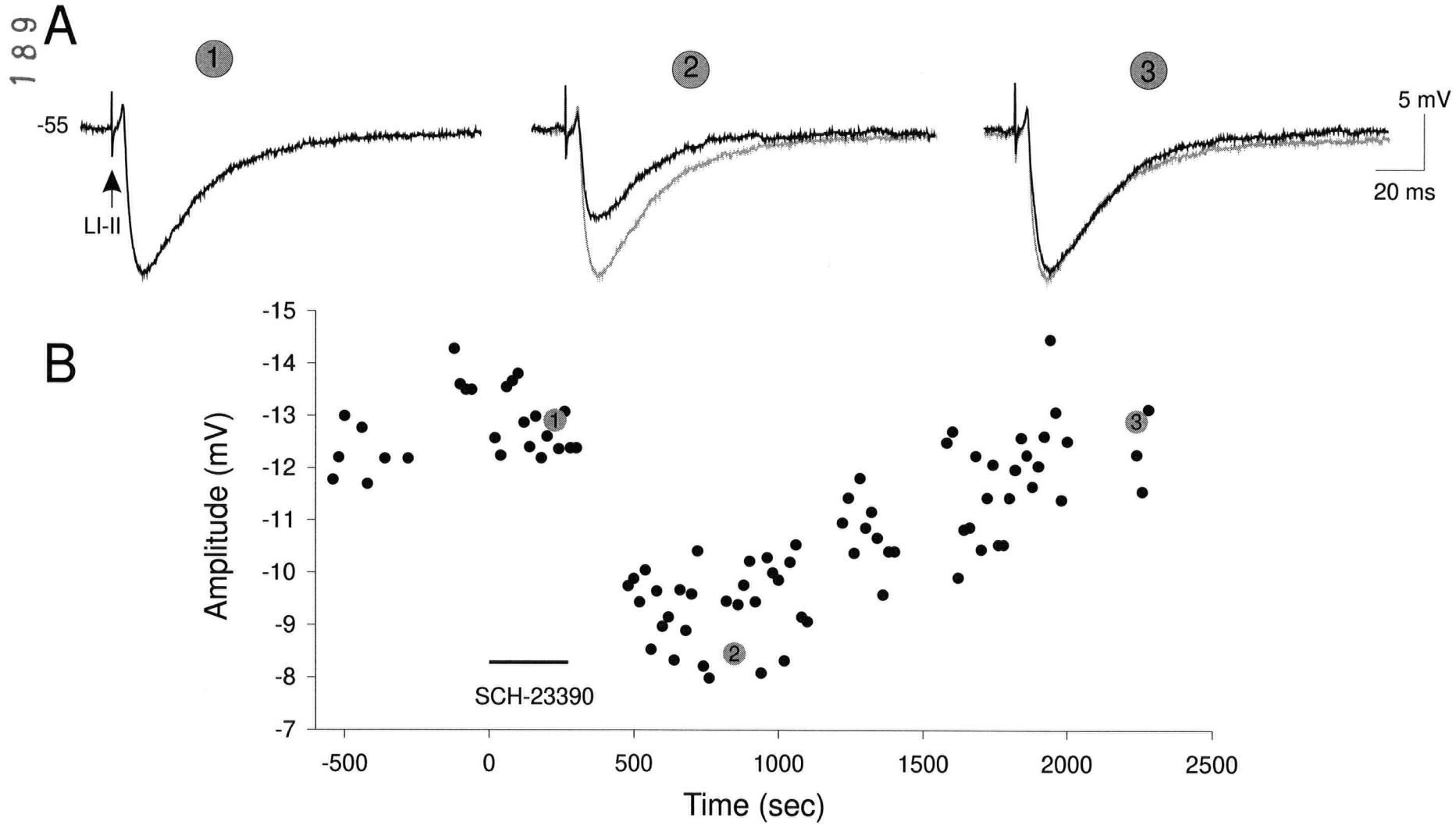

Figure 6-13: D1 receptor blockade reduced layer I-II IPSPs. **A)** (Trace 1) At a somatic V_m of -55 mV an isolated $GABA_A$ IPSP was evoked by layer I-II stimulation in the presence of DNQX (10μM) and APV (50μM). (Trace 2) Bath application of the D1 receptor antagonist SCH-23390 (20μM, for 3min) reduced the amplitude of the IPSP. (Trace 3) The reduction of the synaptic response recovered 40 minutes after SCH-23390 was applied. **B)** Graph of the synaptic response amplitude before, during and after SCH-23390 application. The numbers in the grey circles show the times at which the traces shown in A were obtained. Responses were recorded using an intracellular electrode containing QX-314, 1M CsAc and 2M KAc.

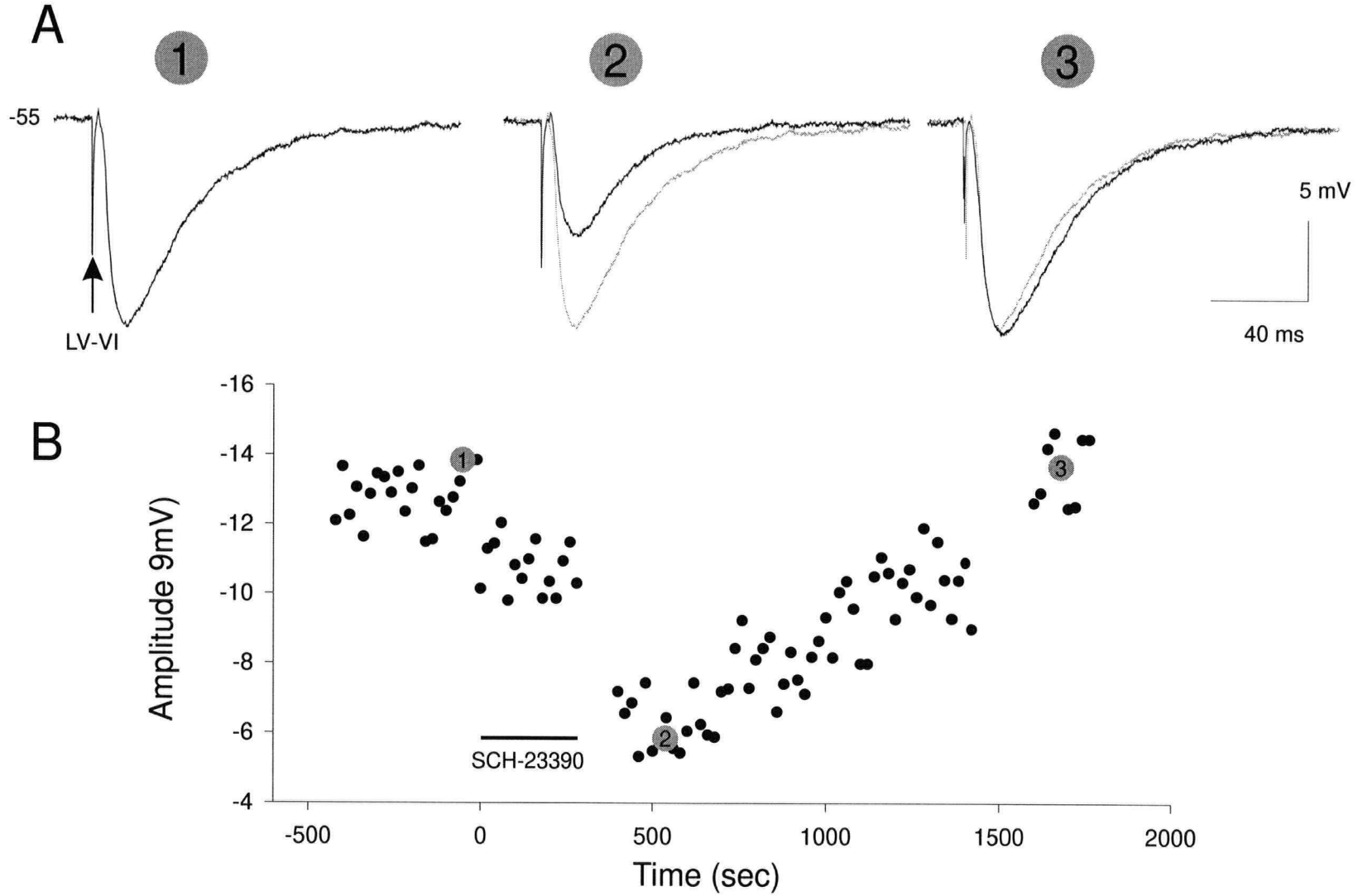

Figure 6-14: D1 receptor blockade reduced layer V-VI IPSPs. **A)** (Trace 1) At a somatic V_m of -55 mV an isolated $GABA_A$ IPSP was evoked by layer V-VI stimulation in the presence of DNQX (10μM) and APV (50μM). (Trace 2) Bath application of the D1 receptor antagonist SCH-23390 (20μM, for 3min) reduced the amplitude of the IPSP. (Trace 3) The reduction of the synaptic response recovered 33 minutes after SCH-23390 was applied. **B)** Graph of the synaptic response amplitude before, during and after SCH-23390 application. The numbers in the grey circles show the times at which the traces shown in A were obtained. Responses were recorded using an intracellular electrode containing QX-314, 1M CsAc and 2M KAc.

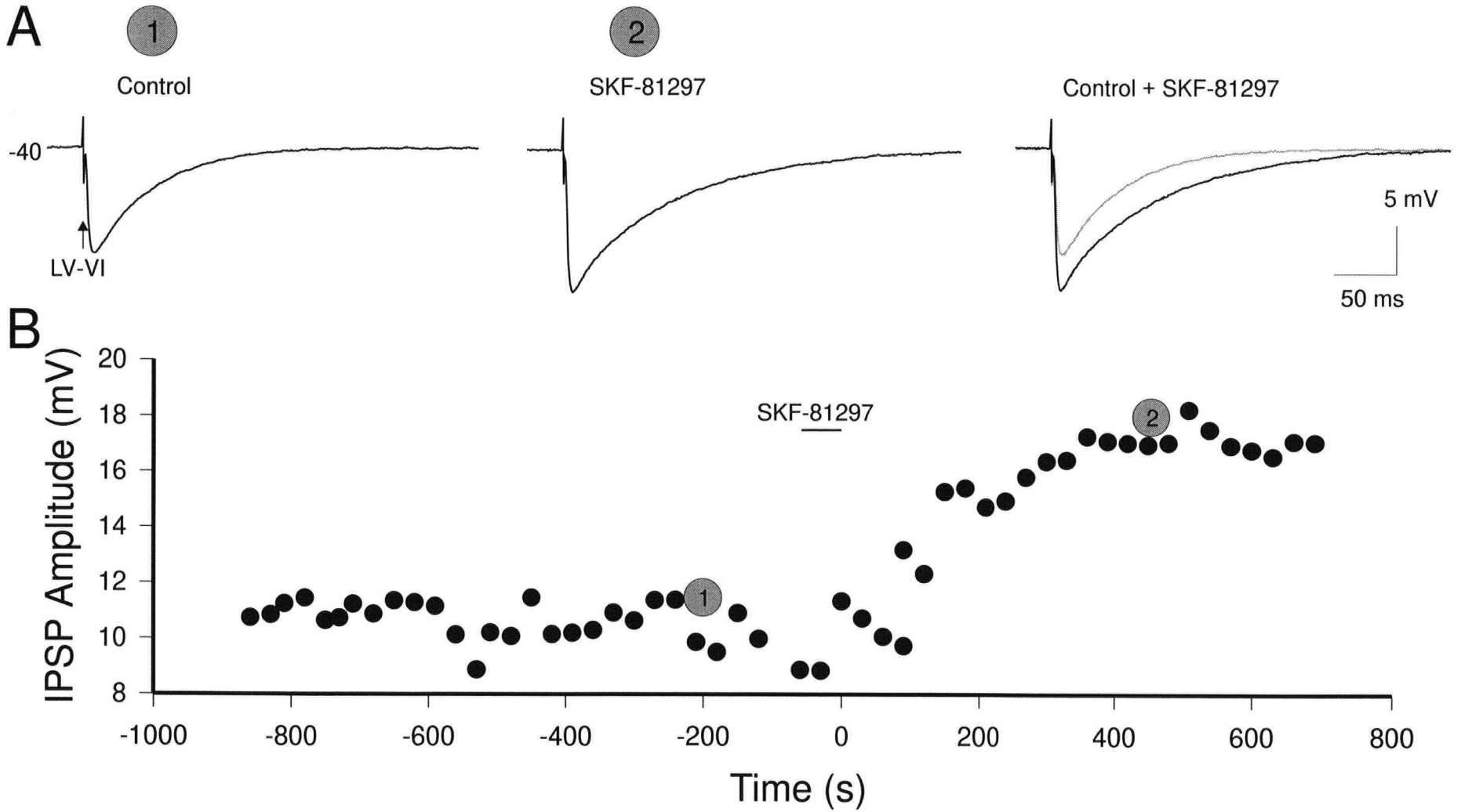

Figure 6-15: D1 receptor stimulation augmented layer V-VI IPSPs. **A)** (Left) At a somatic V_m of -50 mV an isolated $GABA_A$ IPSP was evoked by layer V-VI stimulation in the presence of DNQX (10μM) and APV (50μM). (Middle) Bath application of SKF-81297 (10μM, for 1min) enhanced the amplitude of the IPSP. (Right) The control and SKF-81297 response superimposed showing the magnitude of the ehnancement. **B)** Graph of the synaptic response amplitude before, during and after SKF-81297 application. The numbers in the grey circles show the times at which the traces shown in A were obtained. Responses were recorded using an intracellular electrode containing QX-314, 1M CsAc and 2M KAc.

the reduction in these 2 neurons is not clear. Nevertheless, it appears that in most cases DA, acting through D1 receptors effectively modulates layer I-II and V-VI $GABA_A$ IPSPs in PFC neurons.

Disussion

The results from this study showed that D1 and D2 receptor stimulation induced inconsistent changes in the passive membrane properties of PFC neurons. In contrast, D1, but not D2, receptor activation enhanced the membrane excitability in response to depolarizing current pulses in PFC neurons, presumably by augmenting the voltage-dependent slowly inactivating Na^+ current and by suppressing the voltage-dependent slowly inactivating K^+ current. In addition, D1 receptor stimulation also suppressed high and low threshold Ca^{2+} spikes in layer V-VI PFC neurons. Finally, D1 receptor stimulation enhanced NMDA EPSPs and $GABA_A$-mediated IPSPs in PFC neurons.

In most cells DA or a D1 agonist produced very long-lasting effects, and it was often difficult to obtain wash-out. Washout was generally observed approximately 50min. following drug delivery, and thus only in cases where it was possible to obtain a stable recording for over an hour, was washout observed. The reasons for these long-lasting effects are not known, but may be due to activation of long-lasting intracellular cascades.

Effects of DA on Passive Membrane Properties of PFC neurons

Bath application of DA or its agonists induced small and highly variable changes in resting membrane potential (1-4mV). There was no consistent pattern

of changes in the passive membrane properties even when potential indirect effects of DA on pyramidal output cells via activation of GABAergic interneurons were ruled out by bicuculline application. Though an overall decrease of R_{iN} resulted from both DA and SKF-38393 application, several PFC neurons did show a small enhancement in R_{iN}. In previous studies where higher concentrations of DA were bath-applied, deep layer V-VI PFC neurons showed either a 10-30% increase (with 400μM DA + re-uptake blocker, Penit-Soria et al., 1987) or no change (50-100μM, Law-Tho et al., 1994) in input resistance. Hence, DA does not induce any consistent change in the passive membrane properties of PFC neurons.

D1 receptor regulation of voltage-dependent slowly inactivating Na^+ and K^+ currents.

Two voltage-dependent currents regulate the firing threshold of PFC neurons (see Chapter 3). The first is a TTX-sensitive, slowly inactivating or persistent Na^+ current (I_{NAP}) which activates within 2 to 4 ms at subthreshold voltages by short current pulses but takes many seconds to inactivate. In cortical neurons, this Na^+ current is responsible for both inward rectification and subthreshold membrane oscillations (Alonso and Klink, 1993; Klink and Alonso, 1993; Llinas et al., 1991; Stafstrom et al., 1985). In the present study, following blockade of Ca^{2+} and K^+ currents, the isolated slowly inactivating Na^+ current induced a plateau potential with superimposed membrane oscillations. SKF-38393 increased the duration of this Na^+ plateau potential and shifted its activation threshold to a more negative voltage, perhaps by delaying the

inactivation of the slowly inactivating Na^+ current. This enhancing effect of the slowly inactivating Na^+ current by SKF-38393 is opposite to that observed in striatal neurons where DA D1 receptor activation suppressed both the fast and the slowly inactivating Na^+ currents (Calabresi et al., 1987; Cepeda et al., 1995; Surmeier et al., 1992; Schiffmann et al., 1995). Possible molecular variants of the D1/D5 receptors present in the PFC and striatum may account for the opposite responses which deserve further study.

Tetrodotoxin-senstive Na^+ channels are present in both the dendrites and the soma of pyramidal cells as suggested by electrophysiological and Na^+-imaging data (French et al., 1990; Huguenard et al., 1989; Jaffe et al., 1992; Regehr et al., 1993; Kim and Connors, 1993; Stuart and Sakmann, 1994). While immunohistochemical evidence suggests that the soma and the axon hillock have the densest distribution of Na^+ channel subunits (Westenbroek et al., 1989), cell-attached patch-clamp recordings suggest that Na^+ channels may be uniformly distributed throughout the axon, soma and apical dendrite (Colbert & Johnston 1996; Huegenard et al. 1989; Stuart & Sakmann 1994). As discussed in Chapter 4, although Na^+ channels exist on the apical dendrites of PFC neurons, there is no direct evidence for I_{NAP} current there. Thus it is likely that most of the I_{NAP} recorded in the present series of experiments was due to Na^+ channels near the soma.

Data from single Na^+ channel recordings in acutely isolated cortical pyramidal cell soma favor the idea that a single class of Na^+ channels can switch to a sustained opening mode that is interspersed with short duration transient

openings. When in the sustained opening mode, rapid inactivation of the Na^+ channel is unlikely (Alzheimer et al., 1993; Moorman et al., 1990). Given that the Na^+ plateau potential was activated at a lower voltage threshold and was prolonged by SKF-38393, it suggests that D1 receptor stimulation may modulate the activation and inactivation kinetics of the late Na^+ channel openings. Accordingly, very recent voltage-clamp data indicates that D1 receptor stimulation shifts the activation of I_{NAP} to more negative membrane potentials and slows the inactivation of this current in PFC neurons (Gorelova & Yang 1997). These changes in I_{NAP} by D1 agonists allowed the neuron to fire at a lower threshold while producing a longer sustained depolarization, triggering additional spikes.

Normally the inward rectification by I_{NAP} is balanced by outward rectification mediated by an I_D-like current (see Chapter 3). The pharmacological and biophysical profile of I_D in the PFC (Hammond and Crépel, 1992) resembles slowly inactivating K^+ currents characterized previously in hippocampal and cultured striatal neurons (Foehring and Surmeier, 1993; Nisenbaum et al., 1994; Storm, 1988). The current is inactive at rest but a significant window current is generated near -50mV (Hammond & Crepel 1992). Once I_D is activated within 100-200ms by a depolarizing pulse, it takes many seconds to inactivate. Thus, I_D opposes membrane depolarization and delays firing considerably unless the neuron is activated by long-lasting or repetitive depolarizing inputs (Foehring and Surmeier, 1993; Hammond and Crepel, 1992). Findings from the present study and others (Kitai and Surmeier, 1993) have shown that the D1 stimulation

attenuates the I_D. The reduction of I_D following D1 receptor activation would leave the inwardly rectifying, I_{NAP} unopposed, thus enabling the cell to be more responsive to depolarizing inputs, while promoting repetitive firing.

Little is known about the distribution of the slowly inactivating K^+ channels in single cortical pyramidal neurons although neural computational studies suggest that such functional K^+ channels are likely to be present in both the soma and the dendrites (Bernander et al., 1994; Midtgaard, 1994). The distribution of the transient K^+ I_A increases along the apical dendrite with distance from the soma (Hoffman et al. 1997). As shown in Chapter 4, I_D appeared to control excitability in the apical dendrites. Accordingly, D1 receptor-mediated reduction of I_D would be predicted to increase spike propagation or generation in the distal dendrites. Preliminary data from 1 apical dendritic tuft recording indicated that more spikes were evoked by the same depolarizing current pulse following application of the D1 agonist SKF-38393. If similar effects are observed in additional dendrites, it raises the possibility that DA may enhance associative synaptic plasticity at distal synapses (Magee & Johnston 1996).

D1 receptor-mediated suppression of high and low-threshold Ca^{2+} currents.

The suppressive actions of a D1 agonist on Ca^{2+} spikes is consistent with a DA-mediated suppression of high threshold Ca^{2+} currents shown in other vertebrate and invertebrates neurons (Marchetti et al., 1986; Williams et al., 1990; Paupardin-Tritsch et al., 1985; Surmeier et al., 1995). In the present study, D1 receptor stimulation primarily affected the duration of Ca^{2+} spikes.

Cortical neurons possess all three major types (L, P, N) of high-voltage activated Ca^{2+} channels (Brown et al., 1993; Franz et al, 1986; Sayer et al., 1990; 1993; Ye and Akaike, 1993). While the L-type Ca^{2+} channels are primarily distributed close to the soma (Hell et al., 1993; Westenbroek et al., 1990), the P- and N-channels are located primarily in the more distal dendrites (Hillman et al., 1991; Mills et al., 1994; Westenbroek et al., 1992; Usowicz et al., 1992). The present data indicated that suppressive effects of D1 receptor stimulation on Ca^{2+} spikes were still observed following blockade of L-type Ca^{2+} channels. Moreover, D1 receptor stimulation had very inconsistent effects on the 'hump' potential which was primarily mediated by L-type Ca^{2+} channels (see Figs. 3-6, 4-7, 5-12). These results suggest that Ca^{2+} spikes responsive to D1 receptor modulation were likely generated by P- and N-type Ca^{2+} channels.

Reductions in Ca^{2+} influx through high threshold Ca^{2+} channels was likely responsible for the D1-receptor mediated reduction of burst generation in PFC neurons. As discussed in Chapter 3, burst firing in pyramidal neurons is a complex process which is dependent on a number of factors. However, most data indicates that high and low threshold Ca^{2+} currents are involved. The D1

mediated suppression of Ca^{2+} currents in PFC neurons was likely responsible for the reduction in DAP and AHP amplitude. However, while the DAP was reduced significantly by D1 receptor stimulation, not all neurons fired fewer spikes/burst (e.g., Fig 6-3 A versus B). The D1-mediated suppression of Ca^{2+} currents in these neurons may exert only a small effect on burst initiation. Rather, the slow Ca^{2+}-mediated AHP that followed the burst was clearly reduced by D1 receptor stimulation in all neurons tested. Likewise, DA or D1 agonists also suppress the AHP in hippocampal neurons in studies when possible effects on β adrenergic receptors are ruled out (Pedarzani & Storm 1995; Malenka & Nicoll 1986). As a result in both PFC and hippocampal neurons more spikes were evoked within a given time period. Collectively, the present data indicate that D1 receptor stimulation appeared to bias PFC neurons to fire more spikes in a repetitive manner.

DA Modulation of Synaptic Inputs to PFC Neurons

DA had mixed but primarily inhibitory effects on non-isolated PSPs in PFC neurons, as reported previously (Law-Tho et al. 1994; Penit-Soria et al. 1987). Given that the PSPs in PFC neurons are composed of multiple components (see Chapter 5), this observation provided little insight into the modulatory action of DA.

Previously Law-Tho et al. (1994) showed that the initial slope of isolated NMDA EPSPs was depressed by DA or a D1 agonist in layer V PFC neurons. This effect was not replicated by D1 agonists with a larger number of cells in the

present study. In fact NMDA EPSP amplitude was significantly enhanced by D1 receptor stimulation in the present experiments. The present finding is consistent with the DA-mediated augmentation of responses evoked by NMDA iontophoresis onto cells in human cortical slices (Cepeda et al. 1992). In PFC neurons D1 receptor stimulation also enhances the post-synaptic response evoked by glutamate iontophoresis (Yang et al. 1996). This suggests that the augmentation of NMDA EPSPs by D1 receptor stimulation is at least partially mediated by post-synaptic mechanisms.

D1-Receptor Modulation of IPSPs

DA axons synapse on non-pyramidal neurons in the PFC (Smiley et al 1993) and D1 and D2 immunoreactivity are found on PFC interneurons (Vincent et al. 1995). Recently, Muly et al. (1997) have shown that D1 immunoreactivity on axon terminals of putative parvalbumin containing fast-spiking interneurons in the PFC. DA has been shown to induce a somatic depolarization of interneurons in the PFC that may be mediated by a D1 receptor mechanism (Yang et al. 1997; Zheng et al. 1997).

A previous study reported that DA suppressed the amplitude of IPSPs recorded in PFC pyramidal neurons (Law-Tho et al. 1994). In the present study however, selective stimulation of D1 receptors predominately enhanced IPSPs in PFC neurons, while D1 receptor blockade reduced IPSPs. The reasons for these discrepant findings are unclear, but may reflect differences in the type of interneurons stimulated, and the relative distribution of D1 and D2 receptors

(Vincent et al. 1995; Williams et al. 1996). The present data indicate that endogenous DA acting through D1 receptors augments interneuron activity to effectively enhance fast $GABA_A$ IPSPs onto PFC pyramidal neurons.

This D1-mediated modulation of interneurons and IPSPs in the PFC may explain why most in vivo studies have shown that DA exerts an inhibitory effect on pyramidal cell excitability (Mantz et al. 1982;Sesack & Bunney 1989; Ferron et al. 1984; Godbout et al. 1991; Bunney & Aghajanian 1976; Mora et al. 1976). Indeed, Pirot et al. (1994) has shown that the DA mediated suppression of spontaneous activity in PFC neurons is completely blocked if preceded by iontophoresis of the $GABA_A$ antagonist bicuculline. Therefore, the overall effects of DA on PFC pyramidal neurons may be determined by a complex interplay of direct excitatory effects (via modulation of Na^+, K^+, Ca^{2+} channels and NMDA receptors) and indirect inhibitory effects via interneurons.

General Discussion

The present thesis examined PFC function at both the behavioral and cellular level. Data presented in Chapter 2 demonstrated that bilateral inactivation of the PL specifically impaired prospective foraging on a delayed radial maze task. Moreover, D1 receptor blockade in the PFC, bilaterally or unilaterally in combination with contralateral inactivation of the vSub also disrupted performance of the delayed task. The fact that neither manipulation affected foraging on a single trial task without the aid of prior information, indicated that the PL was involved specifically in working memory processes related to the retrieval and use of information to guide action. Chapters 3-5 examined the basic physiological properties and synaptic responses of the soma and dendrites of deep layer PFC neurons. The apical tuft of PFC neurons appeared to process synaptic signals in a linear manner without amplification by voltage-gated currents. In contrast, Ca^{2+} currents in the apical stem amplified distal EPSPs. In somatic recordings, spike threshold was determined by slowly-inactivating Na^{+} and K^{+} currents and low threshold calcium currents, while both high and low threshold Ca^{2+} currents helped to generate burst firing. Chapter 6 showed that DA, via the D1 receptor, increased the excitability of PFC neurons to depolarizing inputs, allowing more spikes to be evoked in a repetitive manner. D1 receptor stimulation also enhanced IPSPs evoked synaptically. The main purpose of this Chapter is to discuss how these findings may be fitted into a theoretical model of PFC function and its modulation by DA.

A Brief Review of the Cellular Correlates of Working Memory

The neural correlates of working memory are strongly related to the activity of neurons in deep layers of the PFC (Goldman-Rakic 1995a,b; 1996; Quintana & Fuster 1992; Fuster 1995). These neurons show increased activation during a delay period or prior to the initiation of a correct response on working memory tasks (Quintana & Fuster 1992; Fuster 1995; Batuev et al. 1990; Funahasi et al. 1990; Wantanabe 1986). Task performance and task-related activity of PFC neurons is influenced by inputs from other cortical regions (Quintana et al. 1989; Fuster et al. 1985; Chaffe & Goldman-Rakic 1994). The activity of deep layer PFC neurons is thought to be required for holding and manipulation of information relayed from other cortical regions (Goldman-Rakic 1996). Detailed information on signal processing by deep layer PFC neurons is therefore central to an understanding of working memory processes mediated by the PFC.

Single Neuron Computation

Layer V PFC neurons may process synaptic inputs to their apical dendrites from other cortical areas in a potentially unique manner. Based on data presented in Chapter 4, I argue that the apical tuft of PFC neurons may selectively encode the near synchronous arrival of inputs from other cortical regions. One important intrinsic membrane property of the apical tuft of PFC neurons was the fast τ. The effect of a low τ and R_{IN} in the dendrites means that these regions of the neuron can respond to synaptic inputs on faster time scales

than the soma. As shown in Fig 4-1 the passive response of the soma is approximately twice as slow as the apical stem and four times as slow as the apical tuft. A long τ tends to make neurons act as integrators, allowing synaptic inputs to summate within a given temporal window (König et al. 1996). For instance, inputs arriving near the soma within 40-60ms would summate to produce a constant depolarization. Thus the soma could not differentiate between inputs arriving faster than 25Hz. In contrast, because the apical tuft repolarizes passively within 10-14ms, each input in a 70-100Hz train may not summate. As a consequence the apical tuft would not act as an effective integrator of synaptic inputs. The time window for summation is likely even shorter in vivo as constant background synaptic activity tends to decrease the membrane τ (Holmes & Woody 1989; Bernander et al. 1991). As a result, as the synaptic drive increases, the apical tuft may act as a more effective zone for detecting near coincident events.

The lack of Ca^{2+} electrogenesis in the apical tuft is consistent with its hypothesized role in detection of coincident synaptic signals. Specific information encoded by individual EPSPs arriving at different intervals within the apical tuft would not be completely obscured by the large prolonged change in membrane voltage caused by a Ca^{2+} spike. However, as argued in Chapter 4, local Na^+ spike initiation may occur in the apical tuft. Local Na^+ spike initiation may be critical for coincidence detection as it could effectively relay the occurrence of near coincident EPSPs to the soma. Moreover, the high local Na^+ spike threshold may ensure that only the simultaneous arrival of numerous EPSPs is sufficient to

trigger a local spike. Finally, the strong K^+ currents and strong GABA-mediated inhibition in the apical tuft may keep local depolarizations limited in time and spatially. This would also allow for greater temporal precision in processing synaptic inputs. Thus the apical tuft of PFC neurons possess a number of characteristics that are suited for processing nearly coincident synaptic inputs in a linear manner.

The effects of near coincident synaptic inputs to the apical tuft may be amplified by Ca^{2+} currents in regions proximal to the soma (Chapter 5). This proximal amplification may be a means of charging the soma, much like I_{NAP} helps the axon to charge the soma during spike initiation. The apical stem could act as a dynamic coupling zone between the tuft and soma, which could electrically isolate the tuft at resting membrane potentials, or link the tuft and soma by amplifying distal EPSPs in the subthreshold voltage range.

As noted above, the apical tuft of PFC neurons may be targeted by cortico-cortico projections from regions such as the somatosensory/parietal cortex (Johnson & Burkhalter, 1996; Castro-Alamancos & Connors 1997; Cauller & Connors 1992; Mitchell & Cauller 1997). Based on the present hypothesis, near synchronous firing of neurons in the somatosensory/parietal cortex may be most effective in activating the apical tuft of PFC neurons. It has been proposed that the brain may bind related stimuli in the environment together via the synchronous firing of groups of cortical neurons (Singer 1993). Accordingly the apical tuft of PFC neurons would respond best to stimuli that are 'bound' together via the synchronous firing of neurons in somatosensory/parietal cortex. The

effects of synchronous inputs may be transferred to the soma via mechanisms described in Chapter 5, thereby bringing the neuron to spike threshold. The spike output of deep layer PFC neurons may then be transferred along the axon to the striatum (Gorelova & Yang 1996) or other deep layer PFC neurons (see below).

Cortical Circuits:

Cortical neurons make functional connections with other cortical neurons in deep layers III-V via long horizontally projecting axons (Kritzer & Goldman-Rakic 1995; Thomson & Deuchars 1997). These connections may be essential for maintaining recurrent activity amongst small groups of neurons. Recurrently active local circuits have been proposed as a neural mechanism that could briefly retain information in the brain (James, 1961; Hebb 1949). Goldman-Rakic (1996) has proposed that the neural basis of working memory may be mediated by recurrently active subgroups of neurons which form functionally related local circuits in the deep layers of the PFC.

The recurrent activity within a local cortical circuit will be dependent on the type and strength of the synaptic connections. There are numerous types of synaptic interactions between neurons in the cortex, including pyramidal neurons synapsing on pyramidal neurons, pyramidal neurons synapsing on interneurons and interneurons synapsing on pyramidal neurons. Recent dual cell recordings from pairs of cortical neurons *in vitro* have provided new and important insights into local circuit interactions in the cortex which may be applied to our understanding of working memory processes in the PFC.

Pyramidal Cell-Pyramidal Cell Interactions

The majority of connections of pyramidal neurons are with other cortical pyramidal neurons (Keller 1993; Johnson & Burkhalter 1996). Inputs to the basal dendrites of layer III and V neurons arise mainly from neighboring neurons, perhaps within the same cortical column (Kritzer & Goldmann 1995; Markram et al. 1997; Thomson & Deuchars 1994). Unitary EPSPs in layer V neurons evoked by a single action potential in a connected layer V neuron are the strongest and largest of any recorded in the cortex (1-9mV) (Thomson & Deuchars 1997; Markram 1997; Markram et al. 1997). While a single EPSP is sometimes large enough to trigger a spike post-synaptically, usually >10 simultaneous EPSPs are required to evoke a spike in most cases, depending on the reliability of release sites (Thomson et al. 1996; Markram et al. 1997).

Pyramid-pyramid connections in the cortex undergo significant changes in synaptic efficacy. Pyramidal neurons in layer V of the cortex exhibit marked synaptic depression when the pre-synaptic cell fires at > 1Hz and the post-synaptic potential is held below -70mV (Thomson et al. 1993; Markram & Tsodyks 1996). In contrast, at membrane potentials above -65mV, synaptic facilitation rather than depression is observed (Thomson et al. 1995; Thomson & West 1993). At depolarized membrane potentials, the facilitation elicited at higher pre-synaptic firing rates overcomes the effects of depression, and facilitated EPSPs are often able to trigger action potentials in the adjacent post-synaptic neuron (Thomson & West 1993).

Pre-synaptic firing rates of between 5-20 Hz appear to be the most effective in evoking action potentials in the post-synaptic neuron. Furthermore, given that synaptic depression stabilizes after the 3rd pulse in a train (Thomson et al. 1995; Markram & Tsodyks 1996), continuous repetitive firing does not cause greater synaptic depression (Abbott et al. 1996) but allows a greater window for synaptic facilitation or potentiation. Thus continuous repetitive firing may be particularly effective in recruiting neighboring connected neurons in deep layers of the cortex.

Interneuron-Pyramidal Cell Interactions

In the cortex there are at least four main types of interneurons, termed classical fast spiking (FS), fast spiking/ bursting, low threshold spiking (LS), and regular spiking (Thomson & Deuchars 1997; Thomson et al. 1996; Kawaguchi 1995). FS interneurons innervate the soma and proximal regions of layer V pyramidal neurons (Thomson & Deuchars 1997; Thomson et al. 1996; Kawaguchi 1995). FS interneurons generate fast $GABA_A$ IPSPs during paired cell recordings of interneuron pyramidal cell pairs (Thomson et al. 1993; 1995; 1996; 1997). In one of the few studies of FS interneuron-pyramidal interactions, Thomson et al. (1996) showed that single action potentials in FS interneurons can evoke an IPSP in a post-synaptic pyramidal neuron that delays firing by 20-100ms. With long pre-synaptic trains (>20 spikes @ >100Hz) an additional slowly decaying hyperpolarization is evoked. As a result continuous fast firing in pre-

synaptic FS interneurons both significantly delays firing and produces long-lasting hyperpolarizations in post-synaptic pyramidal neurons.

Pyramidal Cell-Interneuron Interactions

Pyramidal neurons also contact and modulate the activity of interneurons in the cortex. The most systematic investigation of pyramidal cell -interneuron interactions in the cortex has been made by Thomson et al. (1995) and Duechars & Thomson (1995). EPSPs in LS or FS interneurons evoked by pre-synaptic action potentials in pyramidal neurons show considerable variability in amplitude. Moreover, at low pre-synaptic firing rates there are a large number of transmission failures (as high as 80%) due to the low probability of release at these synapses (Deuchars & Thomson 1995). However, if the pre-synaptic neuron fires in bursts the number of failures in transmission are decreased dramatically, and pronounced synaptic facilitation is observed. FS interneurons also exhibit a number of intrinsic membrane properties that bias them to respond only to bursts of afferent input. For instance, FS interneurons have depolarized spike thresholds (-41mV), along with strong outward rectification which prevents small EPSPs from evoking spikes (Kawaguchi 1995; 1993; Thomson et al. 1996) and extremely fast membrane τ which prevents effective summation of EPSPs (Thomson & Deuchars 1997; Kawaguchi 1995). Thus both pre- and post-synaptic factors ensure that interneurons are selectively activated by bursts of pre-synaptic and not by moderately high tonic firing rates.

The key differences between pyramid-pyramid and pyramid-interneuron connections in the cortex can be summarized as follows. First, continuous repetitive firing at moderate rates (5-20Hz) appears to be the most effective means of recruiting connected pyramidal neurons in deep layers of the cortex. In contrast very high frequency bursting (>100Hz) in the pre-synaptic neuron is an absolute requirement for activation of interneurons. Thus as noted by Thomson et al. (1993) for a given pyramidal neuron in the cortex, a tonic firing pattern would lead to a preferential recruitment of connected pyramidal neurons, while fast bursts would preferentially recruit interneurons.

Proposed Model of DA Modulation of Cortical Circuit Activity

Most of the evidence that DA modulates neuronal activity in the PFC comes from studies analyzing the effects of this neurotransmitter on single PFC neurons in vivo. Virtually all of these studies have demonstrated that DA exerts an inhibitory effect on pyramidal cell excitability (Pirot et al. 1992; Mantz et al. 1982;Sesack & Bunney 1989; Ferron et al. 1984; Godbout et al. 1991; Bunney & Aghajanian 1976; Mora et al. 1976). However, in a critical experiment, Pirot et al. (1992) showed that this inhibitory effect was abolished if the $GABA_A$ antagonist bicuculline was iontophoresed prior to DA, thereby demonstrating that the inhibitory action of DA was an indirect effect on GABAergic interneurons. This finding is consistent with that of Penit-Soria et al. (1987) who reported that DA substantially increased spontaneous IPSPs in PFC pyramidal neurons. Recently, we have observed that DA (100μM) increases the frequency of spontaneous

IPSPs recorded in PFC pyramidal neurons (Yang et al. 1997). The results shown in Chapter 6 also provided evidence that activation of D1 receptors enhanced evoked IPSPs in pyramidal neurons in the PFC. D1 receptors are present on parvalbumin-containing interneurons in the PFC (Muly et al. 1997), which correspond to the FS type described above (Kawaguchi & Kubota 1993). The D1 mediated enhancements in evoked IPSPs recorded in PFC pyramidal neurons are likely due to direct D1-mediated excitation of interneurons in the PFC, as demonstrated recently by whole-cell recordings from FS and LT interneurons (Yang et al. 1997; Zheng et al. 1997). Thus one action of DA is to increase the activity of local inhibitory interneurons which synapse on pyramidal neurons in the PFC.

In the absence of significant GABA input *in vitro*, DA has no clear effects on the resting membrane properties of pyramidal neurons in the PFC (see Fig 3-1). However, DA acts to enhance the effects of excitatory depolarizing inputs to PFC neurons. In previous studies, DA has been shown to enhance: 1) the excitatory responses of rat PFC neurons to subthreshold doses of NMDA, or acetylcholine (Cépeda et al., 1992; Yang and Mogenson,1990), 2) the response of PFC neurons to hippocampal stimulation and long-term potentiation in the hippocampal PFC pathway (Jay et al. 1996) and 3) the responses of deep layer PFC neurons to injection of intracellular depolarizing current pulses in vitro (Penit-Soria et al. 1993; Henze et al. 1997).

The present study demonstrated that DA acted through a variety of mechanisms to directly enhance the excitability of PFC pyramidal neurons to

depolarizing inputs. First, D1 receptor stimulation enhanced monosynaptic NMDA EPSPs in PFC neurons, and indirectly activated the Ca^{2+} mediated 'hump' potential to amplify NMDA EPSPs further. Second, DA significantly enhanced firing evoked by intracellular current pulses in PFC neurons (Chapter 6; Penit-Soria et al. 1987; Henze et al. 1997) via modulation of two intrinsic ionic conductances, I_{NAP} and I_D. D1 receptor stimulation was shown to enhance the I_{NAP}-mediated plateau potential, by moving the activation threshold to a more negative voltage and prolonging the duration of the plateau. This finding is supported by recent voltage-clamp analyses of I_{NAP} which showed that D1 receptor stimulation shifts the activation of the I_{NAP} to more negative voltages and prolonged the decay of the I_{NAP} in PFC neurons (Gorelova & Yang 1997). Concurrently D1 receptor stimulation was shown to reduce the slowly-inactivating K^+ current I_D, removing outward rectification and allowing more spikes to be evoked by a given depolarizing current pulse. The concurrent modulation of I_{NAP} and I_D by DA allowed spikes to be triggered at a lower membrane voltage while producing a longer depolarization for subsequent spike generation. Finally, D1 receptor stimulation reduced Ca^{2+} spikes, and inhibited Ca^{2+} dependent AHPs and DAPs associated with bursting. As a result of these effects of DA, PFC neurons responded more vigorously to incoming NMDA EPSPs and fired more spikes in a repetitive pattern.

DA may also act to enhance pyramid-pyramid connections in the PFC that are hypothesized to underlie delay-period activity (e.g. Goldman-Rakic 1996). By decreasing Ca^{2+} influx through voltage-gated Ca^{2+} currents, DA via the D1

receptor, would in turn decrease the Ca^{2+}-dependent DAP and AHP, thereby causing bursting PFC neurons to fire more repetitively. Based on the properties of pyramid-pyramid and pyramid/interneuron connections discussed above, biasing PFC neurons to fire repetitively would selectively recruit connected pyramidal neurons, rather than interneurons. As a result excitation amongst interconnected pyramidal neurons would be facilitated, as they would not be inhibited as strongly by interneurons. Although DA may depress pyramidal neurons non-specifically through its action on interneurons, it may actually promote connectivity between local pyramidal cell assemblies. This effect would be augmented further by the other direct action of DA on pyramidal neurons described above.

A Model of DA's action in the PFC

Considerable evidence indicates that DA plays a central role in regulating neural activity within the PFC that is related to working memory. First, 6-OHDA lesions of the PFC disrupt delayed response performance (Brozoski et al. 1979). Second, iontophoresis of DA or low doses of D1 antagonists enhance both delay period activity and anticipatory / response related activity of PFC neurons relative to background activity (Sawaguchi 1987; Sawaguchi et al. 1986; 1990a; Sawaguchi & Matsumura 1985; Williams & Goldman-Rakic 1995). Specifically, Sawaguchi et al. (1990a) reported that in awake monkeys performing a delayed response task, DA increased the average *background* activity by approximately 50% while increasing the *delay* and *response*-correlated activity by 209% and

145% respectively. Third, D1 antagonists iontophoresed into the PFC at high ejection currents disrupt delayed response performance (Chapter 2; Williams & Goldman-Rakic, 1995; Sawaguchi 1987; Sawaguchi et al. 1986; 1990b; Sawaguchi & Goldman-Rakic 1994). Furthermore, the results of Chapter 2 showed that injection of D1 antagonists into the PFC also disrupted selectively executive components of delayed responding, as rats were unable to use previously acquired information effectively to guide responding for food on a spatially-cued radial maze. Collectively, these data suggest a clear role for DA in the modulation of both the mnemonic and response related (executive) functions of PFC neurons during working memory tasks.

I propose that the predominant effect of DA depends on the level of excitation of PFC neurons (Fig 7-1). Spontaneous activity observed in cortical neurons *in vivo* is the result of relatively weak but sustained excitatory synaptic input (Matsumura et al. 1988; Arieli et al. 1996; Britten et al. 1992). Application of DA inhibits spontaneous activity recorded in PFC neurons in anesthetized rats *in vivo* (Mantz et al. 1982; Sesack & Bunney 1989; Ferron et al. 1984; Godbout et al. 1991; Bunney & Aghajanian 1976; Mora et al. 1976). As noted above, this effect appears to be mediated indirectly through GABAergic interneurons in the PFC (Pirot et al. 1992). Thus for PFC neurons receiving low levels of synaptic drive, the primary action of DA is inhibitory (Fig 7-1A).

As the level of synaptic drive increases, the relative effect of DA may be excitatory. During a behavioral task in the awake animal, spontaneous activity is increased above that observed in the anesthetized preparation. Furthermore,

Figure 7-1. The effect of DA depends on the amount of synaptic drive and activity level of deep layer PFC neurons. In all panels, blue lines indicate weak excitatory synaptic inputs, red lines indicate inhibitory inputs and green lines strong excitatory input. The width of each input indicates its relative effectiveness in driving the soma. **A)** (Top) In the anesthetized preparation, there is a low level of tonic excitatory synaptic drive to PFC neurons, and as a result the spike output of PFC neurons is low. (Bottom) When DA is released, interneurons are activated, increasing spontaneous IPSPs and decreasing the overall firing rate of pyramidal neurons (Penit-Soria et al. 1987; Pirot et al. 1984; Yang et al. 1997). **B)** (Top) In the awake animal, excitatory drive is increased relative to the anesthetized preparation, and firing is enhanced (Bottom) When DA is released, the activity level rises further (Sawaguchi et al. 1990). **C)** (Top) During a working memory task, the synaptic drive from intracortical inputs, possibly to the apical tufts, and local inputs to the basal dendrites, is increased (Fuster et al. 1985; Quintana et al. 1989; Goldman-Rakic 1988; 1996). As a result, firing is increased significantly. (Bottom) The level of firing is enhanced further in the presence of DA, by its augmenting effects on NMDA EPSPs and voltage-gated ionic currents which are activated by strong membrane depolarization.

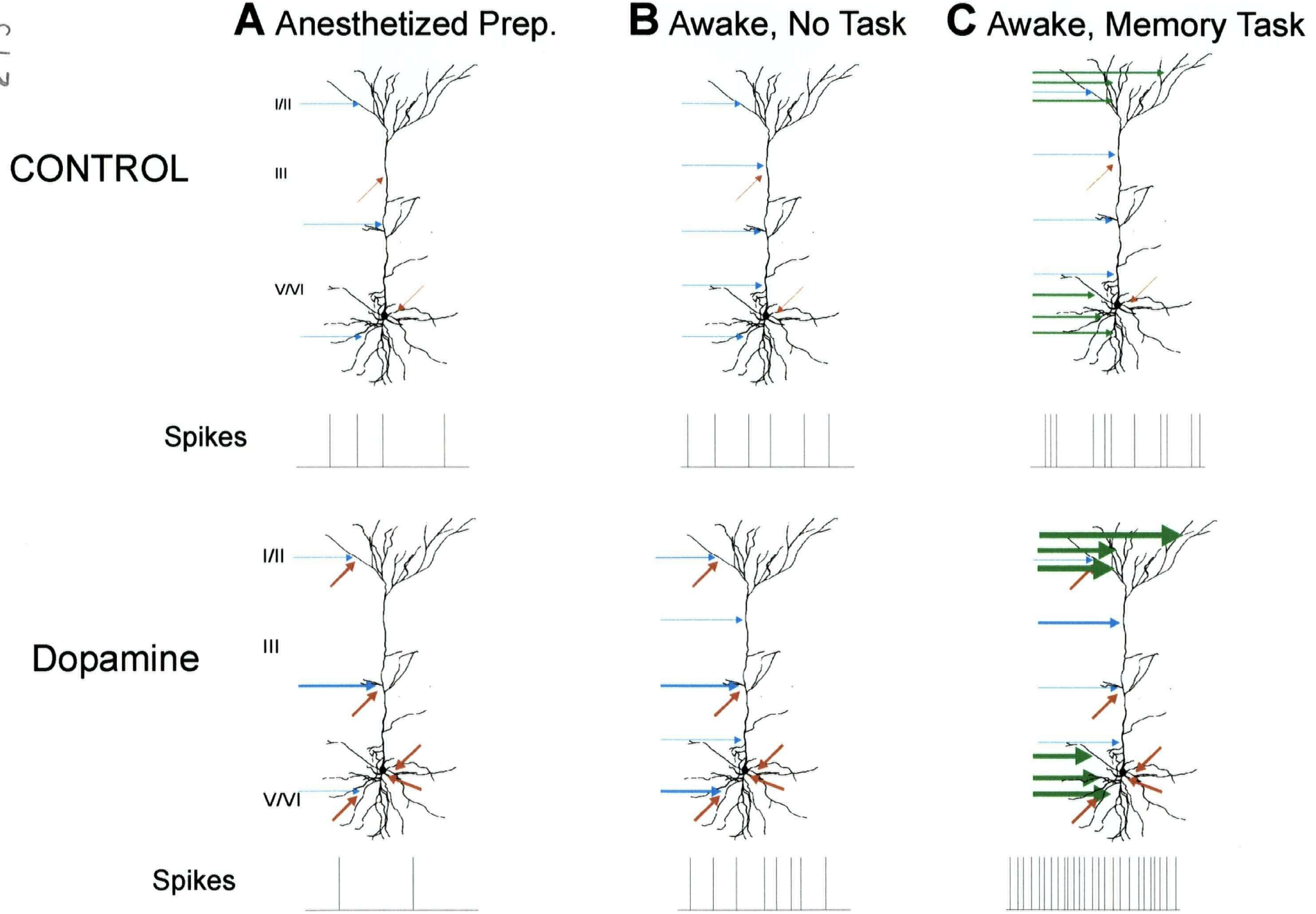
A Anesthetized Prep.
B Awake, No Task
C Awake, Memory Task
CONTROL
I/II
III
V/VI
Spikes
Dopamine
I/II
III
V/VI
Spikes

during a working memory task, delay-active neurons in the PFC receive strong excitatory drive from the parietal and temporal corticies (Fuster et al. 1985; Quintana & Fuster 1989) or neighboring pyramidal neurons (Vaadia et al. 1994; Abeles et al. 1993), and their firing rate increases even further (Funahashi et al. 1989; Fuster 1973). When activity of PFC neurons is increased and the neuron is more strongly depolarized, voltage-dependent NMDA receptors, slowly-inactivating Na^+ currents and high threshold Ca^{2+} currents are considerably more active than when the neuron is at rest or firing at low rates. As a result, under conditions of strong excitatory drive, the effects of DA on NMDA EPSPs and Na^+ and Ca^{2+} currents would predominate and cause an increase in the repetitive firing activity of PFC neurons (Fig 7-1B.C)

One potential problem with such a scheme is that, under conditions of strong excitatory drive, DA may also concurrently activate interneurons. However, rather than simply suppressing pyramidal cell firing, the enhanced inhibition could serve a number of important purposes: First, DA-mediated activation of interneurons may entrain functional cell assemblies in the PFC. Recently, Whittington et al. (1995) have proposed that connected GABAergic interneurons can entrain pyramidal cells in the cortex, with the frequency of entrainment dependent on the net excitation of the interneurons. With strong excitation, oscillations can occur at 40Hz which is significant because neurons coding similar stimulus features may be bound together by synchronous firing at 40Hz (Gray et al. 1989). Field recordings in human subjects indicate that PFC neurons fire synchronously at 40Hz under certain behavioral conditions (R.

Adolfs, personal communication). By exciting interneurons in the PFC, DA may help to entrain activity in connected pyramidal neurons. This processes may be aided by the D1 mediated augmentation of I_{NAP}, which underlies intrinsic membrane oscillations in PFC neurons and other cortical neurons (Chapter 3; Alonso & Llinas 1989).

Second, DA-mediated enhancements in interneuron excitability may tune the task-related firing activity of PFC neurons. In the visual cortex, receptive fields are tuned by local GABAergic interneurons, as receptive fields widen nonspecifically in the presence of bicuculline (Eysel et al. 1996). Goldman-Rakic (1995; 1996) has ascribed a closely related function to interneurons in the PFC. She has suggested that interneurons may inhibit the activity of pyramidal neurons with opposing memory fields. Single-unit recordings during oculomotor delayed response tasks in rats and primates indicate that delay-active neurons are spatially selective, as they fire during the delay only if stimuli were previously presented at a specific spatial location (Batuev et al. 1990; Funahasi et al. 1989). Interneurons show reciprocal activation patterns during the delay, being inactive when adjacent pyramidal neurons are active and active when adjacent pyramidal neurons are inactive. This type of reciprocal activity may serve to regulate pyramidal neuron activity so that pyramidal neurons coding different stimuli features are not co-activated. By stimulating interneurons in the PFC, DA may enhance the tuning of PFC pyramidal neurons, such that only groups of pyramidal neurons coding task-related stimuli are activated. Conversely, manipulations which decrease the effects of interneurons in the PFC (i.e.

bicuculline or SCH-23390) may lead to non-selective and widespread activation of PFC neurons as shown in Chapter 5.

If interneurons connected to the pyramidal neuron in Fig 7-1C had reciprocal activation patterns, then the net effect of DA would be strongly excitatory. Thus, the greater the reciprocal activation pattern of pyramid-interneuron pairs, the more fined tuned is the pyramidal neuron, and the greater the excitatory effect of DA. In poorly tuned interneuron-pyramidal cell pairs, with significant input from the interneurons, the excitatory effects of DA would be reduced by the enhancements in interneuron activity by DA. In this way, DA selectively augments finely tuned local circuit activity.

Third, DA-mediated augmentation of interneuron excitability may help to prime pyramidal neurons in the PFC. If cortical pyramidal neurons are strongly depolarized and firing at high rates, the voltage-gated currents which regulate spike threshold and firing patterns are inactivated to varying degrees (Brown et al. 1993; Storm 1993; Crepel & Hammond 1992; Fleidervish et al. 1996; Huguenard et al. 1988; Fleidervish et al. 1996). As noted in Chapter 3, spike threshold in PFC neurons and spike firing patterns are determined by an interplay of I_{NAP}, I_D and Ca^{2+} currents. Slow inactivation of I_{NAP} causes a slow cumulative adaptation of spike firing in cortical pyramidal neurons, which is expressed as a reduced subthreshold membrane depolarization, progressively increasing inter-spike intervals and elevated spike threshold (Fleidervish et al 1996). This cumulative adaptation is removed with membrane hyperpolarization. Likewise, repeated or prolonged membrane depolarization inactivates I_D in PFC

pyramidal neurons which is also removed by membrane hyperpolarization (Hammond & Crepel 1992). Finally, transient T-type Ca^{2+} currents which are activated in the subthreshold voltage range exhibit fast inactivation when stepped to depolarized membrane potentials (see Fig 2-5). DA augmentation of GABAergic IPSPs in the PFC may not only reduce spontaneous firing, but provide membrane hyperpolarization which resets the ionic currents which determine spike threshold in PFC pyramidal neurons. Once reset, the pyramidal neuron is primed to receive incoming excitatory input.

If the membrane is hyperpolarized or shunted by larger or more frequent IPSPs, stronger depolarizing inputs will be required to depolarize the neuron to near spike threshold in the presence of DA. However, DA concurrently acts directly on NMDA EPSPs and Na^+ and K^+ currents in PFC pyramidal neurons to increase the effectiveness of a depolarizing inputs. Only strong inputs which overcome the effects of the IPSP would be preferentially enhanced by DA, since the activity of NMDA receptors and I_{NAP} is voltage-dependent and are more relevant with membrane depolarization. Thus DA may reduce pyramidal cell activity in the PFC via its effects on interneurons, while concurrently resetting post-synaptic ionic currents and enhancing the effects of strong depolarizing inputs to pyramidal neurons. In this way only those neurons receiving strong excitatory drive, would be enhanced by DA.

Collectively, the hypothesized action of DA via the D1 receptor in the PFC may be summarized as follows. DA may enhance the activity of interneurons in the PFC thereby decreasing spontaneous firing of pyramidal neurons, and

priming these neurons for subsequent excitatory input. DA may also act directly on NMDA EPSPs and intrinsic voltage-gated currents to increase selectively the activity of neurons receiving strong excitatory inputs. In the presence of DA such inputs are more effective in producing repetitive firing. Repetitive firing of these neurons may then help to recruit connected pyramidal neurons into a functional cell assembly. The effects of excitatory inputs from connected neurons may then be maintained by DA's action on intrinsic voltage-gated currents. This model is consistent with the known literature regarding DA's action in the PFC and explains how this transmitter can selectively enhance task-related activity relative to background activity on working memory tasks.

Relating the Cellular Model to Behavior

Shultz (1991) has postulated that:

" ...a major action of DA appears to be a focusing effect by which the function of postsynaptic structures becomes restricted to the processing of the most prominent inputs whereas weaker activity is lost".

The present model describes a mechanism through which this may occur. DA acts via interneurons in the PFC to decrease the spontaneous activity of pyramidal neurons under conditions of low synaptic drive. Concurrently, DA also acts on voltage-gated currents in PFC pyramidal neurons to augment the effects of strong depolarizing inputs from other cortical regions or from functionally connected pyramidal neurons in local cell assemblies. DA may tune the activity of PFC neurons such that firing is more tightly correlated with task relevant

information. On a delayed response task this model would explain how DA increases firing during the delay and response periods more than background activity (Sawaguchi et al. 1990a; Sawaguchi & Matsumura 1985).

A logical extension of this hypothesis is that at higher or 'supranormal' levels of DA or GABA, the spontaneous activity of PFC neurons would be greatly inhibited and only exceptionally strong inputs could drive the neurons to threshold. What would be the consequences of this behaviorally? It has been demonstrated that D1 receptor agonists or GABA microinfusions into the PFC both produce perseverative responding in a T-maze, as rats continue to revisit the recently rewarded spatial location while ignoring the correct spatial location (Zhart et al. 1997; Meneses et al. 1993). This suggests that the rat's behavior was dominated by a limited set of stimuli that had taken on particular significance. The signifigance of a stimulus may be determined by the activity of the DA system in the brain (see General Introduction). The model proposed here suggests that, with respect to the PFC, stimuli which are deemed 'significant' are those that are able to overcome the DA-mediated inhibory mechanisms.

The effect of blocking D1 receptors, would be to decrease task related activity relative to background activity (Sawaguchi 1997). As a result any input would contribute to membrane depolarization and therefore responses would be influenced non-selectively by almost any stimuli. This may explain why, on an oculomotor delayed response task, microinjections of a D1 antagonist into the monkey PFC, disrupt the spatial selectivity of delay-active neurons, and reduce the accuracy of memory-guided saccades (Sawaguchi & Goldman-Rakic 1989;

Williams & Goldman-Rakic 1995). Accordingly in Chapter 2 it was demonstrated that D1 receptor blockade caused random behavior on a task which assessed executive components of working memory in the rat, but not on a simple foraging task which did not. This effect was quite striking because it indicated that D1 antagonists microinjected into the PFC, impaired specifically the ability to use previously acquired spatial information to guide foraging. Moreover, since a similar pattern of errors was observed following unilateral inactivation of the hippocampus in combination with contralateral injections of a D1 antagonist into the PFC, it would appear that D1 receptors specifically modulated hippocampal afferents to the PFC on the delayed task. D1 receptors in the PFC may therefore restrict the types of spatial information transferred from the hippocampus that will be used to guide foraging. In the absence of D1 receptors any type of sensory information from the hippocampus or other brain regions (i.e. inferotemporal cortex or parietal cortex) may influence the activity of PFC neurons involved in response organization thereby causing random or disorganized behaviors.

Summary and Conclusions

The primary function of the PFC appears to be related to the ability to briefly retain and use previously acquired information to guide action. This function is mediated by the activity of deep layer PFC neurons which participate in the active retention of information in recurrently active cell assemblies, in a manner similar to that proposed by Hebb (1968). This recurrent activity may be determined by local synaptic connections and the intrinsic membrane properties

of deep layer PFC neurons. The intrinsic membrane properties and synaptic connections are modulated by DA via the D1 receptor. D1 receptor stimulation augments IPSPs onto deep layer pyramidal neurons, while also augmenting activity evoked by depolarizing inputs. These effects are balanced such that too much or too little DA can be detrimental to cognition but in quantitatively different ways.

I argue that the action of DA in the PFC depends on the state of the neuron and the behavioral situation that the animal is facing. At low stimulation levels, when the PFC is not engaged in any particular task, DA may simply inhibit spontaneous firing in PFC neurons. At higher stimulation levels, DA may tune the activity of PFC neurons such that only the most active neurons which are receiving the most synaptic drive maintain sustained activation. The present model explains why maintaining DA levels within a certain range is necessary for performance of tasks requiring the PFC.

The present model also has implications for disorders of attention such as schizophrenia or attention deficit disorder. If levels of DA are too low in the PFC, thought or action may be undirected or directed towards inappropriate stimuli. Methylphenidate (Ritalin) or related drugs which increase DA levels may help to direct thought or action by tuning the activity of PFC neurons in the manner described above. In schizophrenics, the possible therapeutic effects of increasing DA in the PFC must be balanced by the detrimental effects of increased striatal DA (Grace 1993; Deutch 1993). Perhaps, the most effective anti-psychotic

agents may be those that increase D1 receptor activity in the PFC while reducing DA tone in the striatum.

The present model is based on experiments which were designed to provide a general overview of PFC function and its modulation by DA. This model may be used to make specific predictions regarding the actions of DA in the PFC. Future experiments are necessary to to test these predictions and to determine the validity of the model in explaining the complex yet important action of DA in the PFC.

References

Abeles, M. (1982) Role of the cortical neuron: integrator or coincidence detector? *Isr. J. Med. Sci.* 18, 83-92.

Abeles, M., Bergman, H., Margalit, E., & Vaadia, E. (1993) Spatiotemporal firing patterns in the frontal cortex of behaving monkeys. *J. Neurophysiol.* 70, 1629-1638.

Albert, D.J. & Madryga, F.J. (1980) An examination of the functional spread of 4µl of slowly infused lidocaine. *Behav. & Neural Biol.*, 29, 378-384.

Alonso, A. and Klink, R. (1993) Differential electroresponsiveness of stellate and pyramidal-like cells of medial entorhinal cortex layer II. *J. Neurophysiol.* 70, 128-143.

Alonso, A. and Llinas, R. (1989) Subthreshold Na^+-dependent theta-like rhythmicity in stellate cells of entorhinal cortex layer II. Nature 342, 175-177.

Alonso, A., & Llinas, R. (1992) Electrophysiology of the mammillary complex in vitro. II. Medial mammillary neurons. *J. Neurophysiol.* 68, 1321-1331.

Aghajanian, G.K. & Wang, Y.Y. (1986) Pertussis toxin blocks the outward currents evoked by opiate and α2-agonists in locus coeruleus neurons. *Brain Res.* 371, 390-394.

Alzheimer, C., Schwindt, P.C. , & Crill, W.E. (1993) Modal gating of Na^+ channels as a mechanism of persistent Na^+ current in pyramidal neurons from rat and cat sensorimotor cortex. *J. Neurosci.* 13, 660-673.

Amitai, Y., Friedman, A., Connors, B.W., & Gutnick, M.J. (1993) Regenerative activity in apical dendrites of pyramidal cells in neocortex. *Cerebral Cortex* 3, 26-38.

Andreasen, M., & Hablitz, J.J. (1992) Kinetic properties of a transient outward current in rat neocortical neurons. *J. Neurophysiol.* 68, 1133-1142.

Arieli, A., Sterkin, A., Grinvald, A., & Aertsen, A. (1996) Dynamics of ongoing activity: Explanation of the large variability in evoked cortical responses. *Science* 273, 1868-1871.

Arnsten, A.F.T. (1997) Catecholamine regulation of prefrontal cortex. *J. Psychopharmacol.* in press.

Arnsten, A.F.T., Cai, J.X., Steere, J.C., & Goldman-Rakic, P.S. (1995) Dopamine D2 receptor mechanisms contribute to age-related cognitive decline: the effects of quinpirole on memory and motor performance in monkeys. *J. Neurosci.* 15, 3429-3439.

Avery, R.B., & Johnston, D. (1996) Multiple channel types contribute to the low-voltage-activated calcium current in hippocampal CA3 pyramidal neurons. *J. Neurosci.* 16, 5567-5582.

Bachevalier, J. & Mishkin, M. (1986) Visual recognition impairment follows ventromedial but not dorsolateral prefrontal lesions in monkeys. *Behav. Brain Res.* 20, 249-261.

Baddeley, A. (1986) *Working memory*. Oxford Univ. Press.

Baddeley, A., & Della Sala, S. (1996) Working memory and executive control. *Phil. Trans. Royal. Soc. Lond.* 351, 1397-1404.

Baddeley, A.D., & Hitch, G. (1974) Working memory. In: *The psychology of learning and motivation. Advances in Research and theory.* (ed G.H. Bower), pp 47-89. NY Academic Press.

Barnes, C.A. (1995) Involvement of LTP in memory: Are we "searching under the street light"? *Neuron*, 15, 751-754.

Batuev, A.S., Kurina, N.P. & Shutov, A.P. (1990) Unit activity of the medial wall of the frontal cortex during delayed performance in rats. *Behav. Brain Res.* 41, 95-102.

Benardo, L.S., Masukawa, L.M., & Prince, D.A. (1982) Electrophysiology of isolated hippocampal pyramidal dendrites. *J. Neurosci.* 2, 1614-1622.

Berger, B., Gasper, P., & Verney, C. (1991) Dopaminergic innervation of the cerebral cortex: Unexpected differences between rodents and primates. *Tends Neurosci.* 14, 21-27.

Bergson, C., Mrzlijak, L., Smiley, J.F., Pappy, M., Levenson, R., & Goldman-Rakic (1995) Regional cellular, and subcellular variations in the distribution of D1 and D5 dopamine receptors in the primate brain. *J. Neurosci.* 15, 7821-7836.

Bernander, Ö, Koch, C., & Douglas, R.J. (1994) Amplification and linearization of distal synaptic input to cortical pyramidal neurons. *J. Neurophysiol.* 72, 2743-2753.

Bernander, Ö., Douglas, R.J., Martin, K.A.C., & Koch, C. (1991) Synaptic background activity influences spatiotemporal integration in single pyramidal cells. *Proc. Natl. Acad Sci. U.S.A.* 88, 11569-11573.

Berry, M.S., & Pentreath, V.W. (1976) Criteria for distinguishing between monosynaptic and polysynaptic transmission. *Brain Res.* 105, 1-20.

Brito, G.N.O., & Brito, L.S.O. (1990) Septohippocampal system and the prelimbic sector of frontal cortex: a neuropsychological battery analysis in the rat. *Behav. Brain Res.*, 36, 127-146.

Britten, K.H., Shadlen, M.N., Newsome, W.T., & Movshon, J.A. (1992) The analysis of visual motion: a comparison of neuronal and psychophysical performance. *J. Neurosci.*, 12, 4745-4765.

Bröckers, T.M., Zimmer, M., Müller, A., Bergman, M., Brose, N., & Kreutz, M.R. (1994) Expression of the NMDA R1 receptor in selected human brain regions. *Neuroreport* 5, 965-969.

Broersen, L.M, Heinsbroek, R.P., deBruin, J.P., Uylings, H.B., Oliver, B. (1995b) The role of the medial prefrontal cortex of rats in short-term memory functioning: further support for involvement of cholinergic, rather than dopaminergic mechanisms. *Brain Res.* 674, 221-229.

Broersen, L.M, Heinsbroek, R.P., deBruin, J.P.C., Joosten, R.N.J.M.A., van Hest, A., & Oliver, B. (1995a) Effects of local application of dopaminergic drugs into the dorsal part of the medial prefrontal cortex of rats in a delayed matching to position task: comparison with cholinergic blockade. *Brain Res.* 645, 113-122.

Brown, A.M., Schwindt, P.C., & Crill, W.E. (1993) Voltage-denpendence and activation kinetics of pharmacologically defined components of the high-threshold calcium current in rat neocortical neurons. *J. Neurophysiol.* 70, 1530-1543.

Brozowski, T.S., Brown, R.M., Rosvold, H.E., & Goldman, P.S. (1979) Cognitive deficits caused by regional depletion of dopamine in prefrontal cortex of Rhesus monkey. *Science* 205, 929-932.

Bruce, C.J. (1988) Single neuron activity in the monkey's prefrontal cortex. In (Eds. P. Rakic & W. Singer) *Neurobiology of Neocortex*. pp 297-329. John Wiley & Sons.

Bubser M., & Schmidt W.J. (1990) 6-Hydroxydopamine lesion of the rat prefrontal cortex increases locomotor activity, impairs acquisition of delayed alternation tasks, but does not affect uninterrupted tasks in the radial maze. *Behav. Brain Res.*, 37, 157-68.

Bunney, B.S., & Aghajanian, G.K. (1976) Dopamine and norepinephrine innervated cells in the rat prefrontal cortex: pharmacological differentiation using microiontophoretic techniques. *Life Sci.* 19, 1783-1792.

Calabresi, P., Mercuri, N., Stanzione, P., Stefani, A., & Bernardi, G. (1987) Intracellular studies on the dopamine-induced firing inhibition of neostriatal neurons in vitro: evidence for D1 receptor involvement. *Neurosci.* 20, 757-771.

Carr, D.B., & Sesack, S.R. (1996) Hippocampal afferents to the rat prefrontal cortex: Synaptic targets and relation to dopamine terminals. *J. Comp. Neurol.* 369:1-15.

Cauller, L.J. & Connors, B.W. (1992) Functions of very distal dendrites: Experimental and computational studies of layer I synapses on neocortical pyramidal cells. In: *Single Neuron Computation* (eds: McKenna, T., Davis, J., Zornetzer, S.F.), Academic Press, Inc. p.199-230.

Cauller, L.J., & Connors, B.W. (1994) Synaptic physiology of horizontal afferents to layer I in slices of rat SI neocortex. *J. Neurosci.* 14, 751-762.

Cépeda, C, Walsh, J.P., Peacock, W., Buchwald, N.A., & Levine, M.S. (1994) Neurophysiological, pharmacological and morphological properties of human caudate neurons recorded in vitro. *Neurosci.* 103, 59-89.

Cépeda, C., Radisavljevic, Z., Peacock, W., Levine, M.S., & Buchwald, N.A. (1992) Differential modulation by dopamine of responses evoked by excitatory amino acids in human cortex. *Synapse* 11, 330-341.

Chaffe, M. & Goldman-Rakic, P.S. (1994) Prefrontal cooling dissociates memory- and sensory-guided oculuomotor delayed response functions. *Soc. Neurosci. Abstr.* 15, 786.

Chagnac-Amitai, Y., Luhmann, H.J., Prince, D.A. (1990) Burst generating and regular spiking layer 5 pyramidal neurons of rat neocortex have different morphological features. J. Comp. Neurol. 296, 598-613.

Chang, J.Y., Laubach, M.G., Kirillov, A., & Woodward, D.J. (1994) Neuronal activities in basal ganglia and frontal cortex during delayed match to sample task in freely moving rats. *Soc. for Neurosci. Absts.*, 20, 781.

Colbert, C.M, & Johnston, D. (1996) Axonal action-potential initiation and Na^+ channel densities in the soma and axon initial segment of subicular pyramidal neurons. *J. Neurosci.* 16, 6676-6686.

Condé, F. Marie-Lepoivre, E. , Audinat, E., & Crépel, F. (1995) Afferent connections of the medial frontal cortex of the rat. II. Cortical and subcortical afferents. *J. Comp. Neurol.* 352, 567-593.

Connors, B.W. (1992) $GABA_A$- and $GABA_B$-mediated processes in visual cortex. In, (Eds R.P. Mize, R.E. Marc, & A.M. Sillito) *Progress in Brain Research.* GABA in the retina and central visual system. pp 335-348, Amsterdam, Elsevier.

Connors, B.W., Gutnick, M.J. & Prince, D.A. (1982) Electrophysiological properties of neocortical neurons in vitro. *J. Neurophysiol.* 48: 1302- 1320.

Connors, B.W., Malenka, R.C., & Silva, L.R. (1988) Two inhibitory postsynaptic potentials, and $GABA_A$ and $GABA_B$ receptor-mediated responses in neocortex of rat and cat. *J. Physiol.* 406, 443-468.

Cook, R.G., Brown, R.F., & Riley, D.A. (1985) Flexible memory processing by rats: use of prospective and retrospective information in the radial arm maze. *Anim. Behav. Proc.* 11, 453-469.

Cowan, R.L. & Wilson, C.J. (1994) Spontaneous firing patterns and axonal projections of single corticostriatal neurons in the rat medial agranular cortex. *J. Neurophysiol.* 71, 17-32.

Currie, S.N., Wang, X.F., & Daw, N.W. (1994) NMDA receptors in layers II and III of rat cerebral cortex. *Brain Res.* 662, 103-108.

Deisz, R.A., & Prince, D.A. (1989) Frequency-dependent depression of inhibition in guinea pig neocortex in vitro by $GABA_B$ receptor feedback on GABA release. *J. Physiol. (Lond.)* 412, 513-541.

Descarries, L., LeMay, B., Doucet, G., & Berger, B. (1987) Regional and laminar density of the dopamine innervation in the adult rat cerebral cortex. *Neurosci.* 21, 807-824.

Deuchars, J., & Thomson, A.M. (1995) Single axon fast inhibitory postsynaptic potentials eleicited by a sparsely spiny interneuron in rat neocortex. *Neuroscience*, 65, 935-942.

Deutch, A.Y. (1993) Prefrontal cortical dopamine systems and the elaboration of functional corticostriatal circuits: implications for schizophrenia and Parkinson's disease. *J. Neural Transm. [Gen Sect]* 91, 197-221.

Diamond, A. (1990) The development and neural bases of memory functions as indexed by the A B and delayed response tasks in human infants and infant monkeys. In A. Diamond(Ed.), *The development and neural bases of higher cognitive functions* (pp.267-317) New York: NY Academy of Science Press

Diamond, A., & Goldman-Rakic, P.S. (1989) Comparison of human infants and rhesus monkeys on Piaget's AB task: evidence for dependence on dorsolateral prefrontal cortex. *Exp. Brain Res.* 74, 24-40.

Diamond, J. The third Chimpanzee. pp 32-58, Harper Collins, New York.

Doar, B., Finger, S., & Almli, C.R. (1987) Tactile-visual acquistion and reversal learning deficits in rats with prefrontal cortical lesions. *Exp Brain Res.* 66, 432-434.

Dodt, H.U., Kampe, K., Frink, A., Rüther, T., & Zeiglgänsberger, W. (1995) Differential distribution of excitatory amino acid receptors on rat layer V pyramidal neurons in vitro. *Soc. Neurosci. Abstr.* 21, 144.3.

Dunnett, S.B. (1990) Role of the prefrontal cortex and striatal output systems in short-term memory deficits associated with ageing, basal forebrain lesions, and cholinergic-rich grafts. *Can. J Psych.*, 44, 210-232.

Durstewitz, D., & Seamans, J.K. (1997) The possible function of dendritic HVA calcium channels in prefrontal cortical pyramidal cells: A combined in vitro electrophysiological and compartmental modelling study. *Soc. Neursci. Abstr.* 472.12, 1188.

Eysel, U.T, Eyding, D., & Schweigart, G. (1996) Repetitive visual stimulation elicits LTP-like receptive field plasticity in the mature visual cortex. (In press).

Ferron, A., Thierry, A.M., Le Douarin, C., & Glowinski, J. (1984) Inhibitory influence of the mesocortical dopaminergic system on spontaneous activity or excitatory response induced from the thalamic mediodorsal nucleus in the rat medial prefrontal cortex. *Brain Res.* 302, 257-265.

Fleidervish, I.A., Friedman, A., & Gutnick, M.J. (1996) Slow inactivation of Na^+ current and slow cumulative spike adaptation in mouse and guinea-pig neocortical neurons in slices. *J. Physiol. (Lond.)* 493.1, 83-97.

Floresco, S.B., Seamans, J.K., & Phillips, A.G. (1997) Selective roles for hippocampal prefrontal cortical, and ventral striatal circuits in radial-arm maze tasks with or without a delay. *J. Neurosci.* 17, 1880-1890.

Foehring, R.C. & Surmeier, D.J. (1993) Voltage-gated potassium currents in acutely dissociated rat cortical neurons. *J. Neurophysiol.* 70, 51-63.

Foehring, R.C. & Waters, R.S. (1991) Contributions of low-threshold calcium current and anomalous rectifier (Ih) to slow depolarizations underlying burst firing in human neocortical neurons in vitro. *Neurosci. Lett.* 124, 17-21.

Franceschetti, S., Guatteo, E., Panzica, F., Sancini, G., Wanke, E., & Avanzini, G. (1995) Ionic mechanisms underlying burst firing in pyramidal neurons: Intracellular study in rat sensorimotor cortex. *Brain Res.* 696, 127-139.

Franz, P., Galvan, M., & Constanti, A. (1986) Calcium-dependent activity pattern and the associated inward calcium currents in guinea pig neocortical neurons in vitro. *Brain Res.* 366, 262-267.

French, C.R., Sah, P., Buckett, K.J., & Gage, P.W. (1990) A voltage-dependent persistent sodium current in mammalian hippocampal neurons. *J. Gen. Physiol.* 95, 1139-1157.

Friedman, A. & Gutnick, M.J. (1989) Intracellular calcium and control of bursting generation in neurons of guinea-pig neocortex in vitro. *Eur. J. Neurosci.* 1, 374-381.

Funahashi, S., & Kubota, K. (1994) Working memory and prefrontal cortex. *Neurosci. Res.* 21, 1-11.

Funahashi, S., Bruce, C.J., & Goldman-Rakic, P.S. (1989) Mnemonic coding of visual space in the monkey's dorsolateral prefrontal cortex. *J. Neurophysiol.* 61, 331-349.

Funahashi, S., Chafee, M.V., & Goldman-Rakic, P.S. (1993) Prefrontal neuronal activity in rhesus monkeys performing a delayed anti-saccade task. *Nature*, 365, 753-756.

Fuster, J.M, Bauer, R.H., & Jervey, J.P. (1985) Functional interactions between inferotemporal and prefrontal cortex in a cognitive task. *Brain Res.*, 330, 299-307.

Fuster, J.M. (1973) Unit activity in prefrontal cortex during delayed-response performance: neuronal correlates of transient memory. *J. Neurophysiol.* 36, 61-78.

Fuster, J.M. (1984) Behavioral electrophysiology of the prefrontal cortex. *Trends Neurosci.* 7, 408-414.

Fuster, J.M. (1990) Inferotempoal units in selective visual attention and short-term memory. *J. Neurophysiol.* 64, 681-697.

Fuster, J.M. (1991) The prefrontal cortex and its relation to behavior. *Prog. Brain Res.*, 87, 201-211.

Fuster, J.M. (1993) Frontal Lobes. *Curr. Op. Neurobiol.*, 3, 160-165.

Fuster, J.M. (1995) Memory in the cerebral cortex: an empirical approach to neural networks in the human and nonhuman primate. MIT Press.

Gaspar, P., Bloch, B., & Le Moine, C. (1995) D1 and D2 receptor gene expression in the rat frontal cortex: cellular localization in different classes of efferent neurons. *Eur. J. Neurosci.* 7, 1050-1063.

Ghosh, A. & Greenberg, M.E. (1995) Calcium signalling in neurons: molecular mechanisms and cellular consequences. *Science* 268, 239-247.

Gigg, J., Tan, A., & Finch, D.M. (1994) Glutamatergic hippocampal formation projections to prefrontal cortex in the rat are regulated by GABAergic inhibition and show convergence with glutamatergic projections from the limbic thalamus. *Hippocampus*, 4, 189-198.

Gillessen, T., & Alzheimer, C. (in press) Amplification of EPSPs by low Ni^{2+}- and amiloride-sensitive Ca^{2+} channels in the apical dendrites of rat CA! pyramidal neurons. *J. Neurophysiol.*

Glowinski, J., Tassin. J.P., & Thierry, A.M. (1984) The mesocortico-prefrontal dopaminergic neurons. *Trends Neurosci.* Nov, 415-418.

Godbout, R., Mantz, J., Pirot, S., Glowinski, J., & Thierry, A.-M. (1991) Inhibitory influence of the mesocortical dopaminergic neurons on their target cells: electrophysiological and pharmacological characterization. *J. Pharmacol. Exp. Therap.* 258, 728-738.

Goldman-Rakic, P.S. (1987) Circuitry of the prefrontal cortex and the regulation of behavior by representational knowledge. In *Handbook of Physiology*, (eds. F.Plum & V. Mountcastle), pp 373-417, American Physiological Society, Maryland.

Goldman-Rakic, P.S. (1990) Cellular and circuit basis of working memory in prefrontal cortex of nonhuman primates. *Prog. Brain Res.,* 85, 325-335.

Goldman-Rakic, P.S. (1992) Dopamine-mediated mechanisms of the prefrontal cortex. *The Neurosciences*, 4, 149-159.

Goldman-Rakic, P.S. (1995a) Cellular basis of working memory. *Neuron*, 14, 477-485.

Goldman-Rakic, P.S. (1995b) Architecture of the Prefrontal cortex and the central executive. *Proc. Natl. Acad. Sci (U.S.A.)* 769; 71-83.

Goldman-Rakic, P.S. (1996) The prefrontal landscape: implications of functional architecture for understanding human mentation and the central exectutive. *Phil Trans. Roy. Soc. Lond.* 351; 1445-1453.

Goldman-Rakic, P.S. (1988) Topography of cognition: Parallel distributed networks in primate association cortex. *Ann. Rev. Neurosci.* 11, 137-156.

Goldman-Rakic, P.S. (1990) Cellular and circuit basis of working memory in prefrontal cortex of nonhuman primates. *Prog. Neurobiol.* 85, 325-335.

Goldman-Rakic, P.S. (1991) Prefrontal cortical dysfunction in schizophrenia: the relevance of working memory. In: Psychopathology and the Brain (Eds: B.J. Carroll and J.E. Barrett), Raven Press, 1991,pp 1-23.

Goldman-Rakic, P.S. (1994) Working memory dysfunction in schizophrenia. *J. Neuropsychiatry*, 6, 348-357.

Goldman-Rakic, P.S., Leranth, C., Williams, S.M., Mons, N., & Geffardm, M. (1989) Dopamine synaptic complex with pyramidal neurons in primate cerebral cortex. *Proc. Natl. Acad. Sci. U.S.A.* 86, 9015-9019.

Gorelova, N., Yang, C.R. (1996) Projection of the prefrontal cortex-nucleus accumbens neurons. *Neurosci.* 76, 689-706.

Grace, A.A. (1993) Cortical regulation of subcortical dopamine systems and its possible relevance to schizophrenia. *J. Neural Transm. [Gen. Sect.]* 91: 111-134.

Gray, C.M., König, P., Engel, A.K., Singer, W. (1989) Oscillatory responses in cat visual cortex exhibit inter-columnar synchronization which reflects global stimulus properties. *Nature* 338, 334-337.

Groenewegen, H.J., Berendse, H.W., Wolters, J.G., & Lohman, A.H.M. (1990) The anatomical relationship of the prefrontal cortex with the striatopallidal system, the thalamus and the amygdala: evidence for a parallel organization. *Prog. in Brain Res.* 85, 95-118.

Guatteo, E., Franceschetti, S., Bacci, A., Avanzini, G., & Wanke, E. (1996) A TTX-sensitive conductance underlying burst firing in isolated pyramidal neurons from rat neocortex. *Brain Res.* 741, 1-12.

Hablitz, J.J., & Johnston, D. (1981) Endogenous nature of spontaneous bursting in hippocampal pyramidal neurons. *Cell. & Mol. Neurobiol.* 1, 325-334.

Haj-Dahmane, S., & Andrade, R. (1997) Calcium-activated cation nonselective current contributes to the fast afterdepolarization in rat prefrontal cortex neurons. *J. Neurophysiol.* 78, 1983-1996.

Hammond, C., & Crépel, F. (1992) Evidence for a slowly inactivating K^+ current in prefrontal cortical cells. *Eur. J. Neurosci.* 4, 1087-1092.

Hebb, D. (1977) The frontal lobe. *CMA Journal* 116, 1373-1374.

Hebb, D.O. (1939) Intelligence in man after large removals of cerebral tissue: report of four left frontal lobe cases. *J. Gen. Psychol.* 21, 73-87.

Hebb, D.O. (1949) The Organization of behavior. New York, Wiley.

Hebb, D.O. (1968) Concerning imagery. *Psych. Rev.* 75, 466-477.

Hell, J.W., Westenbroek, R.E., Warner, C., Ahlijanian, M.K., Prystay, W., Gilbert, M.M., Snutch, T.P., & Catterall, W.A. (1993) Identification and differential

subcellular localization of the neuronal class C and class D L-type calcium channel alpha-1 subunits. *J. Cell. Biol.* 123, 949-962.

Henández-López, S., Bargas, J., Surmeier, D.J., Reyes, A., & Galarraga, E. (1997) D1 receptor activation enhances evoked discharge in neostrial medium spiny neurons by modulating an L-type Ca^{2+} conductance. *J. Neurosci.* 17, 3334-3342.

Hestrin, S., Sah, P., & Nicoll, R.A. (1990) Mechanisms generating the time course of dual component excitatory synaptic currents recorded in hippocampal slices. *Neuron* 5, 247-253.

Higashi, H., Tanaka E., & Nishi, S. (1991) Synaptic properties of guinea pig cingulate cortical neurons in vitro. *J. Neurophsiol.* 65, 822-833.

Hille, B. (1984) Ionic channels of excitable membranes. Sinauer Associates Inc., U.S.A.

Hillman, D., Chen, S., Aung, T.T., Chersksey, B., Sugimori, M., & Llinas, R.R. (1991) Localization of P-type calcium channels in the central nervous system. *Proc. Natl. Acad. Sci.,(U.S.A.)* 88, 7076- 7080.

Hirose, S., Ino, T., Takada, M., Kimura, J., Akiguchi, I., & Mizuno, N. (1992) Topographic projections from the subiculum to the limbic regions of the medial frontal cortex in the cat. *Neurosci. Lett.* 139, 61-64.

Hirsch, J.C. & Crepel, F. (1990) Use-dependent changes in synaptic efficacy in rat prefrontal neurons in vitro. *J. Physiol. (Lond.)* 427, 31-49.

Hoffman, D.A., Magee, J.C., Colbert, C.M., & Johnston, D. (1997) K^+ channel regulation of signal propagation in dendrites of hippocampal pyramidal neurons. *Nature* 387, 869-875.

Hoffman, W.H., & Habberly, L.B. (1989) Bursting induces persistent all-or-none EPSPs by an NMDA-dependent process in piriform cortex. *J. Neurosci.* 9, 206-215.

Holmes, W.R. & Woody, C.D. (1989) Effects of uniform and non-uniform synaptic 'activation-distributions' on the cable properties of modeled cortical pyramidal neurons. *Brain Res.* 505, 12-22.

Huguenard, J.R., Haill, O.P., & Prince, D.A. (1989) Sodium channels in dendrites of rat cortical pyramidal neurons. *Proc. Natl. Acad. Sci. (U.S.A.)* 86, 2473-2477.

Huntley, G.W., Vickers, J.C., Janssen, W., Brose, N., Heinemann, S.F., & Morrison, J.H. (1994) Distribution and synaptic localization of immunocytochemically identified NMDA receptor subunit proteins in sensory-motor and visual cortices of monkey and human. *J. Neurosci.* 14, 3603-3619.

Hwa, G.G.C., Avoli, M. (1992) Excitatory postsynaptic potentials recorded from regular-spiking cells in layers II/III of rat sensorimotor cortex. *J. Neurophysiol.* 67, 728-737.

Inoue, M., Oomura, Y., Auo, S., Nishino, H., & Sikdar, S. (1985) Reward related neuronal activity in monkey dorsolateral prefrontal cortex during feeding behavior. *Brain Res.* 326, 307-312.

Jack,J.J.B., Noble, D., & Tsien, R.W. (1975) Electric current flow in excitable cells. London: Oxford University Press.

Jaffe, D.B., Johnston, D., Lasser-Ross, N., Lisman, J.E., Miyakawa, H., & Ross, W.N. (1992) The spread of Na^+ spikes determines the pattern of Ca^{2+} entry into hippocampal neurons. *Nature* 357, 244-246.

Jahnsen, H. & Llinas, R. (1984) Ionic basis for the electroresponsiveness and oscillatory properties of guinea-pig thalamic neurones in vitro. *J. Physiol.* 349, 227-247.

James, W. (1961) Psychology: Briefer Course. New York: Harper. (Original work published in 1892).

Jaskiw, G.E., & Weinberger, D.R. (1992) Dopamine and Schizophrenia - a cortically corrective perspective. *Seminars Neurosci.* 4, 179-188.

Jay, T.M, & Witter, M.P. (1991) Distribution of hippocampal CA1 and subicular efferents in the prefrontal cortex of the rat studied by means of the anterograde transport of Phaseolus vulgaris leucoagglutinin. *J. Comp. Neurol.* 313, 574-586.

Jay, T.M., Burette, F., & Laroche, S. (1996) Dopaminergic modulation of long-term potentiation in the hippocampal-prefrontal cortex pathway. *Soc. Neurosci. Abstr.* 22,332.

Jay, T.M., Glowinski, J., & Thierry, A.M. (1995) Inhibition of hippocampo-prefrontal cortex excitatory responses by the mesocortical DA system. *Neuroreport* 6, 1845-1848.

Jiang, Z.G., & North, R.A. (1991) Membrane properties and synaptic responses of rat striatal neurones in vitro. *J. Physiol. (Lond.)* 443, 533-553.

Johnson, R.B., & Burkhalter, A (1996) Microcircuitry of forward and feedback connections within rat visual cortex. *J. Comp. Neurol.* 368, 383-398.

Johnston, D., & Brown, T.H. (1981) Giant synaptic potential hypothesis for epileptiform activity. *Science* 211, 294-297.

Johnston, D., & Brown, T.H. (1983) Interpretation of voltage-clamp measurements in hippocampal neurons. *J. Neurophysiol.* 50, 464-486.

Johnston, D., Magee, J.C., Colbert, C.M., & Christie, B.R. (1996) Active properties of neuronal dendrites. *Annu. Rev. Neurosci.* 19, 165-186.

Jones, E.G. (1984) Laminar distribution of cortical efferent cells. In: A. Peters and E.G. Jones (eds): Cerevbral Cortex, Vol. 1: Cellular Components of the Cerebral Cortex, New York: Plenum Press, pp. 521-552.

Jones, E.G. (1993) GABAergic neurons and their role in cortical plasticity in primates. *Cereb. Cortex*, 3, 361-372.

Kamondi, A., & Reiner, P.B. (1991) Hyperpolarization-activated inward current in histaminergic tuberomammillary neurons of the rat hypothalamus. *J. Neurophysiol.* 66, 1902-1911.

Kanter, E.D., Kapur, A., & Haberly, L.B. (1996) A dendritic $GABA_A$-mediated IPSP regulates facilitation of NMDA-mediated responses to burst stimulation of afferent fibers in piriform cortex. *J. Neurosci.* 16, 307-312.

Kavalali, E.T., & Plummer, M.R. (1996) Multiple voltage-dependent mechanisms potentiate calcium channel activity in hippocampal neurons. *J. Neurosci.* 16, 1072-1082.

Kawaguchi, Y. (1993) Groupings of nonpyramidal and pyramidal cells with specific physiological and morphological characteristics in rat frontal cortex. *J. Neurophysiol.* 69, 416-431.

Keller, A, (1993) Intrinsic organization of the motor cortex. *Cereb. Cortex* 3, 430-441.

Kesner, R.P. & Holbrook, T. (1987) Dissociation of item and order memory in rats following medial prefrontal cortex lesions. *Neuropsychologia*, 25, 653-664.

Kesner, R.P. (1989) Retrospective and prospective coding of information: role of the medial prefrontal cortex. *Exp. Brain. Res.* 74, 163-167.

Kesner, R.P., DiMattia, B.V., & Crutcher, K.A. (1987) Evidence for neocortical involvement in reference memory. *Behav. & Neural Biol.*, 47, 40-53.

Kim, H.G., & Connors, B.W. (1993) Apical dendrites of the neocortex: Correlation between sodium- and calcium-dependent spiking and pyramidal cell morphology. *J. Neurosci.* 13, 5301-5311.

Kim, H.G., Beierlein, M., & Connors, B.W. (1995) Inhibitory control of excitable dendrites in neocortex. *J. Neurophysiol.* 74, 1810-1814.

Kitai, S.T., & Surmeier, D.J. (1993) Cholinergic and dopaminergic modulation of potassium conductances in neostriatal neurons. *Advances Neurol.* 60, 40-52.

Klassen, A.J., Delrod, B., Burnod, Y., & Guigon, E. Generation and control of sustained discharges in a modeled neocortical pyramidal neuron: role of slowly inactivating potassium and persistent sodium conductances. (in preparation).

Klink, R., & Alonso, A.(1993) Ionic mechanisms for the subthreshold oscillations and differential electroresponsiveness of medila entorhinal cortex layer II neurons. *J. Neurophysiol.* 70, 144-157.

Kobayashi, M., Inoue, T., Matsuo, R., Masuda, Y., Hidaka, O., Kang, Y., & Morimoto, T. (1997) Role of calcium conductances on spike afterpotentials in rat trigeminal motoneurons. *J. Neurophysiol.* 77, 3273-3283.

Koch, C., Rapp, M., & Segev, I. (1996) A brief history of time (constants). *Cereb. Cortex*, 6, 93-101.

Koch, K.W., & Fuster, J.M. (1989) Unit activity in monkey parietal cortex related to haptic perception and temporary memory. *Exp. Brain Res.* 76, 292-306.

Kojima, S. & Goldman-Rakic, P.S. (1982) Delay-related activity of prefrontal neurons in rhesus monkeys performing delayed response. *Brain Res.* 248, 43-49.

Kolb, B. (1984) Functions of the frontal cortex of the rat: a comparative review. *Brain Res. Rev.*, 8, 65-98.

König, P., Engel, A.K., & Singer, W. (1996) Integrator or coincidence detector? The role of the cortical neuron revisited. *Trends Neurosci.* 19, 130-137.

Konnerth, A., Lux, H.D., & Heinemann (1986) Ionic properties of burst generation in hippocampal pyramidal cell somata in vitro. *Exp. Brain Res.* 14, 368-374.

Konow, A., & Pribram, K.H. (1970) Error regognition and utilization produced by injury to the frontal cortex in man. *Neuropsychologia* 8, 489-491.

Kritzer, M.F., & Goldman-Rakic, P.S. (1995) Intrinsic circuit organization of the major layers and sublayers of the dorsolateral prefrontal cortex in the rhesus monkey. *J. Comp. Neurol.* 359: 131-143.

Lampl, I. & Yarom, Y. (1993) Subthreshold oscillations of the membrane potential: a functional synchronizing and timing device. *J. Neurophysiol.* 70, 2181-2186

Larkman, A. & Mason, A. (1990) Correlations between morphology and electrophysiology of pyramidal neurons in slices of rat visual cortex. II Establishment of cell classes. *J. Neurosci.* 10, 1407-1414.

Law-Tho, D., Hirsch, J.C., & Crepel, F. (1994) Dopamine modulation of synaptic transmission in rat prefrontal cortex: an in vitro electrophysiological study. *Neurosci. Res.* 21, 151-160.

Lipowsky, R., Gillessen, T., & Alzheimer, C. (1996) Dendritic Na^+ channels amplify EPSPs in hippocampal CA1 pyramidal cells. *J. Neurophysiol.* 76, 2181-2191.

Ljungberg, T., Apicella, P., & Schultz, W (1992) Responses of monkey dopamine neurons during learning of behavioral reactions. *J. Neurophysiol.* 67, 145-163.

Llinás, R. (1986) Intrinsic electrophysiological properties of mammalian neurons: insights into the central nervous system functions. *Science*, 242, 1654-1664.

Llinás, R., & Sugimori, M. (1980) Electrophysiological properties of in vitro purkinje cell dendrites in mammalian cerebellar slices. *J. Physiol.(Lond)* 305, 197-213.

Llinás, R., Grace, A.A., & Yarom, Y. (1991) In vitro neurons in mammalian cortical layer 4 exhibit intrinsic oscillatory activity in the 10- to 50-Hz frequency range. *Proc. Natl. Acad. Sci. U.S.A.* 88, 897-901.

Magee, J.C., & Johnston, D. (1995a) Synaptic activation of voltage-gated channels in the dendrites of hippocampal pyramidal neurons. *Science* 268, 301-304.

Magee, J.C., & Johnston, D. (1995b) Characterization of single voltage-gated Na^+ and Ca^{2+} channels in apical dendrites of rat CA1 pyramidal neurons. *J. Physiol. (Lond)* 487.1, 67-90.

Magee, J.C., & Johnston, D. (1997) A synaptically controlled, associative signal for hebbian plasticity in hippocampal neurons. *Science* 275, 209-213.

Magee, J.C., Christofi, G., Miyakawa, H., Christie, B., Lasser-Ross, N., & Johnston, D. (1995) Subthreshold synaptic activation of voltage-gated Ca^{2+} channels mediates a localized Ca^{2+} influx into the dendrites of hippocampal pyramidal neurons. *J. Neurophysiol.* 74, 1335-1342.

Mainen, Z.F. & Sejnowski, T.J. (1997) Modeling active dendritic processes in pyramidal neurons. Methods in Neural Modeling (Eds C. Koch, & I. Segev) 2nd Edition. MIT Press, Cambridge.

Mainen, Z.F., Joerges, J., Huguenard, J.R., & Sejnowski, T.J. (1995) A model of spike initiation in neocortical pyramidal neurons. *Neuron* 15, 1427-1439.

Malenka, R.C., & Nicoll, R.A. (1986) Dopamine decreases the calcium-activated afterhyperpolarization in hippocampal CA1 pyramidal cells. *Brain Res.* 379, 210-215.

Mantz, J., Milla, C., Glowinski, J., & Thierry, A.M. (1988) Differential effects of ascending neurons containing dopamine and noradrenaline in the control of spontaneous activity and of evoked responses in the rat prefrontal cortex. *Neurosci.* 27, 517-526.

Marchetti, C., Carbone, E., & Lux, H.D. (1986) Effects of dopamine and noradrenaline on Ca^{2+} channels of cultured sensory and sympathetic neurons of chick. *Pflügers Archiv Eur. J. Physiol.* 406, 104-111.

Markram, H. (1997) A network of tufted layer 5 pyramidal neurons. *Cereb. Cortex.* 7, 523-533.

Markram, H., & Sakmann, B. (1994) Calcium transient in dendrites of neocortical neurons evoked by single subthreshold excitatory postsynaptic potentials via low-voltage-activated Ca^{2+} channels. *Proc. Natl. Acad. Sci. U.S.A.* 91, 5207-5211.

Markram, H., Lübke, J., Frotscher, M., Roth, A., & Sakmann, B. (1997) Physiology and anatomy of synaptic connections between thick tufted pyramidal neurones in the developing rat neocortex. *J. Physiol. (Lond.)* 550.2, 409-440.

Mason, A. & Larkman, A. (1990) Correlations between morphology and electrophysiology of pyramidal neurons in slices of rat visual cortex. II electrophysiology. *J. Neurosci.* 10, 1415-1428.

Masukawa, L.M., & Prince, D.A. (1984) Synaptic control of excitability in isolated dendrites of hippocampal neurons. *J. Neurosci.* 4, 217-227.

Matsumura, M., Cope, T., & Fetz, E.E. (1988) Sustained excitatory synaptic input to motor cortex neurons in awake animals revealed by intracellular recording of membrane potentials. *Exp. Brain Res.* 70, 463-469.

McCormick, D.A. & Feeser, H.R. (1990) Functional implications of burst firing and single spike activity in lateral geniculate relay neurons. *Neurosci.* 39, 103-113.

McCormick, D.A. & Pape, H.-C. (1990) Properties of a hyperpolarization-activated cation current and its role in rhythmic oscillation in thalamic relay neurons. *J. Physiol.* 431, 291-318.

Mel, B. W. (1994) Information processing in dendritic trees. *Neural Computation*, 6: 1031- 1085.

Meneses, S., Galicia, O., & Brailowsky, S. (1993) Chronic infusions of GABA into the medial prefrontal cortex induce spatial alternation deficits in aged rats. *Behav. Brain Res.* 57, 1-7.

Miles, R., Tóth, Gulyás, A.I., Hájos, N., & Freund, T. (1996) Differences between somatic and dendritic inhibition in the hippocampus. *Neuron* 16, 815-823.

Miller, E.K., & Desimone, R. (1994) Parallel neuronal mechanisms for short-term memory. *Science* 263, 520-522.

Miller, E.K., Erickson, C.A., & Desimone, R. (1996) Neural mechanisms of visual working memory in prefrontal cortex of the macaque. *J. Neurosci.* 16, 5154-5167.

Miller, J.P., Rall, W. & Rinzel, J. (1985) Synaptic amplification by active membrane in dendritic spines. *Brain Res.* 325: 325-330.

Mills, L.R., Niesen, C.E., So, A.P., Carlen, P.L., Spigelman, I., & Jones, O.T. (1994) N-type Ca^{2+} channels are located on somata, dendrites, and a subpopulation of dendritic spines on live hippocampal pyramidal neurons. *J. Neurosci.* 14: 6815-6824.

Milner, B. (1963) Effects of different brain lesions on card sorting. The role of the frontal lobes. *Arch. Neurol.*, 9, 90-100.

Milner, B. (1965) Visually-guided maze learning in man: effects of bilateral hippocampal, bilateral frontal and unilateral cerebral lesion. *Neuropyschologia* 3, 317-338.

Milner, B. & Petrides, M. (1984) Behavioral effects of frontal-lobe lesions in man. *Trends Neurosci.*, 7, 403-407.

Mitchell, B.D., & Cauller, L.J. (1997) Cortico-cortical and thalamocortical projections to layer I of the prefrontal/premotor neocortex in rats. *Soc. Neurosci. Abstr.*, 502.5, 1273.

Miyakawa, H., Ross, W.N., Jaffe, D., Callaway, J.C., Lasser-Ross, N., Lisman, J.E., & Johnston, D. (1992) Synaptically activated increases in Ca^{2+} concentration in hippocampal CA1 pyramidal cells are primarily due to voltage-gated Ca^{2+} channels. *Neuron* 9, 1163-1173.

Mogenson, G.J. Brudzynski, S., Wu, M., Yang, C.R. , Yim, C.Y. From motivation to action: a review of dopaminergic regulation of limbic→nucleus accumbens→ventral pallidum→pedunculopontine nucleus circuitries involved in limbic-motor integration. In: *The Mesolimbic Motor Circuit and Neuropsychiatry* (Ed: Kalivas, P. , Barnes, C.) CRC Press, Boca Raton, Florida, 1993.p.193-236.

Moorman, J.R., Kirsch, G.E., Van Dongen, A.M., Joho, R.H., & Brown, A.M. (1990) Fast and slow gating of sodium channels encoded by a single mRNA. *Neuron* 4: 243-252.

Mora, F., Sweeney, K.F., Rolls, E.T., & Sanguinetti, A.M. (1976) Spontaneous firing rate of neurons in the prefrontal cortex of the rat: evidence for a dopaminergic inhibition. *Brain Res.* 116, 516-522.

Müller, W., & Connor, J.A. (1992) Ca^{2+} signalling in postsynaptic dendrites and spines of mammalian neurons in brain slice. *J. Physiol. (Paris)* 86, 57-66.

Muly, E.C., Szigeti, K., & Goldman-Rakic, P.S. (1997) D1 dopamine receptors are present in parvalbumin positive interneurons in macaque prefrontal cortex. *Soc. Neurosci. Abstr.* 692.6, 1772.

Murphy, B.L., Arnsten, A.F.T., Goldman-Rakic, P.S., & Roth, R.H. (1996a) Increased dopamine turnover in the prefrontal cortex impairs spatial working memory performance in rats and monkeys. *Proc. Natl. Acad. Sci. (U.S.A.)* 93, 1325-1329.

Nathan, T., Jensen, M.S., & Lambert, J.D. (1990) The slow inhibitory postsynaptic potential in rat hippocampal CA1 neurons is blocked by intracellular injection of QX-314. *Neurosci. Lett.* 110, 309-313.

Nauta, W.J.H. (1971) The problem of the frontal lobe: A reinterpretation. *J. Psychiat. Res.* 8, 167-187.

Niki, H., & Watanabe, M. (1979) Prefrontal and cingulate unit activity during timing behavior in the monkey. *Brain Res.* 171, 213-224.

Nisenbaum, E.S., Zao, C.X., & Wilson, C.J. (1994) Contribution of a slowly inactivating potassium current to the transition to firing of neostriatal spiny projection neurons. *J. Neurophysiol.* 71: 1174-1189.

Nowak, L., Bregestovski, P., Ascher, P., Herbert, A., & Prochiantz, A. (1984) Magnesium gates glutamate-activated channels in mouse central neurones. *Nature* (*Lond.*) 307, 462-465.

Olton, D.S. & Papas, B.C. (1979) Spatial memory and hippocampal function. *Neuropsychologia*, 17, 669-682.

Overton, F. (1897) Applied Physiology-Intermediate. pp 125-126. American Book Co. New York.

Owen, A.M., Downes, J.J., Sahakian, B.J., Polkey, C.E., & Robbins, T.W. (1990) Planning and spatial working memory following frontal lobe lesions in man. *Neuropsychologia*, 28, 1021-1034.

Owen, A.M., Sahakian, B.J., Semple, J., Polkey, C.E., & Robbins, T.W. (1995) Visuospatial short term recognition memory and learning after temporal lobe excisions, frontal lobe excisions or amygdala hippocampectomy in man. *Neuropsychologia* 33, 1-24.

Packard, M.G., Hirsh, R. & White, N.M. (1989) Differential effects of fornix and caudate nucleus lesions on two radial arm maze tasks: evidence for multiple memory systems. *J. Neurosci.,* 9, 1465-1472.

Packard, M.G., Regenold, W., Quirion, R. & White, N.M. (1990) Post-training injection of the acetylcholine M2 receptor antagonist AF-DX 116 improves memory. *Brain Res.*, 524, 72-76.

Pandya, D.N. & Yeterian, E.H. (1985) Architecture and connections of cortical association areas. In: A. Peters and E.G.Jones (eds.) Cerebral Cortex, Vol. 4 pp. 3-61, Plenum, New York.

Pandya, D.N., & Yeterian, E.H. (1990) Prefrontal cortex in relation to other cortical areas in the rhesus monkey: architecture and connections. *Prog. Brain Res.* vol. 85, 63-94.

Passingham, R.E. (1975) Delayed matching after selective prefrontal lesions in monkeys (Macac mulatta). *Brain Res.* 92 89-102.

Paupardin-Tritsch, D., Colombaioni, L., Deterre, P., & Gerschenfeld, H.M. (1985) Two different mechanisms of calcium spike modulation by dopamine. *J. Neurosci.* 5: 2522-2532.

Paxinos, G. & Watson, C (1986) The rat brain in stereotaxic coordinates, 2nd Ed. NY: Academic.

Paxinos, G. & Watson, C. (1997) *The Rat Brain in Stereotaxic Coordinates* 3rd Ed. N.Y. Academic Press.

Pedarzani, P. & Storm, J.F. (1995) Dopamine modulates the slow Ca^{2+}-activated K^+ current I_{AHP} via cyclic-AMP-dependent protien kinase in hippocampal neurons. *J. Neurophysiol.* 74, 2749-2753.

Penit-Soria, J., Audinat, E., & Crepel, F. (1987) Excitation of rat prefrontal cortical neurons by dopamine: an in vitro electrophysiological study. *Brain Res.* 425, 263-274.

Perkins, K.L., & Wong, R.K.S. (1995) Intracellular QX-314 blocks the hyperpolarization-activated inward current Iq in hippocampal CA1 pyramidal cells. *J. Neurophysiol.* 73, 911-915.

Peters, A. (1987) Number of neurons and synapses in primary visual cortex. In; Cerebral Cortex: Further aspects of cortical function, including hippocampus. Jones, E., Peters, A. (Eds). NY, Phenum, 267-294.

Petrides, M. (1994) Frontal lobes and behaviour. *Curr. Op. Neurobiol.*, 4, 207-211.

Petrides, M. (1989) Frontal lobes and memory. In *Handbook of Neuropsychology*, vol 3 (Ed. F. Boller & J. Graffman) pp 75-90. Amsterdam:Elsevier.

Petrides, M. (1995) Functional Organization of the human frontal cortex for mnemonic processing: Evidence from neuroimaging studies. *Ann. N.Y. Acad. Sci.* 769, 85-96.

Petrides, M. (1996) Specialized systems for the processing of mnemonic information within the primate frontal cortex. *Phil. Trans. Royal Soc. Lond.* 351, 1455-1462.

Pirot, S., Godbout, R., Mantz, J., Tassin, J.-P., & Glowinski, J. , Thierry, A.-M. (1992) Inhibitory effects of ventral tegmental area stimulation on the activity of prefrontal cortical neurons: evience for involvement of both dopaminergic and GABAergic components. *Neurosci.* 49: 857-865.

Quintana, J., & Fuster, J.M. (1992) Mnemonic and predictive functions of cortical neurons in a memory task. *Neuroreport* 3, 721-724.

Quintana, J., Fuster, J.M., & Yajeya, J. (1989) Effects of cooling parietal cortex on prefrontal units on delayed tasks. *Brain Res.* 503, 100-110.

Rall, W. (1964) Theoretical significance of dendritic trees for neuronal input-output relations. In, Neural theory and Modeling (Ed. R.F. Reiss). Palo Alto, Stanford University Press.

Rall, W., & Rinzel, J. (1973) Branch input resistance and steady attenuation for input to one branch of a dendritic neuron model. *Biophys. J.* 13, 648-688.

Ramón y Cajal, S. (1889) Conexión general de los elementos nerviosos. *Medicina Práctica.*

Regehr, W., Kehoe, J., Ascher, P. , & Armstrong, C. (1993) Synaptically triggered action potentials in dendrites. *Neuron* 11: 145-151.

Rétaux, S., Besson, M.J., & Penit-Soria, J. (1991) Opposing effects of dopamine D2 receptor stimulation on the spontaneous and the electrically-evoked release [^{3}H GABA] on rat prefrontal cortex slices. *Neurosci.* 42: 61-71.

Reuveni, I. Friedman, A., Amitai, Y., Gutnick, M.J. (1993) Stepwise repolarization from Ca^{2+} plateaus in neocortical pyramidal cells: evidence for nonhomogeneous distribution of HVA Ca^{2+} channels in dendrites. *J. Neurosci.* 13: 4609-4621.

Rhodes, P. (1997) Functional implications of active currents in the dendrites of pyramidal neurons. In. *Cerebral Cortex*, (Eds. Ulinski, P., Jones, E., Peters, A.) Plenum Press.

Robbins, T.W. (1991) Cognitive deficits in schizophrenia and parkinson's disease: neural basis and the role of dopamine. In: Willner, P & Scheel-Kruger, J. (eds) *The Mesolimbic Dopamine System: From Motivation to Action.* John Wiley and Sons Ltd. pp 497-528.

Robbins, T.W. Dissociating executive functions of the prefrontal cortex. *Phil. Trans. Royal. Soc. Lond.* 351, 1463-1471.

Rogers, D.C., Wright, P.W., Roberts, J.C., Reavill, C., Rothaul, A.L., & Hunter, A.J. (1992) Photothrombotic lesions of the frontal cortex impair the performance of the delayed non-matching to position task by rats. *Behav. Brain Res.*, 49, 231-235.

Romo, R., & Shultz, W. (1990) Dopamine neurons of the monkey midbrain: contingencies of responses to active touch during self-initiated arm movements. *J. Neurophysiol.* 63, 592-606.

Rosário, L.M., Barbosa, R.M., Antunes, C.M., Silva, A.M., Abrunhosa, A.J., & Santos, R.M. (1993) Bursting electrical activity in pancreatic β-cells: evidence that the channel underlying the burst is sensitive to Ca^{2+} influx through L-type Ca^{2+} channels. *Pflügers Arch.* 424, 439-447.

Rose, J.E. & Woolsey, C.N. (1948) Structure and relations of limbic cortex and anterior thalamic nuclei in rabbit and cat. *J. Comp. Neurol.* 89, 279-347.

Rudolf, G.D., Cronin, C.A., Landwehrmeyer, G.B., Standaert, D.G., Penney, J.B., & Young, A.B. (1996) Expression of N-Methyl-D-Aspartate glutamate receptor subunits in the prefrontal cortex of the rat. *Neurosci.* 73, 417-427.

Sah, P. & Nicoll, R.A. (1991) Mechanisms underlying potentiation of synaptic transmission in rat anterior cingulate cortex in vitro. *J. Physiol. (Lond.)* 433: 615-630.

Sakai, M., & Hamada, I. (1981) Intracellular activity and morphology of the prefrontal neurons related to visual attention task in behaving monkeys. *Exp. Brain. Res.* 41: 195-198.

Sakuri, Y., & Sugimoto, S. (1985) Effects of lesions of prefrontal cortex and dorsomedial thalamus on delayed go/no go alternation in rats. *Behav. Brain Res.*, 17, 213-219.

Sawaguchi, T. (1987) Catecholamine sensitivities neuron related to a visual reaction time task in the monkey prefrontal cortex. *J. Neurophysiol.* 48: 1100-1122.

Sawaguchi, T., & Goldman-Rakic, P.S. (1994) The role of D1-dopamine receptor in working memory: local injections of dopamine antagonists into the prefrontal cortex of rhesus monkeys performing an oculomotor delayed-response task. *J. Neurophysiol.* 71: 515-528.

Sawaguchi, T., & Matsumura, M. (1985) Laminar distributions of neurons sensitive to acetylcholine, noradrenaline and dopamine in the dorsolateral prefrontal cortex of the monkey. *Neurosci. Res.* 2, 255-273.

Sawaguchi, T., Matsumura, M. & Kubota, K. (1986) Dopamine modulates neuronal activities related to motor performance in the monkey prefrontal cortex. *Brain Res.* 371, 404-408.

Sawaguchi, T., Matsumura, M., & Kubota, K. (1988) Dopamine enhances the neuronal activity of spatial short-term memory performance in the primate prefrontal cortex. *Neurosci. Res.* 5, 465-473

Sawaguchi, T., Matsumura, M., & Kubota, K. (1990a) Catecholamine effects on neuronal activity related to a delayed response task in monkey prefrontal cortex. *J. Neurophysiol.* 63: 1385-1400.

Sawaguchi, T., Matsumura, M., & Kubota, K. (1990b) Effects of dopamine antagonists on neuronal activity related to a delayed response task in monkey prefrontal cortex. *J. Neurophysiol.* 63: 1401-1412.

Sayer, R.J., Schwindt, P.C., & Crill, W.E. (1990) High- and low-threshold calcium currents in neurons acutely isolated from rat sensorimotor cortex. *Neurosci. Lett.* 120: 175-178.

Schiffmann, S.N., Lledo, P-M., & Vincent J.-D. (1995) Dopamine D1 receptor modulates the voltage-gated sodium current in rat striatal neurons through a protein kinase A. *J. Physiol.* 483: 95-107.

Schiller, J., Helmchen, F., & Sakmann, B. (1995) Spatial profile of dendritic calcium transients evoked by action potentials in rat neocortical pyramidal neurones. *J.Physiol. (Lond.)* 487.3, 583-600.

Schiller, J., Schiller, Y., & Sakmann, B. (1996) Calcium action potentials in apical dendrites of neocortical pyramidal neurons in rat brain slices. *Soc. Neurosci Abstr.* 315.5, pp 794.

Schwindt, P.C. & Crill, W.E. (1995) Amplification of synaptic current by persistent sodium conductance in apical dendrite of neocortical neurons. *J. Neurophysiol.* 74, 2220-2224.

Schwindt, P.C. & Crill, W.E. (1997) Modification of current transmitted from apical dendrite to soma by blockade of voltage- and Ca^{2+}-dependent conductances in rat neocortical pyramidal neurons. *J. Neurophysiol.* 78, 187-198.

Schwindt, P.C. (1992) Ionic currents governing input-output relations of Betz cells. In: Singel Neuron Computation (Eds.: McKenna, T., Davis, J. & Zornetzer, S.F.) Academic Press, Inc. , New York, 1992, p.235-258.

Schwindt, P.C., Spain, W.J. , Crill, W.E. (1992) Calcium-dependent potassium currents in neurons from cat sensorimotor cortex. *J. Neurophysiol.* 67: 216-226.

Schwindt, P.C., Spain, W.J., & Crill, W.E. (1989) Long lasting reduction of excitability by a sodium-dependent potassium current in cat nepcortical neurons. *J. Neurophysiol.* 61: 233-244.

Schwindt, P.C., Spain, W.J., Foehring, R.C., Stafstrom, C.E., Chubb, M.C., & Crill, W.E. (1988) Multiple potassium conductances and their functions in neurons from cat sensorimotor cortex in vitro. *J. Neurophysiol.* 59: 424-449.

Seamans, J.K, Floresco, S.B., & Phillips, A.G. (1995). Functional differences between the prelimbic and anterior cingulate regions of the rat prefrontal cortex. *Behav. Neurosci.* 109: 1063-1073.

Seamans, J.K. & Phillips, A.G. (1994) Selective memory impairments produced by transient lidocaine-induced lesions of the nucleus accumbens in rats. *Behav. Neurosci.* 108: 456-468.

Seamans, J.K., Gorelova, N., & Yang, C.R. (1997) Contributions of voltage-gated Ca^{2+} channels in the proximal versus distal dendrites to synaptic integration in prefrontal cortical neurons. *J. Neurosci.* 17, 5936-5948.

Seeman, P. (1987) Dopamine receptors and the dopamine hypothesis of schizophrenia. *Synapse* 1, 133-152.

Sesack, S.R., & Bunney, B.S. (1989) Pharmacological characterization of the receptor mediating electrophysiological responses to dopamine in rat medial prefrontal cortex: a microiontophoretic study. *J. Pharmacol. Exp. Therap.* 248: 1323-1333.

Sesack, S.R., Deutch, A.Y., Roth, R.H. , & Bunney, B.S. (1989) Topographical organization of the efferent projections of the medial prefrontal cortex in the rat: an anterograde tract-tracing study with phaseolus vulgaris leucoagglutinin. *J. Comp. Neurol.* 290: 213-242.

Shadlen, M.N., & Newsome, W.T. (1994) Noise, neural codes and cortical organization. *Curr. Op. Neurobiol.* 4, 569-579.

Shallice, T. (1982) Specific impairments in planning. *Phil. Trans. Royal Soc. Lond.*, 298, 199-209.

Shallice, T., & Burgess, P. (1996) The domain of supervisory processes and temporal organization of behaviour. *Phil. Trans. Royal Soc. Lond.* 351, 1405-1411.

Shepherd, G.M., Brayton, R.K., Miller, J.P., Segev, I. Rinzel, J. & Rall, W. (1985) Signal enhancement in distal cortical dendrites by means of interactions between active dendritic spines. *Proc. Natl. Acad. Sci. USA* 82: 2192-2195.

Shindou, T., Watanabe, S., Kamata, O., Yamamoto, K., Nakanishi, H. (1994) Calcium-dependent hyperexcitability of hippocampal CA1 pyramidal cells in an in vitro slice after ethanol withdrawl of the rat. *Brain Res.* 656, 432-436.

Shultz, W. (1992) Activity of dopamine neurons in the behaving primate. *The Neurosciences* 4, 129-138.

Shultz, W., Daya, P., & Montague, P.R. (1997) A neural substrate of prediction and reward. *Science* 275, 1583-1599.

Silva, L.R., Amital, Y., & Connors, B.W. (1991) Intrinsic oscillations of neocortex generated by layer 5 pyramidal neurons. *Science*, 251, 432-435.

Silva, M.G., Boyle, M.A., Finger, S., Numan, B., Bouzrara, A.A., & Almli, C.R. (1986) Behavioral effects of large and small lesions of the rat medial frontal cortex. *Exp.Brain Res.*, 65, 176-181.

Singer, W. (1993) Synchronization of cortical activity and its putative role in information processing and learning. *Ann. Rev. Physiol.* 55: 349-374.

Smiley, J.F., & Goldman-Rakic, P.S. (1993) Heterogeneous targets of dopamine synapses in monkey prefrontal cortex demonstrated by serial section electron microscopy: a laminar analysis using the silver-enhanced diaminobenzidone sulfide (SEDS) immunolabeling technique. *Cerebral Cortex* 3: 223-238.

Smiley, J.F., Levey, A., Ciliax, B.J., & Goldman-Rakic, P. (1994) D1 dopamine receptor immunoreactivity in human and monkey cerebral cortex: Predominant and extrasynaptic localization in dendritic spines. *Proc. Natl. Acad. Sci. (U.S.A.)* 91: 5720-5724.

Smith, J.S., Kiloh, L.G., Boots, J.A. (1977) Prospective evaluation of prefrontal leucotomy: Results of 30 months' follow-up. In (Eds. W.H. Sweet, S. Obrador, J.G. Martin-Rodriguez) *Neurosurgical Treatment in Psychiatry, Pain and Epilepsy.* Baltimore: University Park Press, pp217-224.

Softky, W. (1994) Sub-millisecond coincidence detection in active dendritic trees. *Neurosci.* 58, 13-41.

Softky, W.R. (1995) Simple codes versus efficient codes. *Curr. Op. Neurobiol.* 5, 239-247.

Spain, W.J., Schwindt, P.C., & Crill, W.E. (1987) Anomalous rectification in neurones from cat sensorimotor cortex in vitro. *J. Neurophysiol.* 57, 1555-1576.

Spain, W.J., Schwindt, P.C., & Crill, W.E. (1991) Post-inhibitory excitation and inhibition in layer V pyramidal neurones from cat sensorimotor cortex. *J. Physiol. (Lond.)* 434, 609-626.

Spencer, W.A., & Kandel, E.R. (1961) Electrophysiology of hippocampal neurons: IV Fast Prepotentials. *J. Neurophysiol.* 24, 272-285.

Spritzer, N.C. (1984) On the basis of delayed depolarization and its role in reptitive firing of rohon-beard neurons in Xenopus tadpoles. *J. Physiol. (Lond.)* 357, 51-65.

Spruston, N., & Stuart, G. (1996) Voltage attenuation and intracellular resistivity in neocortical pyramidal neurons. *Soc. Neurosci. Abstr.* 315.1.

Spruston, N., Jaffe, D.B., & Johnston, D. (1994) Dendritic attenuation of synaptic potentials and currents: the role of passive membrane properties. *Tends Neurosci.* 17, 161-166.

Spruston, N., Jaffe, D.B., Williams, S.H., & Johnston, D. (1993) Voltage- and space-clamp errors associated with the measurement of electrotonically remote synaptic events. *J. Neurophysiol.* 70, 781-802.

Spruston, N., Jonas, P., & Sakmann, B. (1995) Dendritic glutamate receptor channels in rat hippocampal CA3 and CA1 pyramidal neurons. *J. Physiol. (Lond)* 482.2, 325-352.

Squire, L.R. (1992) Memory and the hippocampus: a synthesis from findings with rats, monkeys, and humans. *Psych. Rev.*, 99, 195-231.

Stafstrom, C.E., Schwindt, P.C., & Crill, W.E. (1982) Negative slope conductance due to a persistent subthreshold sodium current in cat neocortical neurons in vitro. *Brain Res.* 236: 221-226.

Stafstrom, C.E., Schwindt, P.C., & Crill, W.E. (1985) Properties of persistent sodium and calcium conductance of layer V neurons from cat sensorimotor cortex in vitro. *J. Neurophysiol.* 53, 153-170.

Steriade, M., Nunez, A., & Amzica, F.(1993) A novel slow (<1 Hz) oscillation of neocortical neurons in vivo: depoalrizing and hyperpolarizing components. *J. Neurosci.* 13: 3252-3265.

Storm, J.F. (1988) Temporal integration by a slowly inactivating K^+ current in hippocampal neurons. *Nature*, 336: 379-381.

Storm, J.F. (1993) Functional diversity of K^+ currents in hippocampal pyramidal neurons. *Seminars Neurosci.* 5, 79-92.

Stuart, G., & Sakmann, B. (1995) Amplification of EPSPs by axosomatic sodium channels in neocortical pyramidal neurons. *Neuron*, 15, 1065-1076.

Stuart, G.J. & Sakmann, B. (1994) Active propagation of somatic action potentials into neocortical pyramidal cell dendrites. *Nature* 367, 69-72.

Stuss, D.T, Kaplan, E.F., Benson, D.F., Weir, W.S., Chiulli, S., Sarazin, F.F. (1982) Evidence for the involvement of orbitofrontal cortex in memory functions: an interference effect. *J. Comp. Physiol. Psychol.* 96, 913-925.

Stuss, D.T. & Benson, D.F. (1986) *The frontal lobes.* New York, Raven Press.

Surmeier, D.J., Bargas, J., Hemming, Jr., H.C., Nairn, A.C., & Greengard, P. (1995) Modulation of calcium currents by a D1 dopaminergic protein kinase/phosphatase cascade in rat neostriatal neurons. *Neuron* 14: 385-397.

Surmeier, D.J., Eberwine, J., Wilson, C.J., Cao, Y., Stefani, A., & Kitai, S.T. (1992) Dopamine receptor subtypes colocalize in rat striatonigral neurons. *Proc. Natl. Acad. Sci. U.S.A.* 89: 10178-10182.

Sutor, B., & Hablitz, J.J. (1989) EPSPs in rat neocortical neurons in vitro II. Involvement of N-methyl-D-aspartate receptors in the generation of EPSPs. *J. Neurophysiol.* 61, 621-634.

Sutor, B., & Zieglgansberger, W. (1987) A low-voltage activated, transient calcium current is responsible for the time-dependent depolarizing inward rectification of rat neocortical neurons in vitro. *Pflueger Arch. Eur. J. Physiol.* 410: 102-111.

Suzuki, H., & Azuma, M. (1977) Prefrontal neuronal activity during gazing at a spot of light in the monkey. *Brain Res.* 126, 497-508.

Svoboda, K., Denk, W., Kleinfeld, D., & Tank, D.W. (1997) *In vivo* dendritic calcium dynamics in neocortical pyramidal neurons. *Nature* 385, 161-165.

Tanaka, E., Higashi, H., & Nishi, S. (1991) Membrane properties of guinea pig cortical neurons in vitro. J. Neurophysiol. 65, 808-821.

Tasker, J.G., & Dudek, F.E. (1991) Electrophysiology of GABA-mediated synaptic transmission and possible roles in epilepsy. *Neurochem. Res.* 16, 251-262.

Taube, J.S. (1993) Electrophysiological properties of neurons in the rat subiculum in vitro. *Exp. Brain. Res.* 96, 304-318.

Taylor, C.P. (1993) Na^+ currents that fail to inactivate. *Trends Neurosci.* 16: 455-460.

Thomson, A.M. & West, D.C. (1993) Fluctuations in pyramid-pyramid excitatory postsynaptic potentials modified by presynaptic firing pattern and postsynaptic membrane potential using paired intracellular recordings in rat neocortex. *Neurosci.* 54, 329-346.

Thomson, A.M., & Deuchars, J. (1994) Temporal and spatial properties of local circuits in neocortex. *Trends Neurosci.* 17, 119-126.

Thomson, A.M., & Deuchars, J. (1997) Synaptic interactions in neocortical local circuits: Dual intracellular recordings in vitro. *Cereb. Cortex* 7, 510-522.

Thomson, A.M., Deuchars, J. & West, D.C. (1993) Large, deep layer pyramid-pyramid single axon EPSPs in slices of rat motor cortex display paired pulse and frequency-dependent depression, mediated presynaptically and self-facilitation, mediated postsynaptically. *J. Neurophysiol.* 70, 2354-2369.

Thomson, A.M., West, D.C., & Deuchars, J. (1995) Properties of single axon EPSPs elicited in spiny interneurons by action potentials in pyramidal neurones in slices of rat neocortex display unique properties. *Neurosci.* 69, 727-738.

Thomson, A.M., West, D.C., Hahn, J., & Deuchars, J. (1996) Single axon IPSPs elicited in pyramidal cells by three classes of interneurones in slices of rat neocortex. *J. Physiol. (Lond.)* 496, 81-102.

Tsien, R.W., Lipscome, D., Madison, D.V., Bley, K.R., & Fox, A.P. (1988) Multiple types of neuronal calcium channels and their selective modulation. *Trends Neurosci.*, 11, 431-438.

Tsodyks, M.V., & Markram, H. (1997) The neural code between neocortical pyramidal neurons depends on transmitter release probability. *Proc. Natl. Acad. Sci. USA* 94, 719-723.

Usowicz, M.M., Sugimori, M., Cherskey, B., & Llinas, R. (1992) P-type calcium channels in the somata and dendrites of adult cerebellar Purkinje cells. *Neuron* 9: 1185-1199.

Uylings, H.B.M., & van Eden, C.G. (1990) Qualitative and quantitative comparison of the prefrontal cortex in rat and in primates, including humans. *Prog. Brain Res.*, 85, 31-62.

Vaadia, E., Haalman, I., Abeles, M., Bergman, H., Prut, Y., Slovin, H., & Aertsen, A. (1995) Dynamics of neuronal interactions in monkey cortex in relation to behavioural events. *Nature*, 373, 515-518.

van Brederode & Snyder, G.L. (1992) A comparison of the electrophysiological properties of morphologically identified cells in layer 5B and 6 of the rat neocortex. *Neurosci.* 50: 315-337.

van Brederode, J.F.M., & Spain, W.J. (1995) Differences in inhibitory synaptic input between layer II-III and layer V neurons of the cat neocortex. *J. Neurophysiol.* 74, 1149-1166.

van Eden, C.G., Hoorneman, E.M.D., Buijs, R.M., Mathussen, M.A.H., Geffard, M. , & Uylings, H.B.M. (1987) Immunohistochemical localization of dopamine in the prefrontal cortex of the rat at the light, electron microscopical level. *Neurosci.* 22: 849-862.

van Eden, C.G., Lamme, V.A.F., & Uylings, H.B.M. (1992) Heterotopic cortical afferents to the medial prefrontal cortex in the rat. A combined retrograde and anterograde tracer study. *Eur. J. Neurosci.* 4, 77-97.

van Haaren, F., Van Zijderveld, G., Van Hest, A., & Debruin, J.P.C. (1988) Acquisition of conditional associations and operant delayed spatial response

alternation: Effects of lesions in the medial prefrontal cortex. *Behav. Neurosci.*, 102, 481-488.

Vincent, S.L., Khan, Y., & Benes, F.M. (1995) Cellular colocalization of dopamine D1 and D2 receptors in rat medial prefrontal cortex. *Synapse*. 19: 112-120.

Vincent, S.L., Knan, Y., & Benes, F.M. (1993) Cellular distribution of dopamine D1 and D2 receptors in rat medial prefrontal cortex. *J. Neurosci.* 13: 2551-2564.

Wang, X. (1993) Ionic basis for intrinsic 40Hz neuronal oscillations. *Neuroreport* 5, 221-224.

Watanabe, M. (1981) Prefrontal unit activity during delayed conditional discriminations in the monkey. *Brain Res.* 225, 51-65.

Watanabe, M. (1986a) Prefrontal unit activity during delayed conditional go/no-go discrimination in the monkey. I. Relation to the stimulus. *Brain Res.* 382, 1-14.

Watanabe, M. (1986a) Prefrontal unit activity during delayed conditional go/no-go discrimination in the monkey. II. Relation to go and no-go responses. *Brain Res.* 382, 1-14.

Watanabe, M. (1990) Prefrontal unit activity during associative learning in the monkey. *Exp. Brain Res.* 80, 296-309.

Watanabe, M. (1996) Reward expectancy in primate prefrontal neurons. *Nature*, 382, 629-632.

Watanabe, T., & Niki, H. (1985) Hippocampal unit activity and delayed response in the monkey. *Brain Res.* 325, 241-254.

Welsh, J.P., & Harvey, J.A. (1991) Pavlovian conditioning in the rabbit during inactivation of the interpositus nucleus, *J. Physiol. (Lond.)*, 444, 459-480.

Westenbroek, R.E., Ahlijanian, M.K., & Catterall, W.A. (1990) Clustering of L-type Ca^{2+} channels at the base of major dendrites in hippocampal pyramidal neurons. *Nature* 347, 281-284.

Westenbroek, R.E., Hell, J.N., Warner, C., Dubel, S.J., Snutch, T.P., & Catterall, W.A. (1992) Biochemical properties and subcellular distribution of an *N*-type calcium channel $\alpha 1$ subunit. *Neuron* 9, 1099-1115.

Westenbroek, R.E., Merrick, D.K., & Catterall, W.A. (1989) Differential subcellular localization of the R1 and RII Na^+ channel subtypes in central neurons. *Neuron*. 3: 694-704.

Whittington, M.A., Traub, R.D., & Jefferys, J.G.R. (1995) Synchronized oscillations in interneuron networks driven by metabotropic glutamate receptor activation. *Nature*, 373, 612-615.

Wikmark, R.G.E., Divac, I., & Weiss, R. (1973) Retention of spatial delayed alternation in rats with lesions in the frontal lobes. *Brain Behav. & Evol.*, 8, 329-339.

Williams, G.V. & Goldman-Rakic, P.S. (1995) Modulation of memory fields by dopamine D1 receptors in prefrontal cortex. *Nature*, 376: 572-575.

Williams, P.J., MacVicar, B.A., & Pittman, Q.J. (1990) Synaptic modulation by dopamine of calcium currents in rat pars intermedia. *J. Neurosci.* 10: 757-763.

Williams, S.M., & Goldman-Rakic, P.S. (1993) Characterization of the dopaminergic innervation of the primate frontal cortex using a dopamine-specific antibody. *Cerebral Cortex* 3: 199-222.

Wilson, F.A.W., Scalaidhe, S.P.Ó., & Goldman-Rakic, P.S. (1993) Dissociation of object and spatial processing domains in primate prefrontal cortex. *Science*, 260, 1955-1958.

Wolf, C., Waksman, D., Finger, S., & Almi, C.R. (1987) Large and small medial frontal cortex lesions and spatial performance of the rat. *Brain Res. Bull.*, 18, 1-5.

Wong, R.K.S., & Stewart, M. (1992) Different firing patterns generated in dendrites and somata of CA1 pyramidal neurons in guinea-pig hippocampus. *J. Physiol. (Lond.)* 457, 675-687.

Wong, R.K.S., Prince, D.A., & Basbaum, A.I. (1979) Inradendritic recordings from hippocampal neurons. *Proc. Natl. Acad. Sci. U.S.A.* 76, 986-990.

Yajeya, J., Quintana, J., & Fuster, J. (1988) Prefrontal representation of stimulus attributes during delay tasks II. The role of behavioral significance. *Brain Res.* 474, 222-230.

Yang, C.R. , Seamans, J.K, & Gorelova, N.A. (1996) Electrophysiological and morphological properties of layer V-VI principal pyramidal cells in rat prefrontal cortex in vitro. *J. Neurosci.* 16, 1904-1921

Yang, C.R., & Mogenson, G.J. (1990) Dopaminergic modulation of cholinergic responses in rat medial prefrontal cortex: an electrophysiological study. *Brain Res.* 524: 271-281.

Yang, C.R., & Seamans, J.K. (1996) Dopamine D1 receptor actions in layer v-vi rat prefrontal cortex neurons in vitro: Modulation of dendritic-somatic signal integration. *J. Neurosci.*, 16, 1922-1935.

Yang, C.R., Seamans, J.K., & Gorelova, N. (1996) Focal dendritic D1 receptor stimulation differentially modulates layer I-II and V-VI glutamate inputs to deep layer prefrontal cortical pyramidal neurons in vitro. *Soc. Neurosci. Abstr.* 22:1770.

Ye, J.H., & Akaike, N. (1993) Calcium currents in pyramidal neurons acutely dissociated from the rat frontal cortex: a study by the nystatin perforated patch technique. *Brain Res.* 606: 111-117.

Yuste, R., & Tank, D.W. (1996) Dendritic integration in mammalian neurons, a century after Cajal. *Neuron* 16, 701-716.

Yuste, R., Gutnick, M.J., Saar, D., Delaney, K.R., & Tank, D.W. (1994) Ca^{2+} accumulations in dendrites of neocortical pyramidal neurons: An apical band and evidence for two functional compartments. *Neuron* 13, 23-43.

Zahrt, J., Taylor, J.R., & Arnsten, A.F.T. (1996) Supranormal stimulation of dopamine D1 receptors in the prefrontal cortex impairs working memory perfromance in rats. *Soc. Neurosci. Abstr.* 22, 1128.

Zheng, P., Bunney, B.S., & Shi, W.X. (1997) Electrophysiological characterization and effects of dopamine on visually identified non-pyramidal neurons in the prefrontal cortex. *Soc. Neurosci. Abstr.* 481.13, 1212.

Zhu, J.J., & Sakmann, B. (1997) Postnatal development of Ca^{2+}-mediated action potentials in dendritic tufts of rat neocortical pyramidal neurons. *Soc. Neurosci. Abstr.* 891.1, 2283.